SEPARATION AND CHARACTERIZATION OF CLOSED FUNCTIONALIZED DOUBLE-DECKER SHAPED SILSESQUIOXANES

By

David Felipe Vogelsang Suarez

A DISSERTATION

Submitted to
Michigan State University
in partial fulfillment of the requirements
for the degree of

Chemical Engineering — Doctor of Philosophy

2019

ABSTRACT

SEPARATION AND CHARACTERIZATION OF CLOSED FUNCTIONALIZED DOUBLE-DECKER SHAPED SILSESQUIOXANES

By

David Felipe Vogelsang Suarez

Stoichiometric reaction of tetrasilanol octaphenyl double-decker shaped silsesquioxanes (DDSQ-$(Ph)_8(OH)_4$) with difunctional dichlorosilanes ($R_1R_2SiCl_2$) provided a new class of model hybrid organic-inorganic compounds. These model compounds (DDSQ-2(R_1R_2)) have a dimensionally well-defined closed inorganic Si-O core, eight phenyl groups for thermo-oxidative stability and compatibility to aromatic organics, and well-specified R_1 and R_2 for possible further chemical reactions. However, these compounds contain *cis* and *trans* conformations about the DDSQ if R_1 and R_2 are different.

Separation of *cis* and *trans* isomers by liquid chromatography was proposed as the alternative technique to the more tedious fractional crystallization for isolation of pure compounds. It was found polar nature of the R group enables the separation by adsorption chromatography. In contrast, partition chromatography allows separation of isomers of a larger solubility difference. Results of HPLC also provided quantitative measure of the isomer ratio in a *cis* and *trans* DDSQ-2(R_1R_2) mixture with deviations better than ±5%. In contrast, the current quantification of the isomer ratio by ^{29}Si-NMR has been reported to have ±10% deviation from the real value.

HPLC separation was extended to analyze resolution of the elution for DDSQ mixtures with polarity differences. Reaction of DDSQ-$(Ph)_8(OH)_4$ with $R_1R_2SiCl_2$ and $(CH_3)SiCl_3$ mixture followed by hydrolysis, lead to a mixture of DDSQ compounds with zero, one, and two hydroxyl groups. Good separation of the three expected products was made by LC.

Characterization by NMR and mass-spectroscopy allowed identification of each separated product. An asymmetric structure about the DDSQ core with one hydroxyl group (DDSQ-(R_1R_2)((CH_3)(OH)) was obtained.

Scale-up of HPLC separation for the mixture containing zero, one, and two hydroxyl groups was simulated in ASPEN chromatography. Linear adsorption isotherm parameters were obtained by frontal analysis. A correlation between HPLC stationary phase adsorption parameters and preparative stationary phase LC adsorption parameters was obtained. These parameters permitted satisfactory prediction of the column efficiency, the resolution of the elution, and total collection time in a column separation verified with a 5g-scale. In the scale of preparative-LC, fractions collected were of high purity as verified by ^{29}Si NMR. Additionally, for DDSQ-2(R_1OH) a highly *cis* concentrated fraction and a nearly-pure *trans* fraction were also successfully isolated.

DSC experiments were performed for nearly-pure *cis* and *trans* DDSQ-2(R_1R_2), and for DDSQ-2(R_1R_2) mixtures of varying *cis-to-trans* compositions. R_1 was fixed as methyl, and for R_2 aryl groups were selected. It was found *trans* isomer had a higher melting temperature than *cis* isomer and as the size of R_2 increases the melting temperatures of nearly-pure isomers decrease. Interestingly, *cis* and *trans* structures are not miscible in the solid state and form binary eutectic. Binary *cis* and *trans* eutectic temperature and composition can be predicted using the ideal binary assumption.

To my beautiful wife Andrea Garcia. You have been the most important person through my life and along this study. It was because of you that I applied to the scholarship, and it is because of you that I am a better person now. I expect to fulfill your expectations, and I am willing to keep providing more love to our growing family. I am very happy for our projects, for Tommy, for Beyoncé, and for all the good things that are coming for us. I love you.

ACKNOWLEDGMENTS

I would like to acknowledge the institutions that fund my research. First, I want to thank Fulbright-Colombia, and COLCIENCIAS-Colombia for choose me to develop doctoral studies in USA and their economic support. I would like to thank the Office of Naval Research for funding this project through the grant N00014-16-2109. Finally, I want to thank Michigan State University trough the CHEMS department for the unconditional financial support.

I want to acknowledge the work of the professors in my research committee. I highlight the guidance and patience of my advisor Dr. Andre Lee. He accepted me as his student in Fall 2013 and every day he challenges me to become a better researcher teaching me how to think, how to proceed experimentally, and how to formulate questions to find solutions to any scientific problem. His contribution was beyond his duty and he help me to become a better writer and a better speaker. Dr. Robert Maleczka for his guidance through the organic chemistry problems and his disposition to answer my questions every time his door was open. His contributions to this project were invaluable. His advice solved every single issue I had related with the chemistry component of this dissertation. Dr. Carl Lira for his explanations about how to analyze adsorption isotherms and made suggestions to my project that allowed me to generate the chapter 4 of this dissertation. Besides his contribution he was always willing to solve any question I had. Besides his contribution he is an excellent professor and I enjoyed his thermo and distillation column modelling class. Finally, Dr. Dennis Miller for his help when I was his student in the distillation column modelling by ASPEN. Also, his comments were very helpful to enhance the quality of this research. I appreciate he was always willing to help with any question.

Beyond the committee members I would like to express my gratitude to my friends in chemistry. Besides their contributions, their kindness and solidarity make very special my work in the laboratory. From them I would like to highlight the contributions of Jonathan Dannatt, his ideas and explanations help me in such a way that we even wrote research papers together. From this group I also want to remark the contributions of Gayanthi Attanayake, she taught me almost every single organic chemistry technique to develop this research. All faculties in the chemistry department were also very kind offering their help when requested.

I also like to thank to my research group friends Dr. Yuelin Wu, and Dr. Yang Lu because they were a great support in those times where we did not have idea of how to present or read properly papers. Parker Dunk was key person for production of material used in chapter 2 of this work. More recently Aditya Patel join our group and I thank him to be willing to learn and work as a team trying to develop all sort of ideas. I would like to do a mention to the CHEMS department staff, all of them made a great job with paperwork, orders, solving visa issues, and much more. Also, the CHEMS department faculties from whom I learn several new ideas and concepts along seminars, conferences, and classes.

Next, I want to make a special mention to my Latin-American friends specially my parchecito friends. They were my family in USA and these fun moments we enjoyed together make me keep going to reach this goal. This group of people was one of the best parts of my life and I expect we keep being friends forever.

I want to thank my family in Colombia who understood my wish to come to USA to develop PhD studies. They were always supportive thinking in my needs. I expect they keep feeling proud of me and specially from my mother Claudia Suarez who has been always an inspiration to me. She is the toughest person I have known in my entire life.

TABLE OF CONTENTS

LIST OF TABLES

LIST OF FIGURES

LIST OF SCHEMES

KEY TO SYMBOLS AND ABBREVIATIONS

Acronyms

AA	Non-polar symmetric double-decker shaped silsesquioxane
AB	Asymmetric double-decker shaped silsesquioxane
BB	Polar symetric double-decker shaped silsesquioxane
$CDCl_3$	Deuterated chloroform
DCM	Dichloromethane
DDSQ	Double-decker shaped silsesquioxane
DDSQ-$(Ph)_8(OH)_4$	Tetrasilanol double-decker shaped silsesquioxane
DDSQ-$(Ph)_8(ONa)_4$	Tetrasodium cholate double-decker shaped silsesquioxane
DDSQ-2(R1R2)	Double-decker shaped silsesquioxane capped with difunctional dichlorosilanes
DSC	Differential scanning calorimetry
Et_3N	Triethylamine
FC	Fractional crystallization
GC-MS	Gas chromatography – Mass spectroscopy
HPLC	High performance liquid chromatography
IR	Infrared

L	Liquid (in italic)
LC	Liquid chromatography
Me	Methyl
NMR	Nuclear magnetic resonance
NP	Normal phase
PA	*para*-phenylamine
PEP	*para*-phenylethynyl phenyl
Ph	Phenyl
pHPLC	Partition normal phase high performance chromatography
POSS	Polyhedral oligomeric silsesquioxane
R	Functional moiety attached to functional chlorosilanes or to functionalized double-decker shaped silsesquioxane
RP	Reverse phase
R.T.	Room temperature
$R_1R_2SiCl_2$	Difunctional dichlorosilane
S	Solid (in italic)
THF	Tetahydrofurane
TLC	Thin layer chromatography
TMS	Trimethyl silane

UPLC	Ultra-high performance liquid chromatography
UV	Ultraviolet
UV-VIS	Ultraviolet-visible

Symbols

C	Concentration
ΔS_m	Change of entropy at melting
ΔH_m	Change of enthalpy at melting
ε_i	Interparticle void fraction
ε_p	Intraparticle void fraction
ε_t	Total void fraction
E_z	Dispersion coefficient
F_v	Flow rate
γ	Activity coefficient
H	Height of theoretical plate
Hb	Height of packed bed
IP1	Linear adsorption isotherm parameter 1
IP2	Linear adsorption isotherm parameter 2
J	Mass transfer flux

L	Column length
MTC	Mass transfer coefficient
N	Number of theoretical plates or column efficiency
q_v	Concentration of analyte adsorbed in a determinate time and column location
t_0	Hold-up time
R	Universal gas constant (in italic)
R_f	Retardation factor
R_s	Resolution of the elution
t_{ext}	Extra column time
T	Temperature
t	Time
T_E	Eutectic temperature
T_L	Liquidus temperature
T_m	Melting temperature
t_r	Retention time
t_s	Shock time or front time
W	Peak width
x	Isomer fraction

CHAPTER 1.

INTRODUCTION

1. Introduction

1.1 Hybrid organic-inorganic silsesquioxanes: model molecules

Polyhedral oligomeric silsesquioxanes (POSS) are organic-inorganic hybrid materials with a Si-O core surrounded by an organic corona having the common structure $(RSiO_{1.5})_n$. Partially condensed POSS has been functionalized to study properties of hybrid structures in diverse fields including chemistry, engineering, materials science, or medicine.[1–5] The most studied partially condensed POSS has the structure $(RSiO_{1.5})_7(OH)_3$ (**Figure 1-1a**), Condensation of this structure by corner-capping with functionalized trichlorosilanes or alkoxysilanes allow the use of these sructures as model molecules with specific functionalization in vicinal silanols.[6–8]

Recently, tetrasilanol octaphenyl double-decker shaped silsesquioxanes DDSQ-$(Ph)_8(OH)_4$ (**Figure 1-1b**) was developed by Yoshida *et al.*, and further improved by Kawakami *et al.*[9–12] These are oligomeric structures with the formula $(PhSiO_{1.5})_8(O_{0.5}H)_4$. The molecule has an inner Si-O core conformed by two silsesquioxane rings interconnected by two oxygens in opposite edges. The remaining two edges are open, leaving four hydroxyl groups. The core is surrounded by eight phenyl rings bonded to each Si atom. The listed characteristics make DDSQ-$(Ph)_8(OH)_4$ a model molecule to understand hybrid organic-inorganic systems with the benefit of specific number of functionalities in specific sites of the nanostructure.

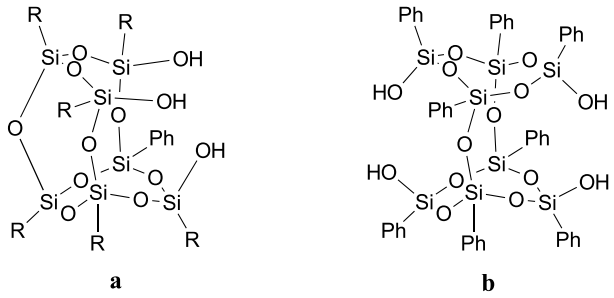

Figure 1-1. Partially condensed oligomeric silsesquioxanes used as model molecules.

1.2 Synthesis of octaphenyl double-decker shaped silsesquioxane

Precursor of DDSQ-$(Ph)_8(OH)_4$ is a tetrasodium salt (DDSQ-$(Ph)_8(ONa)_4$). This salt has been synthesized by reaction of phenyl(trimethoxy)silane with 0.7 equivalents of sodium hydroxide and 1.1 equivalents of water using isobutanol as solvent under reflux for 4h followed by stirring for 15h at room temperature as observed in **Scheme 1-1**.[9,11] Alternative production of DDSQ-$(Ph)_8(ONa)_4$ has been achieved by cleaving fully condensed octaphenyl POSS.[12] This process was performed with 4 equivalents of sodium hydroxide and 2 equivalents of water using isopropanol under reflux or isobutanol at 90°C as seen in **Scheme 1-2.**

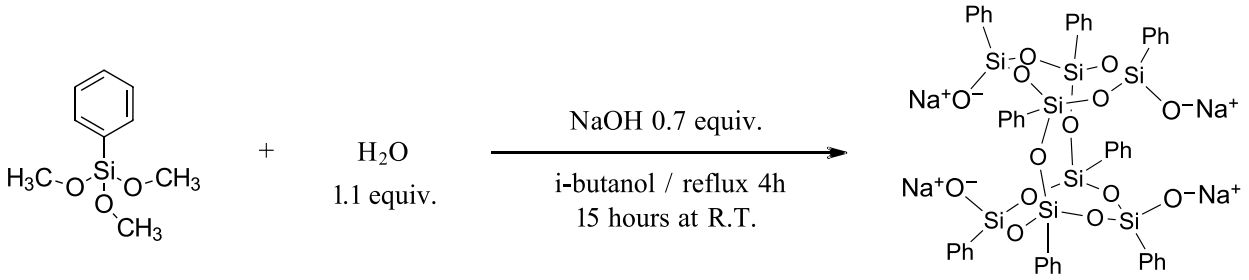

Scheme 1-1. Synthesis of DDSQ-$(Ph)_8(ONa)_4$ from phenytrimethoxysilane

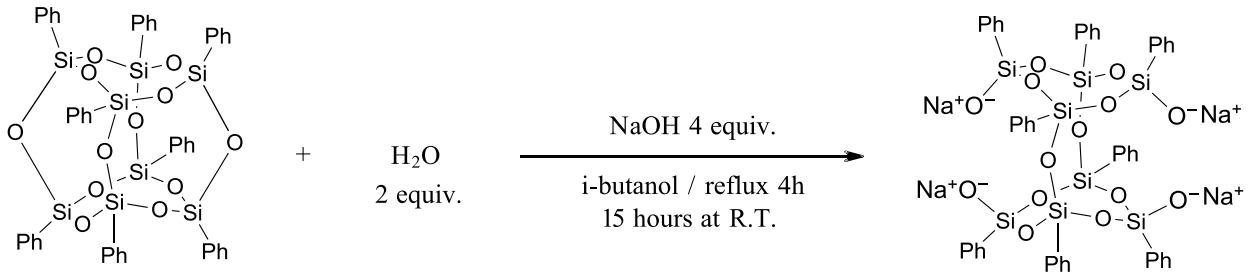

Scheme 1-2. Cleaving of POSS to synthesize DDSQ-$(Ph)_8(ONa)_4$

DDSQ-$(Ph)_8(ONa)_4$ may be very unstable and further acid treatment is done to achieve the more stable DDSQ-$(Ph)_8(OH)_4$ (**1**). This molecule is commercially available and different reactions can be performed with the silanol groups to add specific functionalities.[4–28]

1.3 Side-capping of DDSQ-$(Ph)_8(OH)_4$

The reaction between **1** and difunctional dichlorosilanes produced a closed DDSQ structure that will be label in this document as DDSQ-2(R_1R_2). This reaction, described in **Scheme 1-3**, results in unavoidable production of *cis* and *trans* isomers when R_1 is different than R_2. Examples of DDSQ-2(R_1R_2) have been widely reported in current literature.[4,11,13–17] Applications for DDSQ-2(R_1R_2) have been mainly explored in polymer synthesis because the nanostructures become part of the polymer backbone. Polymers containing DDSQ-2(R_1R_2) are known for their low dielectric constants, hydrophobic properties and high degradation temperatures.[18–28]

Few works have isolated *cis* and *trans* isomers. Separation has been performed by fractional crystallization (FC).[4,13,14,17] FC could be limited by small differences in solubility limits between *cis* and *trans* DDSQ-2(R_1R_2). As an example, the work from Walczak *et al.* was able to isolate only a fraction of the *trans* isomer of DDSQ-2($(CH_3)(H)$). Separation of

the individual isomers is a very interesting topic because structural differences between *cis* and *trans* DDSQ-2(R_1R_2) isomers can affect other properties like melting temperatures between isomers as reported by Schoen, and Moore *et al.* (**Table 1-1**).[15,27] In the study developed by Hoque *et al.*, melting temperature differences were reported in polymers synthesized with pure *cis*, pure *trans*, and a 1:1 *cis*-to-*trans* mixture of DDSQ-2((isobutyl)(OH)). Separation in this work was performed by FC obtaining *cis*-to-*trans* ratios of 2:8 in the precipitated crystals and 8:2 in the solution. This particular study as well as the work developed by Schoen purified the enriched fractions by liquid chromatography.[14,17]

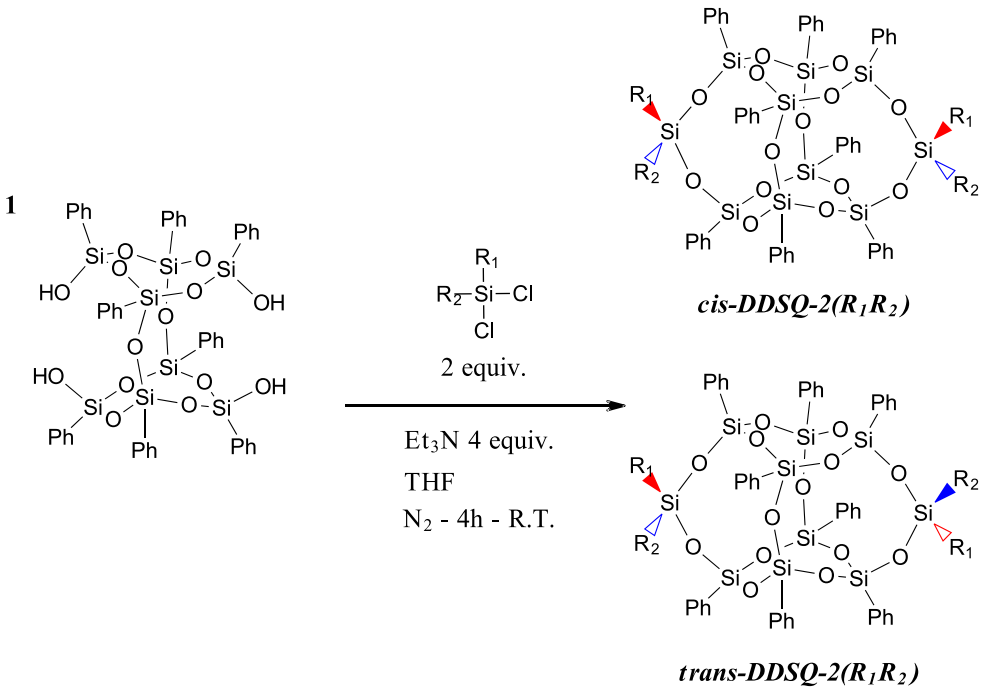

Scheme 1-3. Synthesis of closed DDSQ or DDSQ-2(R_1R_2)

Table 1-1. Differences in melting temperature for *cis* and *trans* isomers for selected systems.[15,27]

Compound	*cis* melting temperature °C	*trans* melting temperature °C
DDSQ-2((*p*-$C_6H_4NH_2$)(CH_3))	275	311
DDSQ-2((*p*-$C_6H_4C_2C_6H_5$)(CH_3))	261	304

1.4 Separation techniques used for separation of DDSQ-2(R_1R_2) systems

1.4.1 Fractional crystallization

FC is a separation technique that is based on differences in the solubility limit between molecules.[29] FC can be performed by dissolving the analyte in a common good solvent and then adding an amount of a poor solvent to crystallize the analyte with the lower solubility limit. An alternative FC is performed by solubilizing the analyte in the minimum amount possible of good solvent and further crystallization by temperature reduction.[14,29–33] FC is usually considered a cost-effective separation. The main inconvenients of this technique are long operation times, requirement of high purity in the sample, as well as impossibility for separation in binary mixtures that may co-crystallize at some specific compositions.[30,33] After separation the solvent mixture must be evaporated and, if possible, the solvent can be recycled. A diagram describing the crystallization process can be observed in **Figure 1-2**.

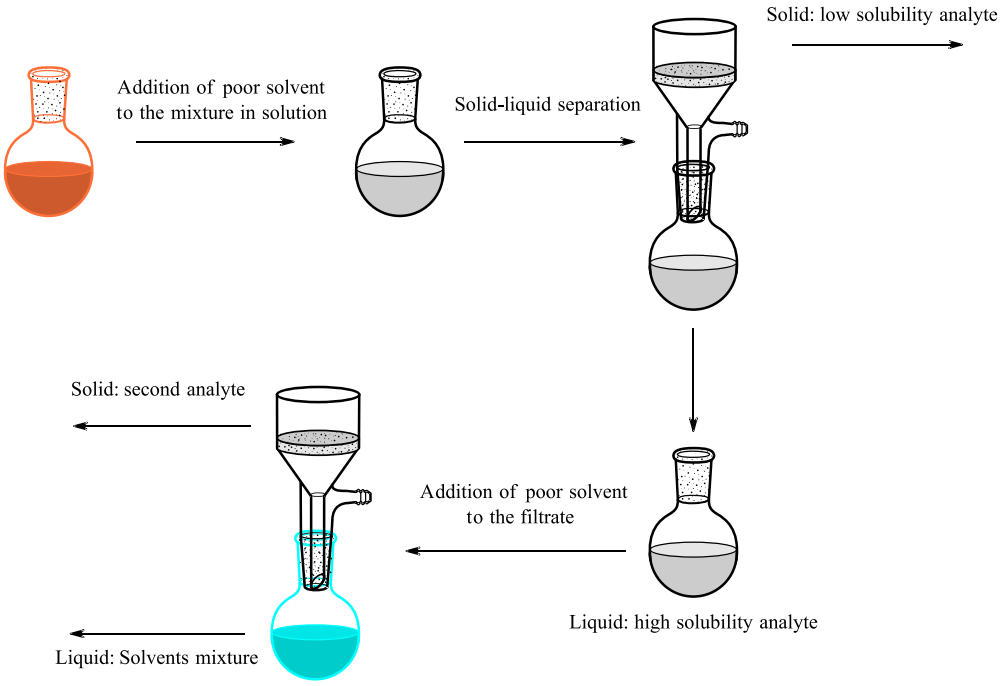

Figure 1-2. Fractional crystallization diagram

1.4.2 Liquid chromatography

Based on the definition provided by Snyder, liquid chromatography or LC is a process in which a liquid mobile phase has contact with a stationary phase. [34] The stationary phase is all the non-moving material in the packed-bed. A mixture of analytes has a specific equilibrium distribution between the two phases. This equilibrium determines the migration rate through the packed-bed. Differences in rates between analytes separate the mixture between their analytes as described in **Figure 1-3**.[34–37] Different classifications for liquid chromatography have been formulated. Modern classification is listed in **Table 1-2**. For this work, adsorption and partition chromatography will be discussed.

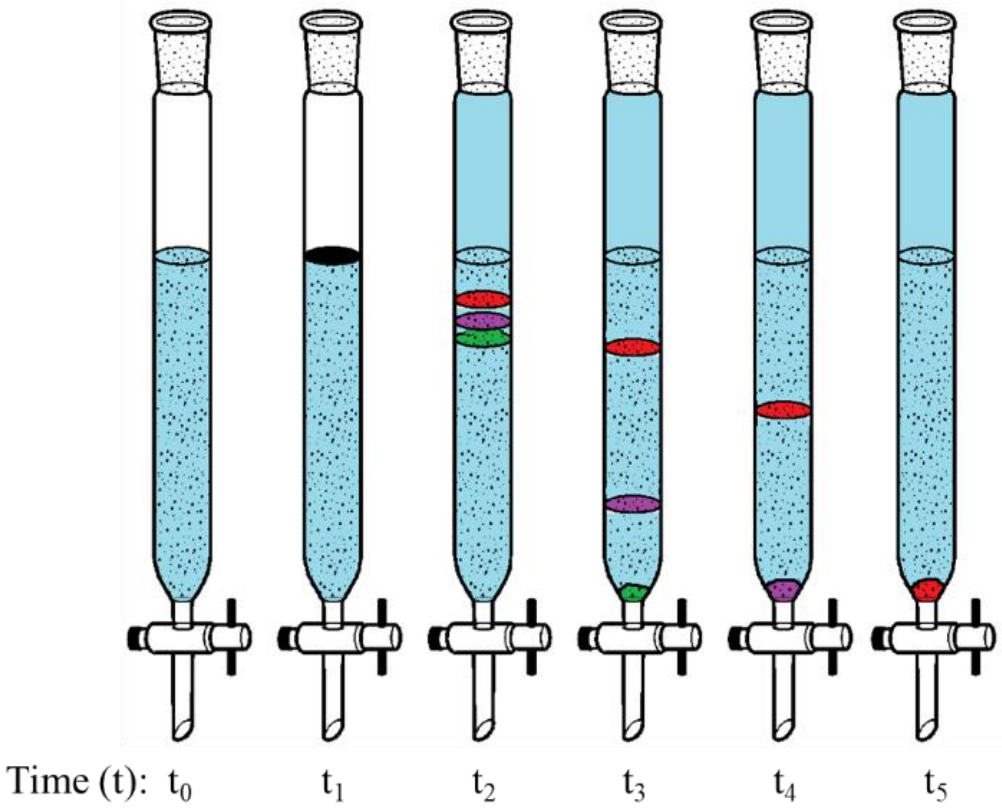

Figure 1-3. Separation by liquid chromatography. t_0 column with stationary phase and wet with mobile phase; t_1 mixture injected on the packed bed; t_2 migration of analytes with different elution rates; t_3, t_4 and t_5 elution of separated components in different times.

Table 1-2. Chromatography classification, adapted from Snyder *et al.* 2013.[36,37]

Class	Example
Adsorption chromatography	Liquid chromatography (Columnar method) Gas-solid chromatography
Partition chromatography	Liquid-liquid partition chromatography Paper chromatography Thin layer chromatography Reverse phase partition chromatography
Ion exchange chromatography	Cation exchange Anion exchange Inorganic exchange Liquid ion chromatography
Exclusion chromatography	Gel-permeation Ion exclusion Molecular sieve
Electrochromatography	Zone electrophoresis Boundary layer method Curtain chromatography Capillary electrophoresis

1.4.2.1 Partition and adsorption chromatography

In partition chromatography the separation process is produced by differences between the solubilities of the components in the mobile and stationary phases.[38] In this process a stagnant layer of solvent is located in the packed bed surface. Depending the chemical composition in the surface, the stagnant layer has different properties compared with the mobile phase. The separation is given by the partition coefficient for an analyte between the two liquid phases.[37,39,40] Usually partition chromatography is subdivided between normal phase and reverse phase, these are defined as a high polar stationary phase and low polar mobile phase, and a low polar stationary phase and high polar mobile phase respectively.

For liquid adsorption chromatography the separation is given by adsorption of an analyte in the stationary phase displacing a previously adsorbed molecule from the mobile

phase. Then desorption of the analyte happens when another molecule of the mobile phase or other analyte displace the already adsorbed analyte.[35,41] Differences in the adsorption isotherms for each analyte in a mixture define the elution rate for each component. Liquid chromatography (LC) has been used for separations in every imaginable field in science requiring a separation step.[42–52]

1.4.3 Scale of separation

Separation can be performed for analytical or processing purposes.[35] Analytical chromatography is usually developed in small densely packed columns with injections of diluted samples usually measured in microliters. high performance liquid chromatography (HPLC) was an improvement over regular liquid chromatography mainly because the use of high pressures to elute the analytes through densely packed columns, allowing reduction in particle sizes and enhancing the resolution of the elution between analytes. Recently ultra-high performance liquid chromatography (UPLC) devices were developed to withstand larger pressures than HPLC allowing better resolution in analytes with similar elution rates. Several detectors have been implemented in these systems including UV, light scattering, mass spectroscopy, IR, flame ionization among others. These detectors allowed elucidation and quantification of the analytes.[35,36]

Other analytical separation technique highly used only for elucidation of analytes is thin layer chromatography. In this, an adsorbent material is located as a layer over a supporting layer. The adsorbent is usually coated with an indicator that emits green at 254 nm under UV light. The mixture is spotted close to the bottom of the layer and the latter one is placed in a container with low amount of solvent that is going to migrate by capillary effect to the top of the layer. Along this migration, the analyte is separated in spots along the layer. These spots covered the indicator

looking as a black spot when evaluated under UV light. If the analyte does not have chromophores, staining solutions allow finding the location of the analyte in the layer.[35]

Large scale chromatography separation is usually done in simulated moving beds for continuous separation of binary mixtures.[53–55] For mixtures containing three or more analytes, a second separation cycle or larger number of columns in the simulated bed may be required. However, large batches of complex mixtures can be separated in large scale using a single packed column working in batches. This process is referred as preparative liquid chromatography.[36,55–57]

1.4.4 Modeling and separation efficiency

Modeling of separation in liquid chromatography columns requires acquisition or estimation of the following parameters: adsorption isotherms, mass transfer coefficient, flow rate, and column geometry[57,58]. Other parameters may be required depending the complexity required in the separation. Adsorption isotherms can be linear or the types I, II, or III as seen in **Figure 1-4**. Further details about modelling are provided in chapter 4 inside this document.

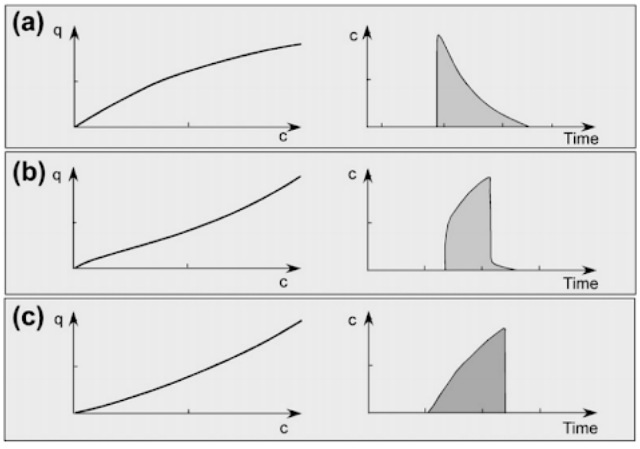

Figure 1-4. Peak shape associated to the adsorption isotherm a) type I, b) type II, and c) type III, adapted from Fornstedt *et al.*, 2013.[57]

Analysis of separation is usually performed calculating the column efficiency. This model assumes that a column with a length (L) is divided in a certain number of theoretical plates (N). Each theoretical plate has the exact same height (H). Value of H can be theoretically calculated by the Van-Deemter equation which is a contributive model based on column path, axial dispersion, and mass transfer terms. Experimentally, the elution profile in the chromatogram can be interpreted as a Gaussian-shaped peak. With the previous analogy, expressions based on the standard deviation and the variance of a normal distribution plot were proposed to calculate N (**Equation 1-1**). Similar analogy between two normal distribution was developed to calculate the resolution of the elution (R_s) (**Equation 1-2**) in which R_s=1.5 is the threshold value to fully separate two analytes. In the listed equations, t_r is the retention time for an analyte and W is the peak width at the baseline. This is measured between the tangent lines as seen in **Figure 1-5**.[36,37]

$$N = 16\left(\frac{t_r}{W}\right)^2 \qquad \textbf{Equation 1-1}$$

$$R_s = \frac{W_i + W_{i+1}}{t_{r\,(1+1)} - t_{r\,(i)}} \qquad \textbf{Equation 1-2}$$

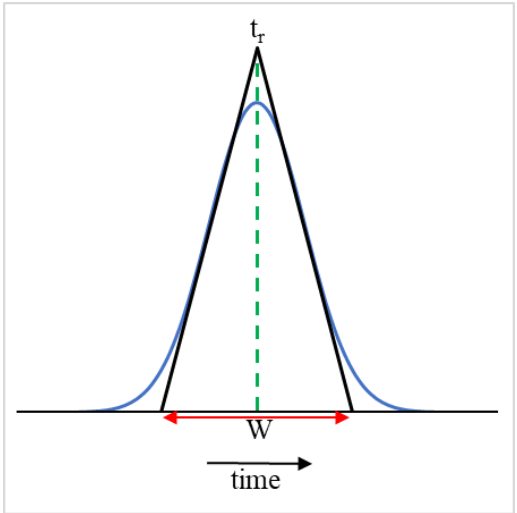

Figure 1-5. Retention time and peak width calculation in the baseline of a gaussian-like elution peak.

1.1 Motivation

DDSQ-2(R_1R_2) molecules, defined previously, have been used as model molecules and building blocks for synthesis of linear hybrid polymers.[17–19,21–25,28,59–62] Resultant materials have enhanced hydrophobicity, reduced dielectric constant, and usually increase in thermal properties without sacrifice in mechanical properties. DDSQ have been applied in minor proportion to other applications such as amphiphilic molecules,[63] support for heterogenous catalysts,[64,65] and nanostructure in composites.[66] But many others are not yet explored.

Most of the studies reported, use the product as synthesized knowing that this is a mixture of *cis* and *trans* isomers.[18,21–25,59,60] Production of these isomers is unavoidable. It has been reported that the use of one of the isomers in synthesis of polymers results in properties with different magnitudes respect to the polymer synthesized with the produced mixture or synthesized with the other isomer.[17] So far, the only method used for separation of these mixtures is fractional crystallization, this tool allowed separation of *cis* and *trans* mixtures with different solubility limits.[4,14,17] However, when the solubility limits are very close, separation is no longer achievable. Besides, to isolate nearly-pure isomers three or more fractional crystallization cycles are required.

1.2 Research goal

This dissertation has the objective of present liquid chromatography as an alternative technique for separation of mixtures containing different varieties of DDSQ-2(R_1R_2). This study was developed by shuffling functional groups in DDSQ-2(R_1R_2) and analyzing the effect of these changes in elution times. This approach allowed production of a variety of unique molecules with potential use for engineering applications not reported previously.

1.3 Research idea

Liquid chromatography is a liquid adsorption separation technique which takes advantage of differences in polarity or other interactions with a stationary phase to elute in different times the analytes in a mixture.[36,55] Knowing that the R_1 and R_2 groups depends of the bridging chlorosilane, polarity can be added to the molecule making feasible the separation of mixtures based on differences in adsorption energies. This idea was evaluated for separation of *cis* and *trans* DDSQ-2(R_1R_2) isomers containing polar groups, and by separating DDSQ-2(R_1R_2) mixtures with different number of a particular polar group.

Simulation of separation process was studied by development of adsorption isotherms based on frontal analysis by high performance liquid chromatography (HPLC). These results allowed scaling up the process to separate mixtures by preparative chromatography column. Thermal behavior of selected isomers of interest was analyzed after isolation by liquid chromatography or by fractional crystallization and quantification by HPLC.

This research highlights the use of liquid chromatography as a chemical engineering unitary operation to achieve high analyte purities.

1.4 Dissertation summary

in Chapter 2 is described the use of HPLC as a tool for separate and characterize ratios between *cis* and *trans* isomers of DDSQ functionalized with polar moieties. Along Chapter 3, HPLC was tested for characterization of DDSQ mixtures with different polarities, synthesis of the mixtures, separation and quantification by HPLC, and isolation of compounds including an asymmetric structure by preparative LC. Chapter 4 discussed the simulation for separation of DDSQ mixtures with different number of hydroxyl groups by ASPEN chromatography in order to scale-up to preparative LC. Finally, the analysis of melting behavior for *cis* and *trans* mixtures

was developed to highlight the benefits of separation achieving eutectic compositions. Findings of this study are described in Chapter 5.

CHAPTER 2.

HPLC CHARACTERIZATION OF *CIS* AND *TRANS* MIXTURES OF DOUBLE-DECKER SHAPED SILSESQUIOXANES

Keywords: Double-decker shaped silsesquioxane (DDSQ), Polarity, cis and trans isomers, separation, HPLC.

This chapter was submitted as a research paper to Silicon journal

2 HPLC characterization of *cis* and *trans* mixtures of double-decker shaped silsesquioxanes

2.1 Introduction

Functionalized double-decker shaped silsesquioxanes (DDSQ) have been used as the building block in polymerization to obtain inorganic-organic hybrid polymers with enhanced dielectric constant, glass transition temperatures, melting temperatures, among other properties of engineering interest.[1–73] DDSQ are usually synthesized from the condensation reaction between the commercially available DDSQ-$(Ph)_8(OH)_4$ **(1)** and $(R^1)(R^2)$-dichlorosilanes in the presence of triethylamine as seen in **Scheme 2-1**. If R^1 is different than R^2, the condensed DDSQ structures have unavoidable *cis* and *trans* isomerism[67, 71, 74–81]. These isomers represent as the product, *cis* and *trans*, show in **Scheme 2-1**.

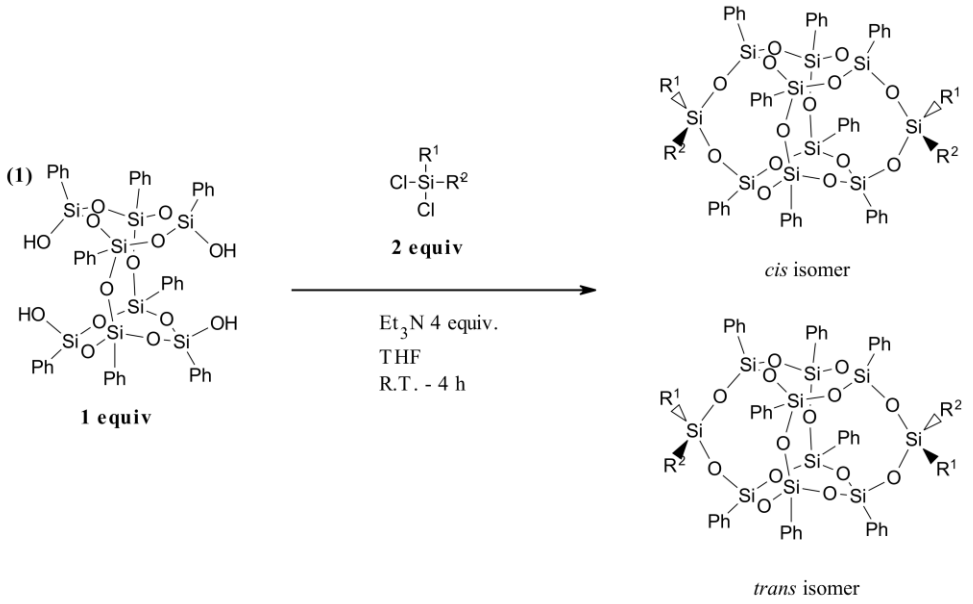

Scheme 2-1. Condensation reaction of DDSQ-$(Ph)_8(OH)_4$ **(1)** with 2 molar equivalent of $R^1R^2SiCl_2$. The resultant product contains *cis* and *trans* isomers DDSQ-2$((R^1)(R^2))$.

These isomers are different in their physical properties such as crystal structure, melting temperature, recrystallization behavior, solubility, etc.[71] It was also reported that a polymer

made from all *cis* isomers have a significantly different melting temperature as compared with the same polymer composed of all *trans* isomer[74]. Quantification of the *cis-trans* ratio in a mixture is often based on ^{29}Si-NMR. However, the ^{29}Si-NMR requires a large amount of functionalized DDSQ and requires a long scan time to reduce the signal-to-noise ratio needed for the analysis. To avoid these complications, 2D NMR was used to identify distinctive peaks in the ^{1}H-NMR between *cis* and *trans* isomers in DDSQ samples with aniline and methyl in the R^1 and R^2 positions.[75] The drawback of this procedure is the need to identify characteristic peaks for each moiety, which will be different depending on the R^1 and R^2 used.

Fractional crystallization is the most common method used to obtain nearly-pure *cis*, and nearly-pure *trans* DDSQ isomers.[71-72,74-75] The separation is based on the solubility differences of *cis* and *trans* isomers in a specific solvent.[76] After the fractional crystallization, a liquid chromatography rectification process is often needed to yield a higher isomeric purity.[71,73–77] Recently, DDSQ-$(Ph)_8(OH)_4$ was condensed with methyltrichlorosilane followed by a hydrolysis reaction producing a mixture of DDSQ cages including *cis* and *trans* isomers functionalized with hydroxyl groups. It was found that *cis* and *trans* isomers may be separated by a preparatory silica column and fractions quantified by HPLC.[74,78,81]

In this work, HPLC was reported as an alternative technique to quantify the *cis*-to-*trans* ratio of DDSQ isomers after the capping reaction and/or separations. The wide availability of HPLC as compared to NMR facility makes this quantification method more readily adoptable. Furthermore, the principle of HPLC separation is mainly based on polarity differences between components. Hence, different polar groups may be bonded to DDSQ which increases the number of molecules that can be quantified. In the following, several different mixtures of *cis* and *trans* compounds are presented and demonstrated a broad applicability of HPLC for the quantification analysis.

2.2 Experimental

2.2.1 Materials

All commercially available chemicals were used as received unless otherwise indicated. $(C_6H_5)_8Si_8O_{10}(OH)_4$ 5,11,14,17-Tetra(hydro)octaphenyltetracyclo[7.3.3.(^{3,7})] octasilsesquioxane DDSQ-$(Ph)_8(OH)_4$ was purchased from Hybrid Plastics (Hattiesburg, MS). 3-[Bis(trimethylsilyl)amino]phenylmagnesium chloride $[(CH_3)_3Si]_2NC_6H_4MgCl$ 1M in THF solution (*m*-PhA$(TMS)_2$-MgCl); Vinyltrichlorosilane $(C_2H_3)SiCl_3$; isopropyltrichlorosilane $(C_3H_7)SiCl_3$; isobutyltrichlorosilane $(C_4H_9)SiCl_3$; and 3-cyanopropylmethyldichlorosilane $(C_3H_6CN)(CH_3)SiCl_2$ were purchased from Gelest. Methyltrichlorosilane $(CH_3)SiCl_3$, phenyltrichlorosilane $(C_6H_5)SiCl_3$, deuterated chloroform with 1 vol % tetramethylsilane ($CDCl_3$-1%TMS) were purchased from Sigma-Aldrich. Triethylamine (Et_3N) was purchased from Avantor and distilled over calcium hydride before use. DDSQ bridged with (methyl)(*para*-aniline)dichlorosilane, (methyl)(*meta*-aniline)dichlorosilane, (isobutyl)(*meta*-aniline)dichlorosilane, and (cyclohexyl)(meta-aniline)dichlorosilane moiety were synthesized for our research group and reported in a previous study.[71] Tetrahydrofuran (THF) was refluxed over sodium/benzophenone and distilled. Reagent grade dichloromethane (DCM) and n-hexanes were degassed with helium for HPLC experiments. The previously listed solvents were purchased from Sigma. Si-gel P-60 was obtained from Silicycle. ^{1}H, ^{13}C, and ^{29}Si were recorded on 500 MHz NMR spectrometers.

2.2.2 Synthesis of (methyl)(meta-Bis(trimethylsilyl)amino]phenyl)dichlorosilane

A 250 mL round bottom flask containing a magnet stirrer under N_2 was sealed with a rubber septum and submerged in an acetone-dry ice bath. 50 mL of THF and 24.0 mmol (4.0 mL) of isobutyltrichlorosilane were injected respectively to the setup. 20 mmol (20.0 mL) of

m-PhA(TMS)$_2$-MgCl was added dropwise for 10 minutes. The ice bath was removed upon completion of the addition, and the solution was stirred overnight until it became a clear yellowish liquid. Volatiles were distilled under N_2 in an oil bath at 90 °C; a second distillation was done under vacuum to collect the expected product as a clear pale-yellow liquid. Spectral information are provided in the Appendix I.

2.2.3 General synthetic procedure

DDSQ-2(R^1R^2) was synthesized following a previously reported method.[75,80,81] In a 250 mL flask purged with dry N_2 for 15 minutes, DDSQ-$(Ph)_8(OH)_4$ **(1)** (2 g, 1.87 mmol, 1 equiv) was dissolved in THF (60 mL) at room temperature. $(R^1)(R^2)SiCl_2$ (3.74 mmol, 2 equiv) was added to the solution followed by Et_3N (1.04 mL, 7.48 mmol, 4 equiv) under vigorous stirring. The addition of triethylamine took about 5 minutes in total, a cloudy suspension was formed and continue stirred for 4 additional hours. The solution was then filtered through a fine fritted-funnel-filter to remove the solid triethylamine hydrochloride. The solution was dried in a rotary evaporator and then passed through a silica-gel column using DCM as a solvent. These cleaning step allowed hydrolysis of Si-Cl bond in cages synthesized with trichlorosilanes. The volatiles were removed from the resulting solution and further dried at 0.4 mbar and 50 °C for 12 hours to afford DDSQ-2(R^1R^2) as a white powder. The structures studied in this work are listed in **Figure 2-1**. NMR spectra for *cis* and *trans* isomer mixtures are provided in the Appendix I.

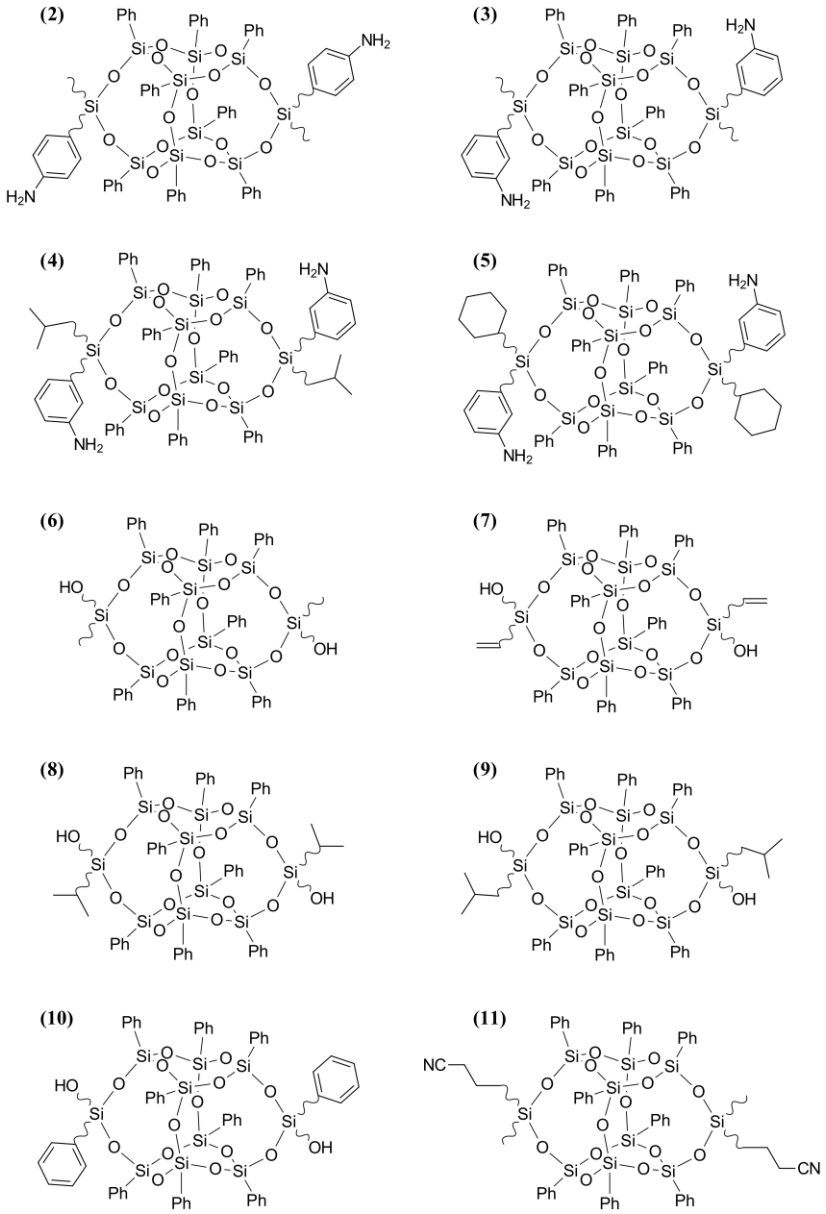

Figure 2-1. DDSQ-2(R^1R^2) isomers studied in this work. **(2)** DDSQ-2((para-aniline)(methyl)), **(3)** DDSQ-2((meta-aniline)(methyl)), **(4)** DDSQ-2((meta-aniline)(isobutyl)), **(5)** DDSQ-2((meta-aniline)(cyclohexyl)), **(6)** DDSQ-2((hydroxyl)(methyl)), **(7)** DDSQ-2((hydroxyl)(vinyl)), **(8)** DDSQ-2((hydroxyl)(isopropyl)), **(9)** DDSQ-2((hydroxyl)(isobutyl)), **(10)** DDSQ-2((hydroxyl)(phenyl)), **(11)** DDSQ-2((cyanopropyl)(methyl)).

2.2.4 Analytical methods

2.2.4.1 Preparatory separation of cis and trans isomers

Liquid chromatography was performed to separate *cis* and *trans* isomers in **2**, **3**, and **11**, and those hydrolyzed structures synthesized with trichlorosilanes in **6** to **10** with a procedure

previously described.[76,78,81] A glass preparatory chromatography column, 60 cm in length and 4 cm internal diameter, with 500 mL round top reservoir was packed with 60 grams of Si-gel resulting with packing height of about 40 cm. DCM was then flushed through the packed bed under pressure generated by a dry N_2 stream. Wetting of the packed bed was complete until no air bubbles, or dry space was observed. A concentrated solution of DDSQ isomeric mixture in DCM (5 mL, 0.2 g/mL) was gently injected from the top of the wet Si-gel bed and moved into the packed bed until no solution was observed above the packed bed. The column was then gently charged with an additional 500 mL of DCM and flushed using the N_2 stream with an average flow rate of 10 mL/min. Fractions of 5 mL were collected at the bottom of the column until the DCM reached the top of the bed. Each fraction was injected in 5 cm TLC plates of Si-gel supported in aluminum. TLC was evaluated with DCM and then analyzed under a 245 nm UV-lamp. Similar fractions were combined and dried for further experiments. The retardation factor (R_f) in **Equation 2-1** was used as a measure of the separation efficiency after the preparatory LC experiments.

$$R_f = \frac{Total\ TLC\ length}{Distance\ traveled\ by\ fraction\ n} \qquad \textbf{(Equation 2-1)}$$

2.2.4.2 UV-VIS spectroscopy

Wavelength sweep readings were developed for isolated isomers **2** to **5** with DCM as the solvent. Individual isomers were solubilized forming master batches of 0.2 mg/mL. Then, the solutions were diluted reaching lower concentrations in progressive steps until a value close to 0.02 mg/mL. All readings were contrasted against a DCM blank

2.2.4.3 Analysis and quantification of isomers by HPLC

All HPLC experiments were performed using an Agilent 1100 HPLC equipped with a UV detector. The columns selected for this work were Supelco LiChrospher® Si-60 for adsorption chromatography and ZORBAX® CN column for partition normal phase chromatography

(pHPLC). DCM was used as the mobile phase for the adsorption chromatography. Different ratios of DCM:hexanes ranging from pure dichloromethane to 70% hexane were used as mobile phase for pHPLC. Solvents were degassed using Helium for a minimum of 15 minutes prior to all HPLC experiments. A flow rate of 1 mL/min at a giving a constant pressure of 32 bars was used. The temperature was set in 25 ^{o}C, and the injection volume was 5 μL. The UV detector was emitting at 254 nm. Once the elution was finished, a blank sample containing mobile phase was injected and flushed trough the column for verification of the baseline and to confirm complete elution of the previous injection.

Standard plate theory of chromatography was used for quantitative analysis of separation.[82] Two different methods were used to evaluate the separation resolution based on peak width (W_n) and full width at half height of the peak ($W_{n@0.5}$) show in **Equation 2-2** and **Equation 2-3**, respectively. The retention time (t_r) is the elution time at the peak maximum. Values of t_r, W_n, and $W_{n@0.5}$ were calculated using the Agilent chemstation software. The theoretical plate number (N) or column efficiency based on Gaussian distribution was calculated using **Equation 2-4**.

$$R_S = \frac{(t_{r2} - t_{r1})}{0.5(W_1 + W_2)} \qquad \textbf{(Equation 2-2)}$$

$$R_{S\,0.5} = \frac{1.18(t_{r2} - t_{r1})}{0.5(W_{1@0.5} + W_{2@0.5})} \qquad \textbf{(Equation 2-3)}$$

$$N = 16\left(\frac{t_r}{W}\right)^2 \qquad \textbf{(Equation 2-4)}$$

2.3 Results and Discussion

2.3.1 Separation of cis and trans isomers

Two spots were observed by TLC for structures **2** to **5** and for **11**. These two spots indicate the presence of *cis* and *trans* isomers; their corresponding retardation factors are listed in **Table**

2-1. The *cis* and *trans* isomers were separated by a preparatory LC, and the isolated fraction was evaluated using ^{29}Si-NMR show in **Figure 2-2**. The spectra obtained for the second fraction was assigned to *trans* isomers; the spectra obtained for the second fraction was assigned to *cis* isomers. A previous report from our research group describes the peak assignments in detail.[76] Mass balance for the material injected in the column resulted in 75% recovery in two main fractions after elution. This result is comparable with a previous report for separation of DDSQ mixtures by LC.[81]

The difference in elution times between *cis* and *trans* isomers is related with the orientation of the polar moieties. For *cis* isomers, both polar groups are pointing at the same direction. This configuration slows the elution rate due to possible stronger adsorption. For *trans* isomers, polar groups are pointing at the opposite direction. Here, only one of the polar groups is attracted to the stationary phase surface increasing the elution rate. A similar relation between positions isomers was reported for small molecules.[83]

Table 2-1. TLC retardation factors, R_f, with dichloromethane as mobile phase for **2** DDSQ-2((*p*-aniline)(methyl)), **3** DDSQ-2((*m*-aniline)(methyl)), **4** DDSQ-2((*m*-aniline)(isobutyl)), **5** DDSQ-2((*m*-aniline)(cyclohexyl)), and **11** DDSQ-2((cyanopropyl)(methyl)).

Compounds	R_f *trans*	R_f *cis*
2	0.28	0.14
3	0.43	0.28
4	0.66	0.44
5	0.77	0.51
11	0.86	0.73

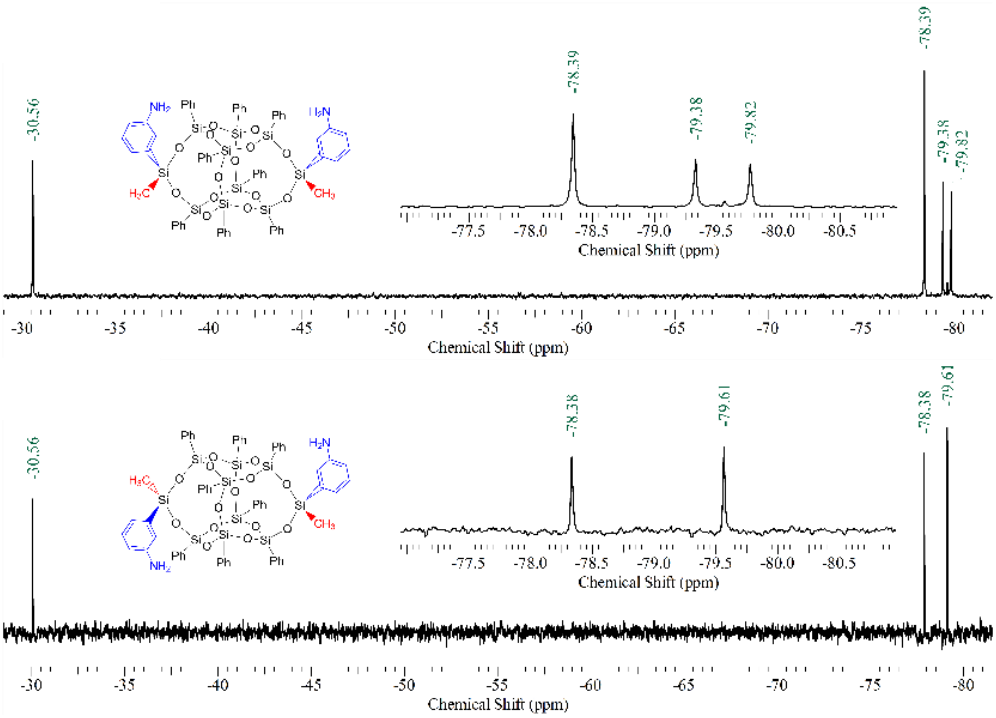

Figure 2-2. ^{29}Si NMR for *cis* and *trans* isomers after separation of **3**. (a) *trans* isomer, corresponding to the first spot in TLC; (b) *cis* isomer, corresponding to the second spot in TLC.

2.3.2 UV absorbance intensity of positional isomers of phenylamine

UV detectors are highly employed in organic chemistry due to its lower concentration limit compared with other class of detection devices. In this work, HPLC detection and quantification was developed by UV. However, other class of detectors with less definition such as refractive index (RI), or with higher resolution like mass spectroscopy can also be used to detect and quantify ratios between *cis* and *trans* DDSQ molecules. *Cis* and *trans* isomers for molecules **2** to **5** show a maximum absorbance at 254 nm which is associated with the chromophores in the phenyl rings.[84] However, at the same concentrations, absorbance values for *meta* molecules are lower when compare to the absorbance values for *para* isomers. It was determined that the slope of absorbance versus concentration for all *para* isomers is twice as that of *meta* isomers show in **Figure 2-3**. This result agrees with previous reports for isomers of positional phenylamine.[82] However, there are no differences in the slope of the absorbance

versus concentration curve between *cis* and *trans* isomer. This result implies for the case of separation by HPLC with a UV detector, the UV absorbance for *cis* and *trans* isomers can be directly correlated to their ratio without concentration correction. In addition, there is no effect on the absorbance values when different R groups were evaluated, as the main contribution to the UV intensity is the eight phenyl groups surrounding the DDSQ, and not the anilines attached to the Si-O core.

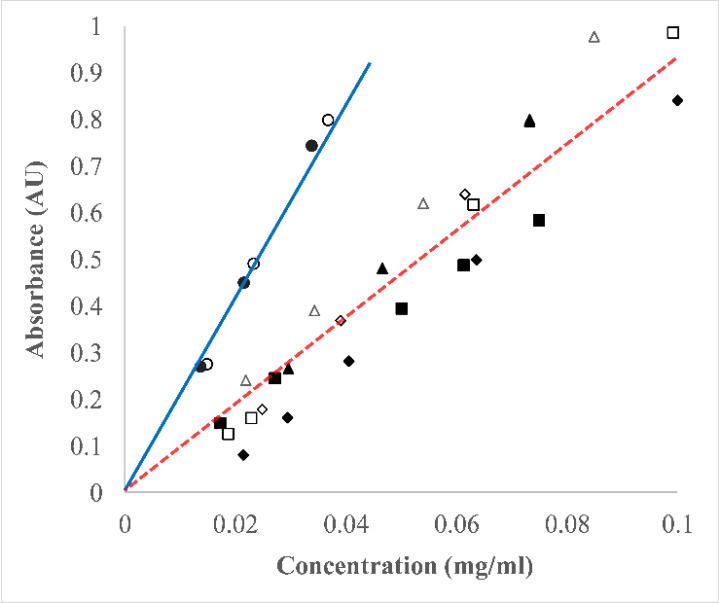

Figure 2-3. UV absorbance results at λ = 254 nm. Open symbols are for *trans* isomers, and filled symbols are for *cis* isomers. ● DDSQ-2((*p*-aniline)(methyl)) **2**; ▲ DDSQ-2((*m*-aniline)(methyl)) **3**; ▪ DDSQ-2((*m*-aniline)(isobutyl)) **4;** ◆ DDSQ-2((*m*-aniline)(cyclohexyl)) **5**. The red dashed line represents the linear trend of all the *para* samples, and the straight blue line is the linear trend for the *meta* samples. The slope of *para* was determined to be two times the slope for *meta.*

2.3.3 Analysis by HPLC of isomeric mixtures and individual isomers.

2.3.3.1 pHPLC of 2 and 3

HPLC evaluation by pHPLC in silica column bonded with cyano (CN) moieties show a single broad peak for the *cis-trans* mixture of **3** while two peaks were clearly observed for the *cis-trans* mixture of **2** using DCM as the mobile phase. By modifying the mobile phase with the addition of hexanes to DCM, the polarity of the mobile phase was reduced; this change increased the retention

time in each peak. The observed effect can be interpreted as a preference of the molecules to be adsorbed in the polar stagnant layer, causing a reduction in the mass transfer between the stagnant layer and the mobile phase. An additional effect of addition of hexanes is the enhancement of R_s as seen in **Figure 2-4**. The R_S value is based on peak analogy to normal distribution and it is an indicative of the separation efficiency. Less than 1% overlapping between two normal distributions has been defined as 6σ or $R_S = 1.5$. R_S calculated with Eq. 2 was improved from 0.77 when only DCM was flushed as the mobile phase to 1.93 when the mobile phase was modified to a 7:3 volumetric ratio of DCM:hexanes. For mobile phase containing less than 10% of hexane, evaluation of peak widths (W) was difficult due to a pronounced overlap. This resulted in a significant error on the calculated value of R_s. Alternatively, resultion of elution based on **Equation 3** may be used for these highly overlapped peaks. Results of the resolution were tabulated in **Table 2-2**.

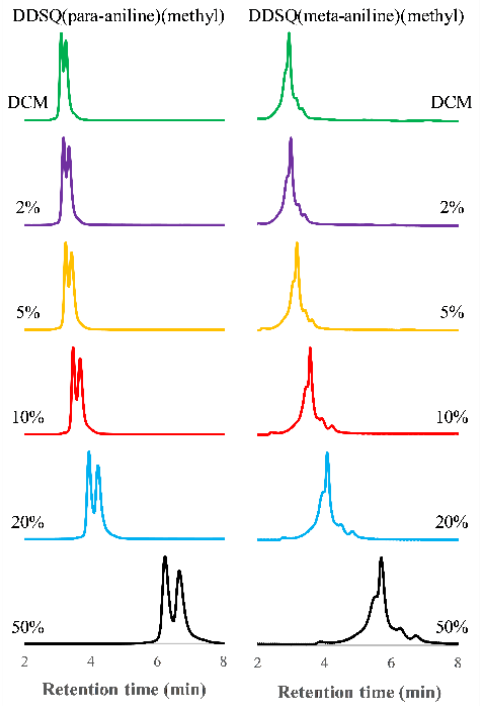

Figure 2-4. Effect of dichloromethane/hexane mobile phase ratios in normal phase pHPLC for *cis-trans* of **2** and **3**. The percentual value indicated represents the volume percentage of hexanes in the mobile phase.

Table 2-2. Comparison of the resolution obtained using equations 2 and 3 in *cis-trans* of **2**

Hexane % v/v in DCM:Hexane solution	0	2	5	10	20	30	50	70
$\mathbf{R_s}$	0.77	1.73	1.63	1.64	1.58	1.68	1.81	1.93
$\mathbf{R_{s0.5}}$	0.36	0.99	0.90	1.03	1.02	1.09	1.04	1.04

2.3.3.2 pHPLC accuracy verification

HPLC experiments were performed for quantification of ratios between *cis* **2** and *trans* **2** isomers mixed from isolated samples. Five mixtures with different *cis* and *trans* ratios described in **Table 2-3** were diluted in DCM. The solutions were injected to pHPLC and eluted with a mobile phase with 1:1 volumetric ratio of DCM:hexanes to achieve optimal R_s. The mixtures with known ratios of isomers were evaluated with the use of a UV detector attached to the HPLC. Eluted chromatograms observed in **Figure 2-5** match with the known ratio of isomers in the mixtures. This result indicates that quantification by HPCL-UV is possible and the standard deviations are lower than 5% as refer in **Table 2-3**.

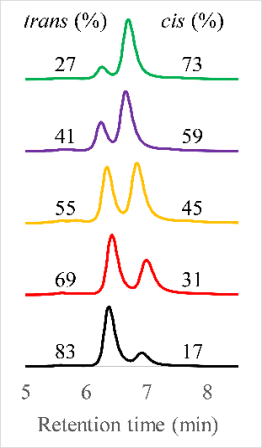

Figure 2-5. Quantitative analysis of *cis-trans* mixtures of DDSQ-2((*p*-aniline)(methyl)) by pHPLC. The individual isomers were first isolated and then mixed to a known ratio for comparison against the area under each peak. The weighted precent of isolated isomers in mixtures was indicated next to each curve.

Table 2-3. Comparison between *cis* and *trans* percentages of **2** calculated by weighting nearly-pure *cis* and nearly-pure *trans* and calculated from the area under the peaks in the chromatograms presented in **Figure 2-5**. The standard deviation was calculated based on the known percentage and the area percentage for each isomer.

% Weighted *cis*	% Weighted *trans*	% Area *cis*	% Area *trans*	Standard deviation *cis* (%)	Standard deviation *trans* (%)
27	73	25	75	1.5	1.5
41	59	44	56	2.3	2.3
55	45	58	41	2.1	2.1
69	31	74	26	3.3	3.4
83	17	86	14	1.9	1.9

2.3.4 Separation by adsorption chromatography

For adsorption chromatography, pure DCM was chosen to activate the Si-OH surface in the stationary phase of the column[83] Different than pHPLC, adsorption chromatography allowed the separation of *meta*-aniline isomers. Resolution of elution between *cis* **2** and *trans* **2** isomers and between *cis* **3** and *trans* **3** isomers are much higher in adsorption chromatography than pHPLC. Using DCM as the mobile phase, resolution of elution has a value of 6 or higher. In addition, as shown in **Table 2-4**, the retention time is high. To reduce t_r, 2% acetonitrile was added to the mobile phase. This change also decreases R_s to an optimal value of 1.5. Like pHPLC, it was observed that in adsorption chromatography *trans* isomers migrate faster than *cis* isomers as could be seen from the retention times presented in **Table 2-4**.

Table 2-4. Retention time (t_r), peak width (W), and plate number (N) after separation by adsorption HPLC with DCM as the mobile phase; Retention time (t_{rAcN}) after separation by adsorption HPLC with a mobile phase composed by DCM:acetonitrile in the volumetric ratio 98:2.

Compound	t_r (min)	W (min)	N	t_{rAcN} (min)
trans **2**	32.1	3.0	1831.8	7.6
cis **2**	60.5	5.0	2342.5	11.4
trans **3**	43.7	4.4	1578.2	8.5
cis **3**	66.4	5.6	2249.4	14.7
trans **4**	23.3	2.3	1642.0	-
cis **4**	47.5	4.7	1634.2	-
trans **5**	20.0	3.0	711.1	-
cis **5**	41.9	6.3	707.7	-

DDSQ with *meta*-aniline moieties has higher retention times compared with *para*-aniline. The reason for this retention time difference is not apparent. However, from crystallographic data, amine groups in DDSQ with *meta* aniline are pointing to the same direction, and it is possible the amine moiety is more exposed than in the *para* position[71, 85].

The number of theoretical plates (N) is a measure of the peak broadening in HPLC. in the column for *cis* **3** and *trans* **3** isomers, resulted in higher values compared with the N value for *cis* **4** and *trans* **4** and for *cis* **5** and *trans* **5** as seen in **Table 2-3**. It is remarkable that the non-polar group attached to the D-Si affects the column efficiency. From the data collected in **Table 2-3**, the column was more efficient resolving **2** and **3** containing methyl group as R^2; followed by **4** with isobutyl as R^2 moiety; and lastly, the lower efficiency was attributed to **5** which has the bulkier cyclohexane group in the R^2 position. Comparison of N between *cis* and *trans* in evaluated molecules does not show a recognizable trend. N for *cis* of **2** and **3** is larger than N for *trans* of **2** and **3**. In this case, N of *cis* was favored by t_r and not by W. However, when t_r was lower for **4** and

5, W had a bigger effect in the calculation of N ending with slightly better N values for *trans* compared against *cis*.

2.3.5 Effect of R^2 groups in retention times

It was observed that the size of organic groups attached to the DDSQ core influences the retention times. For R^1 is *meta*-aniline, the retention time increases as the size of R^2 decreases, $t_r(R^2=\text{methyl}) > t_r(R^2=\text{isobutyl}) > t_r(R^2=\text{cyclohexyl})$. When the polar group was changed from *meta*-aniline to hydroxyl, the retention time was also observed to be affected by the size of R^2 group. Similar to *meta*-anilines, the bulkier group was related to a lower retention time show in **Figure 2-6**. However, for R^2 was phenyl, the retention time was higher as compared to R^2 was isobutyl. This result suggests the isobutyl moiety has a higher steric effect than phenyl, which reduces the overall adsorption between the adsorption site and the hydroxyl group attached to the DDSQ core. Integration of DDSQ-2((OH)(R)) after synthesis by ^{29}Si-NMR results in a mixture with approximately 50% *cis* and 50% *trans* isomers. After separation by HPLC the calculation of the area of each peak in the chromatogram resulted in 50% ± 1.6% of the total area verifying the results obtained previously for DDSQ bonded to para-aniline. Integrations can be observed in the Appendix I.

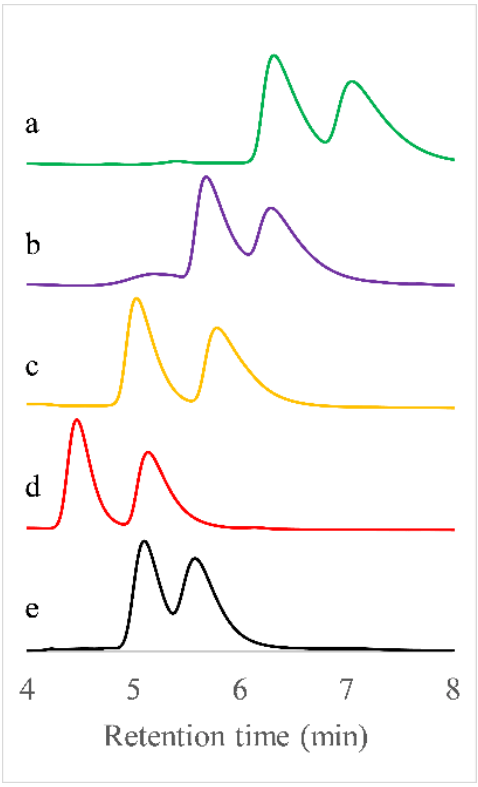

Figure 2-6. Retention times for *cis* and *trans* DDSQ-2((hydroxyl)(R^2)). (a) R^2: methyl **6**; (b) R^2: vinyl **7**; (c) R^2: isopropyl **8**; (d) R^2: isobutyl **9**; and (e) R^2: phenyl **10**.

2.3.6 Effect of polar groups (R^1) in t_r

DDSQ-$(Ph)_8(OH)_4$ was functionalized with different polar groups, *para*-aniline; hydroxyl; or cyanoproproyl, and their separation characteristics evaluated using adsorption chromatography. It was found that the retention time for *trans* **2** (*p*-aniline) was five times longer than the retention times for *trans* **6** (hydroxyl) and *trans* **11** (cyanopropyl). The retention time was ten times higher for *cis* moeity of *p*-aniline than hydroxyl (*cis* **6**) and cyanopropyl (*cis* **11**) as seen in **Table 2-5**.

Table 2-5. Retention time for DDSQ functionalized with methyl and different polar groups. R stands for *para*-aniline **2**, hydroxyl **6**, and cyanopropyl **11**.

DDSQ-2((R)(methyl))	t_r *trans* (min)	t_r *cis* (min)
R: *para*-aniline (**2**)	32.19	61.08
R: hydroxyl (**6**)	6.31	7.03
R: cyanopropyl (**11**)	5.31	6.23

The retention time differences between **6** and **2** could be related to the location of the polar groups. For DDSQ-2((*para*-aniline)(methyl))**,** the amine moiety is extended away from the core of the DDSQ by a phenyl ring to avoid the steric hindrance from the eight phenyl groups surrounding the core. The steric effect weakens the absorption to the stationary phase, which resulted in a significant decrease in retention time. Even it is generally recognized OH has stronger adsorption than NH_2.

For both **2** and **11**, the polar group is not directly attached to the core. However, a difference in the retention time was still observed. This result can be justified based on the hydrogen bonding. For **2**, the oxygen atom from the silanol at the stationary phase and the nitrogen atom from **2** can act as hydrogen acceptors; and both have hydrogen donors. For **11**, the cyano group can act only as the acceptor and forms a weaker hydrogen bonding with the stationary phase as compared with **2**.

2.4 Conclusions

This work confirmed that separation of DDSQ *cis/trans* isomer mixtures by liquid chromatography and quantification by HPLC is possible as the primary separation technique. Evaluation of isomers by NMR and HPLC showed that the isomer expected after separation was present in percentages better than 90% purity. It was observed that the position of the amine group in the aniline affected the UV absorbance values at the same concentration. However, no concentration effect was found in absorbances between *cis* and *trans* isomers. This enables one to determine the *cis/trans* ratio in a mixture directly from the UV detector signal of an HPLC experiment.

Separation by normal phase partition chromatography was distinguished as a technique for identification and quantification of *cis* and *trans* DDSQ-2((*p*-aniline)(methyl)). This

chromatography mode does not permit separation of the *meta* isomers. Adsorption chromatography using silica as stationary phase was a better separation technique allowing optimal resolution of the elution for every case studied in this work.

The moiety next to the polar group has a steric effect that affects the adsorption. Bulkier groups reduced the adsorption energy and in consequence the retention time. However, the elution order is not changed by the adjacent groups it means that for DDSQ functionalized cages, the *trans* isomers will always elute first. Polarity in the DDSQ is a crucial factor for allowance the separation process. In addition, the strength of hydrogen bonding affected by the sterics of the surrounding groups significantly influnced the elution time.

CHAPTER 3.

SEPARATION OF ASYMMETRICALLY CAPPED DOUBLE-DECKER SILSESQUIOXANES MIXTURES

Key Words: Double-decker shaped silsesquioxane (DDSQ), Asymmetric, Separation, HPLC

This chapter was published as a research paper in Polyhedron journal under the following citation: Vogelsang, D. F.; Dannatt, J. E.; Maleczka, R. E.; Lee, A. Separation of Asymmetrically Capped Double-Decker Silsesquioxanes Mixtures. Polyhedron 2018, 155, 189–193.

3 Separation of asymmetrically capped double-decker silsesquioxanes mixtures

3.1 Introduction

Functionalized double-decker silsesquioxanes, DDSQs, are building blocks for diverse applications such as polymer chain modifiers.[86–90] Polymer chains modified with DDSQ can obtain low dielectric constant, enhanced hydrophobicity, and elevated degradation temperature.[88,89,91,92] These materials are derived from the tetrasilanol double-decker silsesquioxane or DDSQ-$(Ph)_8(OH)_4$ (**1**). This compound is composed of two cyclic *syn-cis*-1,3,5,7-tetraoltetraphenyltetrasilsesquioxane bridged by two oxygens and can be functionalized by a side-capping reaction with dichlorosilanes, **Scheme 3-1**, to produce DDSQs that are the building blocks in many polymer applications.[89,92–94]

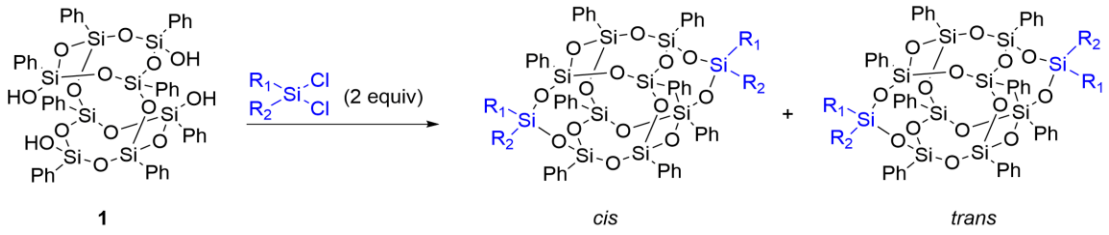

Scheme 3-1. Side capping of DDSQ-$(Ph)_8(OH)_4$ (**1**) with a dichlorosilane.

Side-capping with a dichlorosilane that has two distinct R-groups results in symmetric *cis* and *trans* isomers.[93,94] The products are symmetric because both sides are capped with the same capping agent. Separation of these *cis* and *trans* isomers using fractional crystallization (FC) has been reported.[90,93,94] FC is a technique that allows separation based on solubility differences between two or more analytes in a solution.[95] For example, *cis* and *trans*-DDSQ side-capped with 4-(dichloro(methyl)silyl)aniline were separated with high purity when the initial ratio between *cis* and *trans* isomers was different than 50 % to 50 % *cis*:*trans* using THF as the good solvent and hexane as the poor solvent.[8] DDSQ side-capped with isobutyl trichlorosilane was first separated

using FC, and then subsequently polymerized using mostly a single isomer type was studied.[90] Also, separation of mostly *trans* isomer from the mixture obtained after side-capping of DDSQ-$(Ph)_8(OH)_4$ with methyldichlorosilane was done using FC.[94] However, Schoen *et al.* and Hoque *et al.* reported that further purification via liquid chromatography (LC) was needed, which for polar DDSQ isomers is a separation technique with superior resolution in comparison to FC.[90,93]

LC is a technique that allows isolation of individual molecular compounds even with a partial overlap in retention times.[96–98] For many applications, this technique is faster than FC;[99] furthermore, industrially LC is less expensive despite the differences in initial cost. LC is based mainly on interactions between analytes, stationary phase, and mobile phase.[96,100] Among the many LC operation modes, normal phase (NP) and reverse phase (RP) have been widely used.[101–104] Separation for both NP and RP depend on polarity differences between the analytes. However, in NP analytes interact with a polar stationary phase and a low polar mobile phase.[96] Despite the advantages of LC, there are no reports for the separation of DDSQ compounds using LC except for further purification after FC.

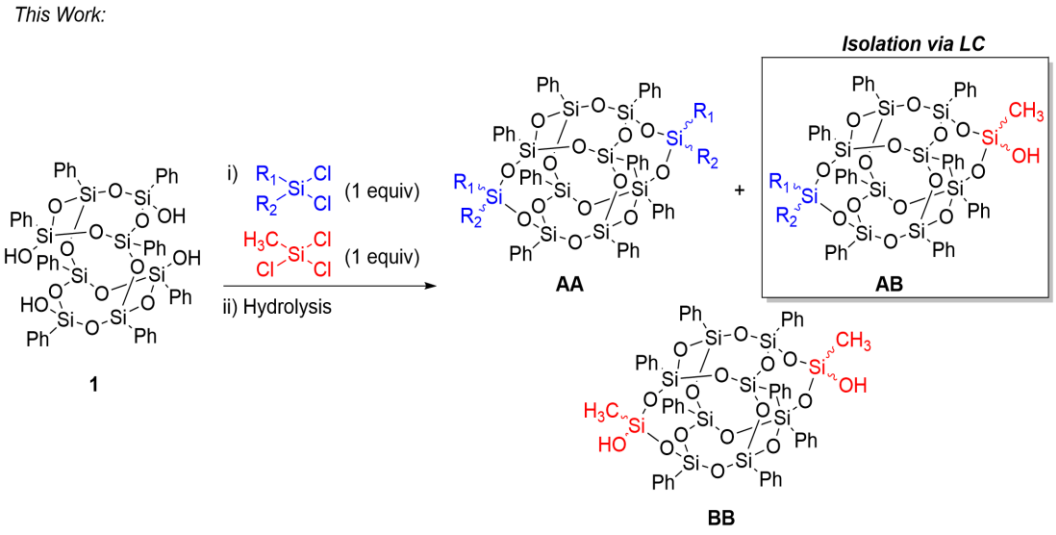

Scheme 3-2. Side capping of DDSQ-$(Ph)_8(OH)_4$ (**1**) with two chlorosilanes.

The use of LC to isolate a DDSQ compound with asymmetric functionalities, ie the **AB** compound in **Scheme 3-2**, is proposed as an engineering solution to expand the field of application for functionalized DDSQs. In this work DDSQ-$(Ph)_8(OH)_4$ was side-capped with two different chlorosilanes which would produce a mixture 3 products, **AA**, **AB**, and **BB**. These DDSQ products have zero, one, and two hydroxyl groups after hydrolysis, and are separable by NP due to their polarity differences. Synthetic procedures, separation technique, and identification of the new **AB** compounds will be described in the following sections.

3.2 Experimental

3.2.1 General information

All commercially available chemicals were used as received unless otherwise indicated. $(C_6H_5)_8Si_8O_{10}(OH)_4$ 5,11,14,17-Tetra(hydro)octaphenyltetracyclo[7.3.3.-$3^{3,7}$]octasilsesquioxane or DDSQ-$(Ph)_8(OH)_4$ was purchased from Hybrid Plastics. Dimethyldichlorosilane $(CH_3)_2SiCl_2$, vinylmethyldichlorosilane $(CH_3)(C_2H_3)SiCl_2$, methyldichlorosilane $(CH_3)HSiCl_2$, and 3-chloropropylmethyldichlorosilane $(CH_3)(C_3H_6Cl)SiCl_2$ were purchased from Gelest. Methyltrichlorosilane $(CH_3)SiCl_3$ was purchased from Sigma-Aldrich. Triethylamine (Et_3N) was purchased from Avantor and distilled over calcium hydride before use. Deuterated chloroform with 1vol.% of tetramethylsilane $CDCl_3$-TMS and deuterated acetone acetone-D_6 were purchased from Cambridge isotopes laboratories. Tetrahydrofuran (THF) was refluxed over sodium/benzophenone ketyl and distilled. Reagent grade dichloromethane (DCM) and n-hexanes were degassed with helium for HPLC experiments. The previously listed solvents were purchased from Avantor. Si-gel P-60 was obtained from Silicycle. ^{1}H, ^{13}C, and ^{29}Si were recorded on 500 MHz NMR spectrometers.

3.2.2 General procedures

3.2.2.1 General procedure A: synthesis of symmetric DDSQ

DDSQ-2((CH$_3$)(R)) was synthesized following the reaction 1-1 shown in **Scheme 3-1**. In a 250 mL flask purged with dry N_2 for 15 minutes, DDSQ-(Ph)$_8$(OH)$_4$ (**1**) (2 g, 1.87 mmol, 1 equiv) was dissolved in THF (60 mL) at room temperature. Dichlorosilane or trichlorosilane (3.74 mmol, 2 equiv.) was added to the DDSQ-(Ph)$_8$(OH)$_4$ solution. Et_3N (1.04 mL, 7.48 mmol, 4 equiv.) was added dropwise to the stirring solution. The addition of triethylamine took 5 minutes in total; a cloudy white suspension was formed and stirred for 4 hours. The solution was then filtered through a fine fritted-funnel-filter to remove the solid triethylamine hydrochloride. The solution was dried in a rotary evaporator and then passed through a silica-gel column using DCM as the solvent. The volatiles was removed from the resulting solution and further dried at 0.4 mbar and 50 °C for 12 hours to afford DDSQ-2((CH$_3$)(R)) as a white powder. It should be noted the reported spectra are of the *cis*/*trans* mixtures. Full experimental details and product characterization are in the Appendix A and I respectivelly.

3.2.2.2 General procedure B: synthesis of DDSQ symmetric and asymmetric mixtures

The synthesis of DDSQ mixture was done following the **Scheme 3-2**. In a 250 mL flask purged with dry N_2 for 15 minutes, DDSQ-(Ph)$_8$(OH)$_4$ (**1**) (2g, 1.87 mmol) was dissolved in THF (60 mL) at room temperature. (CH$_3$)(R)$SiCl_2$ (1.87 mmol, 1 equiv.) and (CH$_3$)$SiCl_3$ (1.87 mmol, 0.24 mL, 1 equiv.) were added to the DDSQ-(Ph)$_8$(OH)$_4$ solution and stirred for 5 minutes.Et_3N (1.04 mL, 7.48 mmol, 4 equiv.) was added dropwise to the stirring solution. The addition of triethylamine took 5 minutes in total which created a cloudy white suspension which was stirred continuously for additional four hours. After,

the solution was filtered through a fine fritted-funnel-filter to remove the solid triethylamine hydrochloride. Volatiles was removed from the resulting solution which produced a white powder. This powder was a mixture of three products as shown in **Scheme 3-2**. The powder was dissolved in a minimum amount of DCM and passed through a silica-gel column using DCM as the solvent. The silica column hydrolyzed the chlorosilanes into silanols which were isolated. The three separated products were dried at 0.4 mbar and 50 °C for 12 hours. Full experimental details and product characterization are in the Appendix A and I respectivelly.

3.2.3 Separation of DDSQ mixtures by LC

A glass preparatory chromatography column with 500 mL round top reservoir (L = 60 cm, D = 4 cm) was packed with Si-gel (60 g, H = 40cm). DCM was flushed through the packed bed under pressure generated by a dry N_2 stream. The packed bed wetting was stopped until no air bubbles, and dry spaces were observed. A concentrated solution of DDSQ mixture in DCM (5 mL, 0.2 g/mL) was gently injected from the top of the wetted Si-gel bed and moved into the packed bed until no solution was above the packed bed. The column was then gently charged with 500 mL of DCM and then flushed using the N_2 stream with an average flow rate of 10 mL/min. Fractions of 5 mL were collected in the bottom of the column until the DCM reached the top of the bed. Each fraction was injected in 5 cm TLC plates of Si-gel supported in Aluminum. TLC was evaluated with DCM and then analyzed under a 245 nm UV-lamp. The graphic description of the TLC separation is shown in the Appendix C.

3.2.4 Characterization of DDSQ materials.

Identification of components and their ratios in the mixture, as well as the fractions separated by LC, were done using an Agilent 1110 HPLC system. The samples were first dissolved in DCM and 5 mL injected into a Supelcosil column (L = 250 mm, ID = 4 mm) and separated at 1

mL/min with DCM as the mobile phase. The components were detected in a UV detector at 245 nm. Mixtures and separated samples were evaluated by NMR taking advantage of the three nuclei of the molecules: ^{1}H, ^{13}C, and ^{29}Si. Dry samples (0.2 g) were dissolved in 0.6 mL of $CDCl_3$-1%TMS and placed in a Variant UNITY Innova 600 at 589 MHz for ^{1}H, and 119.16 MHz for ^{29}Si. Fractions were also characterized by mass spectroscopy in a Waters Xevo G2-XS. The ionization was performed by atmospheric pressure chemical ionization (APCI) using acetonitrile as solvent.

3.3 Results and Discussion

3.3.1 Separation by LC

To obtain asymmetric DDSQ, a dichlorosilane ($R(CH_3)SiCl_2$, **A**) and methyltrichlorosilane (CH_3SiCl_3, **B**) were added to DDSQ-$(Ph)_8(OH)_4$ (**1**) as is shown in **Scheme 3-3**. In addition to the desired **AB** product, two symmetric byproducts are obtained (**AA** and **BB**). This is because the two reactive sides of DDSQ-$(Ph)_8(OH)_4$ are 7 Å apart; thus after capping one side, there is no additional selectivity toward either capping agent **A** or **B**. Assuming the capping rate is independent of chlorosilane used, the probability to bond any chlorosilane to one of the sides is ½ and the probability of the same type of chlorosilane capping the second side is ½. This indicates that probability to synthesize **AA** or **BB** is 25% for each, and the probability to synthesize AB is ½ or 50% when equimolar amounts of **A** and **B** react with DDSQ-$(Ph)_8(OH)_4$ which provides an expected isomer ratio of 25:50:25 **AA**:**AB**:**BB**. However, by using methyltrichlorosilane as the **B** capping agent, the mixture of products will have zero, one and two chloro moieties. During the workup, hydrolysis of the resulting chlorine atom occurs readily leaving zero, one, and two silanols; thus, the final products contain a varying number of silanol groups and separation can be

achieved based on polarity. With silica-gel used as the stationary phase, compound **BB,** with two silanol groups, migrates slower than compounds **AB1-4** which in turn migrate slower than compounds **AA1-4**. This technique allows separation of the product mixtures as long as R on the **A** capping agent is non-polar. This is demonstrated by the retardation factor (R_f) on TLC. A R_f of 0.74 for **BB**, 0.83 for **AB1-4** and 0.93 for **AA1-4** was calculated. These R_f values were independent of the R moiety used in the synthesis.

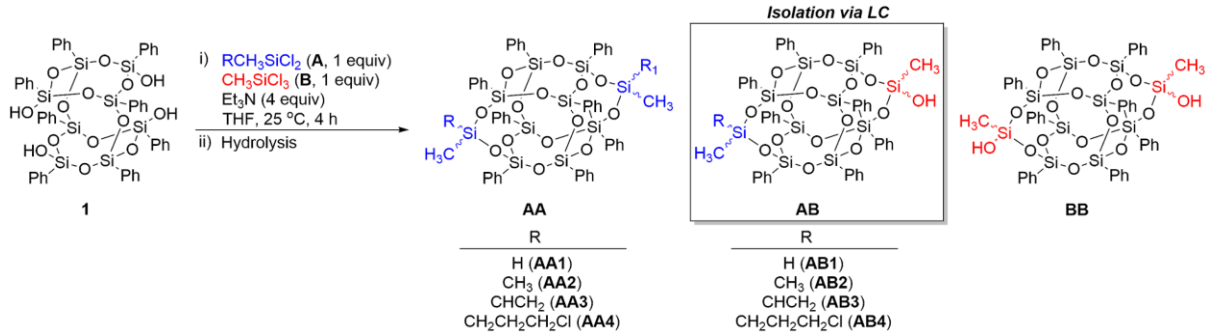

Scheme 3-3. Proposed synthesis to obtain a mixture of AA, AB, and BB.

3.3.2 HPLC Identification

Chromatograms for independently synthesized **AA1-4** exhibit a single peak at t_r = 2.6 min as shown in **Figure 3-1(a-d)**. This finding agrees with TLC results, where R does not have an apparent effect on retention times. Two peaks (t_r = 18 min, t_r = 23 min) were observed for **BB** as shown in **Figure 3-1e**. These peaks correspond to the *trans/cis* configurations. This behavior was reported previously in the separation of DDSQ cages side-capped with phenylamines.[93] Chromatograms for reactions following **Scheme 3-3** have four peaks (t_r = 2.6 min, t_r = 6.5 min, t_r = 18 min, t_r = 23 min) as seen in **Figure 3-1f-i**. Products **AA1-4** and **BB** are present in the reaction mixtures as confirmed by the retention times for independently synthesized compounds (see SI for experimental details). Excitingly, the peak at 6.5 min indicates the presence of asymmetric DDSQs **AB1-4**. To date, no literature in the separation of systems with similar DDSQs has been reported. Nevertheless, previous work in the separation of relatively large or bulky molecules by HPLC

using a Si-gel stationary phase were developed for polyols and polymers with a varying number of hydroxyl groups.[105,106]

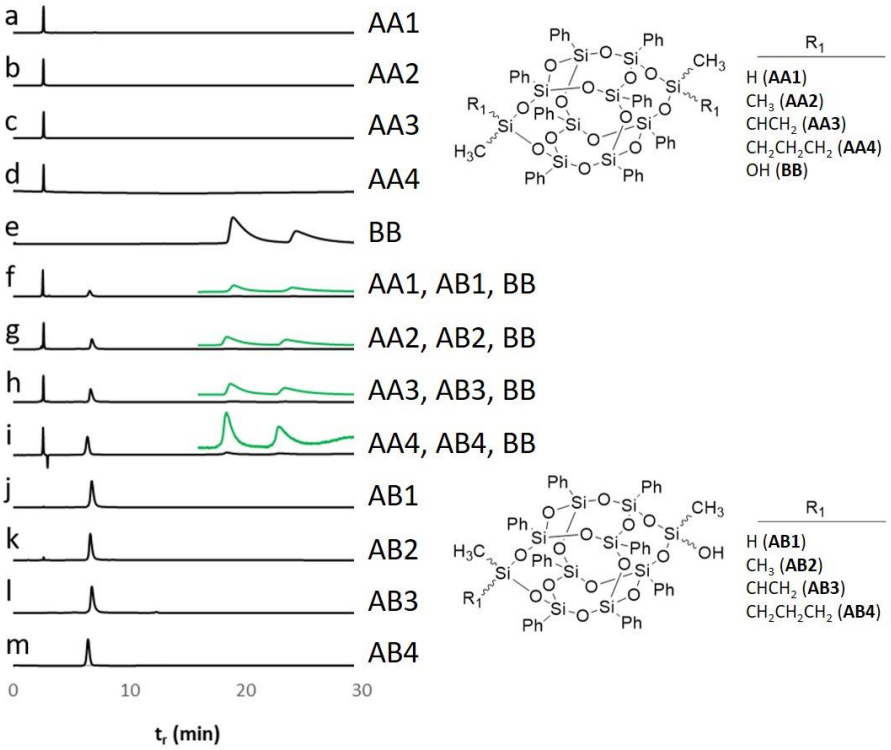

Figure 3-1. Chromatograms for products of pure $(C_6H_5)_8Si_{10}O_{14}(CH_3)_2(R)_2$ obtained following **Scheme 3-1(a-e)**. Chromatograms for mixtures of $(C_6H_5)_8Si_{10}O_{14}(CH_3)_2(R)_2$, $(C_6H_5)_8Si_{10}O_{14}(CH_3)_2(R)(OH)$, and $(C_6H_5)_8Si_{10}O_{14}(CH_3)_2(OH)_2$ following synthesis proposed in **Scheme 3-2**. The absorbance in the region between 15 and 30 minutes is zoomed for reader convenience **(f-i)**. The second fraction separated by LC corresponding to $(C_6H_5)_8Si_{10}O_{14}(CH_3)_2(R)(OH)$ **(j-m)**.

The peaks observed in HPLC chromatograms were sufficiently resolved, so the relative ratio of the three compounds was evaluated. Since each compound has the same number of chromophores, UV was used for quantification. The results are shown in **Table 3-1**. As discussed above, we expected a statistical ratio of 25:50:25 for **AA**:**AB**:**BB**; however, significant variations were observed in the HPLC ratios. These variations were usually favoring capping of the chlorosilane with lower steric hindrance. The smallest chlorosilane in this work was methyldichlorosilane, when this competed with

methyltrichlorosilane the highest yield of **AA** was produced. On the other hand, the bulkiest chlorosilane explored in this work was chloropropyl-methyldichlorosilane, when this competed against methyltrichlorosilane the lowest yield of **AA** was obtained. Overall, the results in **Table 3-1** show that as the sterics of the **A** dichlorosilane increase the amount of **AA** product decreases. This indicates that the rate of side-capping is significantly affected by the sterics of the capping agent.

Table 3-1. The calculated ratio of products in DDSQ mixtures after separation by HPLC.

R	AA (%)	AB (%)	BB (%)
H	42.0	38.8	19.2
CH_3	32.3	48.1	19.6
$CHCH_2$	27.6	50.9	21.5
$CH_2CH_2CH_2Cl$	15.3	39.7	45.0

To verify this, two capping agents, $(CH_3)_2SiCl_2$ and $(Ph)_2SiCl_2$, with distinct steric profiles were selected and reacted with DDSQ-$(Ph)_8(OH)_4$, **Scheme 3-4**. These reactions were followed by ^{1}H-NMR and ^{29}Si-NMR. It was found that DDSQ-$(Ph)_8(OH)_4$ was completely converted to DDSQ-2$(CH_3)_2$ before 59 seconds when the first ^{1}H NMR was collected. However, full capping of DDSQ-$(Ph)_8(OH)_4$ with diphenyldichlorosilane took between 36 minutes and 100 minutes to complete; thus, conclusively demonstrating that the sterics of the chlorosilanes significantly affect the rate of the capping reaction.

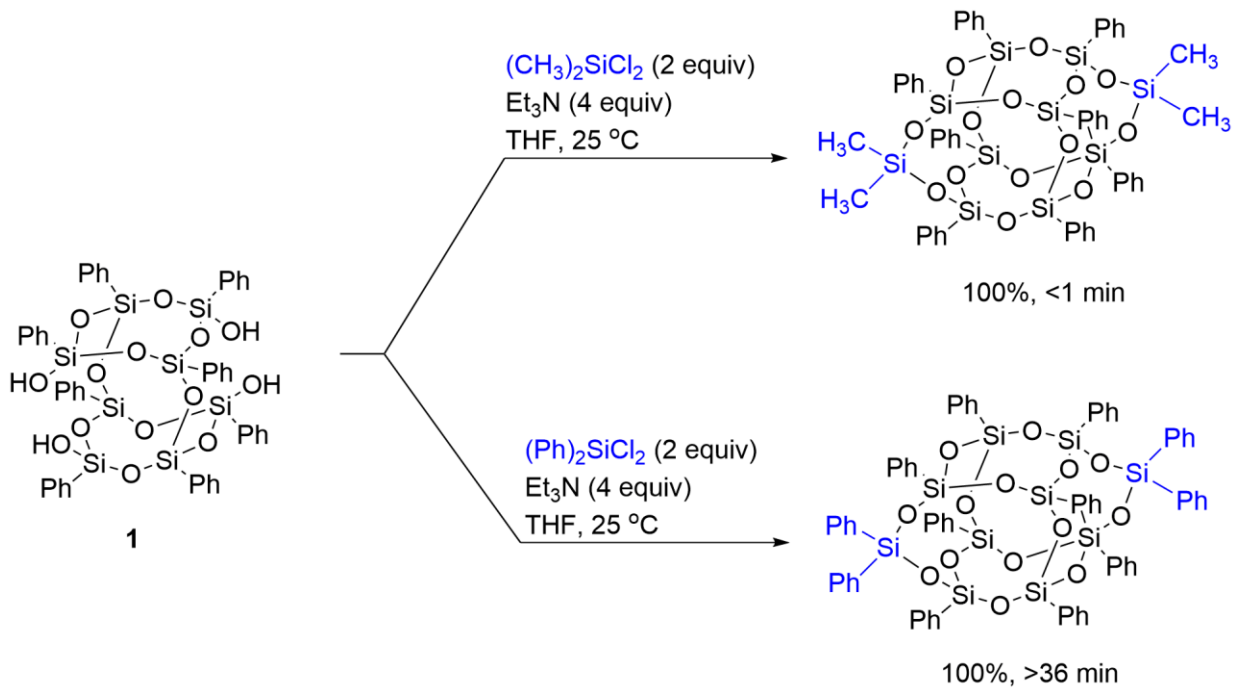

Scheme 3-4. Side-capping of DDSQ-$(Ph)_8(OH)_4$ with chlorosilanes having moieties with different sterics, 100% conversion time for capping with $(CH_3)_2SiCl_2$ less than 1 minute, 100% conversion time for capping with $(C_6H_5)SiCl_2$ higher than 36 minutes.

An unfortunate byproduct of the non-statistical ratios is that in cases where there is a significant difference in sterics between the **A** and **B** capping agent, the ratio of desired **AB** product suffered. For example, in the first and last entry of **Table 3-1**, ~10% loss of **AB** product was observed. To see if this shortcoming could be overcome, we varied the ratios of $H(CH_3)SiCl_2$:$(CH_3)SiCl_3$ from 1.5:0.5 to 0.5:1.5. The HPLC ratios and the mass percentages after separation by liquid chromatography are summarized in **Table 3-2**. In every case, HPLC ratios match closely with the isolated masses from LC. The data in **Table 3-2** indicates a preference towards the formation of DDSQ capped in both sides with methyldichlorosilane just as in **Table 3-1**. However, this is mitigated when an excess of methyltrichlorosilane is used. Excitingly, close to the expected probability of 25:50:25 is obtained when a ratio of 0.8:1.2 was used.

Table 3-2. Mass fraction analysis of products (in precent) after DDSQ mixtures synthesis with different ratios of methyldichlorosilane and methyltrichlorosilane. *HPLC column is calculated based on HPLC peak analysis and Mass column is calculated based on analytic balance measurement after separation by preparatory liquid chromatography Mass.

$H(CH_3)SiCl_2$: $(CH_3)SiCl_3$	**AA1** (%)		**AB1** (%)		**BB** (%)	
	*HPLC	*Mass	*HPLC	*Mass	*HPLC	*Mass
1.5 : 0.5	64.1	65.1	26.7	27.9	9.2	7.0
1.2 : 0.8	49.5	42.3	37.1	45.4	13.4	12.3
1 : 1	42.0	45.2	38.8	32.5	19.2	22.2
0.8 : 1.2	36.6	24.3	44.9	50.7	18.5	25
0.5 : 1.5	6.4	6.0	28.9	30.0	64.7	64.0

3.4 Conclusions

When two different chlorosilanes compete for capping sites on DDSQ-$(Ph)_8(OH)_4$, mixtures of **AA**, **AB**, and **BB** are produced. The separation of these products was possible because a varied number of hydroxyl groups are present in each molecule. HPLC, a valid method to quantify the ratios of products, showed deviations from the expected statistical ratio of 25:50:25 **AA**:**AB**:**BB**. These deviations are due to the rate of side-capping being significantly affected by the sterics of the capping agent. In some cases, this deviation adversely affected the amount of desired **AB** product produced. This was overcome by changing the ratios of the capping agents such that the more sterically hindered capping agent was in excess. Overall, our technique provides a route to **AB** DDSQ systems with an average yield of 30%. This can be further optimized by modifying the ratio between chlorosilanes or modifying the reaction conditions. Isolation of **AB** DDSQ is a step forward to reach block copolymers linked by a single asymmetric DDSQ. Present research efforts are focused on finding a direct synthesis of difunctional DDSQ and exploring the properties of DDSQ based block copolymers.

CHAPTER 4.

PREDICTIVE LIQUID CHROMATOGRAPHY SEPARATION FOR MIXTURES OF FUNCTIONALIZED DOUBLE DECKER SILSESQUIOXANES BASED ON HPLC CHROMATOGRAMS

Keywords: Asymmetric double-decker silsesquioxane, Adsorption isotherms, HPLC, Preparatory liquid chromatography, Chromatogram simulation.

4 Predictive liquid chromatography separation for mixtures of functionalized double decker silsesquioxanes based on HPLC chromatograms

4.1 Introduction

Functionalized DDSQ structures can be obtained by reacting tetrasilanol octaphenyl double-decker shaped silsesquioxane (DDSQ-$(Ph)_8(OH)_4$) **1** with functional chlorosilanes.[107–120] When two equivalent of difunctional dichlorosilanes ($R_1R_2SiCl_2$) are used, generally a closed structure (DDSQ-2(R_1R_2)) is obtained.[109,111,120–122] DDSQ-2(R_1R_2) has been explored for different applications such as amphiphilic molecules in Langmuir-Blodgett films,[123] ionic liquids,[111] or support for heterogeneous catalyst.[124,125] In addition, there are numerous studies using DDSQ-2(R_1R_2) in hybrid inorganic-organic polymers as the resultant hybrid polymers will contain the nanostructure as a part of the chain backbone.[111,116,118,119,126–129] These hybrid polymers have shown enhanced hydrophobic properties,[116,118,127] low dielectric constants,[118,128,130] and improved thermo-oxidative stability without sacrifice of their mechanical performance.[117–119,126]

From chapter 3, a mixture of DDSQ structures functionalized with zero, one, and two hydroxyl groups was produced.[131] These mixtures were made by side-capping DDSQ-$(Ph)_8(OH)_4$ with 1 mol equivalent of $(CH_3)(R)SiCl_2$ and 1 mol equivalent of methyl-trichlorosilane $(CH_3)SiCl_3$ followed by hydrolysis as depicted in **Scheme 4-1**.[131]

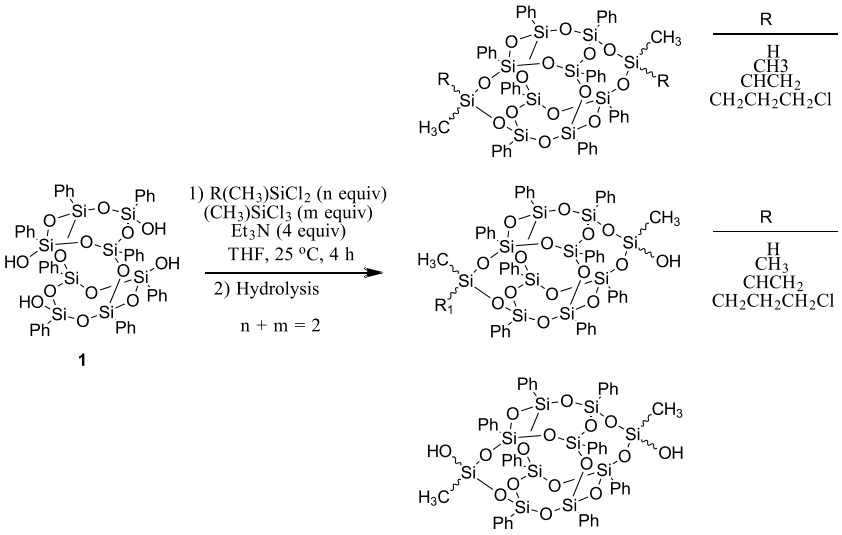

Scheme 4-1. Capping of DDSQ-$(Ph)_8(OH)_4$ with two different chlorosilanes proposed in chapter 3

The structure with a single hydroxyl group (DDSQ-$(CH_3R_2)(CH_3OH)$)was recognized as an asymmetric structure. Separation of this asymmetric structure from the mixture was achieved with optimal resolution of the elution by the use of adsorption HPLC.[131]

In this chapter the asymmetric structure is denoted with the general formula (DDSQ-$(R_1R_2)(R_3OH)$). To further explore engineering applications of asymmetric DDSQ structures, development of large-scale separation methodology to remove the symmetric byproducts is required. Scaling up adsorption HPLC separations to preparative liquid chromatography (LC) requires the use of a different stationary phase. This change usually represents large void volumes, high injection volume, and high concentrated injections, among other factors which may end-up decreasing the resolution of the elution.[132,133] The scope of this work was to simulate the separation of DDSQ-$(R_1R_2)(R_3OH)$ from the mixture by HPLC. In modeling the HPLC column, breakthrough curves were performed by HPLC and analysis of the elution front permit obtention of the adsorption isotherm parameters for each compound in the mixture. Once the simulation converges with experimental

chromatograms, extrapolation of the adsorption parameters can then be used to predict the collection time needed in a large-scale preparative chromatography separation. This prediction allows a proper column configuration to achieve separations with resolutions of the elution large enough to isolate nearly-pure asymmetrical compound.

4.2 Experimental

4.2.1 Materials

All commercially available chemicals were used as received unless otherwise indicated. $(C_6H_5)_8Si_8O_{10}(OH)_4$ 5,11,14,17-Tetra(hydro)octaphenyltetracyclo[7.3.3.-$3^{3,7}$]octasilsesquioxane or DDSQ-$(Ph)_8(OH)_4$ was purchased from Hybrid Plastics. Dimethyldichlorosilane $(CH_3)_2SiCl_2$, methyl trichlorosilane $(CH_3)SiCl_3$, vinyl trichlorosilane $(CH_2CH)SiCl_3$, isobutyl trichlorosilane $((CH_3)_2CHCH_2)SiCl_3$, and deuterated chloroform with 1%vol tetramethylsilane ($CDCl_3$-1%TMS) were purchased from Sigma-Aldrich and from Gelest. Triethylamine (Et_3N) was purchased from Avantor. Tetrahydrofuran (THF) was dried passing through the alumina adsorbent column. Reagent grade dichloromethane (DCM) was degassed with helium for HPLC experiments. The previously listed solvents were purchased from Sigma. Si-gel P-60 was obtained from Silicycle. ^{1}H, ^{13}C, and ^{29}Si were recorded on 500 MHz NMR spectrometers.

4.2.2 Methods

4.2.2.1 Synthesis of DDSQ individual products

DDSQ-2($(CH_3)_2$) **2** and DDSQ-2($(CH_3)(OH)$) **4a** were synthesized following **Scheme 4-2**. In a 500 mL flask purged with dry N_2 for fifteen minutes, DDSQ-$(Ph)_8(OH)_4$ **1** (10 g, 9.35 mmol, 1 equiv.) was dissolved in THF (200 mL) at room temperature. Dimethyldichlorosilane or methyl trichlorosilane (18.7 mmol, 2 equiv.) was added to the DDSQ-$(Ph)_8(OH)_4$ **1** solution. Et_3N (37.4 mmol, 4 equiv.) was added dropwise for a period of about 5 minutes to the stirring

solution; a cloudy white suspension was formed and continue to stir for additional four hours at room temperature. The solution was then filtered through a fine fritted-funnel-filter to remove the solid triethylamine hydrochloride. The volatiles were removed using a rotary evaporator. The sample was then solubilized in a minimum volume of DCM and then passed through a short silica-gel plug using DCM as a solvent to clean the sample and hydrolyze when methyl trichlorosilane was used. The volatiles were removed from the resulting solution and further dried at 0.4 mbar and 50 °C for 12 hours to afford **2** or **4a** as white powders. Spectral information can be found in the Appendix I.

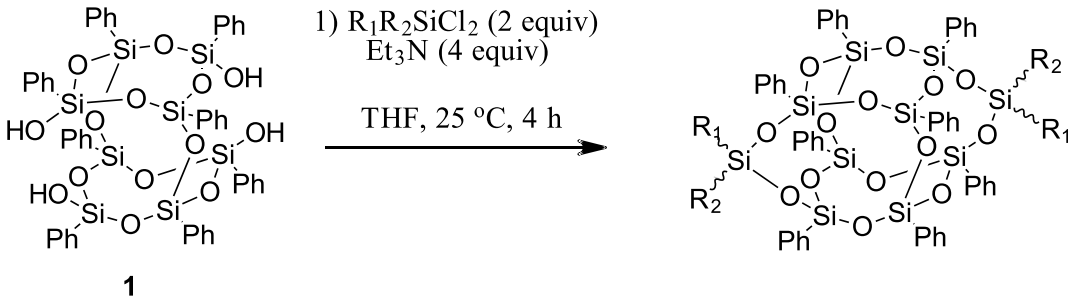

Scheme 4-2. Synthesis of functionalized DDSQ-2(R_1)(R_2). For compound **2**: R_1 and R_2 are CH_3; for compound **4a**: R_1 is CH_3, and R_2 is Cl which is hydrolyzed after the reaction to form hydroxyl (OH)

4.2.2.2 Synthesis of DDSQ mixtures

The synthesis of DDSQ mixtures with zero, one, and two hydroxyl groups was performed following **Scheme 4-3** using a procedure previously described.[114] Synthesis of a mixture containing **2**, **3a**, and **4a** (or mixture **A**) is described as an example. To a 500 mL flask purged with dry N_2 for 15 minutes, **1** (10 g, 9.34 mmol) was added and dissolved in THF (200 mL) at room temperature. Dimethyldichlorosilane (9.34 mmol, 1.14 mL, 1 equiv.) and methyl trichlorosilane (9.34 mmol, 1.10 mL, 1 equiv.) were added to the solution containing **1** and stirred for five minutes. Et_3N (37.4 mmol, 5.22 mL, 4 equiv.) was added in

1 mL installments to the stirring solution. A cloudy white suspension was formed and stirred continuously for additional four hours. The solution was filtered through a fine fritted-funnel-filter to remove the solid triethylamine hydrochloride. Volatiles were removed from the resulting solution which produced a white powder. The powder was dissolved in a minimum amount of DCM and hydrolyzed after addition of 50 mL of water and one hour of stirring. The organic phase was isolated, washed with brine, and then dried with magnesium sulfate. The volatiles were evaporated ending with the mixture **A** as a white powder. Nearly-pure **3a** was then isolated from the mixture **A** using LC. The same procedure was repeated replacing methyl trichlorosilane for vinyl trichlorosilane to produce the mixture **B** (**2**, **3b**, and **4b**), and for isobutyl trichlorosilane to produce the mixture **C** (**2**, **3c**, and **4c**). Spectral information for **3a**, **3b**, and **3c** cages can be seen in the Appendix I.

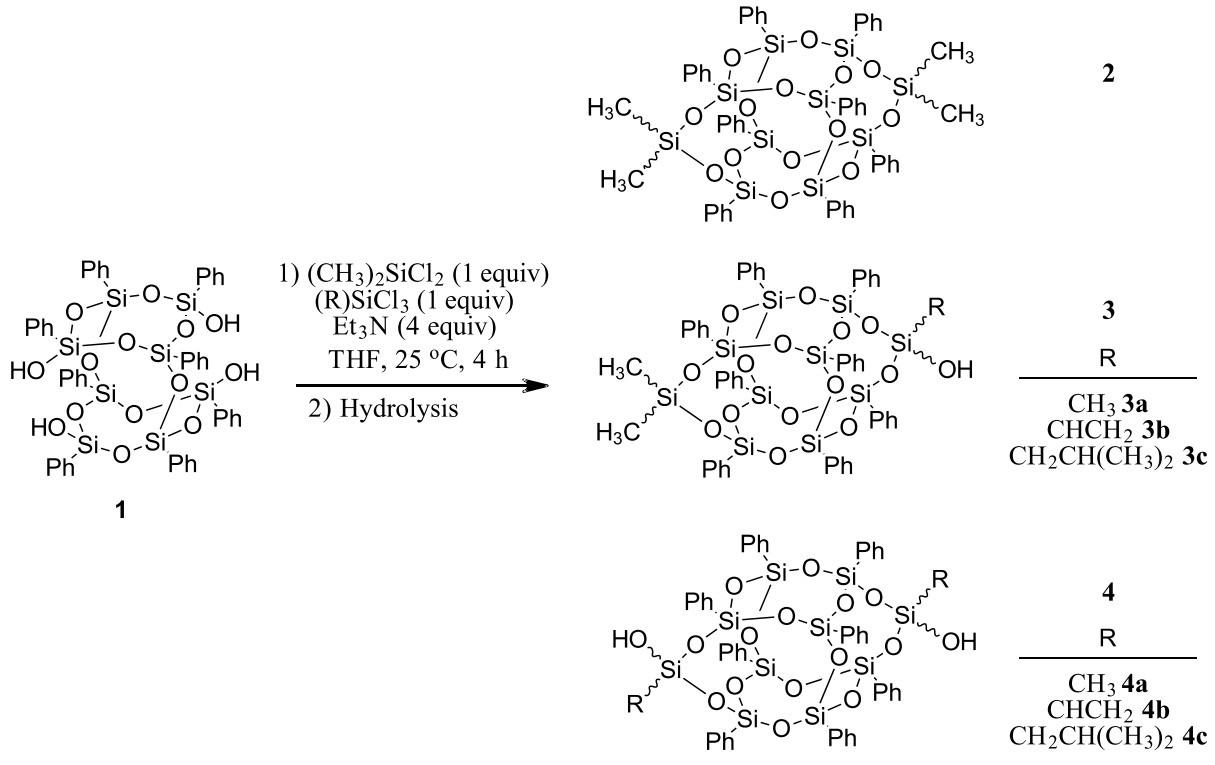

Scheme 4-3. Synthesis of mixtures containing DDSQ-2$(CH_3)_2$ **2**, DDSQ-$(CH_3)_2$(R)(OH) **3**, and DDSQ-2((R)(OH)) **4**, where R is methyl (CH_3), vinyl ($CHCH_2$), or isobutyl ($CH_2CH(CH_3)_2$).

4.2.2.3 Breakthrough curves

Breakthrough curves were generated in an Agilent 1100 HPLC system with a dual pump using a Lichrospher-Si60 column with an inner radius (r) of 0.23 cm and a length (H_b) of 25 cm. Analytes were detected with an UV-detector at 245 nm. Each compound was first solubilized in DCM with varying concentrations listed in **Table 4-1.** The solution was pumped through pump A at a flow rate (F_v) of 1 mL/min for 10 min.; pure DCM was then pumped from pump B for 40 min with the same F_v for complete elution.

Table 4-1. Solutions prepared for obtention of breakthrough curves. Concentrations of 4a are for a 1:1 mixture of cis and trans isomers.

Compound	Concentration (C) (g/L)							
	1	2	3	4	5	6	7	8
2	0.10	0.18	0.30	0.40	1.06	1.60	2.20	-
3a	0.09	0.19	0.33	0.57	0.98	1.83	2.82	6.25
4a	0.14	0.25	0.50	1.20	2.40	3.90	7.00	-

Adsorption isotherms were calculated using **Equation 4-1**,[134] where the hold-up time (t_0) in the column used was found experimentally as 2.0 min. The extra column time (t_{ext}) was calculated based on the channels from the HPLC redirection valve to the beginning of the column, and from the end of the column to the detector. For our HPLC, the value of t_{ext} was found to be 0.7 min. experimentally. The shock time (t_s) was picked from the chromatogram as the half-time of the front located between the baseline and the beginning of the plateau after the detection of DDSQ compounds.

$$q_v = \frac{CF_V(t_s - t_0 - t_{ext})}{\pi H_b r^2 - F_V t_0} \qquad \textbf{Equation 4-1}$$

The experimental adsorption isotherm was fitted to the linear isotherm model, **Equation 4-2**.

$$q_v = IP1 * C + IP2 \qquad \textbf{Equation 4-2}$$

where IP1 and IP2 are isotherm parameters and IP2 was fitted to be zero for all cases here.

4.2.3 HPLC and preparative LC chromatograms

HPLC experiments were configured using DCM as the mobile phase. The solvent was degassed with Helium before pumping to the column. The flow rate was set to be 1 mL/min for all samples, which gave a constant pressure of 34 bars, the temperature was set as 25 ˚C, the injection volume was 10 μL, and the UV detector was set at 254 nm. The number of theoretical plates (N) or column efficiency was calculated with the tangent line method in **Equation 4-3**. For HPLC, retention time (t_r) and peak width at the baseline (W) were calculated using the Agilent Chemstation software.[135] For preparative LC t_r and W were calculated manually from the plots. Resolution of the elution (R_s) was obtained using **Equation 4-4**.

$$N = 16\left(\frac{t_r}{W}\right)^2 \qquad \textbf{Equation 4-3}$$

$$R_s = \frac{2\left(W_{(i)}+W_{(i+1)}\right)}{\left(t_{r(i+1)}-t_{r(i)}\right)} \qquad \textbf{Equation 4-4}$$

Preparative LC was performed to scale-up the results obtained from HPLC experiments. Two different columns were prepared in the following general methodology. DCM was added to dry silica bed inside a glass column. The formed slurry was shaken to remove most air bubbles. Then, the wet bed was flushed with DCM under pressure generated by a dry N_2 stream. The flushing process was stopped until the flow was constant in the column outlet, meaning that air was mostly removed from the column. Void fraction was calculated based on the volume required to elute an injection of toluene through the column at the average flow rate. A

concentrated solution of DDSQ mixture dissolved in DCM was gently injected in the top of the wet Si-gel bed. The injection was flushed until no solution was observed above the packed bed. The column was then gently charged with DCM and the column pressurized by the N_2 stream to elute the analytes. Fractions were collected in the bottom of the column until remaining DCM reached the top of the bed. The concentration in each fraction was obtained by evaporation of the solvent and weighing the solid mass or by HPLC peak areas compared against a standard reference. Elution times in the preparative separation for mixtures **A** and **B** were calculated based on the relation between the volume of each fraction and the average flow rate. For the separation of mixture **C**, the flow rate for every collected fraction was recorded to analyze the effect of flow rate gradients in the simulation results. Dimensions of the columns and parameters for the separations performed can be observed in **Table 4-2.**

Table 4-2. Preparative column dimensions and operational parameters

Column	*Preparative 1*	*Preparative 2*	*Preparative 3*
Mixture	**A** (**2**, **3a**, **4a**)	**B** (**2**, **3b**, **4b**)	**C** (**2**, **3c**, **4c**)
Composition (**2**:**3**:**4**)	32:49:19	42:47:11	40:45:14
Height (Hb) cm	34	43	43
Radius (r) cm	1.7	3.4	3.4
Void fraction	0.7	0.6	0.6
Flow rate (mL/min)	25	54	19 to 87 for 10.4 min 87 to 103 for 13.0 min 54 to finish
Mixture weight (g)	2	4	4
Volume injected (mL)	15	46	46

4.2.4 Chromatogram simulation

ASPEN chromatography V10 was used to simulate the separation process in HPLC as well as in preparative LC. A batch process was drawn starting with an inlet controlling the mobile phase and the injection. This stream was connected to a packed column, and the column was further connected to an outlet stream. To start the modeling, trace-liquid was assumed for the column operation because the density of the liquid along the column is considered to be a constant. Other two assumptions in the mass balance are: (1) no changes in flow rate (F_v); and (2) no additional reaction occur during the separation process. After these assumptions, the resultant mass balance can be observed in **Equation 4-5.**

$$\varepsilon_i E_{zi} \frac{\partial^2 C_i}{\partial z^2} = v_L \frac{\partial C_i}{\partial z} + \varepsilon_t \frac{\partial C_i}{\partial t} + (1 - \varepsilon_t) J_i \qquad \textbf{Equation 4-5}$$

ε_t is the total void fraction which is a function of the interparticle void fraction ε_i and the intraparticle void fraction ε_p which is neglected here. C_i is the concentration of i molecule at a given time and position, and J_i is the mass transfer flux. E_{zi} stands for the axial dispersion coefficient. E_{zi} was calculated based on the theoretical column number of plates (N) described in **Equation 4-6**, where H_b is the packed bed height.

$$E_{zi} = \frac{v_L H_b}{2 N_p \varepsilon_i} \qquad \textbf{Equation 4-6}$$

Linear lumped resistance assumption was made to obtain an expression for J_i (**Equation 4-7**). Under this assumption, the mass transfer driving force for component i is a linear function of the liquid phase concentration.[136] In **Equation 4-7,** q_i^* represents a reference value for component i adsorbed. The mass transfer coefficient MTC was estimated by ASPEN assuming 0.005 cm^2/min as standard value for molecular diffusivity in liquids.

$$J_i = \frac{dq_i}{dt} = MTC(q_i^* - q_i) \qquad \textbf{Equation 4-7}$$

The system was divided into 500 nodes and further solved by finite differences using the quadratic upwind differencing scheme.

4.3 Results and Discussion

4.3.1 Breakthrough curves and calculated adsorption isotherms

Breakthrough curves were obtained for **2**, **3a**, and **4a** as observed in **Figure 4-1**. For **2**, the shock times were the same for all concentrations studied. This occurs as **2** is a molecule without silanol groups and its adsorption to the stationary phase is limited. Breakthrough curves for **3a** showed a slight decrease in t_s when the concentrations were increased. The highly polar **4a** exhibited a larger reduction in t_s as the concentration increases. Two fronts were observed for **4a** corresponding to *trans*-**4a** and *cis*-**4a**. t_s was identified for each one of the fronts in **4a** breakthrough curves. This observation enables the calculation for the adsorption behavior of each isomer and the prediction of *cis* and *trans* separation in the chromatogram simulation. The plateau region for concentrations higher than 10 g/L was above the detection limit. As a result, there was a breakdown of linearity between absorbance and concentration. This implies possible errors in the identification of t_s in the half concentration of the front. In addition, samples at a concentration above 10 g/L had a tendency to form crystals within the HPLC pump pistons and block the flow in the column.

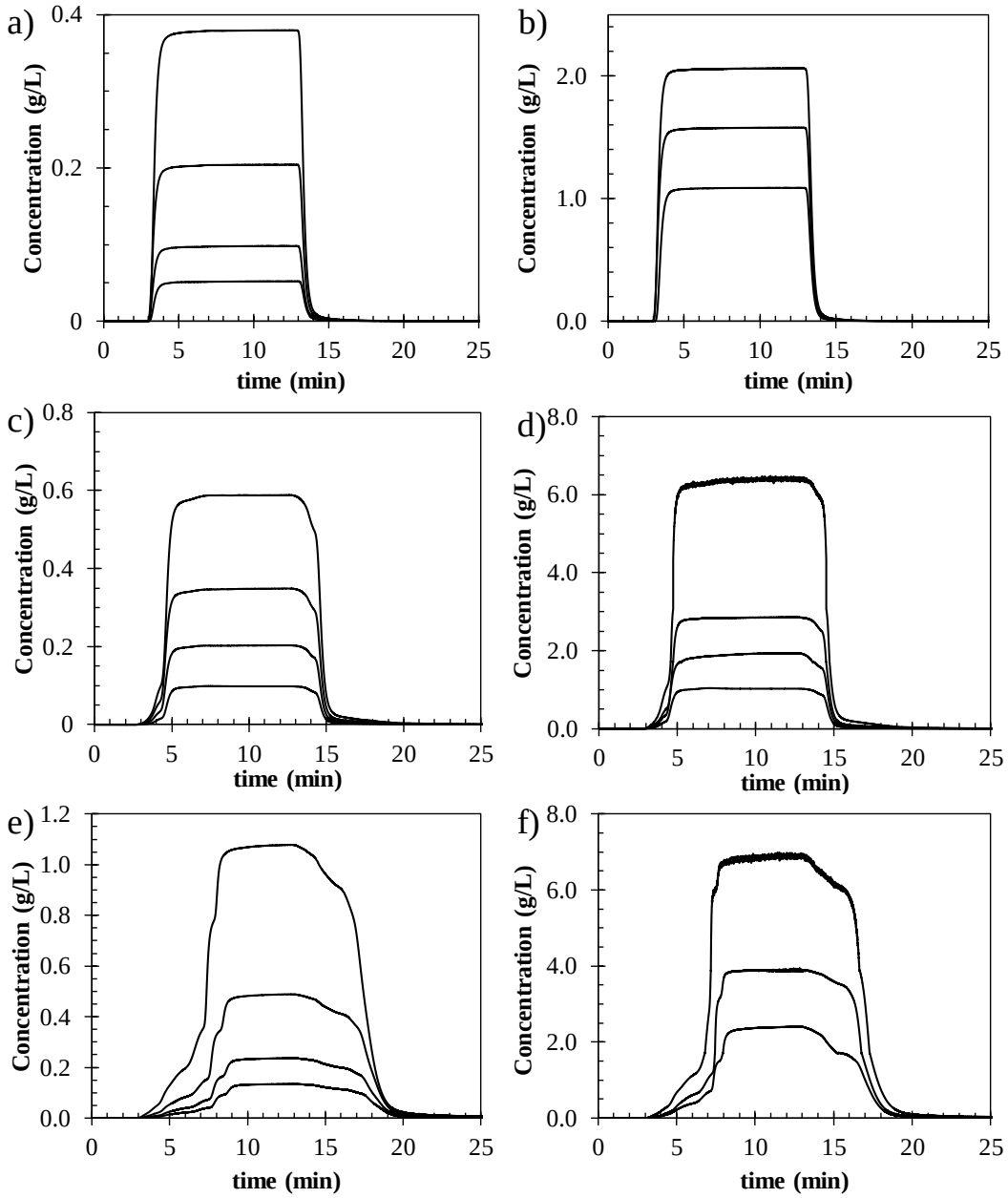

Figure 4-1. Breakthrough curves for a) **2** in low concentrations, b) **2** in high concentrations, c) **3a** in low concentrations, d) **3a** in high concentrations, e) **4a** in low concentrations, and f) **4a** in high concentrations. t_s was calculated from the half-concentration in the curve front.

Experimental results for adsorption equilibrium followed a linear trend. Therefore, the isotherms were fitted with high accuracy into a linear adsorption isotherm model. Adsorption equilibrium data calculated using **Equation 4-1** and fitting of the data in the linear **Equation 4-2** is observed in **Figure 4-2**. The experimental IP1 parameters calculated for HPLC separation for

the components of mixture **A** were tabulated and shown in **Table 4-3**. Some of the effects for high concentrations in the chromatogram such as peak tailing or maximum adsorption capacity were not studied as DDSQ breakthrough curves cannot be obtained at high concentrations.

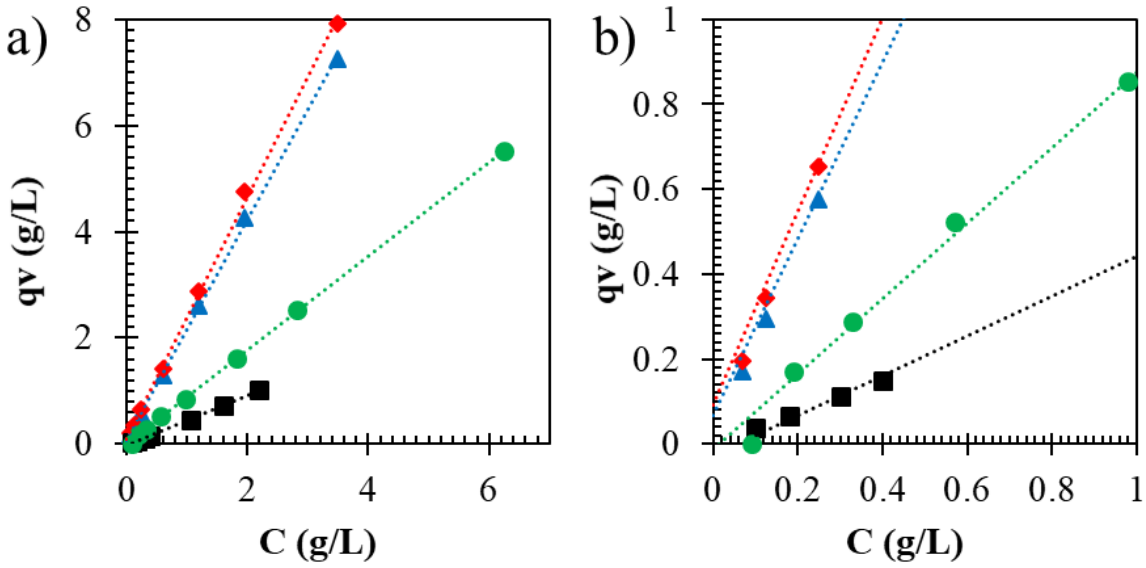

Figure 4-2. Experimental adsorption isotherms and linear fitting for: **2** black squares ■, **3a** green circles ●, *trans*-**4a** blue triangles ▲, and *cis*-**4a** red diamonds ◆. a) full experimental points; b) low concentration points. Color graph can be obtained in the digital version of this document.

4.3.2 Simulation results and parameter fitting

Based on the linear behavior of the adsorption isotherms for the components in mixture **A**. It was hypothesized that isotherms for mixtures **B** and **C** could also be linear. The isotherm parameter IP1 for each component in the mixture **A** was plotted against the retention time correspondent to each peak seen in **Figure 4-3**.

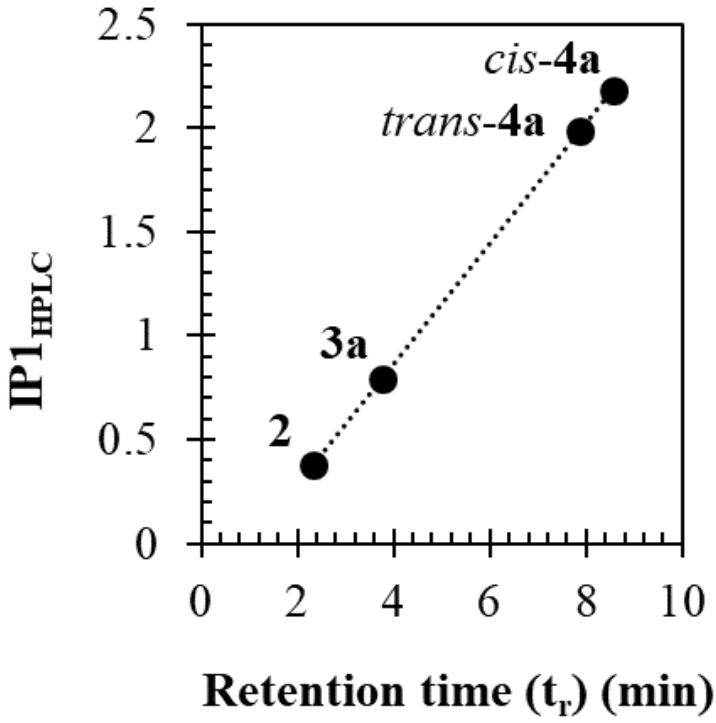

Figure 4-3. Linear behavior between the retention times (t_r) in HPLC and the linear isotherm parameter IP1 obtained from FA for mixture **A**.

The relation between IP1 and t_r for mixture **A** was linear. For instance, **Equation 4-8** was calculated making a linear fitting. **Equation 4-8** was used for calculation of the HPLC IP1 parameters ($IP1_{HPLC}$) for the components in the mixture **B** and in the mixture **C**. These parameters can be observed in **Table 3**. This approximation was made taking into account the similarity of components in the mixtures, as well as the fact that differences in retention times between **4a**, **4b**, and **4c** are mainly affected by the organic group adjacent to the hydroxyl group.[137] The $IP1_{HPLC}$ values obtained were feed into the model, and the HPLC chromatograms for mixture **A**, mixture **B** and for mixture **C** were simulated as seen in **Figure 4-4**.

$$IP1_{HPLC} = 0.2901 t_r - 0.2983 \qquad \textbf{Equation 4-8}$$

Table 4-3. Linear adsorption isotherm parameter (IP1) values obtained experimentally and calculated values.

Compound	IP1 Experimental	IP1 for HPLC column calculated from **Equation 8**	IP1 for preparative column calculated from **Equation 9**
2	0.3753	0.3767	0.0645
3a	0.7940	0.7968	1.6288
trans-**4a**	1.9850	1.9816	6.0937
cis-**4a**	2.1822	2.1844	6.8329
3b	-	0.6899	1.2385
trans-**4b**	-	1.3026	3.5354
cis-**4b**	-	1.5248	4.3684
3c	-	0.5986	0.8963
trans-**4c**	-	0.9373	2.1660
cis-**4c**	-	1.1351	2.9077

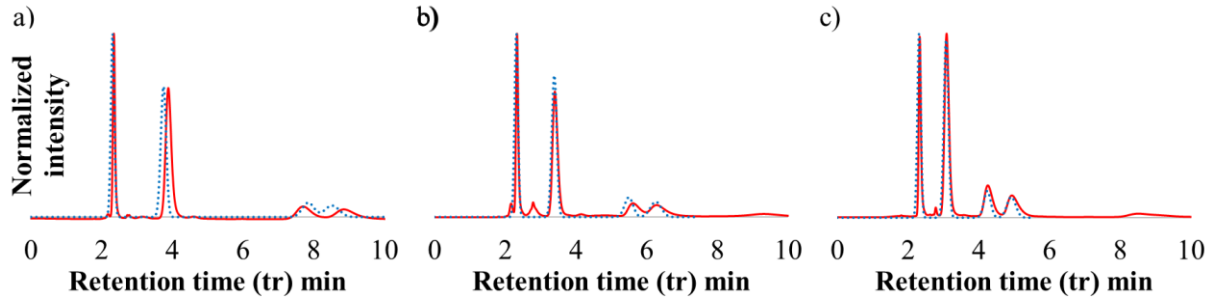

Figure 4-4. Curves in red represent the chromatograms obtained by HPLC. Curves in dotted blue lines represent the simulated chromatograms for a) mixture **A**, b) mixture **B**, c) mixture **C**.

4.3.3 Extrapolation of HPLC parameters to preparative column

The stationary phase in the HPLC column is composed by 5 μm non-porous spherical silica particles densely packed in the column with void fraction around 0.1. On the other hand, the preparative column has silica as a stationary phase with particle size averaging 60 μm, not homogeneous particle shape, porous particles, and once packed in the column the

void fraction can be higher than 0.5. Consequently, HPLC and preparative LC have different adsorption isotherm parameters. A glass column packed with Silicycle P-60 silica was prepared for separation of 2 g of the mixture **A** to obtain the preparatory LC parameters. Fractions of 9.5 mL were collected and every fraction dried and weighed to elaborate the experimental chromatogram observed in **Figure 4-5a**.

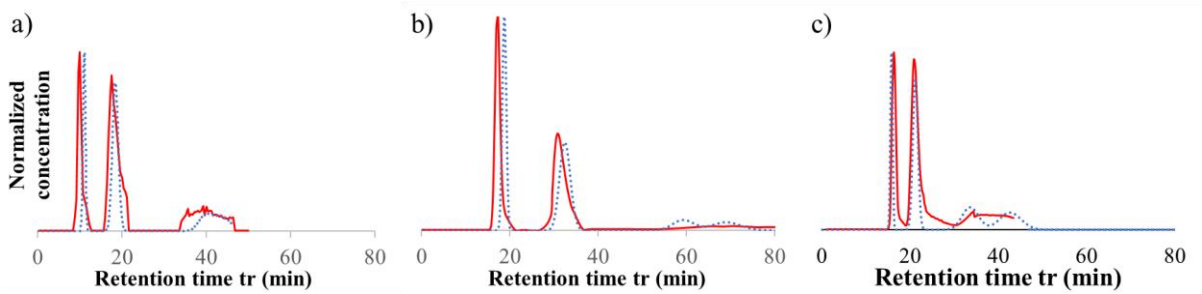

Figure 4-5. Curves in red represent the chromatograms obtained by preparative liquid chromatography. Curves in dotted blue lines represent the simulated chromatograms for a) mixture **A**, b) mixture **B**, c) mixture **C**.

Separation for mixture **A** was simulated by guessing the IP1values in the model. The graph of IP1 against t_r in the preparative column followed a linear behavior like the one observed in the HPLC column. IP1 parameters from the HPLC column were correlated with IP1 parameters from the preparative column. Obtaining the linear correlation observed in **Figure 4-6** as well as in **Equation 4-9**.

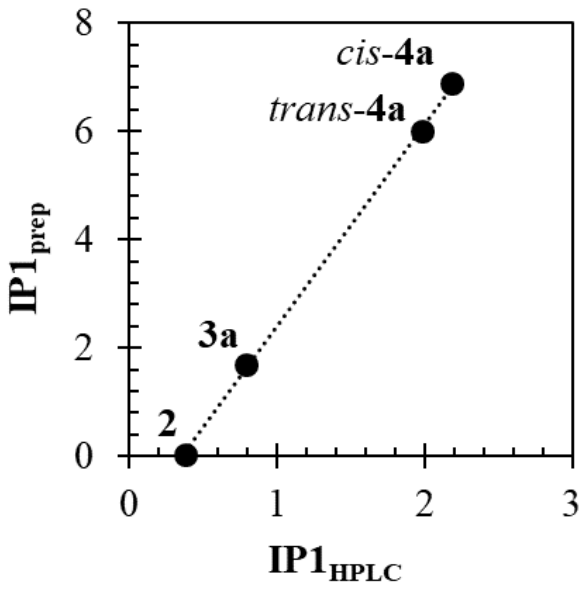

Figure 4-6. The relation between IP1 obtained from HPLC ($IP1_{HPLC}$) and IP1 obtained from Preparative column ($IP1_{prep}$)

$$IP1_{prep} = 3.7488 IP1_{HPLC} - 1.3477 \qquad \textbf{Equation 4-9}.$$

A preparative column was packed for separation of 5 g of mixture **B**, and 5 g of mixture **C** to test the predictive model for columns with Silicycle P-60 silica. Simulation for separation of mixture **B** resulted in an accurate prediction for collection times for every compound. However, retention times were just acceptably predicted. The experimental preparative chromatogram and the simulated chromatogram were compared and shown in **Figure 4-5b**. Analysis of each fraction was performed by HPLC and can be observed in the Appendix G. Separation of mixture **C** was performed as followed: first, the flow rate was increased from 19 mL/min to 87 mL/min in a lapse of 10.4 min.; from 87 mL/min to 103 mL/min for 13 min.; and then suddenly dropped to 54 mL/min for the remaining experiment. Experimental ramps were reposted in the Appendix G. The separation using flow rate gradients was simulated and the results obtained are in acceptable fitting with the

experiment as seen in **Figure 4-5c**. In average, 85% of the initial weight was recovered after the separation process.

Prediction of separation between *cis* and *trans* molecules of **4** indicates that is possible to collect fractions enriched with the *cis* isomers and fractions enriched with the *trans* isomers. The predicted results agree with the experimental results showing that effectively *cis* and *trans* isomers of the DDSQ with two hydroxyl groups can be partially separated using DCM as the mobile phase. Previously separation of *trans* and *cis* DDSQ cages capped with isobutyl trichlorosilane was achieved in a silica column with toluene as mobile phase.[17] Enriched fractions of *cis*-**4b** *trans*-**4b** *cis*-**4c** and *trans*-**4c** can be observed in the HPLC analysis for preparative separations presented in the Appendix G.

4.3.4 Efficiency for preparative columns

Analysis of the column efficiency by **Equation 4-3** was used to estimate the dispersion coefficient by ASPEN chromatography. **Table 4-4** contains the calculated column efficiencies for preparative-1, preparative-2, and HPLC. For compound **2,** the difference in N values between preparative-1 and preparative-2 columns is mainly attributed to the larger diameter and length of preparative-2, larger column diameters generally reduce the injection height, decreasing the initial dispersion in the column. On the other hand, longer columns have a higher number of theoretical plates. The calculated efficiency for separation of **4b** was half of **4a** and **4c** in HPLC due to overlapping of elution peaks. As seen in **Table 4-4**, the values of N for the preparative column are one order of magnitude smaller than the N for HPLC. Calculation of N for preparative columns has the same trend as the N calculated by HPLC.

Table 4-4. Column efficiency (N) calculated from Equation 3 for HPLC and preparative columns. * Value calculated as an individual component.

Compound	N preparative-1	N preparative-2	N HPLC
2	261	603	7178
3a	191	-	2235
3b	-	430	2359
3c	-	-	2635
trans-**4a**	105*	-	1936
cis-**4a**		-	1694
trans-**4b**	-	212	697
cis-**4b**	-	217	853
trans-**4c**	-	-	1427
cis-**4c**	-	-	1117

In **Table 4-5**, values of resolution of the elution (R_s) calculated with **Equation 4-4** are tabulated. R_s between **2** and **3**, and between **3** and **4** were higher than the optimal value, $R_{s\text{-}optimal}$=1.5, in HPLC as well as in preparative LC. These R_s values indicate that every analyte was eluted with high purity. In addition, further improvement may be made to reduce the separation time. Calculations of R_s for HPLC between *cis* and *trans* isomers of **4** resulted in values larger or close to the optimal value for **4a**, and for **4c**. However, for the mixture **B** separation of *trans*-**4b** and *cis*-**4b** has R_s value enough to recognize the components but very low to achieve an optimal resolution between the peaks. This behavior indicates that polarity difference between *cis* and *trans* isomers of **4b** is lower than the difference of polarity for isomers of **4a** and **4c**. For preparative LC separations, R_s between *cis* and *trans* isomers of **4** was not possible to measure because both isomers were overlapped. Different solvents and column lengths may be explored to achieve R_s values close to 1.5 between *trans*-**4**-and *cis*-4 peaks.

Table 4-5. Resolution of the elution between analytes in each mixture after separation by HPLC and preparative LC.

R_s between compounds	R_s by HPLC	R_s by Preparative LC
2 and **3a**	7.1	2.1
2 and **3b**	5.5	3.1
2 and **3c**	4.3	1.8
3a and *trans*-**4a**	7.4	2.0
3b and *trans*-**4b**	3.9	2.9
3c and *trans*-**4c**	3.4	1.7
trans-**4a** and *cis*-**4**	1.5	-
trans-**4b** and *cis*-**4b**	0.8	0.2
trans-**4c** and *cis*-**4c**	1.3	-

4.4 Conclusion

Separation by LC was performed for a mixture of double-decker shaped silsesquioxanes functionalized with zero, one, and two hydroxyl groups. The presence of the polar group allowed different retention times for the mixtures evaluated included the *trans* and the *cis* isomers for the nanostructure functionalized with two hydroxyl groups. It was determined that adsorption of the non-polar compound was neglectable because it migrates through the column without being retained.

Linear adsorption isotherms were identified for the structures dissolved in DCM. Highly concentrated solutions were not studied due to problems with the pump pistons and proximity to the detector limit. However, evaluation of larger concentrations may allow visualization of Langmuir type of isotherms. Nevertheless, linearity is an advantage for scale up the separation process into a preparative column working in batch operations. HPLC was used to predict linear adsorption isotherm parameters that were further extrapolated to find adsorption isotherm

parameters for commercially available silicas. These parameters allowed the prediction of collection intervals in large-scale columns.

Separations performed experimentally with the simulated parameters are accurate in the baseline of the chromatogram. But the peak shapes may require another type of isotherms predictive of tailing or perhaps competition. Other types of separation using this commercial stationary phase can be simulated with the adsorption parameters found in this work. In summary, this work proposes a simple predictive methodology for scale-up HPLC separations of side-capped octaphenyl double-decker shaped silsesquioxanes by the use of commercially available silica.

CHAPTER 5.

PHASE BEHAVIOR OF CIS-TRANS MIXTURES OF DOUBLE-DECKER SHAPED SILSESQUIOXANES FOR PROCESSABILITY ENHANCEMENT

Keywords: Double-decker shaped silsesquioxanes, melting temperature suppression, binary cis and trans eutectic composition, phase diagram.

5 Phase behavior of cis-trans mixtures of double-decker shaped silsesquioxanes for processability enhancement

5.1 Introduction

Functionalized double-decker shaped silsesquioxane (DDSQ-2(R_1R_2)), and corner capped cubic shaped silsesquioxanes (POSS-R_1) (**Figure 5-1**) are cage-like silsesquioxanes with a dimensionally well-defined inorganic core, inert organic groups around the core which provides compatibility with the surround organic matter of interest, and exact specified reactive organic sites.[138,139] These structures have become model compounds to investigate effects of nanostructured inorganic additives on polymer properties.[140-144] Applications of both DDSQ-2(R_1R_2) and POSS-R_1 nanostructures have been explored extensively.[138,140-142,145,146-167] When used in organic polymers, the hybrid characteristics provide enhanced oxidation temperature, improved hydrophobicity, and low dielectric constant.[147-151,156,166,168-173] Recent research extended the use of DDSQ-2(R_1R_2) and POSS-R_1 as supports to reduce the amount of packed bed required in heterogenous catalysts.[142,147,174-177] Other applications for POSS-R_1 include improved ionic liquid performance and its thermal stability,[171,178-180] microstructure modifier to improve mechanical performance of metallic alloys,[162] superhydrophobicity in coatings,[164,181-183] monomer for increased thermal and mechanical performance of thermosetting polymers, [184-187] and use in pharmaceutical applications.[182,188-191]

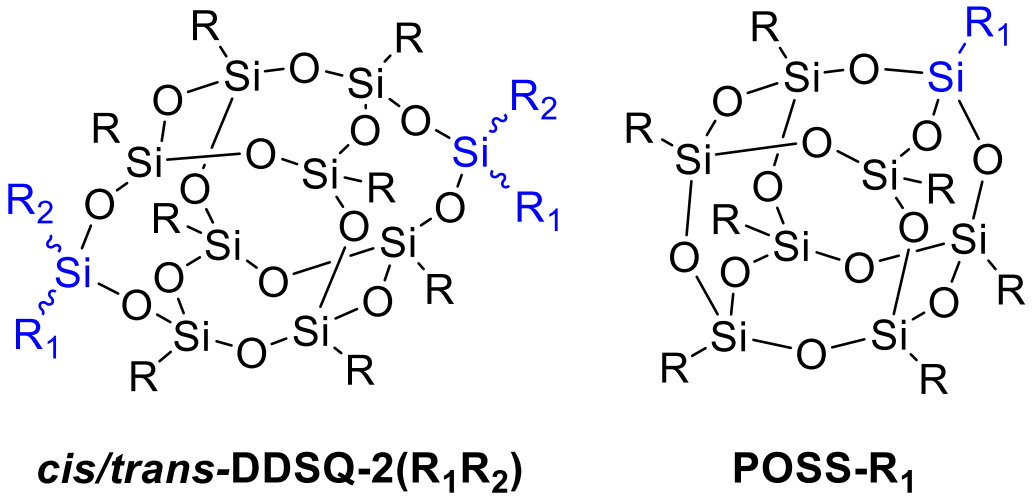

Figure 5-1. Structure of cis/trans-DDSQ-2(R_1R_2) and POSS-R_1 where R are inert organic moieties and R_1 and R_2 are active functional groups.

Incorporation of POSS-R_1 or DDSQ-2(R_1R_2) without the use of solvents is an environmentally friendly method to integrate these cage-like silsesquioxanes into organic polymers and has been achieved by melting the nanostructures.[165,169,192,193] In our prior work on POSS-(phenylethynylphthalimide) where the surrounding R moieties were phenyl or isobutyl, it was observed that hepta-phenyl POSS-(phenylethynylphthalimide) did not melt; however, the isobutyl system could be melt-processed with organic oligomeric phenylethynylphthalimide to form thermosets.[169] Interestingly, it was found that octa-phenyl DDSQ-2((phenylethynylphthalimide)(methyl)), which is structurally similar to hepta-phenyl POSS-(phenylethynylphthalimide), resulted in a material that exhibited melt characteristics.[169,194] It was hypothesized that melting of DDSQ-2(R_1R_2) was caused by higher entropy as compared to POSS-R_1 because the as-synthesized DDSQ-2(R_1R_2) products contain cis and trans isomers about the inorganic core as shown in **Scheme 5-1**.[144,145,192,195-197,198-201]

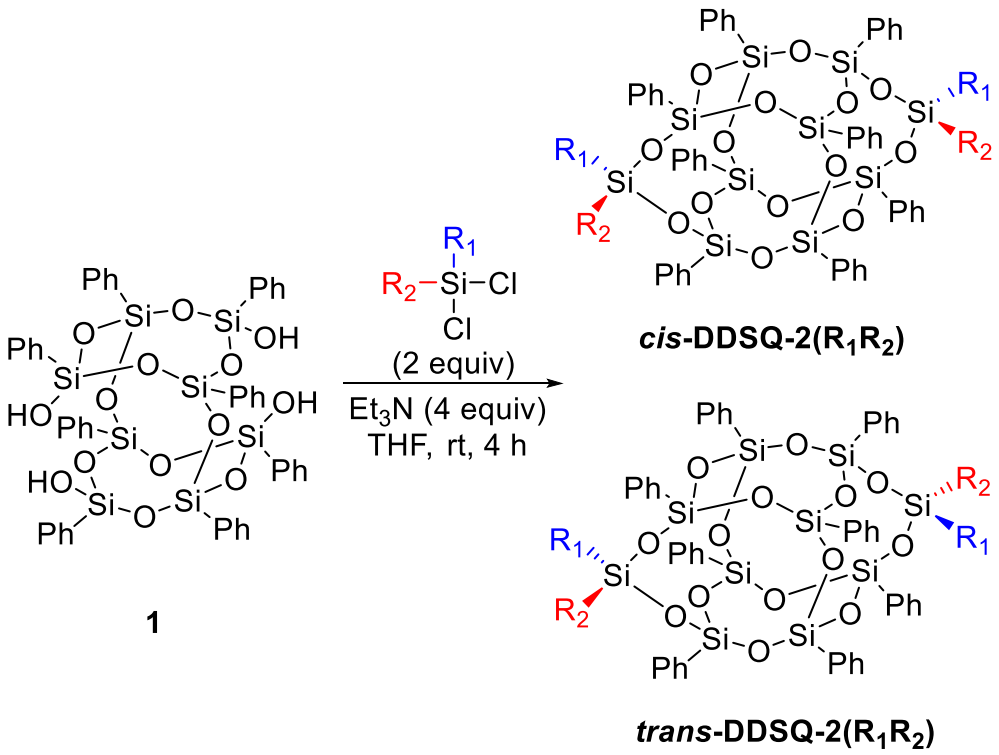

Scheme 5-1. Condensation of 1 with two equivalents of organo-dichlorosilanes

Separation of cis and trans DDSQ-2(R_1R_2) isomers using fractional crystallization (FC), and/or liquid chromatography (LC) has been achieved,[145,199] and it has been demonstrated that polymers synthesized from mostly cis isomers exhibit different thermal characteristics than the same polymer made with mostly trans isomers.[145] In this work we investigate the effect of bulkiness of an aryl group in the R_1 position in DDSQ-2((methyl)(R_1)) on the melting temperature of the cis or trans isomers. In addition, this work focused on a more systematic understanding of the melting behavior of DDSQ compounds with varying cis to trans ratios. Results from the differential scanning calorimetry (DSC) were used to construct the upper portion of the *cis-trans* binary phase diagram. The resulting binary phase diagram can be used to tailor a specified *cis* to *trans* ratio for optimizing the condition needed for melt mixing with organic polymers.

5.2 Experimental

5.2.1 Materials

All commercially available chemicals were used as received unless otherwise indicated. $(C_6H_5)_8Si_8O_{10}(OH)_4$ 5,11,14,17-tetra(hydro)octaphenyltetracyclo[7.3.3.-$3^{3,7}$]octasilsesquioxane (DDSQ-$(Ph)_8(OH)_4$) **1** was purchased from Hybrid Plastics. Methyltrichlorosilane, 4-[bis(trimethylsilyl)amino]phenyl(bromo)magnesium, 4-bromoiodobenzene, phenylacetylene, phenylmethyldichlorosilane, $Pd(PPh_3)_2Cl_2$, CuI, activated magnesium turnings, $CDCl_3$ with 1% TMS, dichloromethane (DCM), hexanes, ethyl acetate, and THF were all purchased from commercial sources and used directly unless specified. THF was refluxed over sodium/benzophenone ketyl and distilled.

5.2.2 Synthetic procedures

5.2.2.1 Synthesis of dichloro(methyl)(4-(phenylamine(bis(trimethylsilyl))))silane

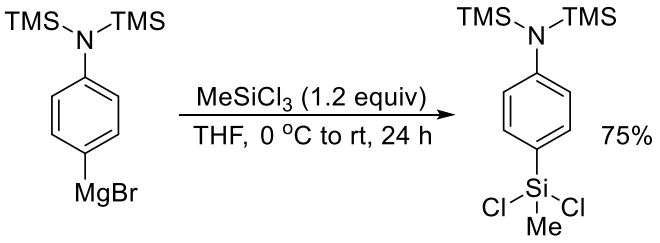

Scheme 5-2. Synthesis of dichloro(methyl)(4-(phenylamine(bis(trimethylsilyl))))silane

Under an N_2 atmosphere, a solution of 0.5 M 4-[bis(trimethylsilyl)amino]phenyl(bromo)-magnesium in THF (30 mL, 15 mmol) was injected dropwise into a flask containing a solution of freshly distilled THF (10 mL) and 18 mmol of methyltrichlorosilane (1.2 equiv, 2.11 mL) that was cooled by an ice bath (**Scheme 5-2**). This mixture was allowed to warm to room-temperature and then stir for 24 h after which a clear yellow-pale solution was observed. At the end of the reaction, the excess THF and $MeSiCl_3$ were removed by distillation under N_2 in an oil bath at 90

°C. The product was then distilled at 120 °C under 0.1 mmHg vacuum producing a clear yellow liquid (3.95 g, 11.26 mmol, 75 % yield). The spectra match previously reported data.[195,199]

^{1}H NMR (500 MHz, $CDCl_3$) δ: 7.58 (m, 2H), 7.01 (m, 2H), 1.02 (s, 3H, CH_3), 0.10 (s, 18H, TMS). ^{29}Si NMR (99 MHz, $CDCl_3$) δ 18.89 (1Si), 5.12 (2Si).

5.2.2.2 Synthesis of 1-bromo-4-(phenylethynyl)benzene

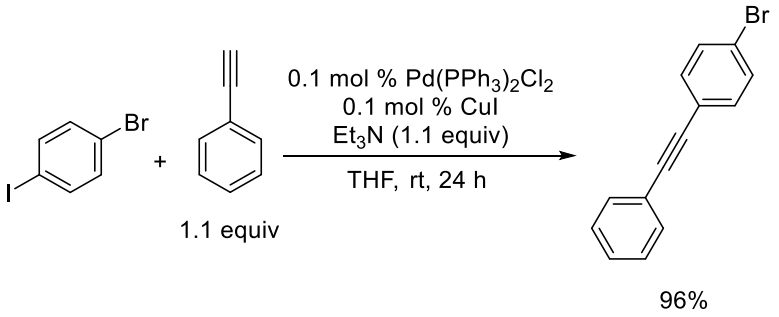

Scheme 5-3. Synthesis of 1-bromo-4-(phenylethynyl)benzene

This procedure was adapted from previous literature and described in **Scheme 5-3**.[198,201] To a 500 mL round bottom flask was added 4-bromoiodobenzene (100 g, 353 mol, 1 equiv.), $Pd(PPh_3)_2Cl_2$ (0.2481 g, 0.353 mmol, 0.1 mol %), CuI (0.0673 g, 0.353 mmol, 0.1 mol %), and a stir bar. The flask was sealed with a rubber septum and flushed with nitrogen then 300 mL freshly distilled THF was added. Triethylamine (54.3 mL, 0.389 mol, 1.1 equiv.) was distilled over CaH_2 and added to the reaction mixture. Finally, phenylacetylene (42.7 mL, 0.389 mol, 1.1 equiv.) was added dropwise to the reaction mixture. The reaction solution eventually turned a brown color with a white precipitate. The white precipitate is likely Et_3NI. The reaction was allowed to stir for 12 hours at room temperature. At the end of the reaction, the solvent was removed, and the resulting solid was extracted with DCM/H_2O. The solid from the organic layer was then purified by silica column chromatography

(hexanes) to afford 87.25 g of a white flaky solid (96% yield) with NMR matching previous literature.[202]

^{1}H NMR (500 MHz, $CDCl_3$) δ 7.57 – 7.53 (m, 2H), 7.52 – 7.48 (m, 2H), 7.44 – 7.39 (m, 2H), 7.39 – 7.35 (m, 3H). ^{13}C NMR (126 MHz, $CDCl_3$) δ 133.04, 132.52, 131.62 (d, J = 2.3 Hz), 128.53, 128.42, 122.92, 122.49, 122.25, 90.53, 88.34.

5.2.2.3 Synthesis of dichloro(methyl)(4-(phenylethynyl)phenyl)silane

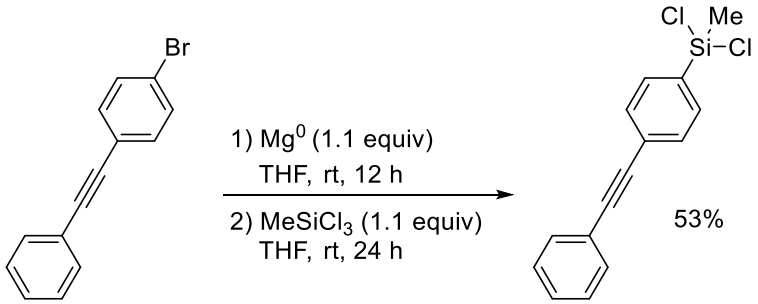

Scheme 5-4. Synthesis of dichloro(methyl)(4-(phenylethynyl)phenyl)silane.

Following **Scheme 5-4**, to a 250 mL round bottom flask were added Mg^0 turnings (2.08 g, 0.085 mol, 1.1 equiv.) and a stir bar. The Mg^0 turnings were stirred under vacuum for 2 hours after which the flask was put under an N_2 atmosphere. 1-bromo-4-(phenylethynyl)benzene (20 g, 0.077 mol, 1 equiv.) was dissolved in 80 mL freshly distilled THF and injected into the flask containing the Mg^0 turnings. This mixture was allowed to stir for 12 h after which a green solution was observed. An aliquot of the solution was dissolved in methanol, and a GC/MS showed only one peak with a mass of 178 suggesting full Grignard formation was achieved. In a 500 mL round bottom flask equipped with a stir bar under an N_2 atmosphere, $MeSiCl_3$ (10 mL, 0.085 mol, 1.1 equiv.) was placed in 40 mL THF. The $MeSiCl_3$ was freshly distilled over CaH_2. The Grignard solution was cannula transferred dropwise into the 500 mL flask containing $MeSiCl_3$. The cannula transfer took approximately 45 minutes. The reaction mixture was allowed to stir for 24 h at which time GC-MS showed full conversion. It should be noted that the initial

color of the solution was clear colorless which turned first yellow, then green and finally a yellow-orange color. At the end of the reaction, the excess THF and $MeSiCl_3$ were removed leaving behind a yellow powder. Fresh hexanes (~300 mL) were added to the powder creating a slurry. This slurry was filtered through a medium fritted funnel with the use of hexanes (~200 mL) to aid transfer and wash the solid on the frit. The solvent from the filtrate was removed producing a yellow solid which was dried under vacuum overnight at room temperature. Once dry, the solid was subjected to sublimation at 70 °C under 0.01 torr. It should be noted after the first batch a crystalline product has collected the temperature of the sublimation was raised to 95 °C. Dichloro(methyl)(4-(phenylethynyl)phenyl)silane was collected as white crystals (12.1 g, 53% yield) with a melting point of 78 °C.

^{1}H NMR (500 MHz, $CDCl_3$) δ 7.71 (d, J = 8.2 Hz, 2H), 7.65 – 7.58 (m, 2H), 7.58 – 7.53 (m, 2H), 7.37 (dd, J = 4.8, 1.9 Hz, 3H), 1.05 (s, 3H).^{13}C NMR (126 MHz, $CDCl_3$) δ 133.20, 132.98, 131.75, 131.24, 128.70, 128.43, 126.72, 122.78, 91.64, 88.69, 5.52. ^{29}Si NMR (99 MHz, $CDCl_3$) δ 18.39.

5.2.3 Capping of DDSQ-(Ph)$_8$(OH)$_4$

DDSQ-2((Me)(R)) where R = *para*-phenylamine (PA) **2**, *para*-(phenylethynyl)phenyl (PEP) **3**, and for phenyl (Ph) **4** were synthesized following **Scheme 5-1** and are shown in **Figure 5-2**. A 250 mL flask was charged with DDSQ-$(Ph)_8(OH)_4$ (**1**) (2.0 g, 1.87 mmol, 1 equiv) and a stir bar then purged with dry N_2 for 15 minutes followed by the addition of THF (60 mL) at room-temperature. To the solution was added $Cl_2Si(Me)(R)$ (3.74 mmol, 2 equiv) followed by dropwise addition of Et_3N (1.04 mL, 7.48 mmol, 4 equiv). The addition of triethylamine took 5 minutes in total, and a cloudy white suspension was formed. The reaction mixture was stirred for 4 hours. The solution was then filtered through a fine fritted-

funnel-filter to remove the solid triethylamine hydrochloride. The solution was dried by rotary evaporation to afford *cis*-to-*trans* mixtures of DDSQ-2((Me)(R)) as a white powder. Compound **2** was obtained after deprotection of the trimethylsilyl groups using previously reported methods of methanol acidified with acetic acid and further evaporation of the volatiles.[195,199]

These reactions generated two geometrical arrangements for Me and R. When both moieties are facing in the same directions, they are referred to *cis* isomers, and when they are facing in opposite directions, they are identified as *trans* isomers. The structures synthesized under this procedure are listed in **Figure 5-2**.

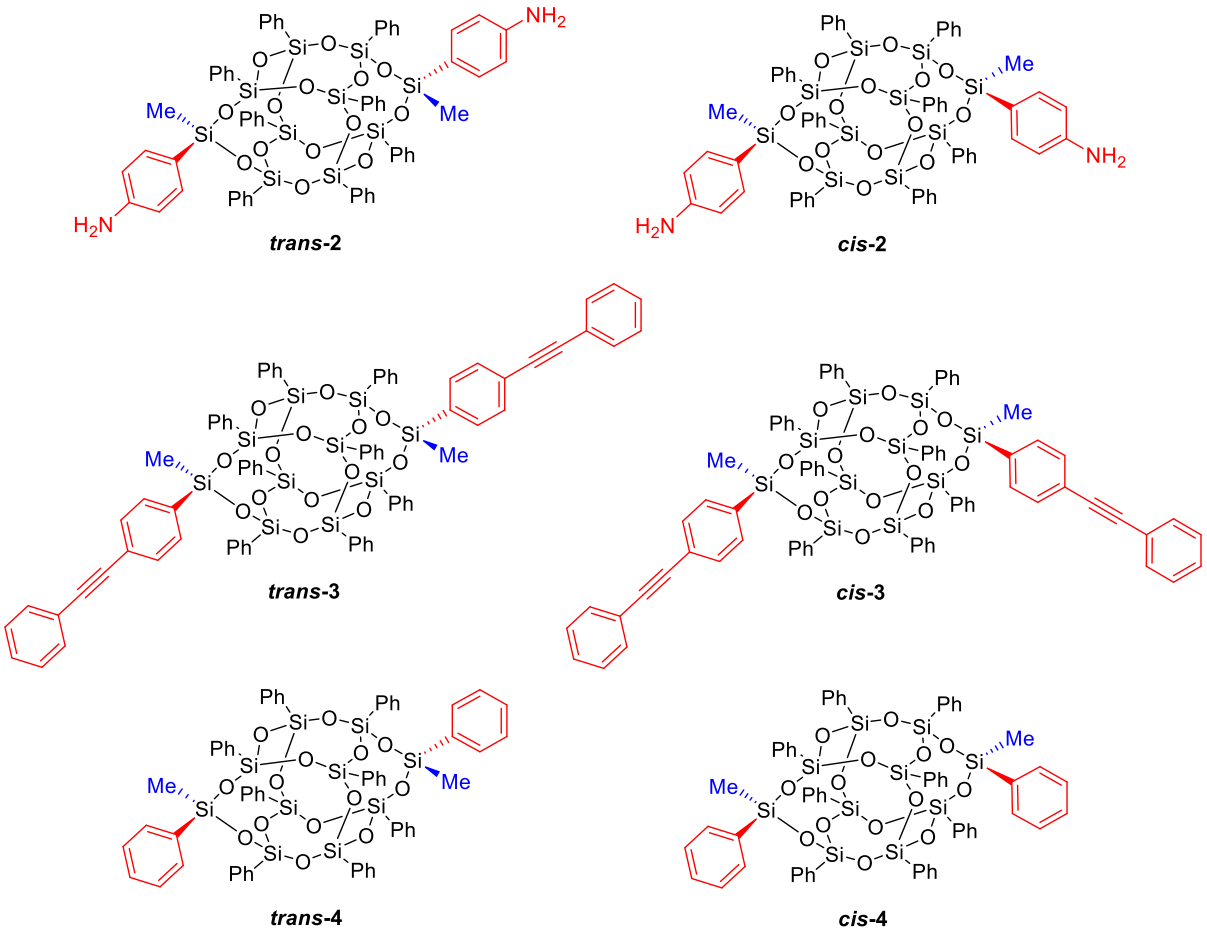

Figure 5-2. Structures synthesized and studied in this work.

5.2.4 Analytical methods

^{1}H, ^{13}C, and ^{29}Si NMR spectroscopy were used to identify synthesized products. The *cis*-to-*trans* ratio of all samples investigated was first estimated using ^{29}Si NMR. Detailed quantification for the *cis*-to-*trans* ratio in **2** was performed based on ^{1}H NMR using a 2-D NMR technique previously described[195].

In general, separation of isomers was by fractional crystallization (FC) with THF as a good solvent and hexanes as a poor solvent using a procedure specified elsewhere[14]. Several cycles of fractional crystallization were needed for required isomer purity. Isolated isomers were crystallized by slow evaporation of THF and crystals obtained were mounted on a nylon loop with paratone oil and analyzed on a Bruker APEX-II CCD diffractometer. The crystal was kept at a constant temperature of 173 K during data collection.

Thermal behavior of isomers with purities superior to 95%, or nearly pure isomers, and mixtures of *cis* and *trans* isomers was studied by DSC Q2000 equipped with a mechanical cooling accessory. Typically, the temperature range of investigation was from 50 °C to 350 °C with a constant heating rate of 10 °C/min.

5.3 Results and discussion

5.3.1 Separation and identification of nearly-pure isomers

Nearly-pure *trans* and enriched *cis* DDSQ-2((Me)(R)) isomers can be obtained by fractional crystallization;[199] however, the ease of isolating nearly-pure *cis* or *trans* isomers varied depending on the R-group. In general, the as-synthesized DDSQ-2((Me)(R)) mixtures were dissolved in THF, and addition of hexanes resulted in crystallization and precipitation of the *trans* isomers. This in turn enriched the solution with the *cis* isomer. The isolation process was repeated until sufficiently isomerically pure compounds were obtained.

Isolation of nearly-pure *cis* and *trans* isomers by FC was easily achieved for **3**. However, separation of the *cis and trans* isomers of **4** required multiple recrystallizations. The nearly-pure *trans*-**4** was obtained in the first cycle with this technique, but further removal of trans from the mother liquor could not be achieved after a threshold of 75 wt% cis and 25 wt% trans was reached. Unfortunately, further purification via LC was unable to increase the *cis* isomer ratio due to non-polar R groups in **4**.[197,203] *Trans* isomers were isolated by FC for **2**. Due to the polar nature of phenylamines in **2**, liquid chromatography proved effective for the isolation of nearly-pure *cis* fraction.[147,151] The isolated isomers were analyzed by ^{29}Si NMR, as seen in **Figure 3**. Analysis by HPLC can be observed in the Appendix G.

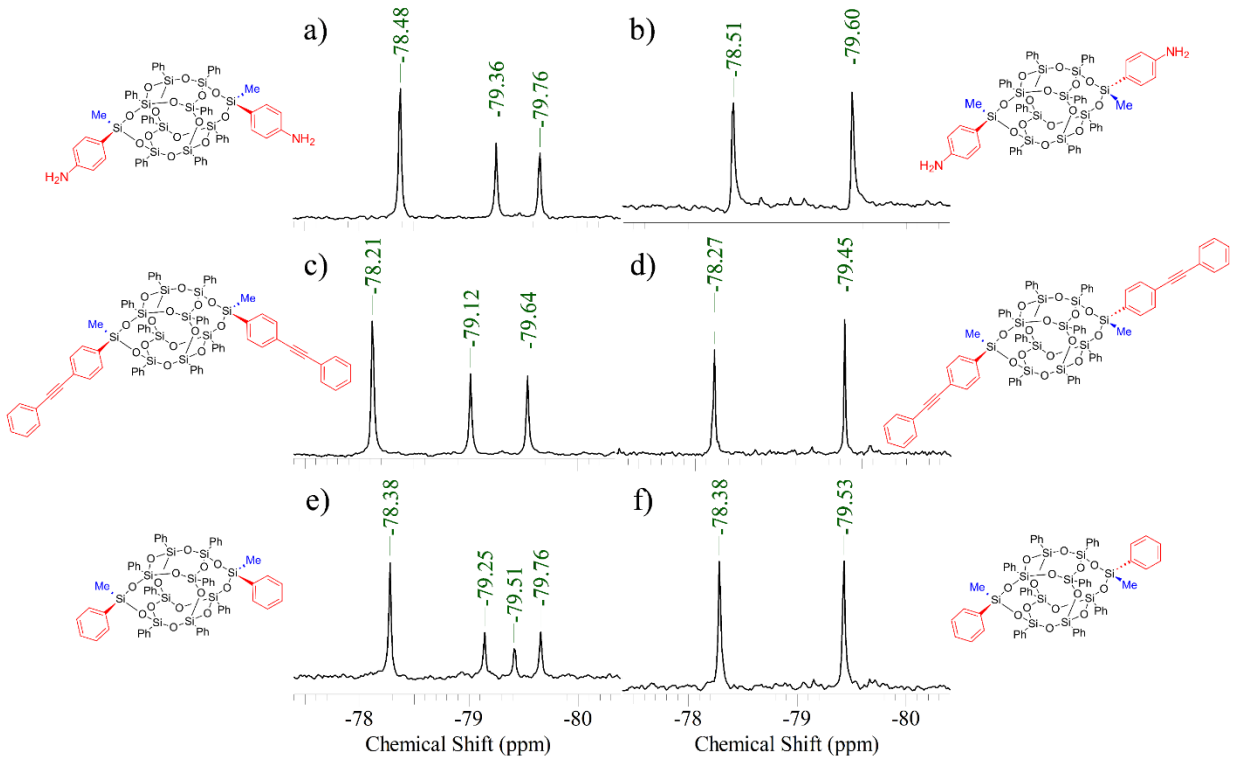

Figure 5-3. ^{29}Si NMR peaks representing the nearly-pure isomers after separation; a) *cis*-**2**, b) *trans*-**2**, c) *cis*-**3**, d) *trans*-**3**, e) 75% *cis*-**4**, and f) *trans*-**4**.

Isolated isomers were crystallized by slow evaporation of THF to form single crystals needed for crystallographic analysis. We obtained crystallographic data for each compound; however, it should be noted that cis/trans-**2** and cis/trans-**3** were previously reported.[201,204] Data from these crystal structures are shown in **Table 5-1**. Crystalline packing density for the *cis* isomer is less than for the *trans* isomer and packing density was reduced as the size of R group in DDSQ-2((Me)(R)) increases.

Table 5-1. Crystallization of individual isomers

Compound	Density (g/cm^3)	Crystal system	Space group	Unit cell axes dimension (Å)		Unit Cell inclination angles (°)	
cis-**2**	1.366	Triclinic	$P\bar{1}$ (2)	a	13.77	α	87.11
				b	17.50	β	79.16
				c	27.50	γ	87.39
trans-**2**	1.390	Monoclinic	$P\,2_1/n$ (14)	a	10.05	α	90.00
				b	43.57	β	91.66
				c	14.59	γ	90.00
cis-**3**	1.321	Triclinic	$P\bar{1}$ (2)	a	14.44	α	85.92
				b	14.90	β	74.70
				c	18.54	γ	79.89
trans-**3**	1.341	Triclinic	$P\bar{1}$ (2)	a	10.77	α	91.39
				b	13.45	β	108.68
				c	13.61	γ	91.69
trans-**4**	1.382	Triclinic	$P\bar{1}$ (2)	a	9.90	α	65.65
				b	13.51	β	71.77
				c	14.03	γ	69.54

5.3.2 Thermal behavior of nearly-pure isomers

Melting behavior as expressed in DSC trace for pure compounds is usually observed as a single sharp endothermic peak in which the onset temperature (T_{onset}) is very similar to the peak temperature (T_{peak}). This was observed for *cis*-**2**, *trans*-**2**, and *trans*-**3** indicating the purity of these samples was >95% based on the difference between T_{onset} and T_{peak} and the ^{29}Si NMR spectra shown in **Figure 5-3**. However, for *cis*-**3** and *trans*-**4** approximately 6 °C difference in T_{onset} and T_{peak} was large enough to indicate these compounds may not be as

pure as suggested by ^{29}Si NMR. In fact a first small endo peak with an onset temperature near 267 °C was observed for DSC trace of nearly-pure *trans*-**4**. Melting temperatures (T_m) calculated from the T_{onset} in the endo peak were higher for *trans* isomers than for *cis* isomers as seen in **Table 5-2**. The calculated entropy at melting (ΔS_m) for *trans* isomers is higher than *cis* isomers. This suggests the solid state of the *trans* isomer is more ordered than that of the *cis* isomer. From **Table 5-2**, it was observed that the size of the R group could affect the value of T_m. Larger R has a lower value of T_m. The T_m reduction is most likely related to the packing density as reported in **Table 5-1**.

Table 5-2. Experimental values obtained from nearly-pure *cis* and *trans* DDSQ-2((Me)(R)) by DSC. $\Delta S_m = \Delta H_m/T_m$

Compound	T_{peak} (°C)	T_m (°C)	ΔH_m (kJ/mol)	ΔS_m (J/mol K)
cis-**2**	278	276	37.8	69
trans-**2**	313	311	54.6	94
cis-**3**	270	263	46.7	87
trans-**3**	303	300	63.7	128
trans-**4**	321	314	58.9	99

5.3.3 Phase behavior of cis-trans binary mixtures

Knowing that evaluated isomers have different crystal structures we hypothesized that they may be immiscible in the solid state. Hence, it is possible for a mixture with a specified *cis*-to-*trans* ratio to exhibit eutectic transition. From the thermal analysis results for individual isomers, solid-liquid phase diagrams were calculated from the Schröder-van Laar equation (**Equation 5-1**),[205] where x_i is the mole fraction of the isomer i in the mixture, ΔH_{mi} is the heat of fusion of the pure compound i, R is the gas constant, T is variable temperature, and T_{mi} is the melting

temperature of compound i. Ideal behavior in the phase equilibrium was assumed, such that the activity coefficient (γ_i) value was set to 1. Mixtures with near-eutectic compositions based on the calculated phase diagrams were prepared from the previously isolated isomers.

$$ln(x_i, \gamma_i) = \frac{\Delta H_{mi}}{RT}\left(1 - \frac{T}{T_{mi}}\right) \qquad \textbf{Equation 5-1.}$$

Analysis of DSC curves for different *cis* to *trans* ratios was done based on the standard methodology used in the analysis of binary metallic alloys[206]. Here, the onset temperature of the lowest endo peak is denoted as the eutectic temperature (T_E), and the peak temperature of the highest endo peak is the liquidus temperature (T_L).

*5.3.3.1 Solid-liquid phase equilibrium of DDSQ-2((Me)(PA)) **2***

Binary mixtures of **2** were prepared using the FC method by gradual removal of *trans* isomers and their compositions reported within were estimated by NMR. Most DSC traces of **2** have two endo peaks corresponding to eutectic and liquidus transition (**Figure 5-4a**). It was observed the value of T_L decreases as the amount of *cis* isomer increases in the mixture up to the eutectic composition. When x_{trans} in the mixture reaches a value of 0.33, only one peak was resolved. The onset temperature of this DSC trace is very similar to the onset of the first endo peak in DSC traces for up 0.7 of x_{trans} as shown in **Figure 5-4a**. This T_{onset} represents a near-eutectic composition. Below the eutectic point, where x_{trans} = 0.20, the melting endotherm appears to be very broad and is representative of two overlapping melting endotherms. T_{onset} in the first endo peak agrees with the previously described eutectic temperature. For x_{trans} = 0.50 three endothermic transitions can be observed; it is hypothesized that cocrystal behavior was formed possibly by interactions between amine moieties. Experimental onset temperatures and liquidus temperatures were plotted, and a

solid-liquid binary phase diagram of varying *cis-to-trans* ratios was constructed as shown in Error! Reference source not found.**b**. The experimental results are relatively close to the ideal eutectic as described by **Equation 5-1**.

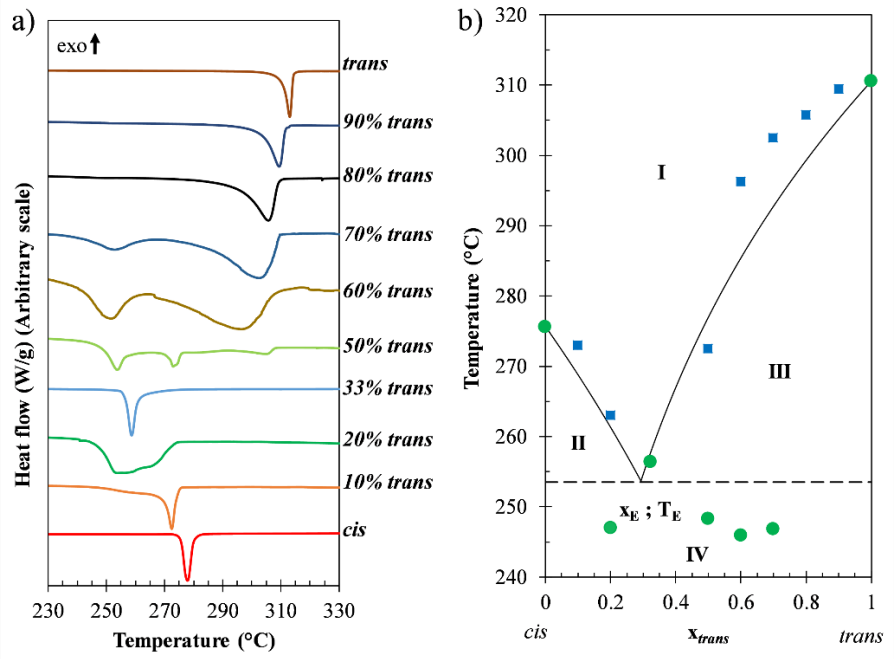

Figure 5-4. **a)** DSC curves for compound **2**. Every curve was normalized for better identification of peaks. The reported x_{trans} was estimated using NMR. **b)** Binary phase diagram for structure **2**. Green dots (●) are the onset temperatures of the first endothermic transition in DSC trace. Blue squares (■) represent the peak temperature of the highest endothermic transition. The solid line represents the ideal eutectic as calculated using **Equation 5-1**; dashed line (---) represents the calculated eutectic temperature T_E which matches the transition temperature observed using a sample with the predicted eutectic composition. Phase I: $L_{(cis\ +\ trans)}$; Phase II: $L_{(cis\ +\ trans)}$ + S_{cis}; Phase III: $L_{(cis\ +\ trans)}$ + S_{trans}; Phase IV: S_{cis} + S_{trans}.

*5.3.3.2 Solid-liquid phase equilibrium of DDSQ-2((Me)(PEP)) **3***

Phenylamine was replace with a larger non-polar PEP group to reduce possible polar interactions. Nearly-pure *cis*-**3** and nearly-pure *trans*-**3** were separated and their purities analyzed by ^{29}Si-NMR and HPLC using a hypercarb® column and ethyl acetate as mobile phase. The nearly-pure isomers were physically mixed, solubilized in THF and dried using a dynamic vacuum. Three mixtures were prepared with x_{trans} = 0.3, 0.5, and 0.7. DSC traces for nearly-pure

isomers and their binary mixtures can be observed in **Figure 5-5a**. The trace for x_{trans} = 0.3 has a single peak relatively sharp. In contrast, traces for x_{trans} = 0.5 and 0.7 have two endo peaks. For these traces, $T_{liquidus}$ was decreased as the fraction of *cis* isomer increased in the sample. T_{onset} in the first endotherm transition for x_{trans} = 0.5 and 0.7 is similar to that of x_{trans} = 0.3. This result is distinguishing for eutectic temperature. T_{onset} of nearly-pure *cis* is higher than T_{onset} of x_{trans} = 0.3 confirming the existence of a eutectic composition close to x_{trans} = 0.3. The calculated phase diagram is close to the collected data indicating proximity to ideal eutectic behavior for compound **3**. In **Figure 5-5b** are plotted the eutectic temperature and liquidus temperature for each mixture as well as the solid-liquid phase diagram. DSC traces for nearly-pure *cis* and nearly-pure *trans* in **Figure 5-5a** are similar to the same traces reported in a prior study[201]. However, the DSC trace for x_{trans} = 0.5 is inconsistent between this work and the work reported by Moore *et al.* as they overlooked the existence of the eutectic reaction.

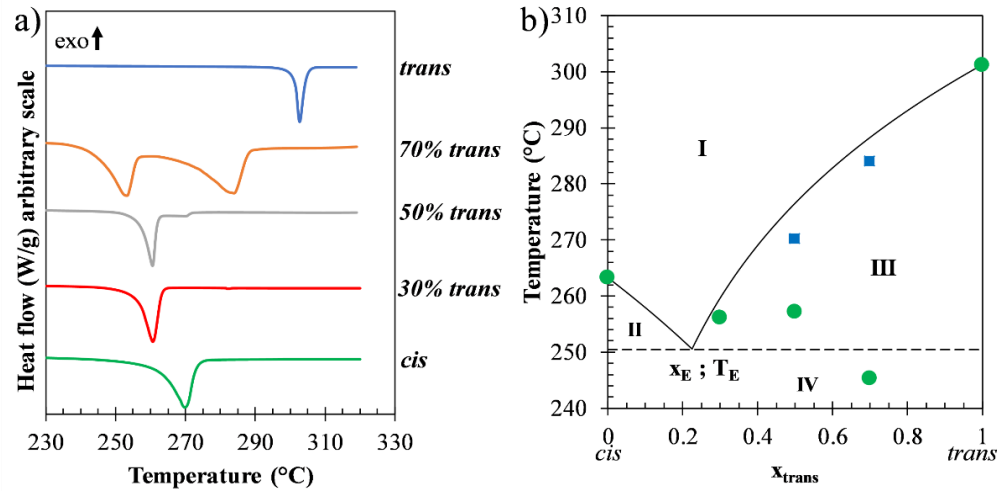

Figure 5-5. **a)** DSC curves for compound **3**. Every curve was normalized for better identification of peaks. **b)** Binary phase diagram for structure **3**. Green dots (●) are the onset temperatures of the first endothermic transition in DSC trace. Blue squares (■) represent the peak temperature of the highest endothermic transition. The solid line represents the ideal eutectic as calculated using **Equation 5-1**; dashed line (---) represents the calculated eutectic temperature $T_{E.}$. Phase I: $L_{(cis\ +\ trans)}$; Phase II: $L_{(cis\ +\ trans)}$ + S_{cis}; Phase III: $L_{(cis\ +\ trans)}$ + S_{trans}; Phase IV: S_{cis} + S_{trans}.

*5.3.4 Solid-liquid phase equilibrium of DDSQ-2((Me)(Ph)) **4***

Structure **4** was analyzed to reveal the phase behavior of a DDSQ structure with the smallest aryl group possible. After synthesis of **4**, *trans* isomers were progressively removed by FC. DSC trace for x_{trans} = 0.33 resulted in a single peak. Two endotherms were identified in all others including nearly-pure *trans*-**4**. $T_{liquidus}$ steadily decreased as the fraction of *cis* isomer increased up to x_{trans} = 0.33. T_{onset} of the first endo peak has similar value as the T_{onset} for the single peak observed in x_{trans} = 0.33, which represents the eutectic temperature (**Figure 5-6a**). For x_{trans} = 0.25, its DSC trace has a main peak and a shoulder. The first main peak has a T_{onset} similar to the eutectic temperature. The shoulder located between 275 °C and 285 °C is the $T_{liquidus}$ for the excess *cis* isomer-rich phase in the mixture. Pure *cis*-**4** was never isolated despite several crystallization attempts. It is believed that samples with compositions of *cis* isomers larger than 75% may be forming co-crystals making further removal of *trans-**4*** very difficult. The phase diagram in **Figure 5-6b** is near to the ideal for the hypereutectic *trans*-rich portion. The experimentally near-eutectic composition (x_{trans}=0.33) is extracted by fitting with the calculated trace for *trans*-**4**. The eutectic composition cannot be calculated due to the lack of available nearly-pure *cis*-**4**.

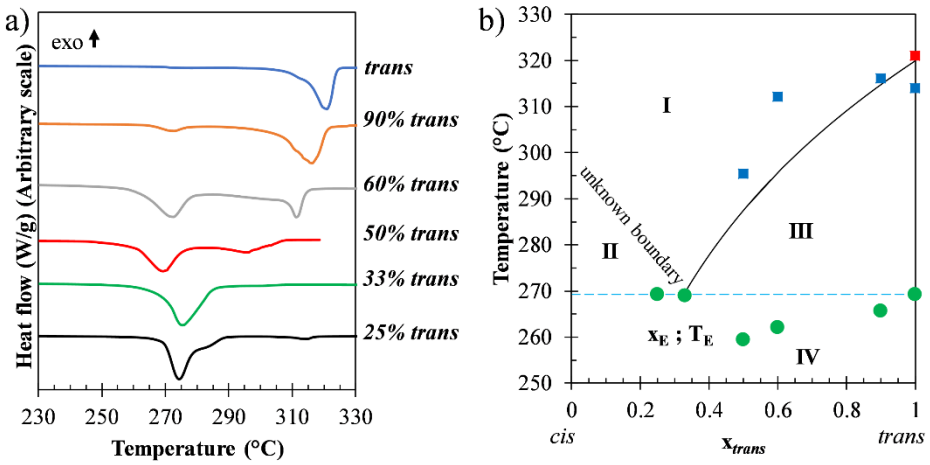

Figure 5-6. **a)** DSC curves for compound **4**. Every curve was normalized for better identification of peaks. **b)** Partial binary phase diagram for structure **4**. Green dots (●) are the onset temperatures of the first endothermic transition in DSC trace. Blue squares (■) represent the peak temperature of the highest endothermic transition. The solid line represents the ideal solid-liquid equilibrium, light blue dashed line (---) represents the experimental eutectic temperature T_E. For nearly-pure *trans*-**4** are depicted the nearly-eutectic temperature from the first endo peak(●), the onset temperature from the second endo peak(■), and the peak temperature from the second endo peak (■). Phase I: $L_{(cis + trans)}$; Phase II: $L_{(cis + trans)}$ + S_{cis}; Phase III: $L_{(cis + trans)}$ + S_{trans}; Phase IV: S_{cis} + S_{trans}.

5.4 Conclusions

Eutectic temperatures were observed for the DDSQ-2((Me)(R)) mixtures studied in this work. The eutectic composition was generally located near x_{trans} = 0.3. Excitingly, the eutectic temperature was on average 50 °C lower than the melting temperature of nearly-pure *trans* isomers. DSC traces for the composition obtained after reaction (x_{trans} = 0.5) have liquidus temperatures 20 °C larger than the temperatures in the eutectic composition. This result indicates that liquid processing of materials containing DDSQ-2((Me)(R)) is milder from a temperature perspective if a near-eutectic composition is used for such process. Onset temperature in the endothermic transition for nearly-pure and for nearly-eutectic composition is inversely proportional to the size of the R group. This result indicates that selection of high steric R groups will result in lower melting temperatures for the nearly-

pure isomers, as well as at the eutectic transition. These data allow users to tune the melting temperature of the materials by either adjusting the sterics in the system or by adjusting the ratio of *cis*-to-*trans* isomers.

CHAPTER 6.

SIGNIFICANCE AND PERSPECTIVES

6 Significance and perspectives

6.1 Significance

This research provides a new technique for separation of DDSQ mixtures. The most significant findings are listed in the following bullets.

- Using adsorption HPLC, *cis* and *trans* DDSQ isomers were resolved with optimal resolution of the elution by adjusting the solvent quality. Chromatograms obtained leaded to well defined peaks allowing quantitative analysis. Mixtures of isomers prepared from nearly-pure *cis* and nearly-pure *trans* were analyzed by HPLC; the ratio between the peak areas matched with the weighted ratio. Therefore, for the first time we were able to use HPLC for quantification of ratios in DDSQ isomeric mixtures.
- Mixtures containing DDSQ bonded with zero, one, and two hydroxyl groups were separated by HPLC using adsorption chromatography. It is believed that silanol groups in DDSQ structures are interacting with the silanol groups in the stationary phase. In consequence, DDSQ without hydroxyl groups migrates faster than DDSQ with a single hydroxyl group. Also, DDSQ with two hydroxyl groups eluted in longer times. Also, this was separated between *cis* and *trans* isomers confirming our previous finding. Exact quantification of the mixtures was performed by HPLC. The resultant ratio favors functionalization of DDSQ capped with the less bulk chlorosilane. A major finding in this research was the isolation for the first time of an asymmetric DDSQ.
- Linear adsorption isotherm parameters for the model mixture containing different number of hydroxyl groups in an analytical Si-HPLC column were obtained experimentally by frontal analysis of breakthrough curves. It was observed that the relation between the retention times and the adsorption isotherm parameters for the DDSQ in the mixture was linear. Thanks to this

linearity, adsorption parameters were extrapolated to preparative-LC packed with a commercial type of silica. Simulation in ASPEN chromatography was performed with the obtained parameters to estimate collection times in large-scale separations. Simulations predicted accurately the collection times to isolate highly-pure asymmetric DDSQ. The simulation was then validated by preparative-LC. This is the first time that DDSQ mixtures with different functionalities are separated in preparative-scale.

- DDSQ functionalized with *para*-phenylethynyl phenyl was separated easily between *cis* and *trans* by fractional crystallization. This was not the case for DDSQ functionalized with *para*-phenylamine or with phenyl. However, LC offered a solution for isolation of nearly-pure *cis* and *trans* fractions in the polar para-phenylamine DDSQ. Crystal structures showed that *cis* and *trans* isomers of DDSQ bonded to large groups have larger configuration differences and for instance larger solubility differences between them. Melting temperature differences were identified between nearly-pure *cis* and nearly-pure *trans* isomers and these differences are proportional to the structure density. Evaluation of mixtures with compositions about x_{trans} = 0.3 resulted in a single endotherm with low onset temperature compare with the nearly-pure isomers. This was recognized as the eutectic composition. In conclusion, *cis* and *trans* isomers are not miscible in the solid state and they obey the ideal mixing rule in the liquid state showing a eutectic composition. Besides, the size of the aryl moiety is inversely proportional to the melting temperature of pure isomers, and the eutectic temperature of binary isomeric mixtures.

6.2 Perspectives

- From a separation perspective it is proposed to evaluate other stationary phases for separation of isomer systems containing non-polar molecules. Separation of isomers and ternary mixtures of non-polar DDSQ compounds was achieved along this research with the use of a hypercarb

column when and aryl group was present in the structure. I think the use of partition chromatography using columns bonded with C_{30} could allow the separation of non-polar DDSQ isomers bonded with alkyl groups.

- Beyond separation, it is possible the synthesis of asymmetric DDSQ structures by a direct chemistry route. Currently, efforts to synthesize this material has been made in our research group using boron-siloxane bonds following a route consisting in protection, capping, deprotection, and second capping. This route has showed positive results but there are challenges related with premature deprotection caused by the capping solvents and reagents that should be perfected. I consider that other routes such as immobilization in solid-carbon substrates should be explored to achieve improved yields and reduce loss of starting material.
- Better understanding of DDSQ chemistry such as the effects of metals and solvents in the stability of the structures is suggested. Several reports in reported washed with methanol, but it is possible that byproducts of that washing could be harmful for the structures. Condensation of DDSQ-$(Ph)_8(OH)_4$ could be done with other solvents as we are currently exploring with DCM, as well as with other bases different than Et_3N. Along this research SOP for functionalization using THF and Et_3N was elaborated. Nevertheless, a paper describing the possible outcomes for DDSQ structures under different treatments will be highly appreciated for synthetic and training purposes. Finally, the identification of rate constants for DDSQ capping will be helpful to reduce reaction times in functionalization under THF considering the reactivity differences between chlorosilanes.
- Siloxane bonds to condense DDSQ structures can be done with chlorosilanes and methylallyloxysilanes. Silanes and other alkoxysilanes could be potentially used for capping.

These groups are less reactive and for instance more cleaning techniques could be done to avoid several issues related with the synthesis and isolation of chlorosilanes.

- DDSQ structures surrounded by other groups different than phenyl will allow better compatibility with organic compounds that are not constituted by aryl groups. From a material science perspective, synthesis of these DDSQ can broad the application spectrum for new materials and composites.
- Perspectives for asymmetric DDSQ structures are related with configuration of the functional groups to develop diverse grafting chemistry. I see these structures as modular building blocks with up to four connections for addition of different modules.
- Finally, solid-liquid behavior between binary or ternary mixtures of DDSQ structures closed with different groups could generate better understanding about miscibility in the liquid or in the solid phase. This knowledge is helpful for synthesis of DDSQ molecules that could serve as melting point depressors based on their chemical structure. Also, studies of ternary mixtures including an asymmetric structure allow understanding the effect of DDSQ as compatibilizers between two otherwise immiscible structures.

APPENDICES

APPENDIX A.

SYNTHETIC PROCEDURES

A. Synthetic procedures

General Procedure A.

In a 250 mL flask purged with dry N_2 for 15 minutes, DDSQ-$(Ph)_8(OH)_4$ (**1**) (2 g, 1.87 mmol, 1 equiv) was dissolved in THF (60 mL) at room temperature. Dichlorosilane or trichlorosilane (3.74 mmol, 2 equiv.) was added to the DDSQ-$(Ph)_8(OH)_4$ solution. Et_3N (1.04 mL, 7.48 mmol, 4 equiv.) was added dropwise to the stirring solution. The addition of triethylamine took 5 minutes in total; a cloudy white suspension was formed and stirred for 4 hours. The solution was then filtered through a fine fritted-funnel-filter to remove the solid triethylamine hydrochloride. The solution was dried in a rotary evaporator and then passed through a silica-gel column using DCM as the solvent. The volatiles was removed from the resulting solution and further dried at 0.4 mbar and 50 °C for 12 hours to afford DDSQ-2((CH_3)(R)) as a white powder. It should be noted the reported spectra are of the *cis*/*trans* mixtures.

*Synthesis of $(C_6H_5)_8Si_{10}O_{14}(CH_3)_2(H)_2$ 7,17-dimethyl-7,17-dihydro-1,3,5,9,11,13,15,1-octaphenylhexacyclo[9.13.1^{1,9}.1^{3,15}.1^{5,13}.1^{11,19}]decasiloxane (Compound **AA1**)*

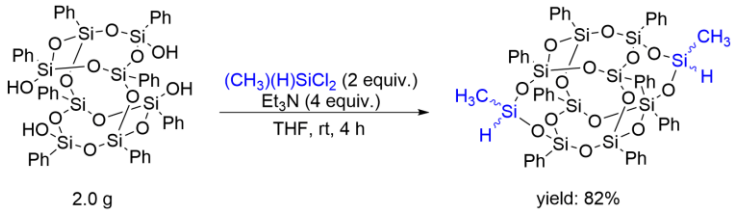

Scheme A-1. Synthesis of DDSQ-2((methyl)(hydro))

Compound **AA1** was synthesized using the general procedure A with $(CH_3)(H)SiCl_2$ (3.74 mmol, 0.39 mL, 2 equiv). This provided 1.78 g (82% yield) of compound **AA1** as a white powder.

^{1}H NMR (500 MHz, $CDCl_3$): $\boldsymbol{\delta}_H$ 0.37 (6H), 5.03 (2H), 7.16-7.56 (40H).

^{13}C NMR (125 MHz, $CDCl_3$): $\boldsymbol{\delta}_C$ 134.27, 134.11, 134.07, 134.04, 133.94, 131.60, 130.83, 130.76, 130.70, 130.52, 130.43, 130.41, 127.86, 127.70, 127.67, 127.64, 0.67.

^{29}Si NMR (99 MHz, $CDCl_3$): $\boldsymbol{\delta}_{Si}$ -32.77 (2Si), -77.81 (4Si), -79.09 (*cis*, 1Si), -79.30 (*trans*, 2Si), -79.50 (*cis*, 1Si).

*Synthesis of $(C_6H_5)_8Si_{10}O_{14}(CH_3)_2(CH_3)_2$ 7,7,17,17-tetramethyl-1,3,5,9,11,13,15,1-octaphenylhexacyclo[9.13.1^{1,9} .1^{3,15} .1^{5,13} .1^{11,19}]decasiloxane (Compound **AA2**)*

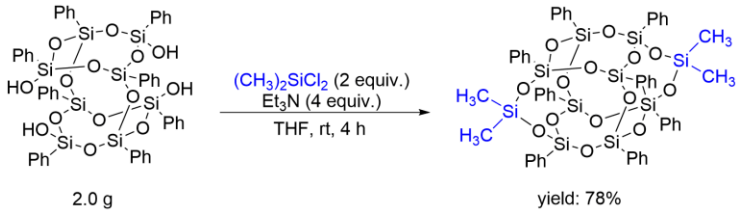

Scheme A-2. Synthesis of DDSQ-2(methyl)$_2$

Compound **AA2** was synthesized using the general procedure A with $(CH_3)_2SiCl_2$ (3.74 mmol, 0.46 mL, 2 equiv). This provided 1.72 g (78% yield) of compound **AA2** as a white powder.

^{1}H NMR (500 MHz, $CDCl_3$): $\boldsymbol{\delta}_H$ 0.39 (12H), 7.16-7.56 (40H).

^{13}C NMR (125 MHz, $CDCl_3$): $\boldsymbol{\delta}_C$ 134.30, 134.10, 133.98, 132.17, 131.13, 130.37, 127.83, 127.68, 0.61.

^{29}Si NMR (99 MHz, $CDCl_3$): $\boldsymbol{\delta}_{Si}$ -16.52 (2Si), -78.57 (4Si), -79.56 (4Si).

Synthesis of $(C_6H_5)_8Si_{10}O_{14}(CH_3)_2(CHCH_2)_2$ *7,17-dimethyl-7,17-divinyl-1,3,5,9,11,13,15,1-octaphenylhexacyclo[9.13.*$1^{1,9}$ *.*$1^{3,15}$ *.*$1^{5,13}$ *.*$1^{11,19}$ *]decasiloxane (Compound* ***AA3****)*

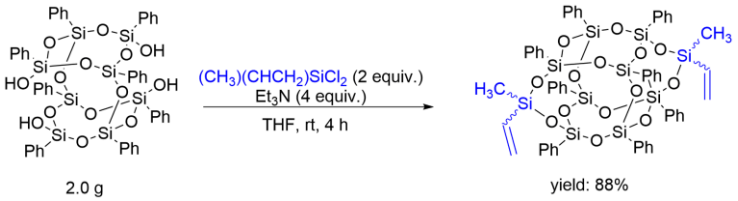

Scheme A-3. Synthesis of DDSQ-2((methyl)(vinyl))

Compound **AA3** was synthesized using the general procedure A with $(CH_3)(CHCH_2)SiCl_2$ (3.74 mmol, 0.48 mL, 2 equiv). This provided 2.00 g (88% yield) of compound AA3 as a white powder.

^{1}H NMR (500 MHz, $CDCl_3$): $\boldsymbol{\delta}_H$ 0.37 (6H), 5.91-6.01 (4H), 6.12-6.19 (2H) 7.16-7.56 (40H).

^{13}C NMR (125 MHz, $CDCl_3$): $\boldsymbol{\delta}_C$ 135.07, 134.33, 133.96, 133.95, 133.94, 133.84, 131.80, 130.90, 130.87, 130.84, 130.25, 130.21, 130.17, -1.26.

^{29}Si NMR (99 MHz, $CDCl_3$): $\boldsymbol{\delta}_{Si}$-31.39 (2Si), -78.37 (4Si), -79.55 (4Si*)*

^{29}Si NMR (99 MHz, Acetone-D_6): $\boldsymbol{\delta}_{Si}$ -31.08 (2Si), -78.07 (4Si), -79.26 (*cis*, 1Si*)*, -79.30 (*trans*, 2Si), -79.35 (*cis*, 1Si).

*Synthesis of $(C_6H_5)_8Si_{10}O_{14}(CH_3)_2(CH_2CH_2CH_2Cl)_2$ 7,17-dimethyl-7,17-chloropropyl-1,3,5,9,11,13,15,1-octaphenylhexacyclo[9.13.1^{1,9} .1^{3,15} .1^{5,13} .1^{11,19}]decasiloxane (Compound **AA4**)*

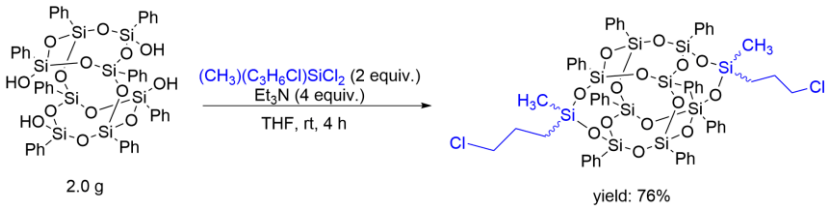

Scheme A-4. Synthesis of DDSQ-2((methyl)(3-propyl chloride))

Compound **AA4** was synthesized using the general procedure A with $(CH_3)(C_3H_6Cl)SiCl_2$ (3.74 mmol, 0.59 mL, 2 equiv). This provided 1.86 g (76% yield) of compound **AA4** as a white powder.

^{1}H NMR (500 MHz, $CDCl_3$): $\boldsymbol{\delta}_H$ 0.31 (6H), 0.83-0.86 (4H), 1.83-1.89 (4H) 3.37-3.40 (4H), 7.18-7.54 (40H).

^{13}C NMR (125 MHz, $CDCl_3$): $\boldsymbol{\delta}_C$ 134.29, 134.13, 134.11, 134.09, 134.07, 134.05, 133.92, 131.82, 130.94, 130.85, 130.77, 130.52, 130.50, 130.47, 127.92, 127.76, 47.50, 26.41, 14.42, -0.84 (d, J = 1.4 Hz).

^{29}Si NMR (99 MHz, $CDCl_3$): $\boldsymbol{\delta}_{Si}$ -18.29 (2Si), -78.46 (4Si), -79.37 (*cis*, 1Si), -79.41 (*trans*, 2Si), -79.46 (*cis*, 1Si).

*Synthesis of $(C_6H_5)_8Si_{10}O_{14}(CH_3)_2(OH)_2$ 7,17-dimethyl-7,17-diol-1,3,5,9,11,13,15,1-octaphenylhexacyclo[9.13.1^{1,9} .1^{3,15} .1^{5,13} .1^{11,19}]decasiloxane (Compound **BB**)*

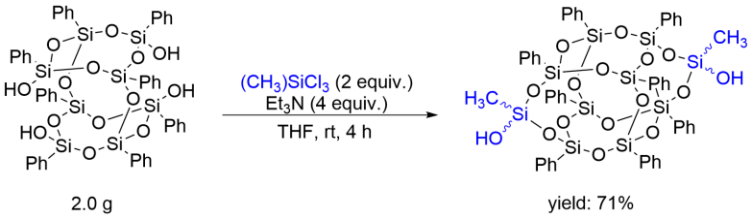

Scheme A-5. Synthesis of DDSQ-2((methyl)(hydroxyl))

Compound **BB** was synthesized using the general procedure A with $(CH_3)SiCl_3$ (3.74 mmol, 0.49 mL, 2 equiv). This provided 1.58 g (71% yield) of compound **BB** as a white powder.

^{1}H NMR (500 MHz, $CDCl_3$): $\boldsymbol{\delta}_H$ 0.35 (6H), 7.16-7.57 (40H).

^{13}C NMR (125 MHz, $CDCl_3$): $\boldsymbol{\delta}_C$ 134.09, 134.05, 134.01, 133.96, 131.37, 130.67, 130.61, 130.59, 130.55, 130.53, 127.89, 127.76, 127.73, 127.71, -3.84.

^{29}Si NMR (99 MHz, $CDCl_3$): $\boldsymbol{\delta}_{Si}$ -53.99 (2Si), -78.59 (4Si), -79.03 (*cis*, 1Si), -79.14 (*trans*, 2Si), -79.24 (*cis*, 1Si).

General procedure B

In a 250 mL flask purged with dry N_2 for 15 minutes, DDSQ-$(Ph)_8(OH)_4$ (**1**) (2g, 1.87 mmol) was dissolved in THF (60 mL) at room temperature. $(CH_3)(R)SiCl_2$ (1.87 mmol, 1 equiv.) and $(CH_3)SiCl_3$ (1.87 mmol, 0.24 mL, 1 equiv.) were added to the DDSQ-$(Ph)_8(OH)_4$ solution and stirred for 5 minutes.Et_3N (1.04 mL, 7.48 mmol, 4 equiv.) was added dropwise to the stirring solution. The addition of triethylamine took 5 minutes in total which created a cloudy white suspension which was stirred continuously for additional four hours. After, the solution was filtered through a fine fritted-funnel-filter to remove the solid triethylamine hydrochloride. Volatiles was removed from the resulting solution which produced a white powder. The powder was dissolved in a minimum amount of DCM and passed through a silica-gel column using DCM as the solvent. The silica column hydrolyzed the chlorosilanes into silanols which were isolated. The three separated products were dried at 0.4 mbar and 50 °C for 12 hours.

*Synthesis of $(C_6H_5)_8Si_{10}O_{14}(CH_3)(OH)(CH_3)(H)$ 7,17-dimethyl-7-hydro-17-ol-1,3,5,9,11,13,15,1-octaphenylhexacyclo[9.13.1^{1,9} .1^{3,15} .1^{5,13} .1^{11,19}]decasiloxane (Compound **AB1**)*

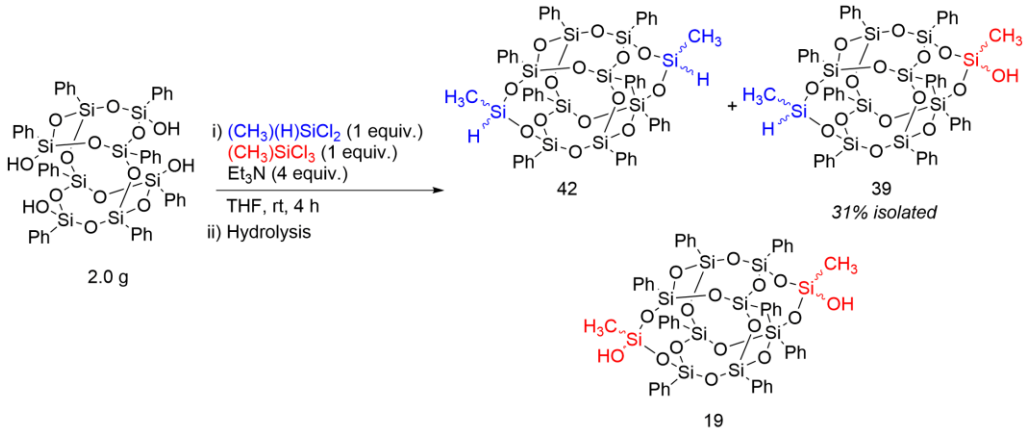

Scheme A-6. Synthesis of DDSQ-(methyl)(hydro)(methyl)(hydroxyl)

Compound **AB1** was synthesized using the general procedure B with $(CH_3)(H)SiCl_2$ (1.87 mmol, 0.19 mL, 1 equiv). This procedure produced compounds **AA1**, **AB1**, and **BB** (1.66 g, 80% yield) in a ratio of 42:39:19 respectively. Compound **AB1** was isolated as a white powder (0.65 g, 31% yield).

^{1}H NMR (500 MHz, $CDCl_3$): $\boldsymbol{\delta}_H$ 0.35 (3H), 0.37 (3H), 4.99 (1H) 7.16-7.58 (40H)

^{13}C NMR (125 MHz, $CDCl_3$): $\boldsymbol{\delta}_C$ 134.08, 134.05, 134.04, 134.01, 133.95, 133.92, 131.52, 131.42, 130.73, 130.68, 130.67, 130.62, 130.55, 130.52, 130.47, 130.45, 127.86, 127.85, 127.71, 127.69, 127.68, 127.66, 0.64, -3.86 (d, J = 1.4 Hz).

^{29}Si NMR (99 MHz, $CDCl_3$): $\boldsymbol{\delta}_{Si}$ -32.71 (1Si), -54.02 (1Si), -77.60 (2Si), -78.78 (2Si), -79.06 (1Si), -79.15 (1Si), -79.26 (1Si), -79.36 (1Si).

MS (APCI) *m/z* $[M+H]^+$: calculated 1169.07 found 1169.06

*Synthesis of $(C_6H_5)_8Si_{10}O_{14}(CH_3)(OH)(CH_3)(CH_3)$ 7,7,17-dimethyl-17-ol-1,3,5,9,11,13,15,1-octaphenylhexacyclo[9.13.1^{1,9} .1^{3,15} .1^{5,13} .1^{11,19}]decasiloxane (Compound **AB2**)*

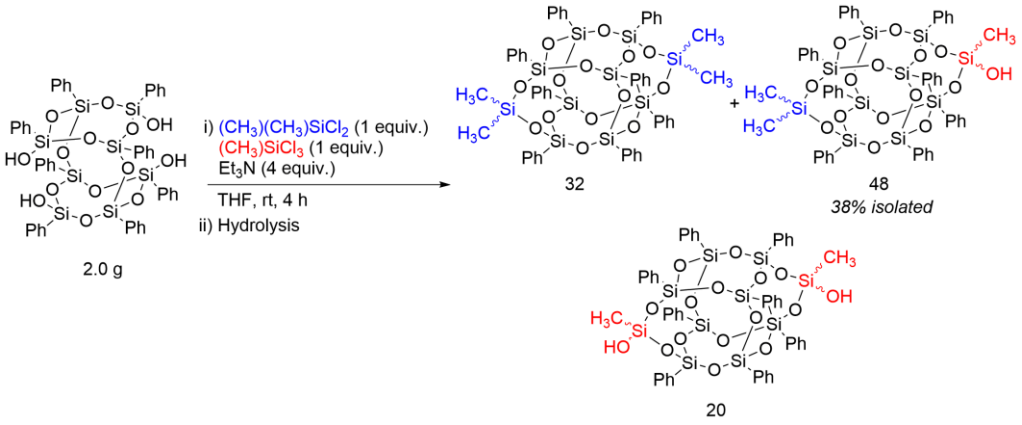

Scheme A-7. DDSQ-(methyl)$_2$(methyl)(hydroxyl)

Compound **AB2** was synthesized using the general procedure for DDSQ symmetric and asymmetric mixtures using $(CH_3)(CH_3)SiCl_2$ (1.87 mmol, 0.23 mL, 1 equiv). This procedure produced compounds **AA2**, **AB2**, and **BB** (1.67 g, 79% yield) in a ratio of 32:48:20 respectively. Compound **AB2** was isolated as a white powder (0.80 g, 38% yield).

^{1}H NMR (500 MHz, $CDCl_3$): $\boldsymbol{\delta}_H$ 0.32 (6H), 0.35 (3H), 7.14-7.46 (40H)

^{13}C NMR (125 MHz, $CDCl_3$): $\boldsymbol{\delta}_C$ 134.17, 134.13, 134.08, 134.02, 132.11, 131.60, 130.97, 130.92, 130.63, 130.54, 130.51, 127.95, 127.93, 127.80, 127.78, 0.67, -3.72.

^{29}Si NMR (99 MHz, $CDCl_3$): $\boldsymbol{\delta}_{Si}$ -16.35 (1Si), -54.07 (1Si), -78.45 (2Si), -78.64 (2Si), -79.26 (2Si), -79.36 (2Si).

MS (APCI) *m/z* $[M+H]^+$: calculated 1183.08 found 1183.07

*Synthesis of $(C_6H_5)_8Si_{10}O_{14}(CH_3)(OH)(CH_3)(CHCH_2)$ 7,17-dimethyl-7-vinyl-17-ol-1,3,5,9,11,13,15,1-octaphenylhexacyclo[9.13.1^{1,9} .1^{3,15} .1^{5,13} .1^{11,19}]decasiloxane (Compound **AB3**)*

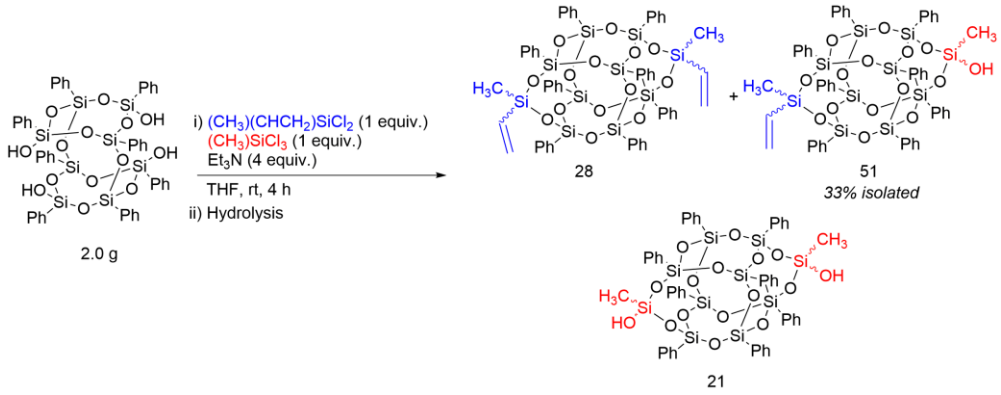

Scheme A-8. DDSQ-(methyl)(vinyl)(methyl)(hydroxyl)

Compound **AB3** was synthesized using the general procedure for DDSQ symmetric and asymmetric mixtures using $(CH_3)(CHCH_2)SiCl_2$ (1.87 mmol, 0.24 mL, 1 equiv). This procedure produced compounds **AA3**, **AB3**, and **BB** (1.43 g, 64% yield) in a ratio of 28:51:21 respectively. Compound **AB3** was isolated as a white powder (0.73 g, 33% yield).

^{1}H NMR (500 MHz, $CDCl_3$): $\boldsymbol{\delta}_H$ 0.35 (3H), 0.37 (3H), 5.91-6.02 (2H), 6.12-6.19 (1H), 7.16-7.58 (40H)

^{13}C NMR (125 MHz, $CDCl_3$): $\boldsymbol{\delta}_C$ 135.12, 134.49, 134.06 (d, J = 1.4 Hz), 134.03 (d, J = 1.6 Hz), 133.95, 133.94, 131.80, 131.46, 130.83, 130.79, 130.73, 130.71, 130.51, 130.42, 127.83, 127.79, 127.69, 127.67, 127.64, 127.62, -1.16, -3.88.

^{29}Si NMR (99 MHz, $CDCl_3$): $\boldsymbol{\delta}_{HSi}$ -31.29 (1Si), -54.03 (1Si), -78.32 (2Si), -78.67 (2Si), -79.30 (2Si), -79.42 (2Si).

^{29}Si NMR (99 MHz, Acetone-D_6): $\boldsymbol{\delta}_{Si}$ -31.10 (1Si), -55.65 (1Si), -78.04 (2Si), -78.86 (2Si), -79.19 (1Si), -79.24 (1Si), -79.35 (1Si), -79.40 (1Si).

MS (APCI) *m/z* $[M+H]^+$: calculated 1195.08 found 1195.09

*Synthesis of $(C_6H_5)_8Si_{10}O_{14}(CH_3)(OH)(CH_2CH_2CH_2Cl)(CH_3)$ 7,17-dimethyl-7-chloropropyl-17-ol-1,3,5,9,11,13,15,1-octaphenylhexacyclo[9.13.1^{1,9} .1^{3,15} .1^{5,13} .1^{11,19}]decasiloxane (Compound **AB4**)*

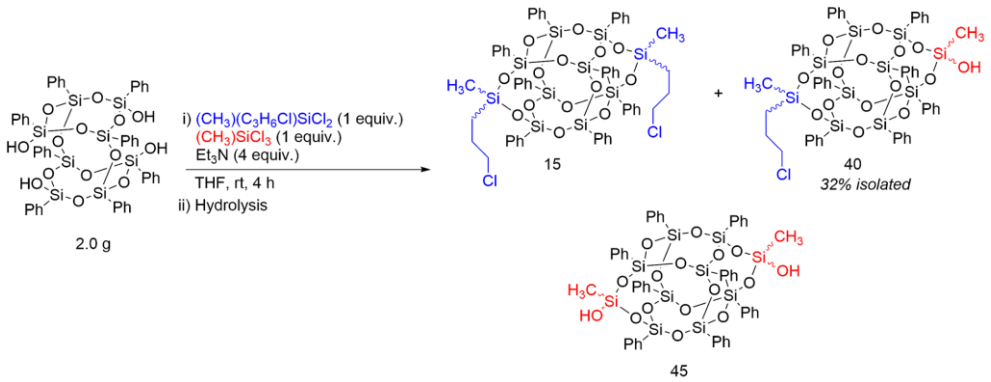

Scheme A-9. DDSQ-(methyl)(3-propyl chloride)(methyl)(hydroxyl)

Compound **AB4** was synthesized using the general procedure for DDSQ symmetric and asymmetric mixtures using $(CH_3)(C_3H_6Cl)SiCl_2$ (1.87 mmol, 0.29 mL, 1 equiv). This procedure produced compounds **AA4**, **AB4**, and **BB** (1.23 g, 62% yield) in a ratio of 15:40:45 respectively. Compound **AB4** was isolated as a white powder (0.47 g 20% yield).

^{1}H NMR (500 MHz, $CDCl_3$): $\boldsymbol{\delta}_H$ 0.33 (3H), 0.35 (3H), 0.83-0.86 (2H), 1.84-1.89 (2H), 3.37-3.39 (2H), 7.16-7.58 (40H)

^{13}C NMR (125 MHz, $CDCl_3$): $\boldsymbol{\delta}_C$ 134.16, 134.14, 134.12, 134.10, 134.06, 133.97, 131.84, 131.50, 130.88, 130.82, 130.78, 130.73, 130.66, 130.61, 130.58, 127.99, 127.97, 127.84, 127.83, 127.82, 127.80, 47.54, 26.47, 14.47, -0.78, -3.74.

^{29}Si NMR (99 MHz, $CDCl_3$): $\boldsymbol{\delta}_{Si}$ -18.14 (1Si), -54.08 (1Si), -78.36 (2Si), -78.65 (2Si), -79.16 (1Si), -79.22 (1Si), -79.27 (1Si), -79.32 (1Si).

MS (APCI) *m/z* $[M+H]^+$: calculated 1245.08 found 1245.08

*General procedure for synthesis of $(C_6H_5)_8Si_{10}O_{14}(CH_3)(OH)(CH_3)(H)$ 7,17-dimethyl-7-hydro-17-ol-1,3,5,9,11,13,15,1-octaphenylhexacyclo[9.13.$1^{1,9}$.$1^{3,15}$.$1^{5,13}$.$1^{11,19}$]decasiloxane (Compound **AB1**) varying the chlorosilanes equivalents*

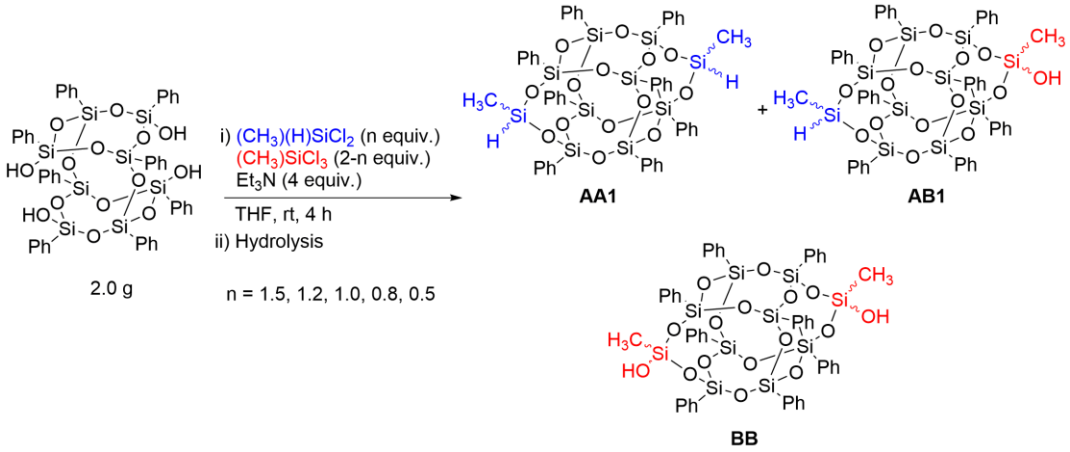

Scheme A-10. DDSQ-(methyl)(hydro)(methyl)(hydroxyl) varying equivalents

Compound **AB1** was synthesized using the general procedure B varying the mol equivalents for $(CH_3)(H)SiCl_2$ between 0.5, 0.8, 1.0, 1.2, and 1.5 equiv. $(CH_3)SiCl_3$ was added to complete 2 equiv. of chlorosilanes. This procedure produced compounds **AA1**, **AB1**, and **BB** in different ratios. Compound **AB1** was isolated in the four cases as a white powder.

^{1}H NMR (500 MHz, $CDCl_3$): $\boldsymbol{\delta}_H$ 0.35 (3H), 0.37 (3H), 4.99 (1H) 7.16-7.58 (40H)

^{13}C NMR (125 MHz, $CDCl_3$): $\boldsymbol{\delta}_C$ 134.08, 134.05, 134.04, 134.01, 133.95, 133.92, 131.52, 131.42, 130.73, 130.68, 130.67, 130.62, 130.55, 130.52, 130.47, 130.45, 127.86, 127.85, 127.71, 127.69, 127.68, 127.66, 0.64, -3.86 (d, J = 1.4 Hz).

^{29}Si NMR (99 MHz, $CDCl_3$): $\boldsymbol{\delta}_{Si}$ -32.71 (1Si), -54.02 (1Si), -77.60 (2Si), -78.78 (2Si), -79.06 (1Si), -79.15 (1Si), -79.26 (1Si), -79.36 (1Si).

MS (APCI) *m/z* $[M+H]^+$: calculated 1169.07 found 1169.06

APPENDIX B.

PERCENTAGES AFTER SEPARATION OF MIXTURES WITH ZERO, ONE, AND TWO HYDROXYL GROUPS

B. Percentages after separation of mixtures with zero, one, and two hydroxyl groups

Table B-1. Isolated yield after column for components in the ternary mixture

$H(CH_3)SiCl_2$: $(CH_3)SiCl_3$	**AA1** (%)		**AB1** (%)		**BB** (%)	
	HPLC	Mass	HPLC	Mass	HPLC	Mass
1.5 : 0.5	64.1	65.1	26.7	27.9	9.2	7.0
1.2 : 0.8	49.5	42.3	37.1	45.4	13.4	12.3
1 : 1	42.0	45.2	38.8	32.5	19.2	22.2
0.8 : 1.2	36.6	24.3	44.9	50.7	18.5	25
0.5 : 1.5	6.4	6.0	28.9	30.0	64.7	64.0

APPENDIX C.

TLC FOR SEPARATION OF DDSQ MIXTURE WITH EACH SEPARATED FRACTION

C. TLC for separation of DDSQ mixture with each separated fraction

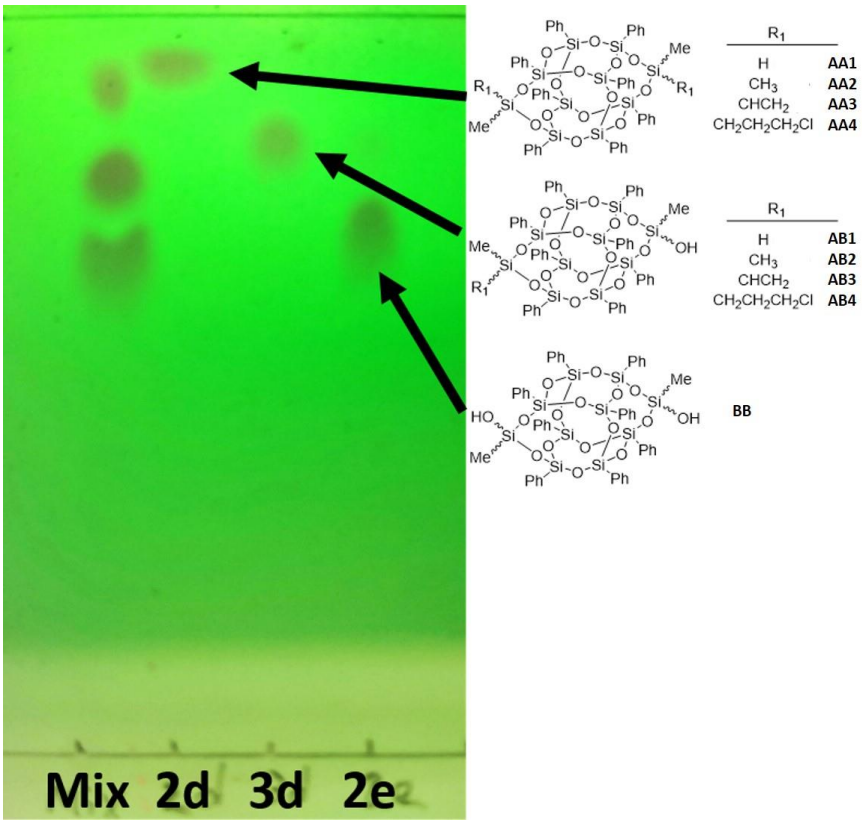

Figure C-1. TLC after separation of ternary DDSQ mixture

APPENDIX D.

STRUCTURAL ANALYSIS OF AB1-D BY ^{29}Si-NMR AND MASS SPECTROSCOPY

D. Structural analysis of AB1-D by ^{29}Si-NMR and mass spectroscopy

Structural Analysis for asymmetric compounds

The ^{29}Si-NMR for **3** *$(C_6H_5)_8Si_{10}O_{14}(CH_3)_2(R)(OH)$* have eight peaks. Each Si atom was numbered in **Figure 2** for reader clarity. Si#1 bonded to R was expected to be between -10 and -40 ppm this peak is typical for silicas linked to two oxygens and two carbons. Si#2 bonded to hydroxyl group was expected to be between -50 and -60 ppm. This is a common value for silicon atoms connected to one carbon and three oxygens, being one of them a hydroxyl group. Assuming there is a *cis* and a *trans* configuration, six peaks between -70 and -80 ppm were expected for the eight Si atoms forming the DDSQ corners. One of this peaks was assigned to two silicon atoms Si#3 in proximity to the edge capped with $(CH_3)(R)SiCl_2$. The other peak was assigned to two silicon atoms Si#4 in proximity to the edge capped with $(CH_3)SiCl_3$. The remaining four peaks were assigned to the four silicas Si#5a, Si#5b, Si#6a, and Si#6b in the corners exposed to four different environments. First peak for the environment containing R and OH (Si#5a, *cis*), a second peak for the environment having two CH_3 groups (Si#5b *cis*), a third peak for the environment involving R and CH_3 (Si#6a *trans*) and a fourth peak for OH and CH_3 (Si#6b *trans*) in the same environment. Exact molecular mass was determined using the mass spectroscopy for each *$(C_6H_5)_8Si_{10}O_{14}(CH_3)_2(R)(OH)$*. The theoretical mass matched with the exact mass found in the spectrum when one unit was subtracted from the experimental value due to the presence of a proton ionizing the molecule.

LC could not separate a mixture of cages synthesized following the general procedure B with R as H and 3-chloropropylmethyldichlorosilane instead of the methyltrichlorosilane. The resultant product after the column resulted in one single spot by TLC. ^{1}H-NMR, ^{13}C-NMR, and ^{29}Si-NMR were used to analyze the product. ^{29}Si-NMR spectra showed extra peaks in the

region between -77 ppm and -80 ppm plus the peaks for products **AA1** and **AA4**. The region between 0 ppm and -40 ppm have two peaks near the -18 ppm region and two peaks near the -32 ppm region. Two of the four mentioned peaks are the characteristic peaks for the Si atom capped at the edges of products **AA1** and **BB**. The two other peaks suggest the presence of an extra product possibly a DDSQ cage with hydrogen and methyl to one side, and 3-chloropropyl and methyl to the other side.

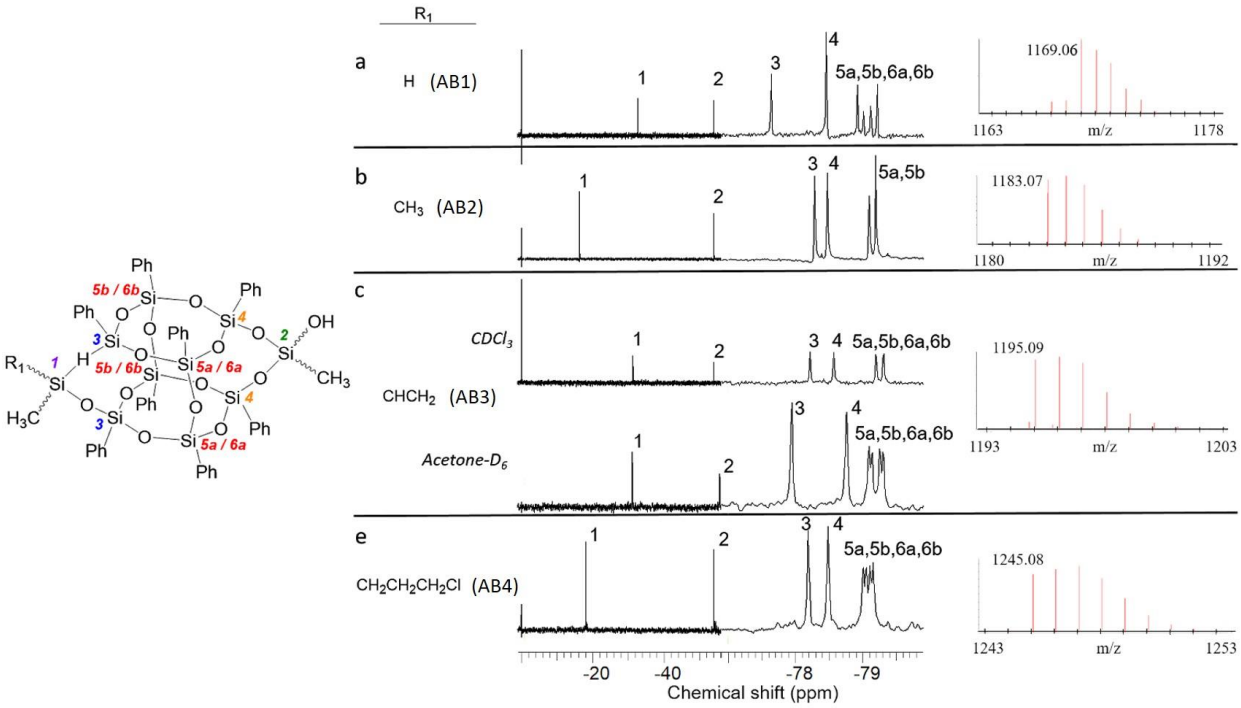

Figure D-1. ^{29}Si-NMR and mass spectrums obtained after characterization of DDSQ-(methyl)(R)(methyl)(hydroxyl) products obtained as the second fraction of the separation by LC of DDSQ mixtures. a) R = hydrogen, b) R = methyl, c) R = vinyl, d) R = 3-propyl chloride.

APPENDIX E.

STRUCTURAL ANALYSIS OF A NON - POLAR MIXTURE BY ^{29}Si NMR

E. Structural analysis of a non - polar mixture by ^{29}Si NMR

Analysis of a non-polar ternary mixture

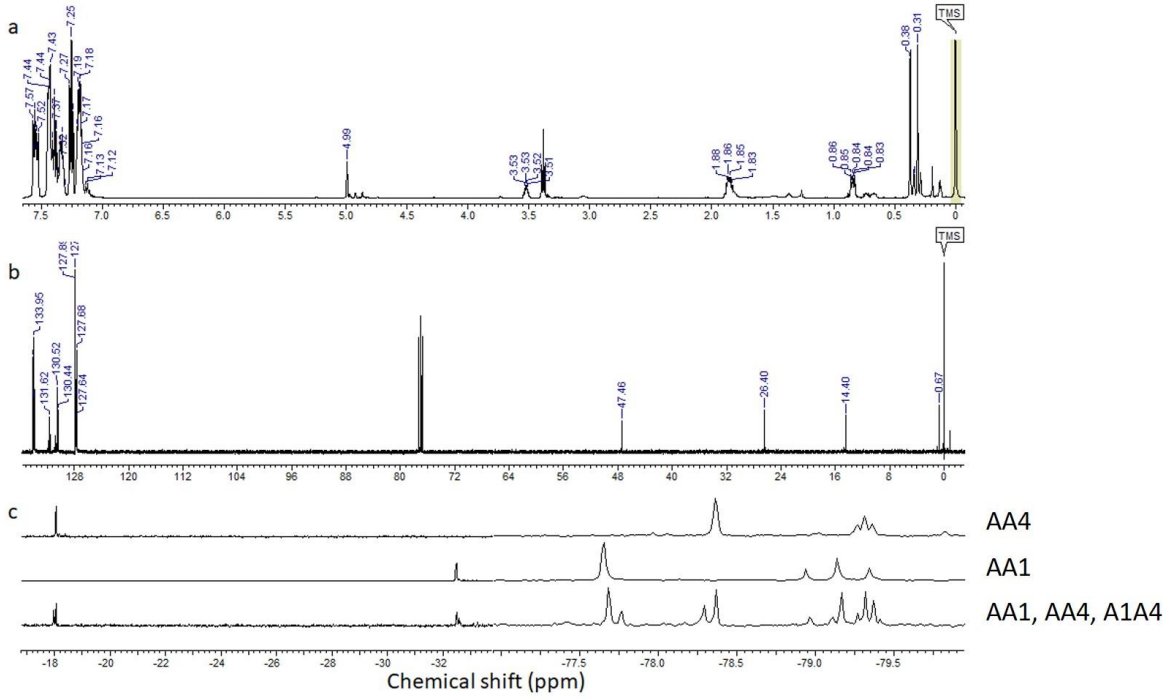

Figure E-1. ^{1}H (a), ^{13}C (b), and ^{29}Si-NMR (c), for non-polar mixture of DDSQ-2((methyl)(hydro)) AA1, DDSQ-2(methyl)(3-propyl chloride) AA4, and DDSQ-(methyl)(hydro)(methyl)(3-propyl chloride) A1A4 synthesized from $Cl_2Si(H)(CH_3)$ and $Cl_2Si(CH_2CH_2CH_2Cl)(CH_3)$. ^{29}Si-NMR is compared against pure AA1 and pure AA4 obtained following general procedure B. This mixture is not separable by the methods employed in this work due to lack of polar moieties in the functionalized DDSQ.

APPENDIX F.

KINETIC ANALYSIS OF DDSQ-$(PH)_8(OH)_4$ SIDE-CAPPED WITH DICHLOROSILANES WITH DIFFERENT STERIC GROUPS

F. Kinetic analysis of DDSQ-$(Ph)_8(OH)_4$ side-capped with dichlorosilanes with different steric groups

Conversion of DDSQ-$(Ph)_8(OH)_4$ to DDSQ-$2(Ph)_2$ analyzed by ^1H NMR at different times

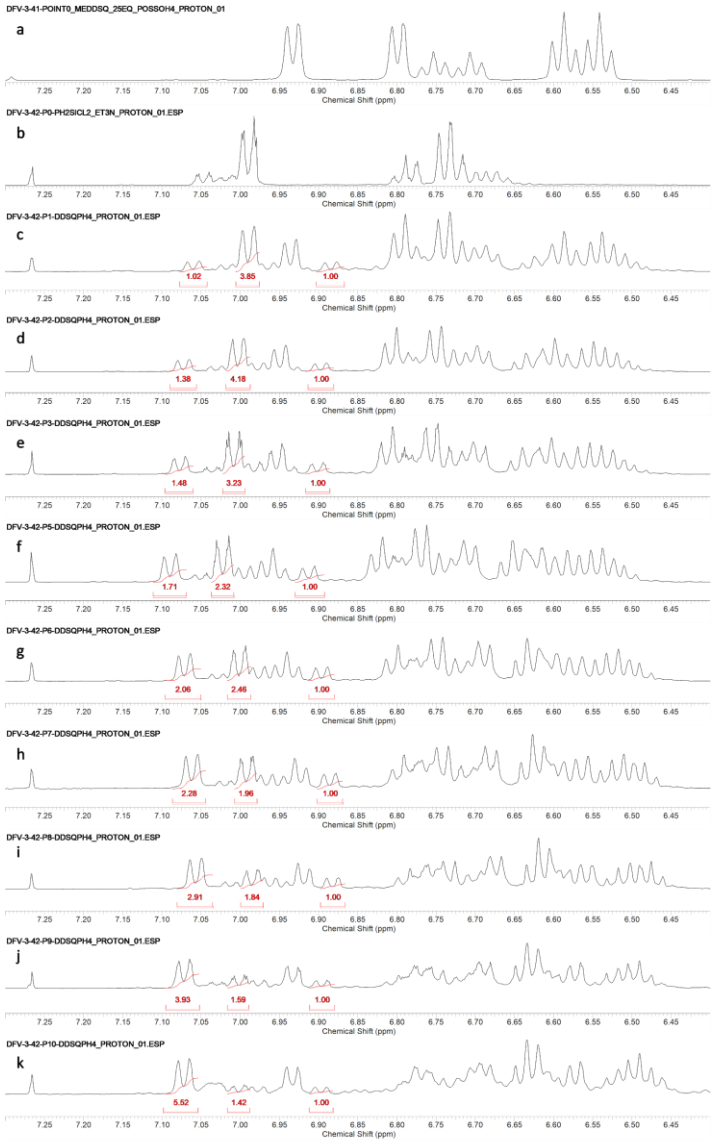

Figure F-1. Conversion of DDSQ-$(Ph)_8(OH)_4$ to DDSQ-$2(Ph)_2$ in different times analyzed by ^{1}H-NMR (500 MHz, $CDCl_3$) after quench with MeOH: a = DDSQ-$(Ph)_8(OH)_4$, b = Ph_2SiCl_2, c = 0.67 min , d = 1.35 min, e = 2.03 min, f = 4.63 min, g = 6.85 min, h = 10.83 min, i = 20 min, j = 36 min, k = 100 min

Conversion of DDSQ-$(Ph)_8(OH)_4$ to DDSQ-2$(Ph)_2$ analyzed by ^{29}Si NMR at different times

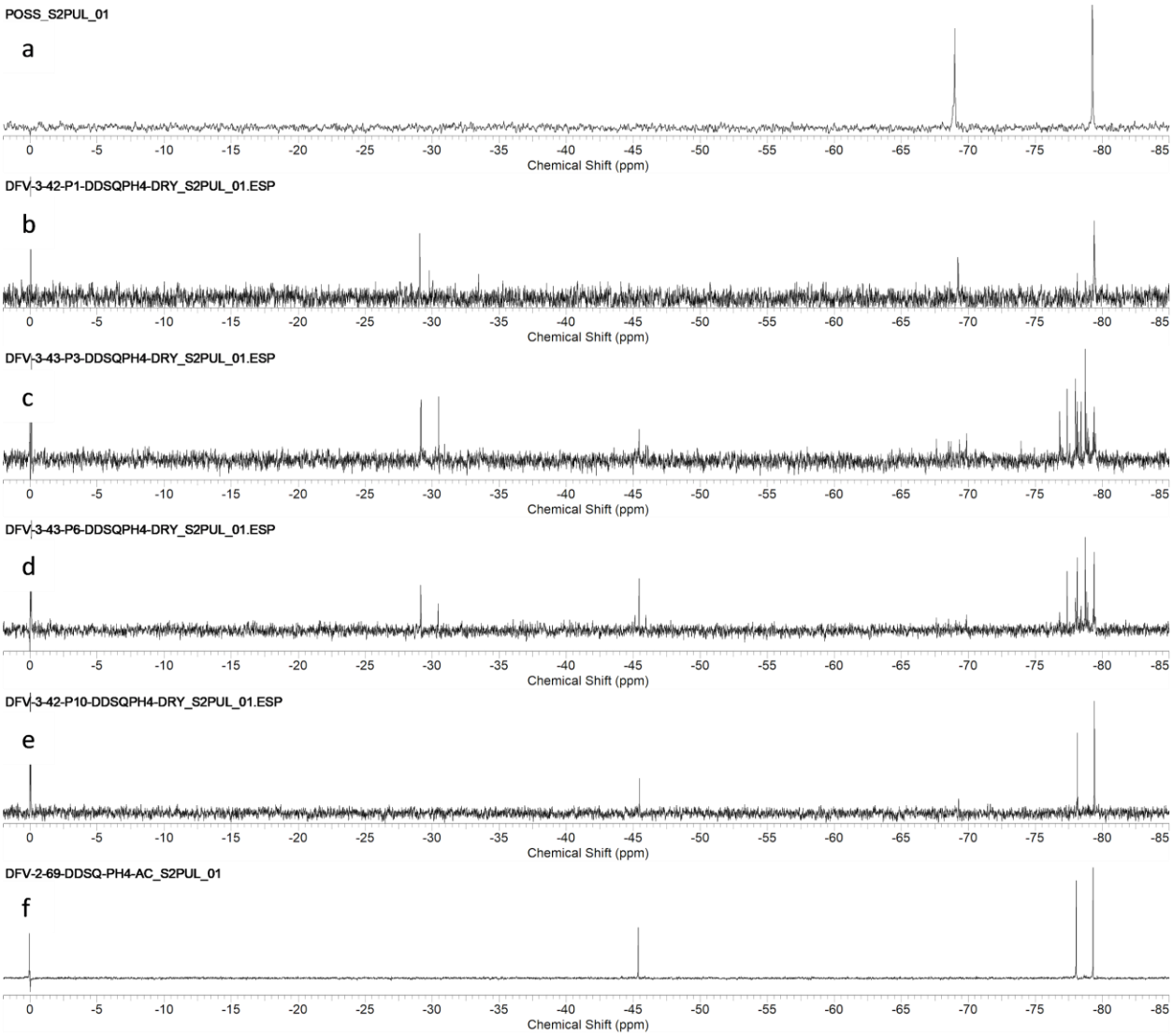

Figure F-2. Conversion of DDSQ-$(Ph)_8(OH)_4$ to DDSQ-2$(Ph)_2$ at different times analyzed by ^{29}Si-NMR (99 MHz, $CDCl_3$) after quench with MeOH and solvents evaporation (times in minutes): a=DDSQ-$(Ph)_8(OH)_4$, b = 0.67 min, c = 2.03 min, d = 6.85 min, e = 100 min, f = DDSQ-2$(Ph)_2$ completed after 4 hours reaction

Conversion of DDSQ-$(Ph)_8(OH)_4$ to DDSQ-$2(Me)_2$ analyzed by ^1H NMR at different times

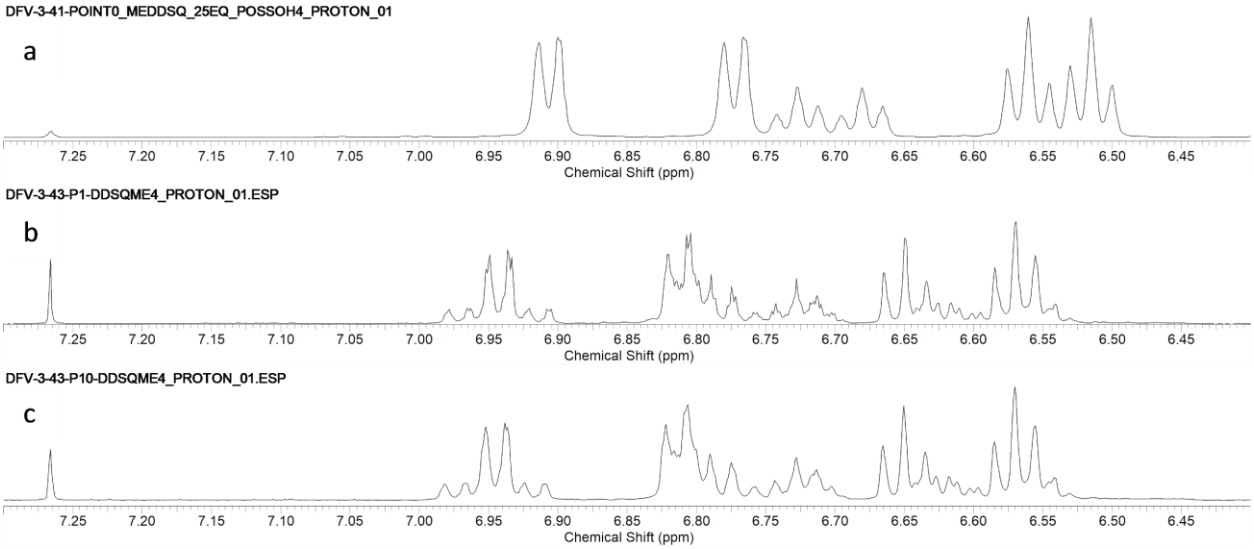

Figure F-3. Conversion of DDSQ-$(Ph)_8(OH)_4$ to AA1 or DDSQ-$2(Me)_2$ in different times analyzed by ^{1}H-NMR (500 MHz, $CDCl_3$) after quench with MeOH. Times in minutes: a = 0 only DDSQ-$(Ph)_8(OH)_4$, b = 0.98 min, c = 100 min.

Conversion of DDSQ-$(Ph)_8(OH)_4$ to DDSQ-$2(Me)_2$ analyzed by ^{29}Si NMR at different times

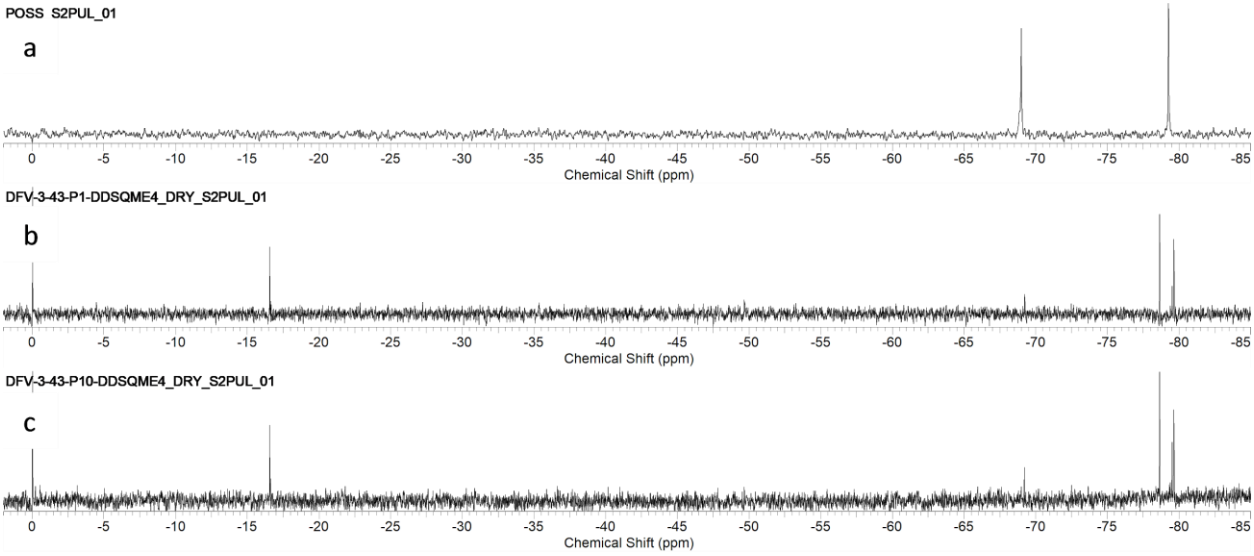

Figure F-4. Time conversion of DDSQ-$(Ph)_8(OH)_4$ to AA1 or DDSQ-$2(Me)_2$ analyzed by ^{29}Si-NMR (99 MHz, $CDCl_3$) after quench with MeOH and solvents evaporation: a=DDSQ-$(Ph)_8(OH)_4$, b = 0.98 min, c = 100 min.

Reaction kinetics for the reaction DDSQ-$(Ph)_8(OH)_4$ + A_2SiCl_2 + B_2SiCl_2 → DDSQ-A_4 + DDSQ-A_2B_2 + DDSQ-B_4

Kinetics were modeled to analyze how much deviated were the experimental results from the theoretical results. Experiments run with less than 2 equivalents of a single chlorosilane behaves as theoretically predicted. However, $(CH_3)SiCl_3$ competing with $R'RSiCl_2$ resulted in an unexpected ratio.

Model 1: single chlorosilane

Model developed for prediction of ratios when less than two equivalents of chlorosilanes react with tetrahydroxyl octaphenyl double decker-shaped silsesquioxane

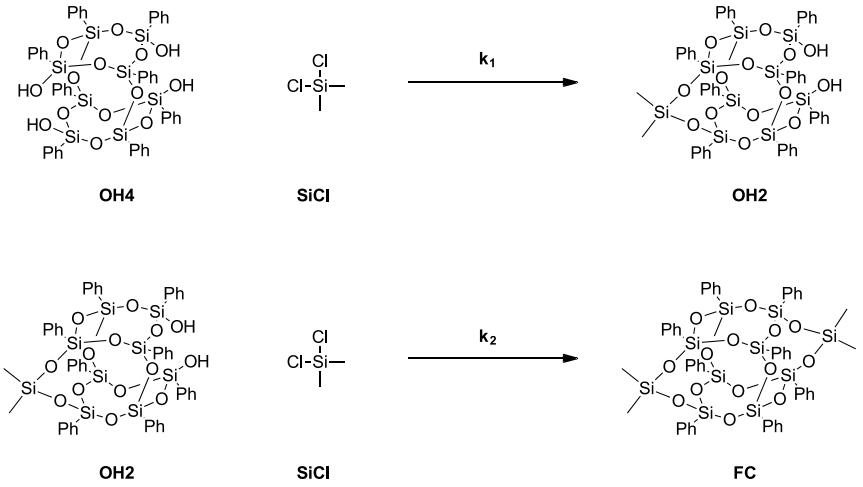

Scheme F-1. $DDSQ(OH)_4$ capping reactions generated for model 1

Rates:

$$-r_{1\,(OH4)} = k_1 C_{OH4} C_{SiCl}$$

$$-r_{2\,(FC)} = k_2 C_{OH2} C_{SiCl}$$

Rate laws

$$-r_{1\,(OH4)} = -r_{1\,(SiCl)} = r_{1\,(OH2)}$$

$$-r_{2\,(OH2)} = -r_{2\,(SiCl)} = r_{2\,(FC)}$$

Material balance for batch reactor

$$\frac{dC_{SiCl}}{dt} = r_{1\,(SiCl)} + r_{2\,(SiCl)}$$

$$\frac{dC_{OH4}}{dt} = r_{1\,(OH4)}$$

$$\frac{dC_{OH2}}{dt} = r_{1\,(OH2)} + r_{2\,(OH2)}$$

$$\frac{dC_{FC}}{dt} = r_{2\,(FC)}$$

Rate constant simplification (this step is required because the constants are unknown)

$$n = \frac{k_2}{k_1}$$

Replacing rates in the mol balance

$$\frac{dC_{SiCl}}{dt} = -k_1 C_{OH4} C_{SiCl} - nk_1 C_{OH2} C_{SiCl}$$

$$\frac{dC_{OH4}}{dt} = -k_1 C_{OH4} C_{SiCl}$$

$$\frac{dC_{OH2}}{dt} = k_1 C_{OH4} C_{SiCl} - nk_1 C_{OH2} C_{SiCl}$$

$$\frac{dC_{FC}}{dt} = nk_1 C_{OH2} C_{SiCl}$$

Initial conditions for the case using 1 equivalent of chlorosilane

$$t = 0\ ;\ C_{SiCl} = 0.036\frac{mmol}{ml}\ ;\ C_{OH4} = 0.036\frac{mmol}{ml}\ ;\ C_{OH2} = 0\frac{mmol}{ml}\ ;\ C_{FC} = 0\frac{mmol}{ml}$$

MATLAB code specifying model equations

```
function f = moles(t, C)
%Derivative system for DDSQ functionalization
%   Concentrationn (mol) balance for Reactions DDSQ(OH)4 + R2SiCl2
%   -->DDSQR2(OH)2 and DDSQR2(OH)2 + R2SiCl2 --> DDSQR4. Reaction rates
%   were replaced in the balance.
%   C(1) stands for Concentration of OH4
%   C(2) stands for Concentration of SiCl
%   C(3) stands for Concentration of OH2
%   C(4) stands for Concentration of FC
k1=1; %ml/(mmol*t) arbitrarily selected
n=1; % n=1 means that first capping is equally fast as second capping
f(1,1)=-k1*C(1)*C(2);
f(2,1)=-k1*C(1)*C(2)-n*k1*C(3)*C(2);
f(3,1)=k1*C(1)*C(2)-n*k1*C(3)*C(2);
f(4,1)=n*k1*C(3)*C(2);
end
```

MATLAB code solving the model

```
[tv, Cv]=ode45('moles',[0 100],[0.36 0.36 0 0]);
%Derivative system for DDSQ functionalization
%   Concentrationn (mol) balance for Reactions (OH)4 + SiCl
%   -->(OH)2 and (OH)2 + SiCl2 --> FC. Reaction rates
%   were replaced in the balance.
%   C(1) stands for Concentration of OH4
%   C(2) stands for Concentration of SiCl
%   C(3) stands for Concentration of OH2
%   C(4) stands for Concentration of FC
plot(tv,Cv(:,1),'r')
hold on
plot(tv,Cv(:,2),'g')
plot(tv,Cv(:,3),'b')
plot(tv,Cv(:,4),'c')
hold off
title ('DDSQ(OH)2 kinetic model')
ylabel('Concentration (mmol/ml)')
xlabel('time (s)')
legend('DDSQ(OH)4','A2SiCl2','DDSQ(OH)2','DDSQA4')
```

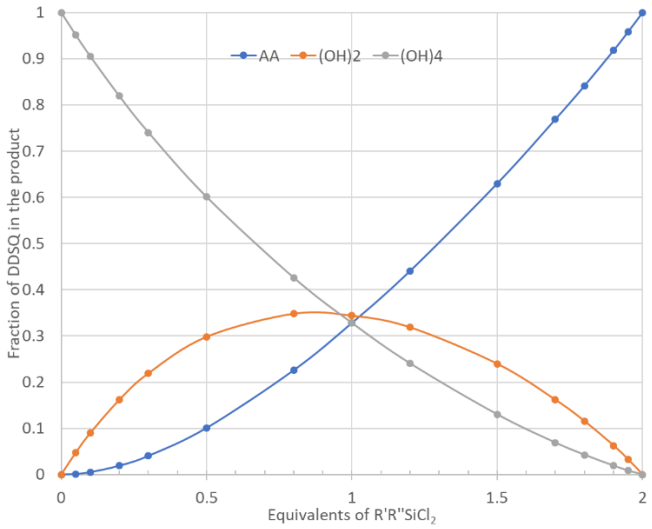

Figure F-5. Fractions of $DDSQ(OH)_4$ (grey line), DDSQ-2(R_1R_2) (blue line), and $DDSQ(OH)_2$ (orange line) obtained from model 1 after evaluation with different equivalents of chlorosilane.

Model 2: two chlorosilanes

Model developed for prediction of ratios when a mixture of two different chlorosilanes react with tetrahydroxyl octaphenyl double decker-shaped silsesquioxane

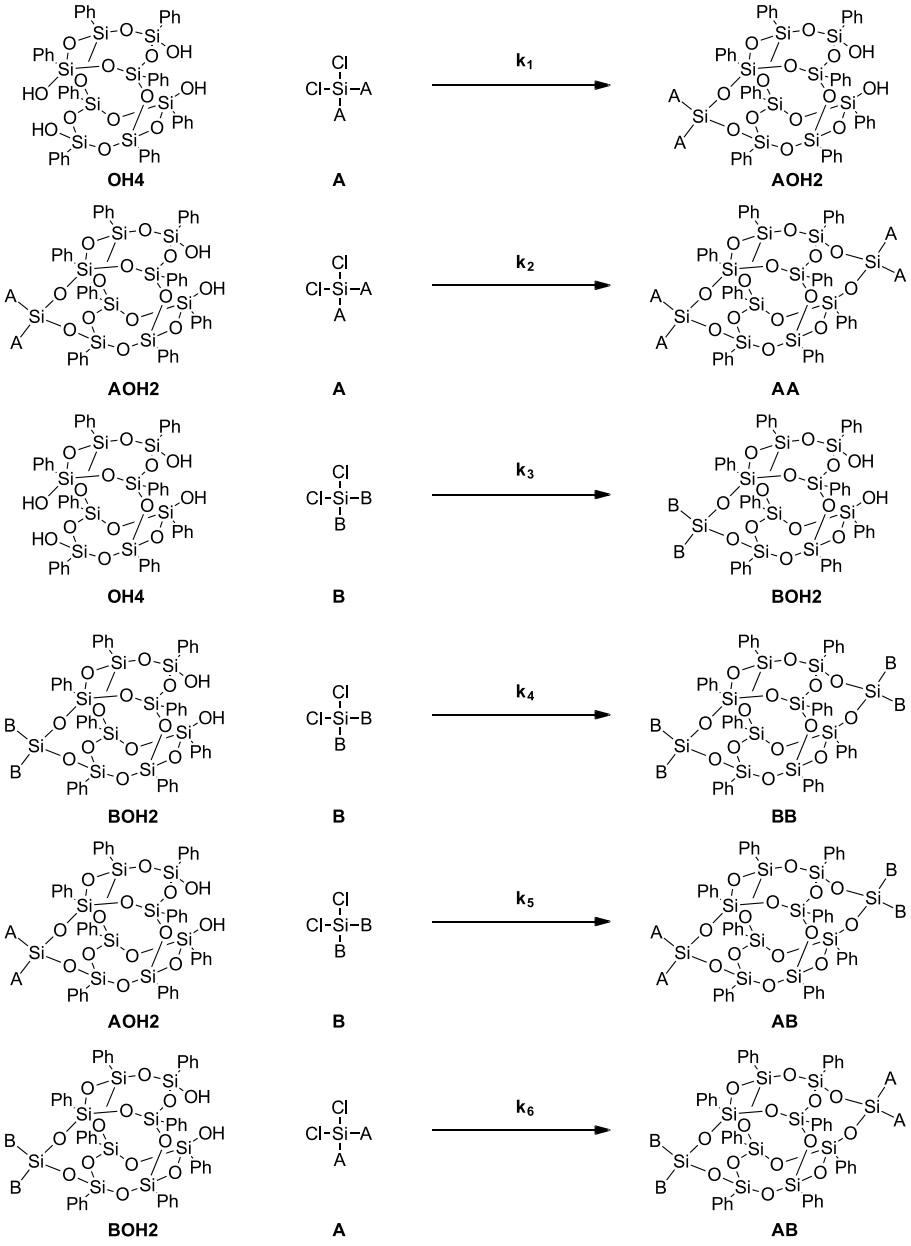

Scheme F-2. DDSQ(OH)$_4$ Capping reactions generated for model 2

Rates:

$$-r_{1\,(OH4)} = k_1 C_{OH4} C_A$$

$$-r_{2\,(AA)} = k_2 C_{AOH2} C_A$$

$$-r_{3\,(OH4)} = k_3 C_{OH4} C_B$$

$$-r_{4\,(BB)} = k_4 C_{BOH2} C_B$$

$$-r_{5\,(AB)} = k_5 C_{AOH2} C_B$$

$$-r_{6\,(AB)} = k_6 C_{BOH2} C_A$$

Rate laws

$$-r_{1\,(OH4)} = -r_{1\,(A)} = r_{1\,(AOH2)}$$

$$-r_{2\,(AOH2)} = -r_{2\,(A)} = r_{2\,(AA)}$$

$$-r_{3\,(OH4)} = -r_{3\,(B)} = r_{3\,(BOH2)}$$

$$-r_{4\,(BOH2)} = -r_{4\,(B)} = r_{4\,(BB)}$$

$$-r_{5\,(AOH2)} = -r_{5\,(B)} = r_{5\,(AB)}$$

$$-r_{6\,(BOH2)} = -r_{6\,(A)} = r_{6\,(AB)}$$

Material balance for batch reactor

$$\frac{dC_{OH4}}{dt} = r_{1\,(OH4)} + r_{3\,(OH4)}$$

$$\frac{dC_{AOH2}}{dt} = r_{1\,(AOH2)} + r_{2\,(AOH2)} + r_{5\,(AOH2)}$$

$$\frac{dC_{BOH2}}{dt} = r_{3\,(BOH2)} + r_{4\,(BOH2)} + r_{6\,(BOH2)}$$

$$\frac{dC_{AA}}{dt} = r_{2\,(AA)}$$

$$\frac{dC_{BB}}{dt} = r_{2\,(BB)}$$

$$\frac{dC_{AB}}{dt} = r_{5\,(AB)} + r_{6\,(AB)}$$

$$\frac{dC_{A}}{dt} = r_{1\,(A)} + r_{2\,(A)} + r_{6\,(A)}$$

$$\frac{dC_{B}}{dt} = r_{3\,(B)} + r_{4\,(B)} + r_{5\,(B)}$$

Replacing rates in material balances

$$\frac{dC_{OH4}}{dt} = k_1 C_{OH4} C_A - k_3 C_{OH4} C_B$$

$$\frac{dC_{AOH2}}{dt} = k_1 C_{OH4} C_A - k_2 C_{AOH2} C_A - k_5 C_{AOH2} C_B$$

$$\frac{dC_{BOH2}}{dt} = k_3 C_{OH4} C_B - k_4 C_{BOH2} C_B - k_6 C_{BOH2} C_A$$

$$\frac{dC_{AA}}{dt} = k_2 C_{AOH2} C_A$$

$$\frac{dC_{BB}}{dt} = k_4 C_{BOH2} C_B$$

$$\frac{dC_{AB}}{dt} = k_5 C_{AOH2} C_B + k_6 C_{BOH2} C_A$$

$$\frac{dC_A}{dt} = -k_1 C_{OH4} C_A - k_2 C_{AOH2} C_A - k_6 C_{BOH2} C_A$$

$$\frac{dC_B}{dt} = -k_3 C_{OH4} C_B - k_4 C_{BOH2} C_B - k_5 C_{AOH2} C_B$$

Constants assumptions

First capping and second capping are similar

$$k_1 = \frac{k_2}{n}$$

$$k_3 = \frac{k_4}{m}$$

Reactions for A are faster than reactions for B

$$k_1 = p k_3$$

Capping rate of A in BOH2 is equal to second capping rate of A in AOH2

$$k_2 = k_5$$

Capping rate of B in AOH2 is equal to second capping rate of B in BOH2

$$k_4 = k_6$$

Reorganizing all constants in function of k_1

$$k_2 = n k_1 \; ; \; k_3 = \frac{k_1}{p} \; ; \; k_4 = \frac{m}{p} k_1 \; ; \; k_5 = n k_1 \; ; k_6 = \frac{m}{p} k_1$$

If first capping with A is no different than second capping with A, and if first capping with B is no different than second capping with B, then:

$$n = m = 1$$

Capping rate depend of A and B species, the factor p indicates that reaction of A is p times faster than reaction of B

Initial conditions for the case using 1 equivalent of A and 1 equivalent of B

$$t = 0\ ;\ C_A = 1\frac{mmol}{ml}\ ;\ C_B = 1\frac{mmol}{ml}\ ;\ C_{OH4} = 1\frac{mmol}{ml}\ ;\ C_{AOH2} = 0\frac{mmol}{ml}\ ;$$

$$C_{BOH2} = 0\frac{mmol}{ml}\ ;\ C_{AA} = 0\frac{mmol}{ml}\ ;\ C_{BB} = 0\frac{mmol}{ml}\ ;\ C_{AB} = 0\frac{mmol}{ml}$$

MATLAB code specifying model equations

```
function f = AB(t, C)
%Derivative system for DDSQ functionalization
%   Reaction rates were replaced in the balance.
%   C(1) stands for Concentration of OH4
%   C(2) stands for Concentration of A2OH2
%   C(3) stands for Concentration of B2OH2
%   C(4) stands for Concentration of AA
%   C(5) stands for Concentration of BB
%   C(6) stands for Concentration of AB
%   C(7) stands for Concentration of A
%   C(8) stands for Concentration of B
k1=1000; %ml/(mmol*t)
n=1;
m=1;
p=100; %   Assuming A is 100 times faster than B
k2=k1*n;
k3=k1/p;
k4=k3*m;
k5=k4;
k6=k2;
f(1,1)=-k1*C(1)*C(7)-k3*C(1)*C(8);
f(2,1)=k1*C(1)*C(7)-k2*C(2)*C(7)-k5*C(2)*C(8);
f(3,1)=k3*C(1)*C(8)-k4*C(3)*C(8)-k6*C(3)*C(7);
f(4,1)=k2*C(2)*C(7);
f(5,1)=k4*C(3)*C(8);
f(6,1)=k5*C(2)*C(8)+k6*C(3)*C(7);
f(7,1)=-k1*C(1)*C(7)-k2*C(2)*C(7)-k6*C(3)*C(7);
```

```
f(8,1)=-k3*C(1)*C(8)-k4*C(3)*C(8)-k5*C(2)*C(8);
end
```

MATLAB code solving the model

```
[tv, Cv]=ode45('AB',[0 50],[1 0 0 0 0 0 1 1]); % DDSQ AOH2 BOH2 AA BB AB A B
plot(tv,Cv(:,1),'r')
hold on
plot(tv,Cv(:,4),'g')
plot(tv,Cv(:,5),'b')
plot(tv,Cv(:,6),'c')
plot(tv,Cv(:,7),'m')
plot(tv,Cv(:,8),'p')
plot(tv,Cv(:,2),'o')
plot(tv,Cv(:,3),'k')
hold off
title ('AB kinetic model')
ylabel('Concentration (mmol/ml)')
xlabel('time (s)')
legend('OH4','AA','BB','AB','A','B','AOH2','BOH2')
```

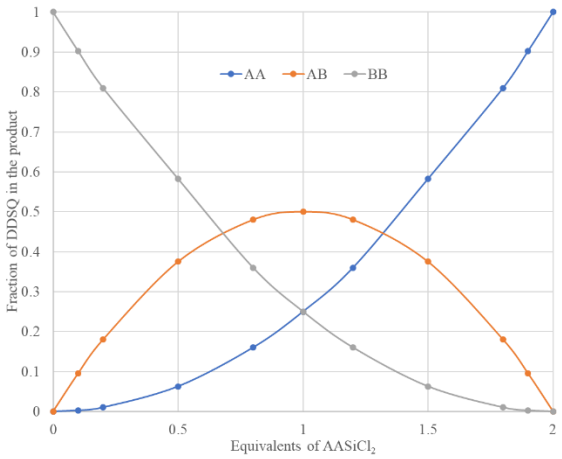

Figure F-6. Fractions of DDSQ-$(B)_4$ or BB (grey line), DDSQ-$(A)_4$ or AA (blue line), and DDSQ-(A_2B_2) or AB (orange line) obtained from model 2 after evaluation with different equivalents of A and completion to two equivalents with B assuming A and B are equally reactive.

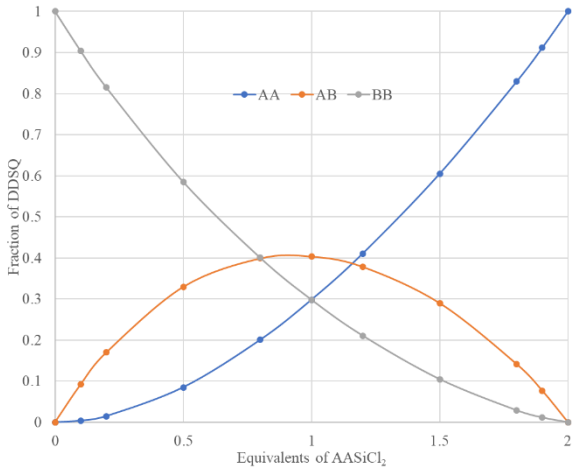

Figure F-7. Fractions of DDSQ-$(B)_4$ or BB (grey line), DDSQ-$(A)_4$ or AA (blue line), and DDSQ-(A_2B_2) or AB (orange line) obtained from model 2 after evaluation with different equivalents of A and completion to two equivalents with B assuming A is ten times faster than B (p = 10).

Model 3: two chlorosilanes with byproducts condensed by triethylamine

Model developed for prediction of ratios when a mixture of two different chlorosilanes react with tetrahydroxyl octaphenyl double decker-shaped silsesquioxane. Also, condensation generated by triethylamine was included in this model.

Reactions proposed and brief explanation:

Formation of a complex between chlorosilanes and triethylamine. Formation of this complex has been described in literature and only happen between one molecule of chlorosilane and one molecule of triethylamine. Triethylamine can be also consumed by HCl product of the rection between chlorosilanes and DDSQ-$(Ph)_8(OH)_4$. It is assumed that these reactions proceed extremely fast compared with the other reactions in this model. Also it is assumed that $k_{16} = k_{17} = k_{18}$

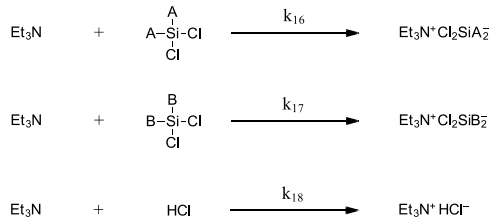

Scheme F-3. Formation of triethylamine complex with chlorinated species

Reaction between the chlorosilane complex with DDSQ tetraol or diol, this condensation produces triethylamine hydrochloride. In here, it is assumed that the remaining Cl in the chlorosilane reacts instantaneously with the remaining hydroxyl forming HCl. In here, the capping made by A is faster than the capping made by B. $k_1 > k_2$, $k_1 = k_3 = k_6$, and $k_2 = k_4 = k_5$

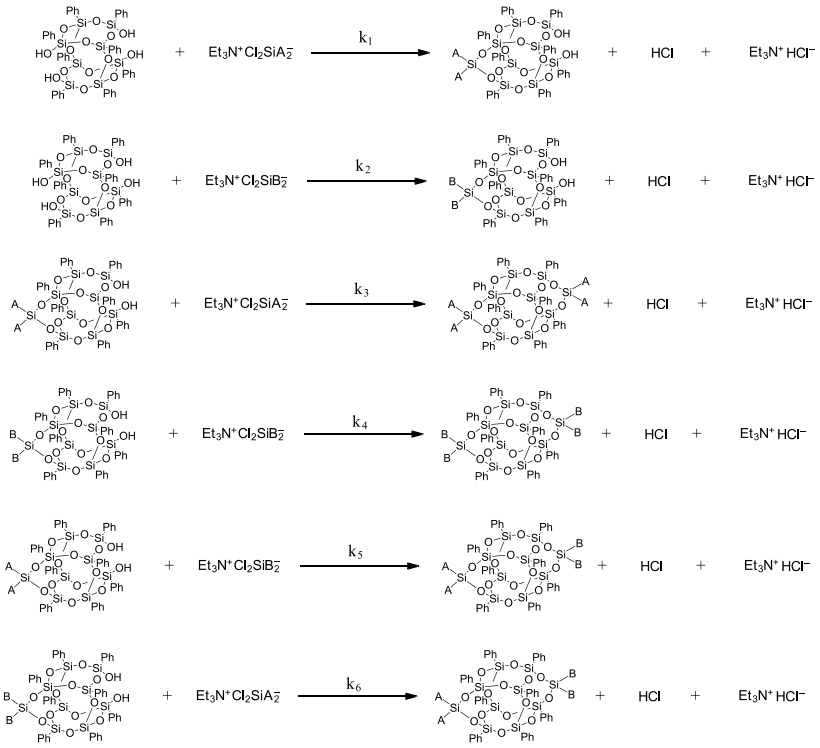

Scheme F-4. Capping of $DDSQ(OH)_4$ with chlorosilane triethylamine complex.

So far, the reactions observed do not differ from model 2. Now a series of complexities involving byproducts will be discussed and at some extend allow understanding of yields and ratios obtained after reaction. It is known that triethylamine may act as a catalyst for condensation of silanols. Remarkably, from the published paper it was recognized that the reaction rate between chlorosilane and DDSQ tetrasilanol depends from the chlorosilane bulkiness. Also, it was described that a chlorosilane form complex with a single triethylamine. Based on the previous descriptions it may be inferred that if the capping reaction rate is low, free triethylamine can remain in solution generating condensation between silanols. These condensation rates are slower than the chlorosilanes capping rates. $k_7 << k_1$, $k_7 < k_2$, and $k_7 = k_8 = k_9 = k_{10}$

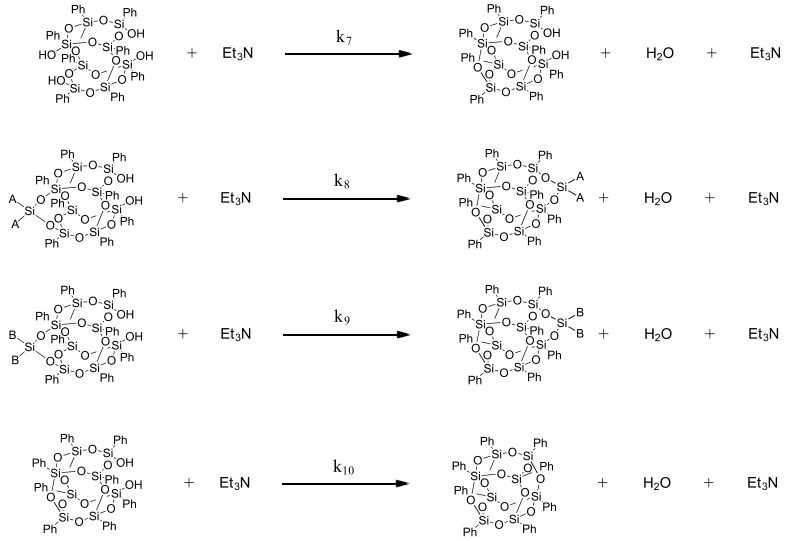

Scheme F-5. Formation of byproducts from condensation reactions in $DDSQ(OH)_4$ catalyzed by triethylamine.

It is highly possible that a chlorosilane complex may react with structures condensed in one side by triethylamine. For these $k_{11} = k_1$ and $k_{12} = k_2$

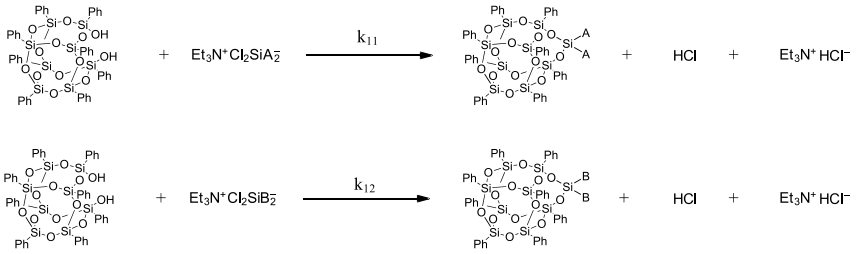

Scheme F-6. Functionalization of $POSS(OH)_2$ with dichlorosilanes as other possible side reactions.

Other reactions such as polycondensation of chlorosilanes generated by the produced water were considered but not used due to extensive simulation times. For these extra reactions it was assumed that the products of the condensation between two chlorosilanes end up as a chlorinated polymer chain (Cl-Poly-Cl) and these chains are assumed as a single specie that is consuming chlorosilanes if there is water present. Based on these reactions it is

believed that the amount of DDSQ-B_4 and the amount of DDSQ-A_2B_2 should be lower than the value reported for the simulation without this set of byproducts.

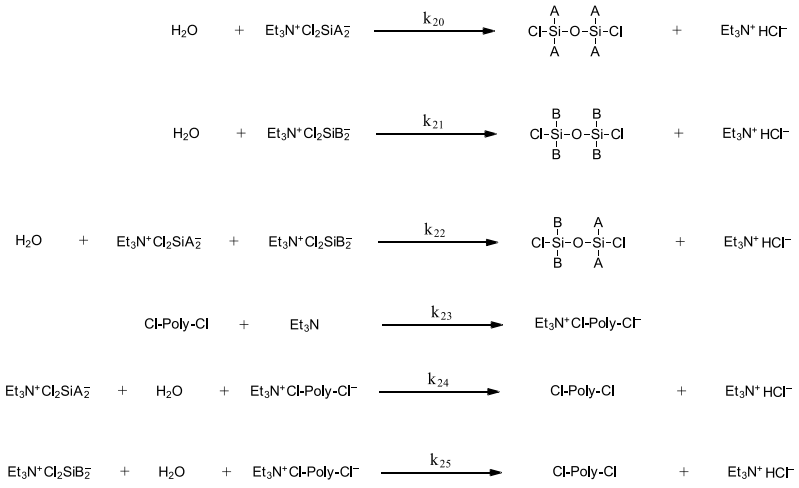

Scheme F-7. Production of polysiloxanes promoted by water production in DDSQ(OH)4 condensation. These reactions were not yet included in the model but they are highly likely based on multiple peaks observed by ^{29}Si-NMR in the D-Si region

Rates:

$$-r_{16\,(A_2SiCl_2)} = k_{16} C_{Et_3N} C_{A_2SiCl_2}$$

$$-r_{17\,(B_2SiCl_2)} = k_{17} C_{Et_3N} C_{B_2SiCl_2}$$

$$r_{18\,(Et_3NHCl)} = k_{18} C_{Et_3N} C_{HCl}$$

$$-r_{1\,(DDSQ(OH)_4)} = k_1 C_{DDSQ(OH)_4} C_{A_2SiCl_2Et_3N}$$

$$-r_{2\,(DDSQ(OH)_4)} = k_2 C_{DDSQ(OH)_4} C_{B_2SiCl_2Et_3N}$$

$$r_{3\,(DDSQA_4)} = k_3 C_{A_2DDSQ(OH)_2} C_{A_2SiCl_2Et_3N}$$

$$r_{4\,(DDSQB_4)} = k_4 C_{B_2DDSQ(OH)_2} C_{B_2SiCl_2Et_3N}$$

$$r_{5\,(DDSQA_2B_2)} = k_5 C_{B_2DDSQ(OH)_2} C_{A_2SiCl_2Et_3N}$$

$$r_{6\,(DDSQA_2B_2)} = k_6 C_{A_2DDSQ(OH)_2} C_{B_2SiCl_2Et_3N}$$

$$-r_{7\,(DDSQ(OH)_4)} = k_7 C_{DDSQ(OH)_4} C_{Et_3N}$$

$$-r_{8\,(A_2DDSQ(OH)_2)} = k_8 C_{A_2DDSQ(OH)_2} C_{Et_3N}$$

$$-r_{9\,(B_2DDSQ(OH)_2)} = k_9 C_{B_2DDSQ(OH)_2} C_{Et_3N}$$

$$-r_{10\,(POSS(OH)_2)} = k_{10} C_{POSS(OH)_2} C_{Et_3N}$$

$$r_{11\,(POSSA_2)} = k_{11} C_{POSS(OH)_2} C_{A_2SiCl_2Et_3N}$$

$$r_{12\,(POSSB_2)} = k_{12} C_{POSS(OH)_2} C_{B_2SiCl_2Et_3N}$$

Rate laws

$$-r_{1\,(DDSQ(OH)_4)} = -r_{1\,(A_2SiCl_2Et_3N)} = r_{1\,(A_2DDSQ(OH)_2)} = r_{1\,(HCl)} = r_{1\,(Et_3NHCl)}$$

$$-r_{2\,(DDSQ(OH)_4)} = -r_{2\,(B_2SiCl_2Et_3N)} = r_{2\,(B_2DDSQ(OH)_2)} = r_{2\,(HCl)} = r_{2\,(Et_3NHCl)}$$

$$r_{3\,(DDSQA_4)} = r_{3\,(HCl)} = r_{3\,(Et_3NHCl)} = -r_{3\,(A_2DDSQ(OH)_2)} = -r_{3\,(A_2SiCl_2Et_3N)}$$

$$r_{4\,(DDSQB_4)} = r_{4\,(HCl)} = r_{4\,(Et_3NHCl)} = -r_{4\,(B_2DDSQ(OH)_2)} = -r_{4\,(B_2SiCl_2Et_3N)}$$

$$r_{5\,(DDSQA_2B_2)} = r_{5\,(HCl)} = r_{5\,(Et_3NHCl)} = -r_{5\,(B_2DDSQ(OH)_2)} = -r_{5\,(A_2SiCl_2Et_3N)}$$

$$r_{6\,(DDSQA_2B_2)} = r_{6\,(HCl)} = r_{6\,(Et_3NHCl)} = -r_{6\,(A_2DDSQ(OH)_2)} = -r_{6\,(B_2SiCl_2Et_3N)}$$

$$-r_{7\,(DDSQ(OH)_4)} = -r_{7\,(Et_3N)} = r_{7\,(POSS(OH)_2)} = r_{7\,(Et_3N)} = r_{2\,(H_2O)}$$

$$-r_{8\,(A_2DDSQ(OH)_2)} = -r_{8\,(Et_3N)} = r_{8\,(POSSA_2)} = r_{8\,(Et_3N)} = r_{8\,(H_2O)}$$

$$-r_{9\,(B_2DDSQ(OH)_2)} = -r_{9\,(Et_3N)} = r_{9\,(POSSB_2)} = r_{9\,(Et_3N)} = r_{9\,(H_2O)}$$

$$r_{10\,(POSS)} = r_{10\,(Et_3N)} = r_{10\,(H_2O)} = -r_{10\,(POSS(OH)_2)} = -r_{10\,(Et_3N)}$$

$$-r_{11\,(POSS(OH)_2)} = -r_{11\,(A_2SiCl_2Et_3N)} = r_{11\,(HCl)} = r_{11\,(POSSA_2)} = r_{11\,(Et_3NHCl)}$$

$$-r_{12\,(POSS(OH)_2)} = -r_{12\,(B_2SiCl_2Et_3N)} = r_{12\,(HCl)} = r_{12\,(POSSB_2)} = r_{12\,(Et_3NHCl)}$$

$$-r_{16\,(A_2SiCl_2)} = -r_{16\,(Et_3N)} = r_{16\,(A_2SiCl_2Et_3N)}$$

$$-r_{17\,(B_2SiCl_2)} = -r_{17\,(Et_3N)} = r_{17\,(B_2SiCl_2Et_3N)}$$

$$r_{18\,(Et_3NHCl)} = -r_{18\,(HCl)} = -r_{18\,(Et_3N)}$$

Material balance for batch reactor

$$\frac{dC_{A_2SiCl_2}}{dt} = r_{16}$$

$$\frac{dC_{B_2SiCl_2}}{dt} = r_{17}$$

$$\frac{dC_{Et_3N}}{dt} = r_{16} + r_{17} + r_{18}$$

$$\frac{dC_{DDSQ(OH)_4}}{dt} = r_1 + r_2 + r_7$$

$$\frac{dC_{A_2DDSQ(OH)_2}}{dt} = r_1 + r_3 + r_6 + r_8$$

$$\frac{dC_{B_2DDSQ(OH)_2}}{dt} = r_2 + r_4 + r_5 + r_9$$

$$\frac{dC_{A_2SiCl_2Et_3N}}{dt} = r_1 + r_3 + r_5 + r_{11} + r_{16}$$

$$\frac{dC_{B_2SiCl_2Et_3N}}{dt} = r_2 + r_4 + r_6 + r_{12} + r_{17}$$

$$\frac{dC_{DDSQA_4}}{dt} = r_3$$

$$\frac{dC_{DDSQB_4}}{dt} = r_4$$

$$\frac{dC_{DDSQA_2B_2}}{dt} = r_5 + r_6$$

$$\frac{dC_{HCl}}{dt} = r_1 + r_2 + r_3 + r_4 + r_5 + r_6 + r_{11} + r_{12} + r_{18}$$

$$\frac{dC_{Et_3NHCl}}{dt} = r_1 + r_2 + r_3 + r_4 + r_5 + r_6 + r_{11} + r_{12} + r_{18}$$

$$\frac{dC_{H_2O}}{dt} = r_7 + r_8 + r_9 + r_{10}$$

$$\frac{dC_{POSS(OH)_2}}{dt} = r_7 + r_{10} + r_{11} + r_{12}$$

$$\frac{dC_{POSSA_2}}{dt} = r_8 + r_{11}$$

$$\frac{dC_{POSSB_2}}{dt} = r_9 + r_{12}$$

$$\frac{dC_{POSS}}{dt} = r_{10}$$

Replacing rates in material balances

$$\frac{dC_{A_2SiCl_2}}{dt} = k_{16} C_{Et_3N} C_{A_2SiCl_2}$$

$$\frac{dC_{B_2SiCl_2}}{dt} = k_{17} C_{Et_3N} C_{B_2SiCl_2}$$

$$\frac{dC_{Et_3N}}{dt} = k_{16}C_{Et_3N}C_{A_2SiCl_2} + k_{17}C_{Et_3N}C_{B_2SiCl_2} + k_{18}C_{Et_3N}C_{HCl}$$

$$\frac{dC_{DDSQ(OH)_4}}{dt} = k_1C_{DDSQ(OH)_4}C_{A_2SiCl_2Et_3N} + k_2C_{DDSQ(OH)_4}C_{B_2SiCl_2Et_3N} + k_7C_{DDSQ(OH)_4}C_{Et_3N}$$

$$\frac{dC_{A_2DDSQ(OH)_2}}{dt} = k_1C_{DDSQ(OH)_4}C_{A_2SiCl_2Et_3N} + k_3C_{A_2DDSQ(OH)_2}C_{A_2SiCl_2Et_3N} + k_6C_{A_2DDSQ(OH)_2}C_{B_2SiCl_2Et_3N} + k_8C_{A_2DDSQ(OH)_2}C_{Et_3N}$$

$$\frac{dC_{B_2DDSQ(OH)_2}}{dt} = k_2C_{DDSQ(OH)_4}C_{B_2SiCl_2Et_3N} + k_4C_{B_2DDSQ(OH)_2}C_{B_2SiCl_2Et_3N} + k_5C_{B_2DDSQ(OH)_2}C_{A_2SiCl_2Et_3N} + k_9C_{B_2DDSQ(OH)_2}C_{Et_3N}$$

$$\frac{dC_{A_2SiCl_2Et_3N}}{dt} = k_1C_{DDSQ(OH)_4}C_{A_2SiCl_2Et_3N} + k_3C_{A_2DDSQ(OH)_2}C_{A_2SiCl_2Et_3N} + k_5C_{B_2DDSQ(OH)_2}C_{A_2SiCl_2Et_3N} + k_{11}C_{POSS(OH)_2}C_{A_2SiCl_2Et_3N} + k_{16}C_{Et_3N}C_{A_2SiCl_2}$$

$$\frac{dC_{B_2SiCl_2Et_3N}}{dt} = k_2C_{DDSQ(OH)_4}C_{B_2SiCl_2Et_3N} + k_4C_{B_2DDSQ(OH)_2}C_{B_2SiCl_2Et_3N} + k_6C_{A_2DDSQ(OH)_2}C_{B_2SiCl_2Et_3N} + k_{12}C_{POSS(OH)_2}C_{B_2SiCl_2Et_3N} + k_{17}C_{Et_3N}C_{B_2SiCl_2}$$

$$\frac{dC_{DDSQA_4}}{dt} = k_3C_{A_2DDSQ(OH)_2}C_{A_2SiCl_2Et_3N}$$

$$\frac{dC_{DDSQB_4}}{dt} = k_4C_{B_2DDSQ(OH)_2}C_{B_2SiCl_2Et_3N}$$

$$\frac{dC_{DDSQA_2B_2}}{dt} = k_5C_{B_2DDSQ(OH)_2}C_{A_2SiCl_2Et_3N} + k_6C_{A_2DDSQ(OH)_2}C_{B_2SiCl_2Et_3N}$$

$$\frac{dC_{HCl}}{dt} = k_1 C_{DDSQ(OH)_4} C_{A_2SiCl_2Et_3N} + k_2 C_{DDSQ(OH)_4} C_{B_2SiCl_2Et_3N} + k_3 C_{A_2DDSQ(OH)_2} C_{A_2SiCl_2Et_3N}$$
$$+ k_4 C_{B_2DDSQ(OH)_2} C_{B_2SiCl_2Et_3N} + k_5 C_{B_2DDSQ(OH)_2} C_{A_2SiCl_2Et_3N}$$
$$+ k_6 C_{A_2DDSQ(OH)_2} C_{B_2SiCl_2Et_3N} + k_{11} C_{POSS(OH)_2} C_{A_2SiCl_2Et_3N}$$
$$+ k_{12} C_{POSS(OH)_2} C_{B_2SiCl_2Et_3N} + k_{18} C_{Et_3N} C_{HCl}$$

$$\frac{dC_{Et_3NHCl}}{dt} = k_1 C_{DDSQ(OH)_4} C_{A_2SiCl_2Et_3N} + k_2 C_{DDSQ(OH)_4} C_{B_2SiCl_2Et_3N}$$
$$+ k_3 C_{A_2DDSQ(OH)_2} C_{A_2SiCl_2Et_3N} + k_4 C_{B_2DDSQ(OH)_2} C_{B_2SiCl_2Et_3N}$$
$$+ k_5 C_{B_2DDSQ(OH)_2} C_{A_2SiCl_2Et_3N} + k_6 C_{A_2DDSQ(OH)_2} C_{B_2SiCl_2Et_3N}$$
$$+ k_{11} C_{POSS(OH)_2} C_{A_2SiCl_2Et_3N} + k_{12} C_{POSS(OH)_2} C_{B_2SiCl_2Et_3N} + k_{18} C_{Et_3N} C_{HCl}$$

$$\frac{dC_{H_2O}}{dt} = k_7 C_{DDSQ(OH)_4} C_{Et_3N} + k_8 C_{A_2DDSQ(OH)_2} C_{Et_3N} + k_9 C_{B_2DDSQ(OH)_2} C_{Et_3N}$$
$$+ k_{10} C_{POSS(OH)_2} C_{Et_3N}$$

$$\frac{dC_{POSS(OH)_2}}{dt} = k_7 C_{DDSQ(OH)_4} C_{Et_3N} + k_{10} C_{POSS(OH)_2} C_{Et_3N} + k_{11} C_{POSS(OH)_2} C_{A_2SiCl_2Et_3N}$$
$$+ k_{12} C_{POSS(OH)_2} C_{B_2SiCl_2Et_3N}$$

$$\frac{dC_{POSSA_2}}{dt} = k_8 C_{A_2DDSQ(OH)_2} C_{Et_3N} + k_{11} C_{POSS(OH)_2} C_{A_2SiCl_2Et_3N}$$

$$\frac{dC_{POSSB_2}}{dt} = k_9 C_{B_2DDSQ(OH)_2} C_{Et_3N} + k_{12} C_{POSS(OH)_2} C_{B_2SiCl_2Et_3N}$$

$$\frac{dC_{POSS}}{dt} = k_{10} C_{POSS(OH)_2} C_{Et_3N}$$

Reorganizing all constants to write them in function of k_1

$$k_2 = k_4 = k_6 = k_{12} = \frac{k_1}{n}$$

$$k_3 = k_5 = k_{11} = k_1$$

$$k_7 = k_8 = k_9 = k_{10} = \frac{k_1}{p}$$

$$k_{16} = m * k_1$$

$$k_{17} = o * k_1$$

$$k_{18} = q * k_1$$

These constants were described previously. To satisfy the assumptions made for this model the values of m, n, o, p, and q must be higher than 1

Initial conditions for the case using 1 equivalent of A chlorosilane and 1 equivalent of B chlorosilane

$$t = 0\ ;\ C_{A_2SiCl_2} = 1\frac{mmol}{ml}\ ;\ C_{B_2SiCl_2} = 1\frac{mmol}{ml}\ ;\ C_{DDSQ(OH)_4} = 1\frac{mmol}{ml}\ ;\ C_{Et_3N} = 4\frac{mmol}{ml}$$

Concentrations for intermediate and final products were set to zero.

MATLAB code specifying model equations

```
function f = AB_w_Et3N(t, C)
%Derivative system for DDSQ functionalization
%   Concentrationn (mol) balance for Reactions DDSQ(OH)4 + R2SiCl2
%   -->DDSQR2(OH)2 and DDSQR2(OH)2 + R2SiCl2 --> DDSQR4. Reaction rates
%   were replaced in the balance.
%   C(1) stands for Concentration of DDSQ(OH)4
%   C(2) stands for Concentration of DDSQA2(OH)2
%   C(3) stands for Concentration of DDSQB2(OH)2
%   C(4) stands for Concentration of A2SiCl2Et3N
%   C(5) stands for Concentration of B2SiCl2Et3N
%   C(6) stands for Concentration of DDSQA4
%   C(7) stands for Concentration of DDSQB4
%   C(8) stands for Concentration of DDSQA2B2
```

```
    %   C(9) stands for Concentration of HCl
    %   C(10) stands for Concentration of HClEt3N
    %   C(11) stands for Concentration of H2O
    %   C(12) stands for Concentration of POSS(OH)2
    %   C(13) stands for Concentration of POSSA
    %   C(14) stands for Concentration of POSSB
    %   C(15) stands for Concentration of POSS
    %   C(16) stands for Concentration of A2SiCl2
    %   C(17) stands for Concentration of B2SiCl2
    %   C(18) stands for Concentration of Et3N

    k1=100; %ml/(mmol*t)
    n=100; %if n>1, A capping faster than B capping
    m=10; %Et3N to Chlorosilane A complex formation
    o=10; %Et3N to Chlorosilane B complex formation
    p=1000; %Condensation promoted by Et3N in DDSQ(OH)n species
    q=1000; %Formation of the Et3NHCl salt, assumed to be super-fast
    k2=k1/n;
    k3=k1;
    k4=k2;
    k5=k1;
    k6=k2;
    k7=k1/p;
    k8=k7;
    k9=k7;
    k10=k7;
    k11=k1;
    k12=k2;
    k16=m*k1;
    k17=o*k1;
    k18=q*k1;

    f(1,1)=-k1*C(1)*C(4)-k2*C(1)*C(5)-k7*C(1)*C(18);
    f(2,1)=k1*C(1)*C(4)-k3*C(2)*C(4)-k6*C(2)*C(5)-k8*C(2)*C(18);
    f(3,1)=k2*C(1)*C(5)-k4*C(3)*C(5)-k5*C(3)*C(4)-k9*C(3)*C(18);
    f(4,1)=k16*C(18)*C(16)-k1*C(1)*C(4)-k3*C(2)*C(4)-k5*C(3)*C(4)-
k11*C(12)*C(4);
    f(5,1)=k17*C(18)*C(17)-k2*C(1)*C(5)-k4*C(3)*C(5)-k6*C(2)*C(5)-
k12*C(12)*C(5);
    f(6,1)=k3*C(2)*C(4);
    f(7,1)=k4*C(3)*C(5);
    f(8,1)=k5*C(3)*C(4)+k6*C(2)*C(5);
    f(9,1)=-
k18*C(18)*C(9)+k1*C(1)*C(4)+k2*C(1)*C(5)+k3*C(2)*C(4)+k4*C(3)*C(5)+k5*C(3)
*C(4)+k6*C(2)*C(5)+k11*C(12)*C(4)+k12*C(12)*C(5);
    f(10,1)=k18*C(18)*C(9)+k1*C(1)*C(4)+k2*C(1)*C(5)+k3*C(2)*C(4)+k4*C(3)*
C(5)+k5*C(3)*C(4)+k6*C(2)*C(5)+k11*C(12)*C(4)+k12*C(12)*C(5);
    f(11,1)=k7*C(1)*C(18)+k8*C(2)*C(18)+k9*C(3)*C(18)+k10*C(12)*C(18);
    f(12,1)=k7*C(1)*C(18)-k10*C(12)*C(18)-k11*C(12)*C(4)-k12*C(12)*C(5);
    f(13,1)=k8*C(2)*C(18)+k11*C(12)*C(4);
    f(14,1)=k9*C(3)*C(18)+k12*C(12)*C(5);
    f(15,1)=k10*C(12)*C(18);
    f(16,1)=-k16*C(18)*C(16);
    f(17,1)=-k17*C(18)*C(17);
    f(18,1)=-k16*C(18)*C(16)-k17*C(18)*C(17)-k18*C(18)*C(9);
    end
```

Solver for model 3

```
    [tv, Cv]=ode45('AB_w_Et3N',[0 100],[1 0 0 0 0 0 0 0 0 0 0 0 0 0 0 1 1 4]);
% [OH4 AOH2 BOH2 AEt3N BEt3N A4 B4 AB HCl Et3NHCl H20 POSSOH2 POSSA POSSB
POSS ASi BSi Et3N]
    plot(tv,Cv(:,1),'-s','color',1/255*[255 0
0],'MarkerSize',4,'MarkerEdgeColor',1/255*[255 0
0],'MarkerFaceColor',1/255*[255 0 0],'MarkerIndices',1:50000:length(Cv))
    hold on
    plot(tv,Cv(:,6),'-*','color',1/255*[255 0
255],'MarkerSize',4,'MarkerEdgeColor',1/255*[255 0
255],'MarkerFaceColor',1/255*[255 0 255],'MarkerIndices',1:50000:length(Cv))
    plot(tv,Cv(:,7),'-x','color',1/255*[154 0
255],'MarkerSize',4,'MarkerEdgeColor',1/255*[154 0
255],'MarkerFaceColor',1/255*[154 0 255],'MarkerIndices',1:50000:length(Cv))
    plot(tv,Cv(:,8),'-d','color',1/255*[0 0
255],'MarkerSize',4,'MarkerEdgeColor',1/255*[0 0
255],'MarkerFaceColor',1/255*[0 0 255],'MarkerIndices',1:50000:length(Cv))
    plot(tv,Cv(:,13),'-p','color',1/255*[0 255
255],'MarkerSize',4,'MarkerEdgeColor',1/255*[0 255
255],'MarkerFaceColor',1/255*[0 255 255],'MarkerIndices',1:50000:length(Cv))
    plot(tv,Cv(:,14),'-h','color',1/255*[0 255
0],'MarkerSize',4,'MarkerEdgeColor',1/255*[0 255
0],'MarkerFaceColor',1/255*[0 255 0],'MarkerIndices',1:50000:length(Cv))
    plot(tv,Cv(:,15),'-+','color',1/255*[0 0
0],'MarkerSize',4,'MarkerEdgeColor',1/255*[0 0 0],'MarkerFaceColor',1/255*[0
0 0],'MarkerIndices',1:50000:length(Cv))
    plot(tv,Cv(:,11),'-o','color',1/255*[67 142
58],'MarkerSize',4,'MarkerEdgeColor',1/255*[67 142
58],'MarkerFaceColor',1/255*[67 142 58],'MarkerIndices',1:50000:length(Cv))
    hold off
    title ('DDSQA2B2 kinetic model')
    ylabel('Concentration (mmol/ml)')
    xlabel('time (s)')
    legend('DDSQ(OH)4','DDSQA4','DDSQB4','DDSQA2B2','POSSA','POSSB','POSS','H2
0')
```

Results for the proposed model

For the case in which the reaction rate of chlorosilane A is higher than the rate of the B chlorosilane and using the m, n, o, p, and q constants as described in the Matlab code.

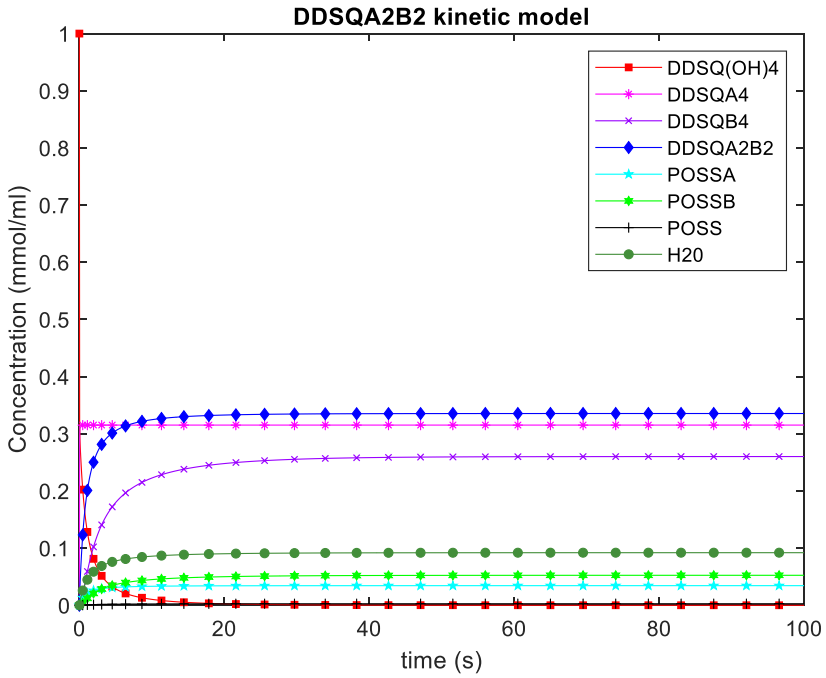

Figure F-8. Modelling of functionalization of $DDSQ(OH)_4$ with two different chlorosilanes including the formation of byproducts. The kinetic constants are not real values but related to k1 based on experimental observations.

From this plot it can be observed how production of DDSQ-A_4 is favored compared to that of DDSQ-B_4. It is also remarkable that under the conditions modeled byproducts add a total of 0.1 mmol/ml. It should be noticed that this result was obtained assuming that condensation caused by triethylamine is 1000 times slower than capping of the A chlorosilane and 10 times slower than capping of the B chlorosilane. These assumptions were made based on experimental observations.

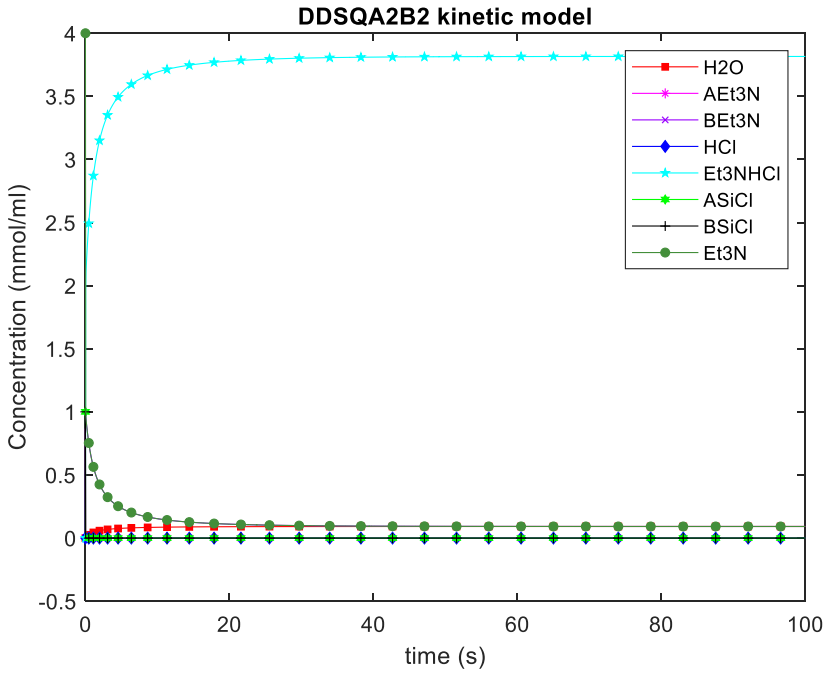

Figure F-9. Evolution of triethylamine, triethylamine complexes, and water production in the DDSQ-$(OH)_4$ functionalization.

The behavior of chlorosilanes and triethylamine showed fast consumption of both pure chlorosilanes to form the complex with triethylamine. However, triethylamine and the complex from the chlorosilane B cannot react anymore and end up as byproducts after synthesis. It is believed that these must react with water to produced siloxane polymers or cycles. Experimentally once the reaction is finished, filtered, and dried it is possible to watch HCl smoke once DCM is added to dissolve the material.

It is possible to infer that the model may be predicting the reaction byproducts, and at some extent explaining the reaction yield as well as the ratios between DDSQ-A_4, DDSQ-A_2B_2, and DDSQ-B_4 quantified experimentally after column. The products condensed by Et_3N were not identified experimentally because these may be stuck in the column stationary phase.

APPENDIX G.

LC AND FC SEPARATIONS ANALYZED BY HPLC

G. LC and FC separations analyzed by HPLC

Fraction analysis for separation of mixture B by HPLC

Chromatograms processed by HPLC for each fraction collected along the preparatory column for mixture B containing **2** DDSQ-2($(CH_3)_2$), **3b** DDSQ-2($(CHCH_2)(CH_3)$), and **4b** DDSQ-2($(CHCH_2)(OH)$). The flow rate was variable, and fractions of 19 mL were collected. At 59 min fractions were rich in *trans*-**4b**. Final fractions were *cis*-**4b** rich fraction.

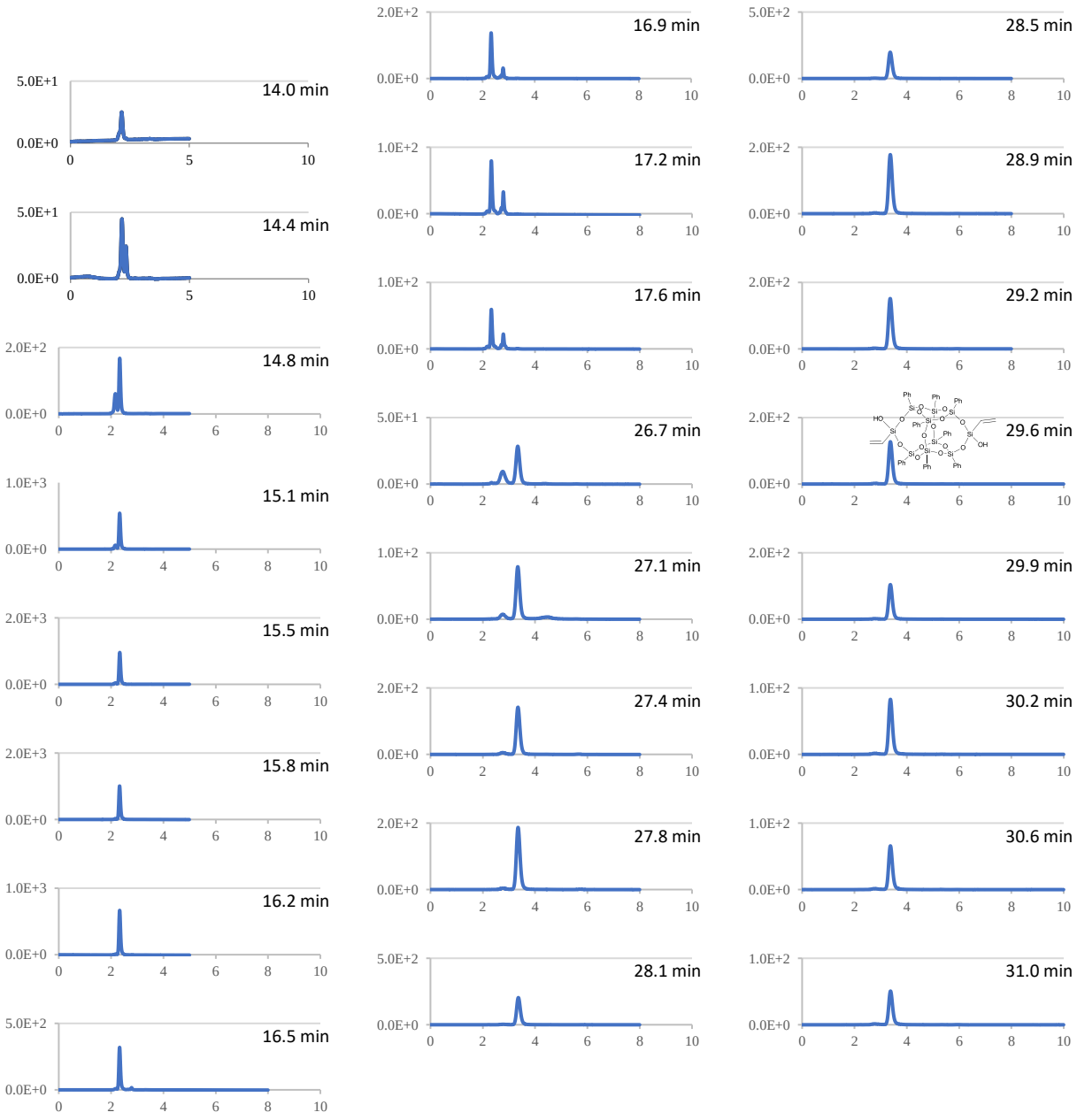

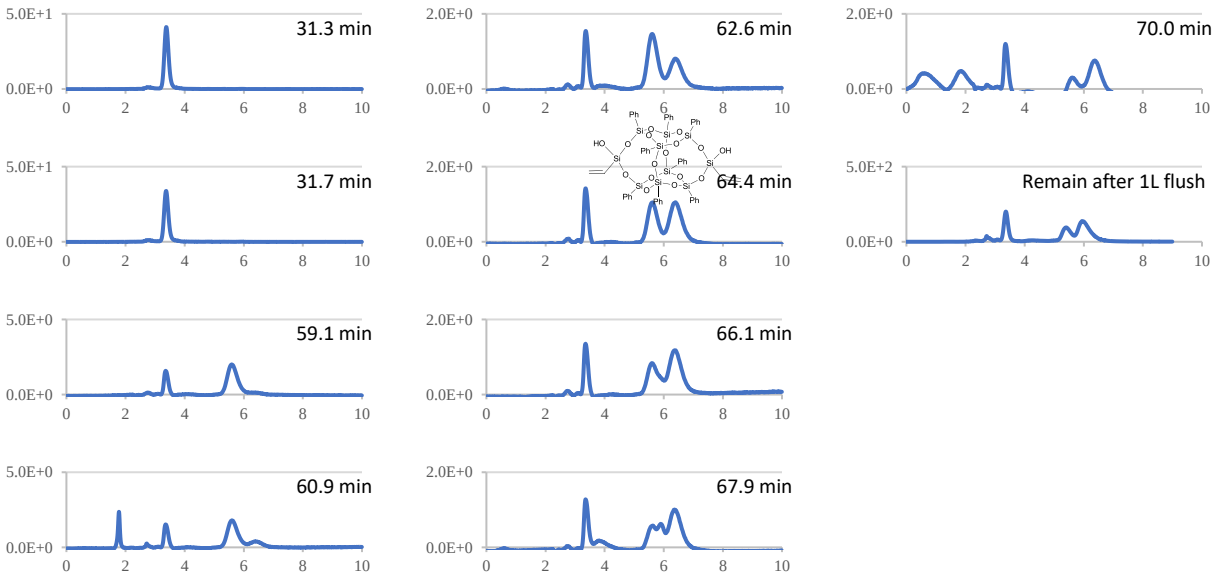
31.3 min
62.6 min
70.0 min
31.7 min
64.4 min
Remain after 1L flush
59.1 min
66.1 min
60.9 min
67.9 min

HPLC flow rate profile for preparatory column separating mixture C

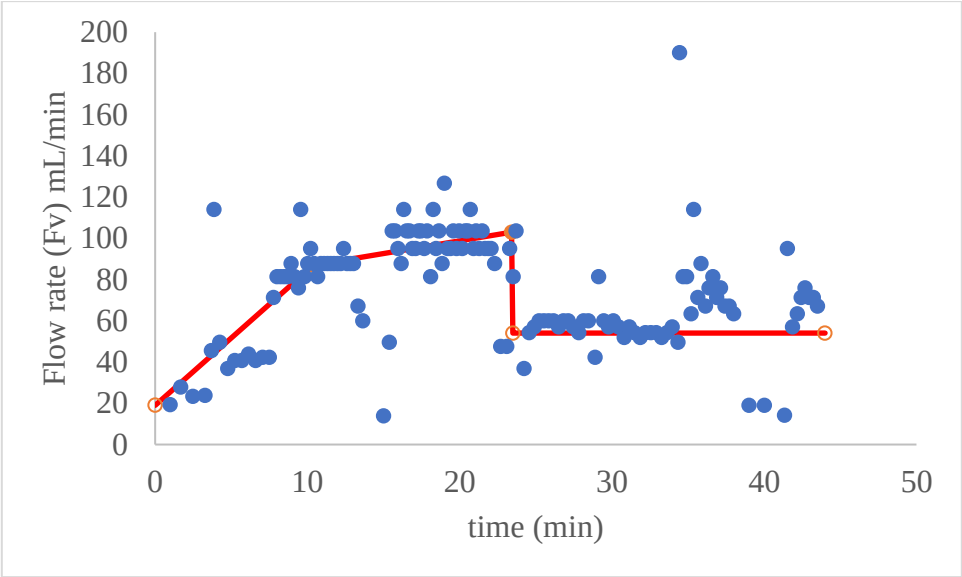

Figure G-1. Flow rate ramps for preparative column under non-constant flow rate.

Dots in this graph are experimentally measured flow rates. Each point is defined as the lapse of time for completion of 19 mL. Points below 25 mL/min represent reservoir refilling times when the pressure was relieved to add more solvent. Linear flow rate ranging 52 to 56 mL/min was obtained only when the pressure was reduced.

Fraction analysis for separation of mixture C by HPLC

Chromatograms processed by HPLC for each fraction collected along the preparatory column for mixture IB containing the molecules **2** DDSQ-2($(CH_3)_2$), **3c** DDSQ-2($(CH_2CH(CH_3)_2)(CH_3)$), and **4c** DDSQ-2($(CH_2CH(CH_3)_2)(OH)$). The flow rate was variable, and fractions of 19 mL were collected. From 32 min to 37 min fractions were rich in *trans*-**4c**. Final fraction was a fraction rich in *cis*-**4c**.

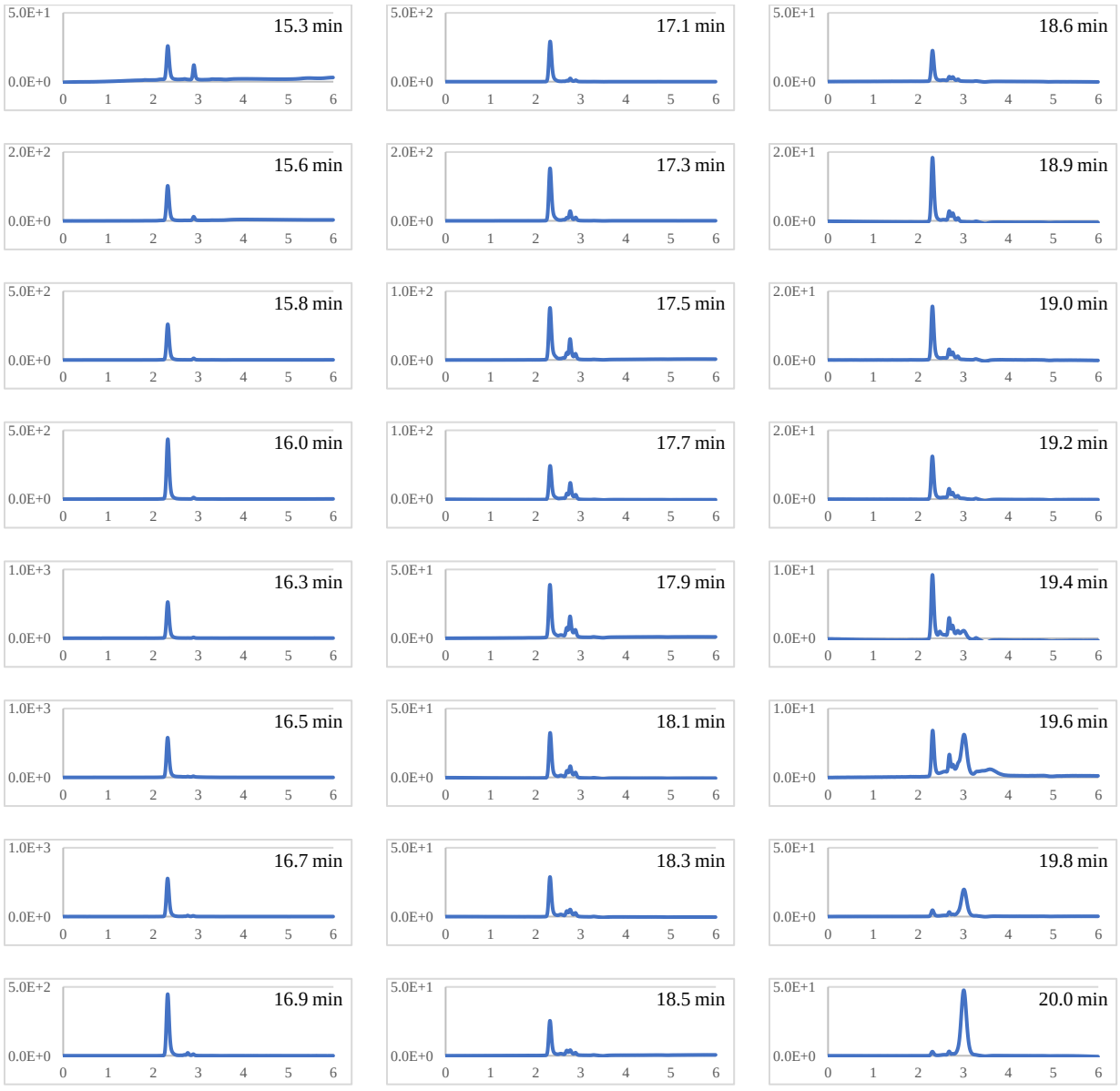

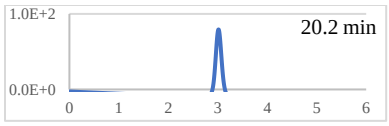
1.0E+2
0.0E+0
0 1 2 3 4 5 6
20.2 min

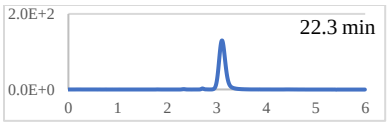
2.0E+2
0.0E+0
0 1 2 3 4 5 6
22.3 min

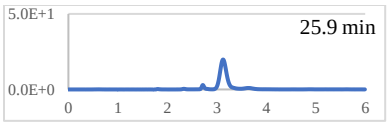
5.0E+1
0.0E+0
0 1 2 3 4 5 6
25.9 min

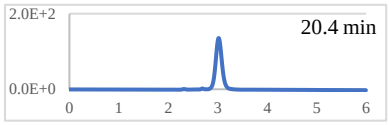
2.0E+2
0.0E+0
0 1 2 3 4 5 6
20.4 min

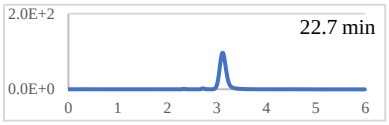
2.0E+2
0.0E+0
0 1 2 3 4 5 6
22.7 min

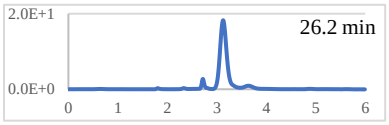
2.0E+1
0.0E+0
0 1 2 3 4 5 6
26.2 min

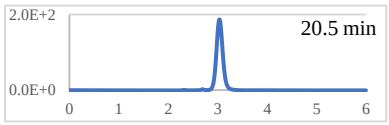
2.0E+2
0.0E+0
0 1 2 3 4 5 6
20.5 min

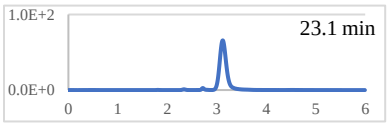
1.0E+2
0.0E+0
0 1 2 3 4 5 6
23.1 min

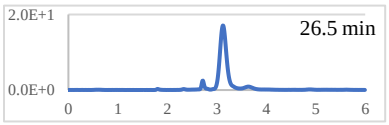
2.0E+1
0.0E+0
0 1 2 3 4 5 6
26.5 min

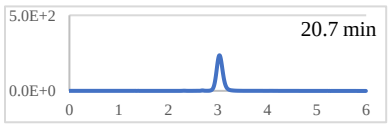
5.0E+2
0.0E+0
0 1 2 3 4 5 6
20.7 min

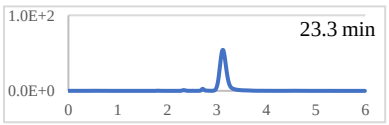
1.0E+2
0.0E+0
0 1 2 3 4 5 6
23.3 min

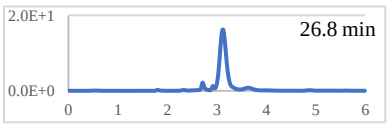
2.0E+1
0.0E+0
0 1 2 3 4 5 6
26.8 min

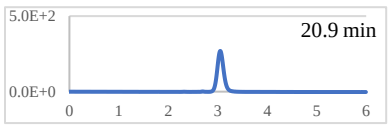
5.0E+2
0.0E+0
0 1 2 3 4 5 6
20.9 min

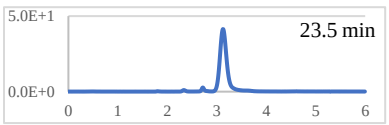
5.0E+1
0.0E+0
0 1 2 3 4 5 6
23.5 min

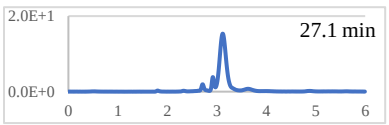
2.0E+1
0.0E+0
0 1 2 3 4 5 6
27.1 min

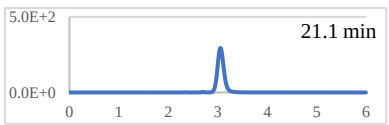
5.0E+2
0.0E+0
0 1 2 3 4 5 6
21.1 min

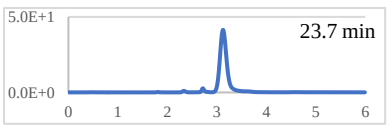
5.0E+1
0.0E+0
0 1 2 3 4 5 6
23.7 min

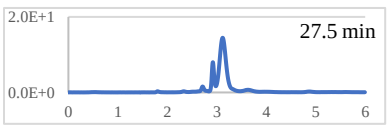
2.0E+1
0.0E+0
0 1 2 3 4 5 6
27.5 min

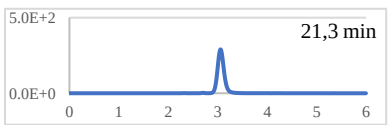
5.0E+2
0.0E+0
0 1 2 3 4 5 6
21,3 min

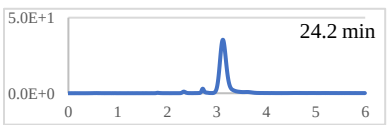
5.0E+1
0.0E+0
0 1 2 3 4 5 6
24.2 min

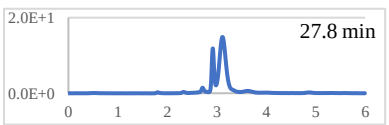
2.0E+1
0.0E+0
0 1 2 3 4 5 6
27.8 min

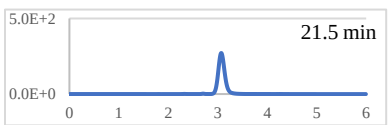
5.0E+2
0.0E+0
0 1 2 3 4 5 6
21.5 min


5.0E+1
0.0E+0
0 1 2 3 4 5 6
24.6 min

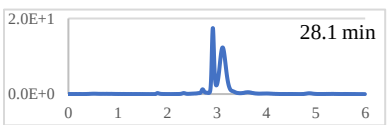
2.0E+1
0.0E+0
0 1 2 3 4 5 6
28.1 min

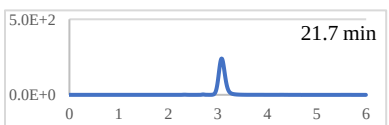
5.0E+2
0.0E+0
0 1 2 3 4 5 6
21.7 min


5.0E+1
0.0E+0
0 1 2 3 4 5 6
24.9 min


5.0E+1
0.0E+0
0 1 2 3 4 5 6
28.5 min

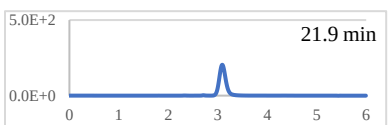
5.0E+2
0.0E+0
0 1 2 3 4 5 6
21.9 min


5.0E+1
0.0E+0
0 1 2 3 4 5 6
25.2 min

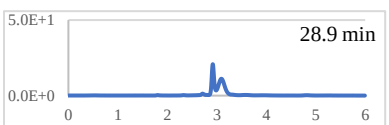
5.0E+1
0.0E+0
0 1 2 3 4 5 6
28.9 min

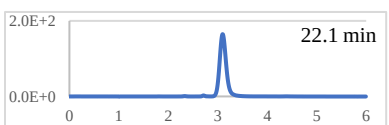
2.0E+2
0.0E+0
0 1 2 3 4 5 6
22.1 min


5.0E+1
0.0E+0
0 1 2 3 4 5 6
25.5 min

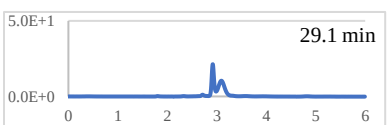
5.0E+1
0.0E+0
0 1 2 3 4 5 6
29.1 min

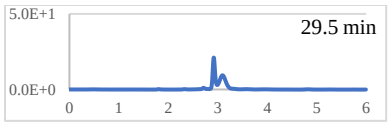
5.0E+1
0.0E+0
29.5 min
0 1 2 3 4 5 6

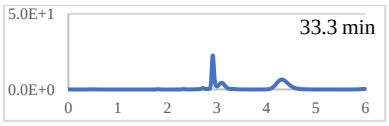
5.0E+1
0.0E+0
33.3 min
0 1 2 3 4 5 6

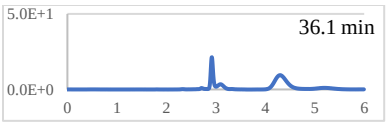
5.0E+1
0.0E+0
36.1 min
0 1 2 3 4 5 6

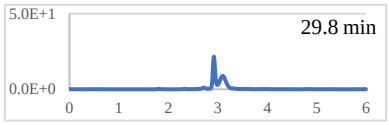
5.0E+1
0.0E+0
29.8 min
0 1 2 3 4 5 6


5.0E+1
0.0E+0
33.6 min
0 1 2 3 4 5 6

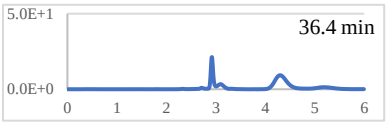
5.0E+1
0.0E+0
36.4 min
0 1 2 3 4 5 6

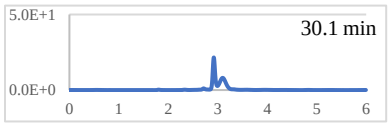
5.0E+1
0.0E+0
30.1 min
0 1 2 3 4 5 6


5.0E+1
0.0E+0
34.0 min
0 1 2 3 4 5 6

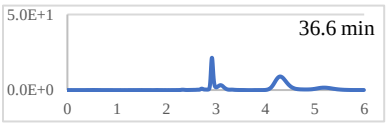
5.0E+1
0.0E+0
36.6 min
0 1 2 3 4 5 6

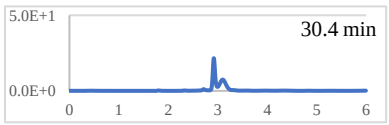
5.0E+1
0.0E+0
30.4 min
0 1 2 3 4 5 6

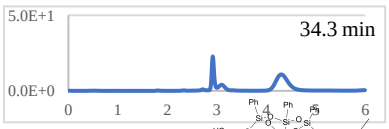
5.0E+1
0.0E+0
34.3 min
0 1 2 3 4 5 6

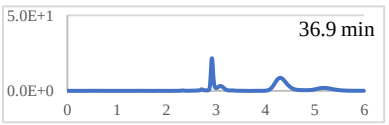
5.0E+1
0.0E+0
36.9 min
0 1 2 3 4 5 6

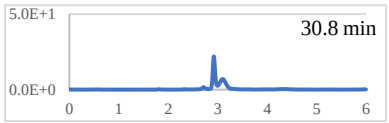
5.0E+1
0.0E+0
30.8 min
0 1 2 3 4 5 6

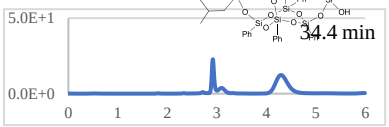
5.0E+1
0.0E+0
34.4 min
0 1 2 3 4 5 6

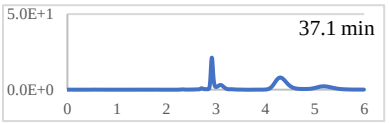
5.0E+1
0.0E+0
37.1 min
0 1 2 3 4 5 6

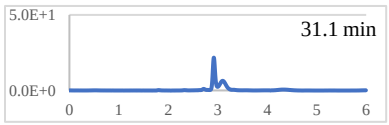
5.0E+1
0.0E+0
31.1 min
0 1 2 3 4 5 6


5.0E+1
0.0E+0
34.7 min
0 1 2 3 4 5 6

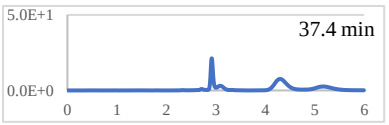
5.0E+1
0.0E+0
37.4 min
0 1 2 3 4 5 6

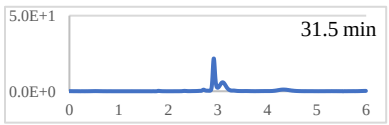
5.0E+1
0.0E+0
31.5 min
0 1 2 3 4 5 6

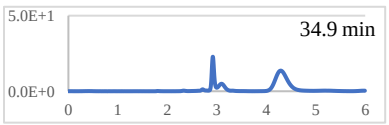
5.0E+1
0.0E+0
34.9 min
0 1 2 3 4 5 6

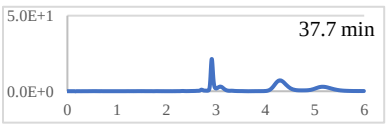
5.0E+1
0.0E+0
37.7 min
0 1 2 3 4 5 6

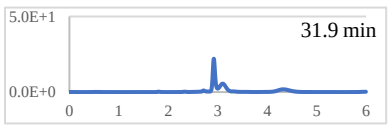
5.0E+1
0.0E+0
31.9 min
0 1 2 3 4 5 6

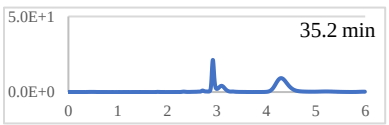
5.0E+1
0.0E+0
35.2 min
0 1 2 3 4 5 6

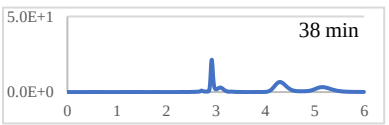
5.0E+1
0.0E+0
38 min
0 1 2 3 4 5 6

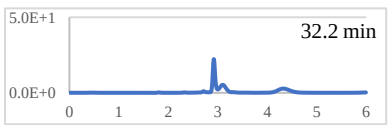
5.0E+1
0.0E+0
32.2 min
0 1 2 3 4 5 6

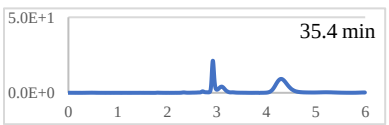
5.0E+1
0.0E+0
35.4 min
0 1 2 3 4 5 6

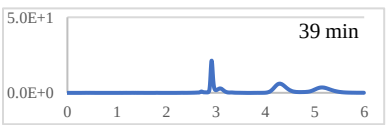
5.0E+1
0.0E+0
39 min
0 1 2 3 4 5 6

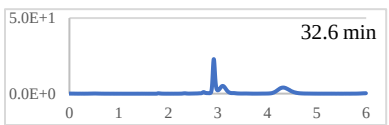
5.0E+1
0.0E+0
32.6 min
0 1 2 3 4 5 6

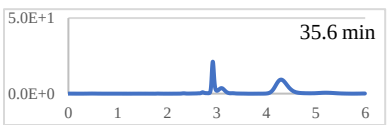
5.0E+1
0.0E+0
35.6 min
0 1 2 3 4 5 6

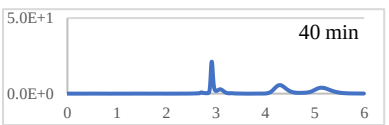
5.0E+1
0.0E+0
40 min
0 1 2 3 4 5 6


5.0E+1
0.0E+0
32.9 min
0 1 2 3 4 5 6


5.0E+1
0.0E+0
35.9 min
0 1 2 3 4 5 6

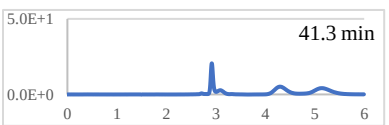
5.0E+1
0.0E+0
41.3 min
0 1 2 3 4 5 6

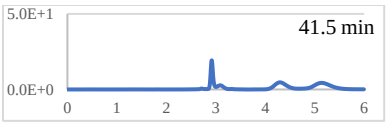
5.0E+1
0.0E+0
41.5 min
0 1 2 3 4 5 6

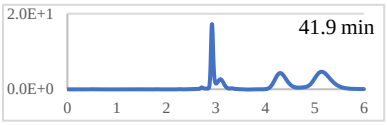
2.0E+1
0.0E+0
41.9 min
0 1 2 3 4 5 6

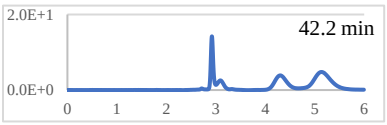
2.0E+1
0.0E+0
42.2 min
0 1 2 3 4 5 6

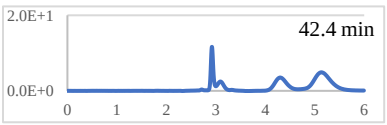
2.0E+1
0.0E+0
42.4 min
0 1 2 3 4 5 6

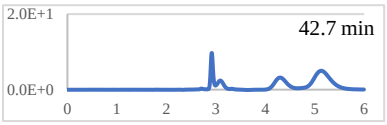
2.0E+1
0.0E+0
42.7 min
0 1 2 3 4 5 6

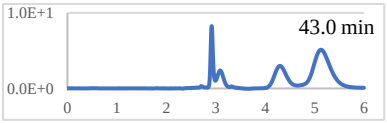
1.0E+1
0.0E+0
43.0 min
0 1 2 3 4 5 6

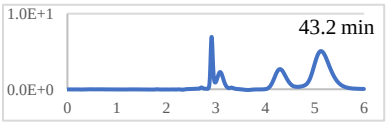
1.0E+1
0.0E+0
43.2 min
0 1 2 3 4 5 6

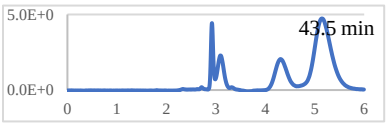
5.0E+0
0.0E+0
43.5 min
0 1 2 3 4 5 6

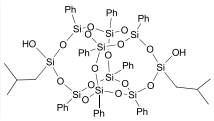
Ph
Si
O
HO
OH

Purity analysis after FC of cis and trans DDSQ-2((Me)(PEP)) 3 by HPLC

Samples evaluated in a hypercarb® column of 10 cm length and 0.46 cm internal diameter. Ethyl acetate was used as mobile phase with a flow rate of 0.4 ml/min. The eluent was analyzed by a UV detector

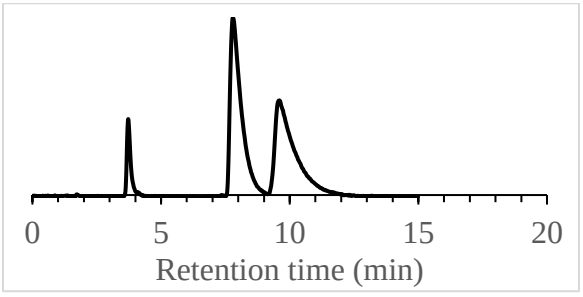

Figure G-2. 50% *trans* and 50% *cis* mixture of DDSQ-2((methyl)(para-phenylethynyl phenyl))after hypercarb column

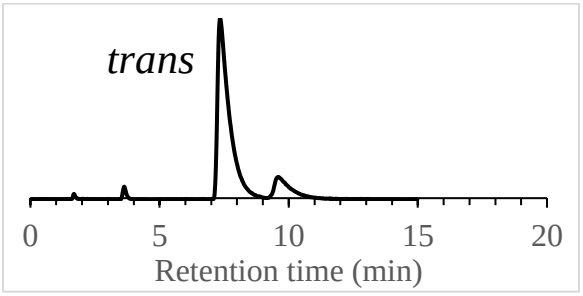

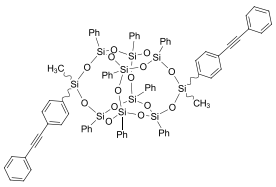

Figure G-3. Mostly *trans* isomer of DDSQ-2((methyl)(para-phenylethynyl phenyl))after hypercarb column

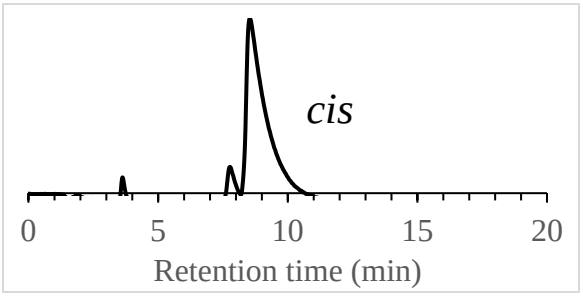

Figure G-4. Mostly *cis* isomer of DDSQ-2((methyl)(para-phenylethynyl phenyl))after hypercarb column

Separation of a non-polar ternary mixture

Samples evaluated in a hypercarb® column of 10 cm length and 0.46 cm internal diameter. Ethyl acetate was used as mobile phase with a flow rate of 0.4 ml/min. The eluent was analyzed by a UV detector

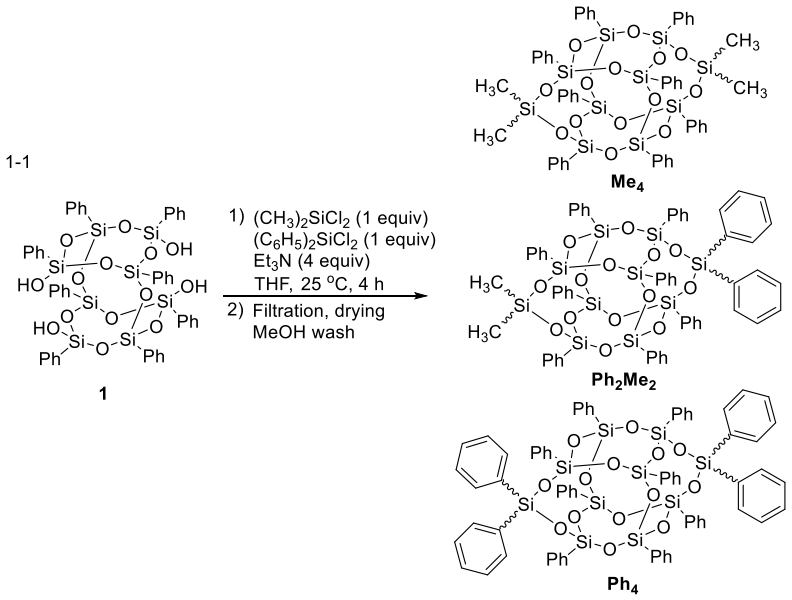

Scheme G-1. Synthesis of a ternary non-polar mixture with diphenyldichlorosilane and dimethyldichlorosilane.

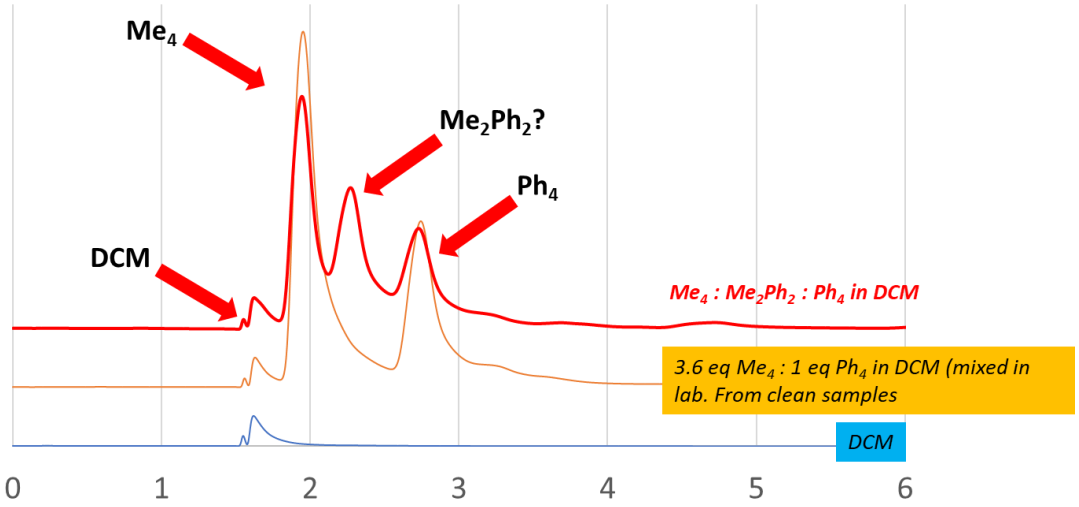

Figure G-5. Possible separation of the ternary mixture described in **Scheme G-1**. Synthesis of a ternary non-polar mixture with diphenyldichlorosilane and dimethyldichlorosilane.**Scheme G-1** using 98:2 DCM:Acetonitrile as mobile phase. Blue line represents the chromatogram with a

DCM injection; yellow line is the chromatogram for a mixture of tetramethyl DDSQ and tetraphenyl DDSQ. Red line represents the chromatogram for the ternary mixture.

APPENDIX H.

SUMMARIZED EUTECTIC AND LIQUIDUS COMPOSITIONS

H. Summarized eutectic and liquidus compositions

Summarized onset and liquidus temperatures in DSC traces

Table H-1. Eutectic temperature (T_E) and liquidus temperatures (T_L) for binary *cis*-to-*trans* mixtures of compound **2**.

x_{trans}	T_E (°C)	T_L (°C)
0	-	275
0.1	-	272
0.2	247	263
0.3	256	-
0.5	248	272
0.6	245	296
0.7	246	302
0.8	-	305
0.9	-	309
≈ 1	-	310

Table H-2. Eutectic temperature (T_E) and liquidus temperatures (T_L) for binary *cis*-to-*trans* mixtures of compound **3**.

x_{trans}	T_E (°C)	T_L (°C)
≈ 0	-	263
0.3	256	-
0.5	257	270
0.7	245	284
≈ 1	-	301

Table H-3. Eutectic temperature (T_E) and liquidus temperatures (T_L) for binary *cis*-to-*trans* mixtures of compound **4**.

x_{trans}	T_E (°C)	T_L (°C)
0.25	269	280 ± 5
0.33	269	-
0.5	259	295
0.6	262	312
0.9	269	316
≈ 1	269	320

Analysis of the experimental eutectic temperatures shows that TE for 2 and 3 is 14 °C lower than TE for 4. However, the eutectic composition is similar for the three cases studied

in this work. It was observed that the TE for 3 is 26 °C lower than the liquidus temperature of the as synthesized mixture (xtrans = 0.5), for 2 the difference is 20 °C, and for 4 the difference is 14 °C. These results suggest that the use of large aryl groups decreased the melting temperature of pure components and had a pronounced effect decreasing the eutectic temperature.

APPENDIX I.

NMR SPECTRA FOR COMPONENTS SYNTHESIZED AND SEPARATED IN THIS WORK

I. NMR spectra for components synthesized and separated in this work

(Isobutyl)(para-aniline(trimethylsilyl))dichlorosilane

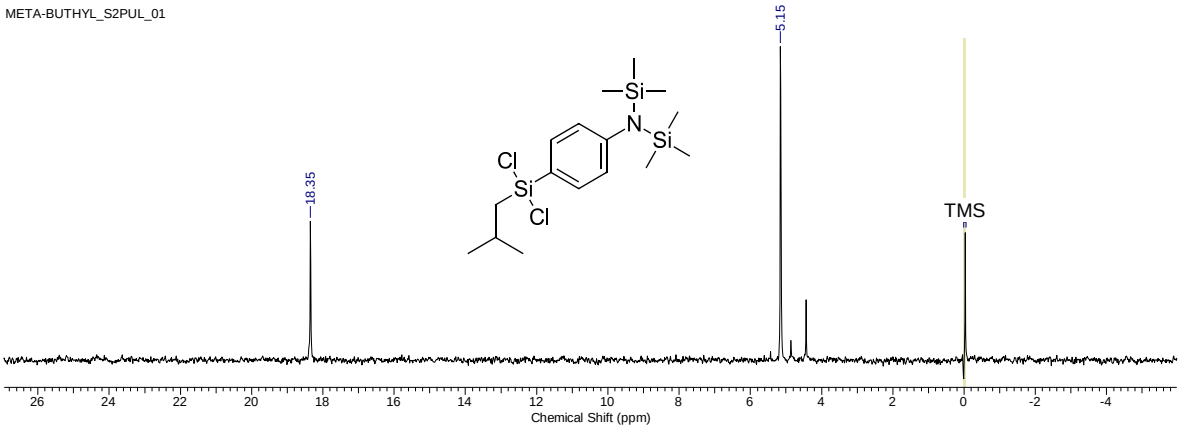

Figure I-1. ^{29}Si-NMR ($CDCl_3$, 99 MHz) for (isobutyl)(para-aniline(trimethylsilyl))dichlorosilane

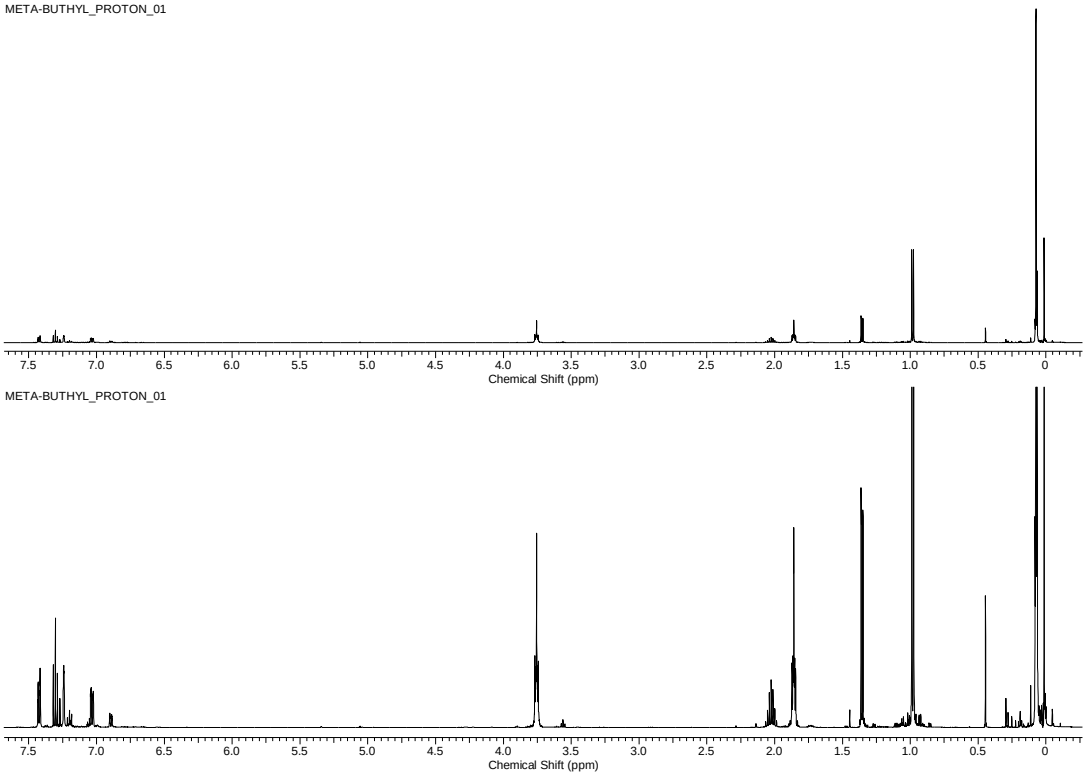

Figure I-2. ^{1}H-NMR ($CDCl_3$, 500 MHz) for (isobutyl)(para-aniline(trimethylsilyl))dichlorosilane

DDSQ-2((methyl)(para-aniline))

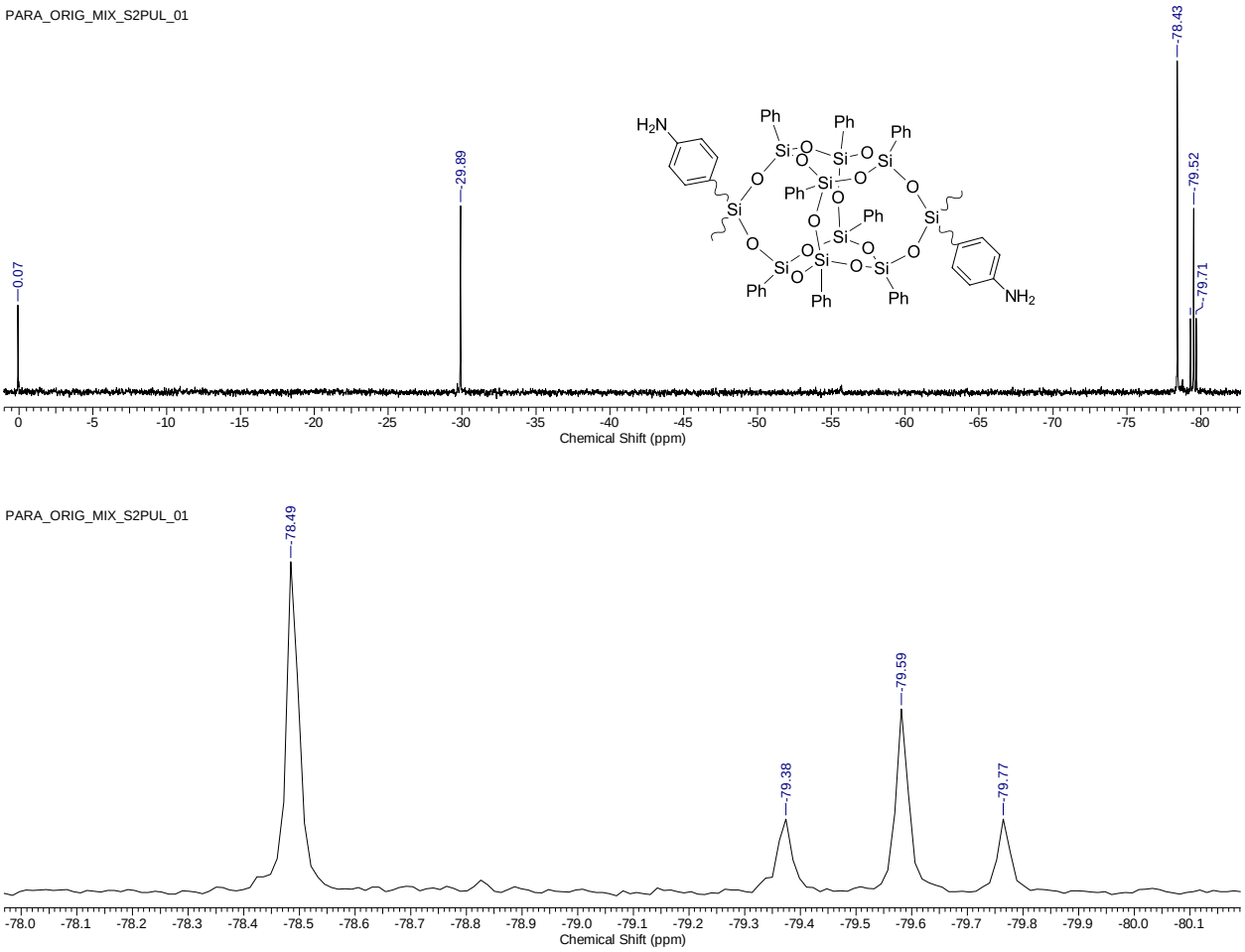

Figure I-3. ^{29}Si-NMR ($CDCl_3$, 99 MHz) for DDSQ-2((methyl)(para-aniline))

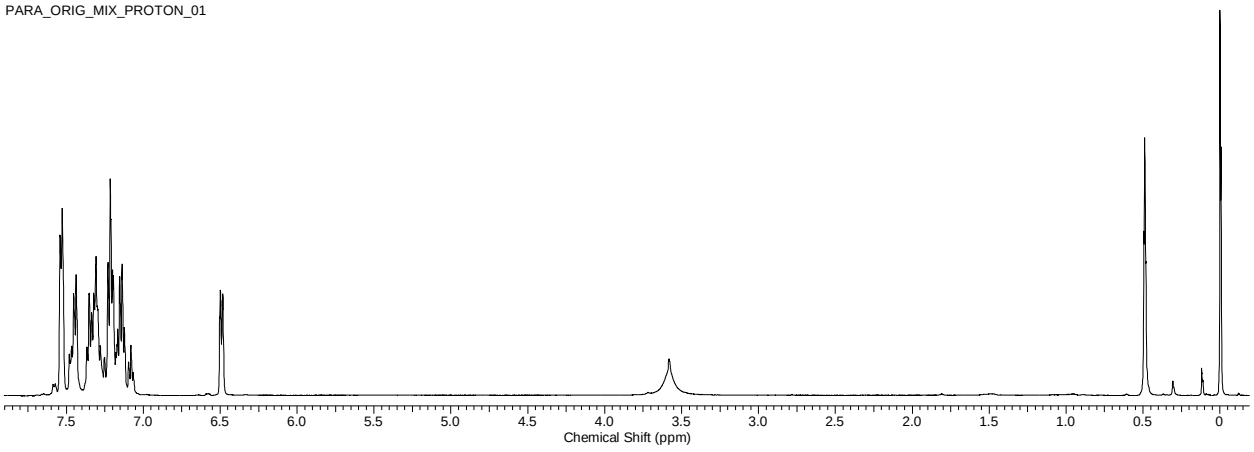

Figure I-4. ^{1}H-NMR ($CDCl_3$, 500 MHz) for DDSQ-2((methyl)(para-aniline))

DDSQ-2((methyl)(meta-aniline))

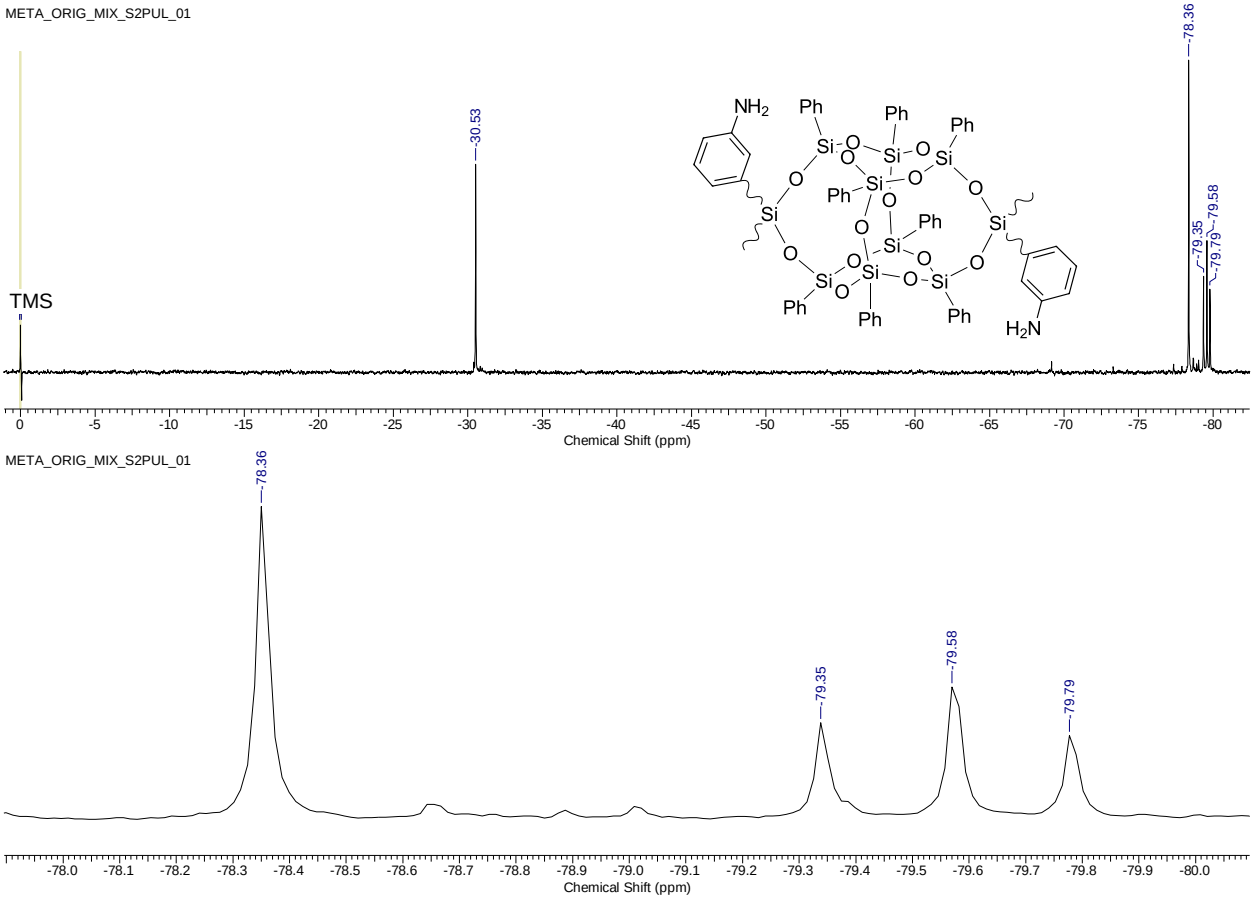

Figure I-5. ^{29}Si-NMR ($CDCl_3$, 99 MHz) DDSQ-2((methyl)(meta-aniline))

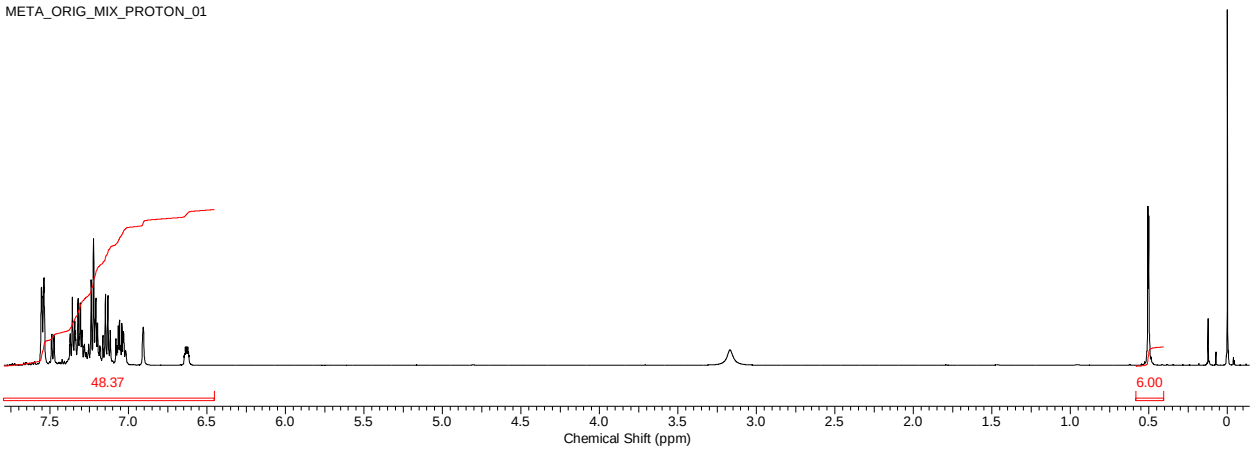

Figure I-6. ^{1}H-NMR ($CDCl_3$, 500 MHz) for DDSQ-2((methyl)(meta-aniline))

DDSQ-2((isobutyl)(meta-aniline))

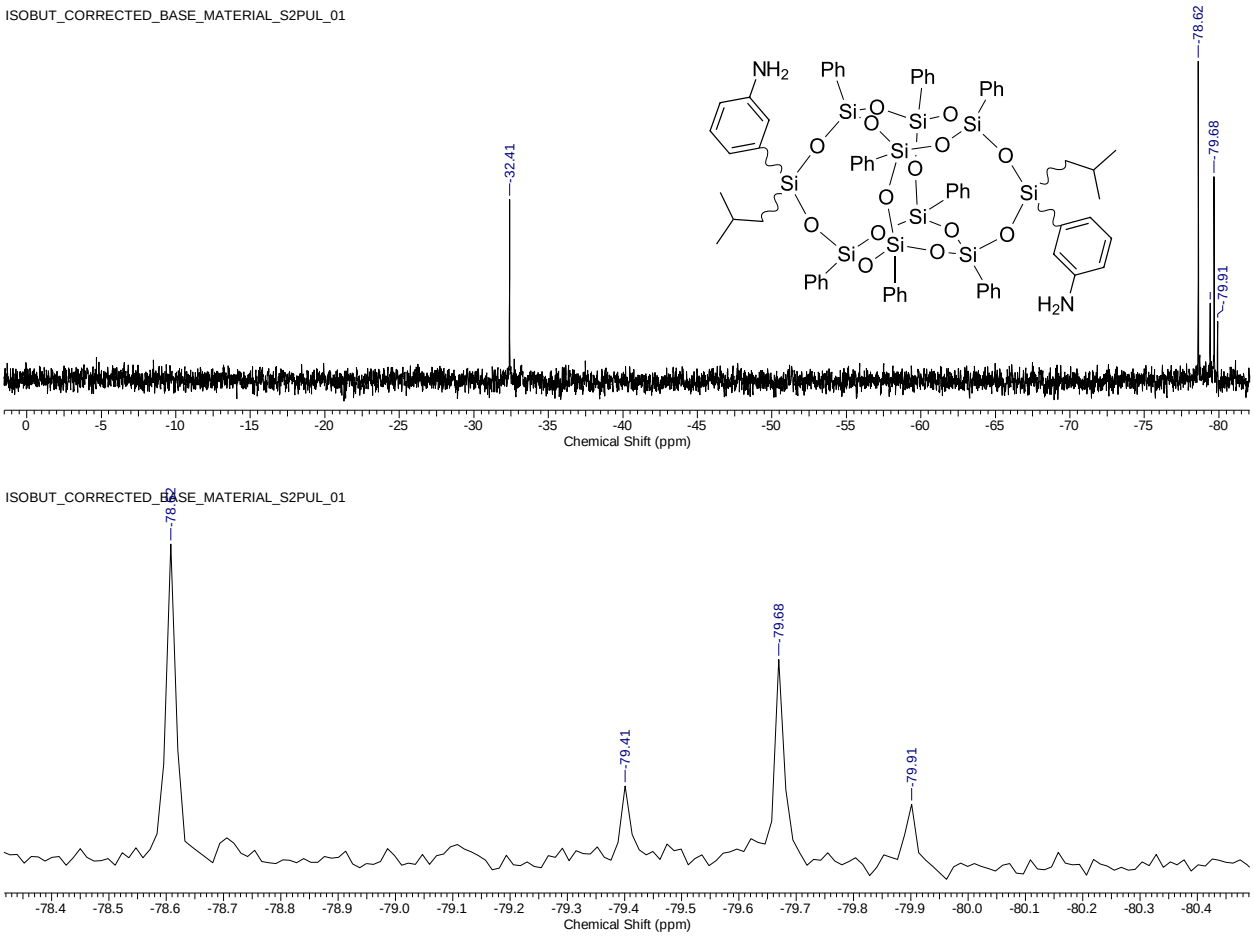

Figure I-7. ^{29}Si-NMR ($CDCl_3$, 99 MHz) for DDSQ-2((isobutyl)(meta-aniline))

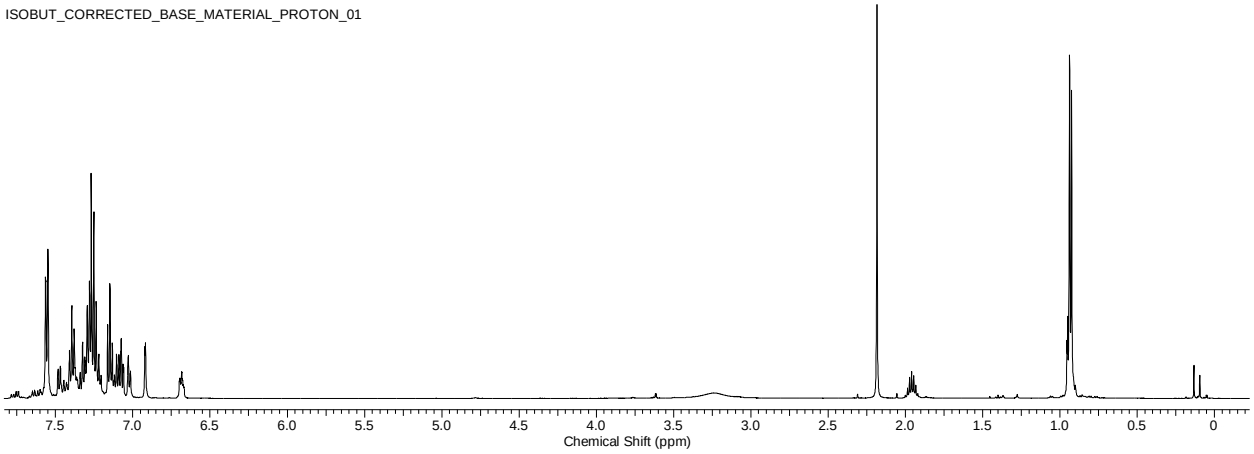

Figure I-8. ^{1}H-NMR ($CDCl_3$, 500 MHz) for DDSQ-2((isobutyl)(meta-aniline))

DDQS-((cyclohexyl)(meta-aniline))

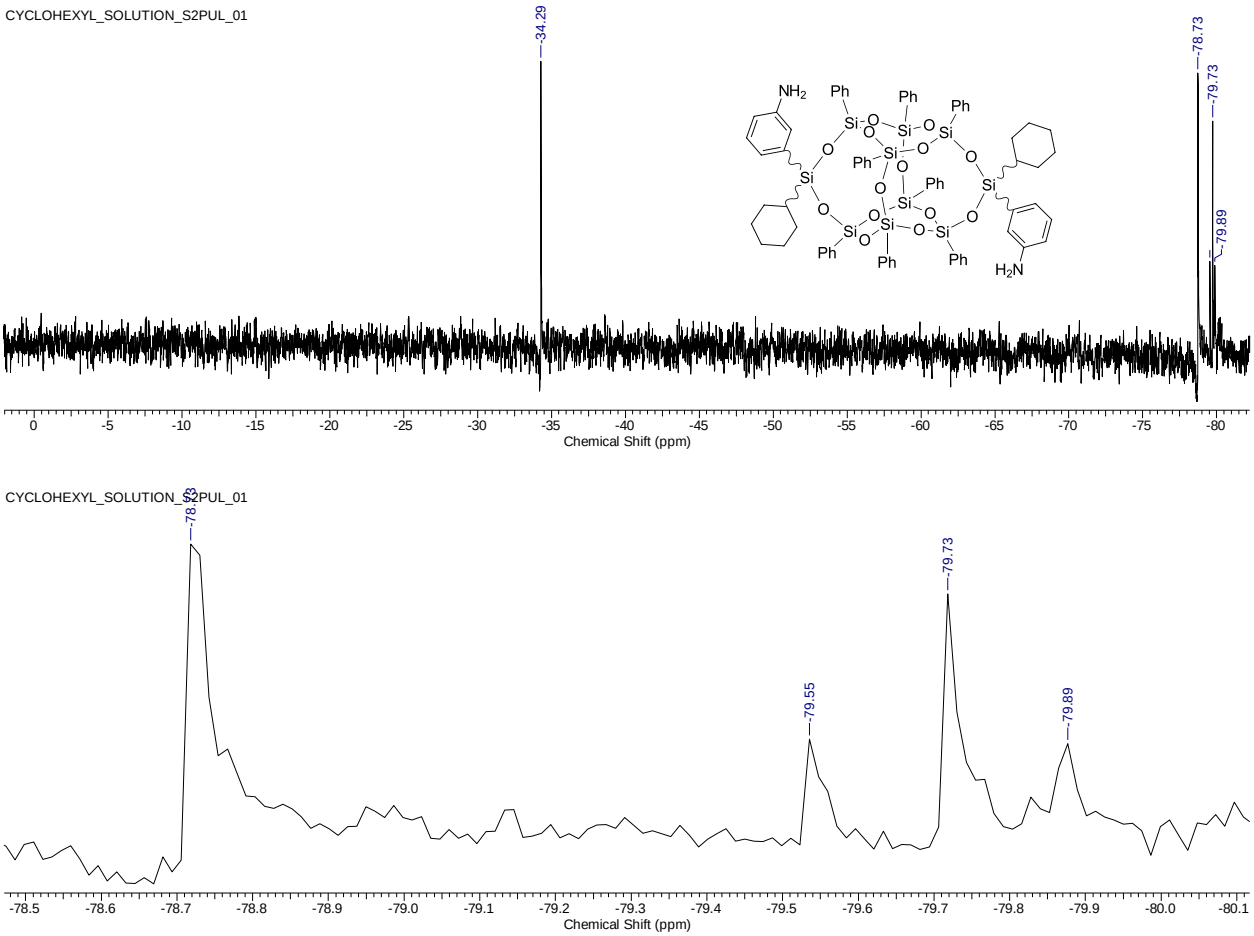

Figure I-9. ^{29}Si-NMR ($CDCl_3$, 99 MHz) for DDQS-((cyclohexyl)(meta-aniline))

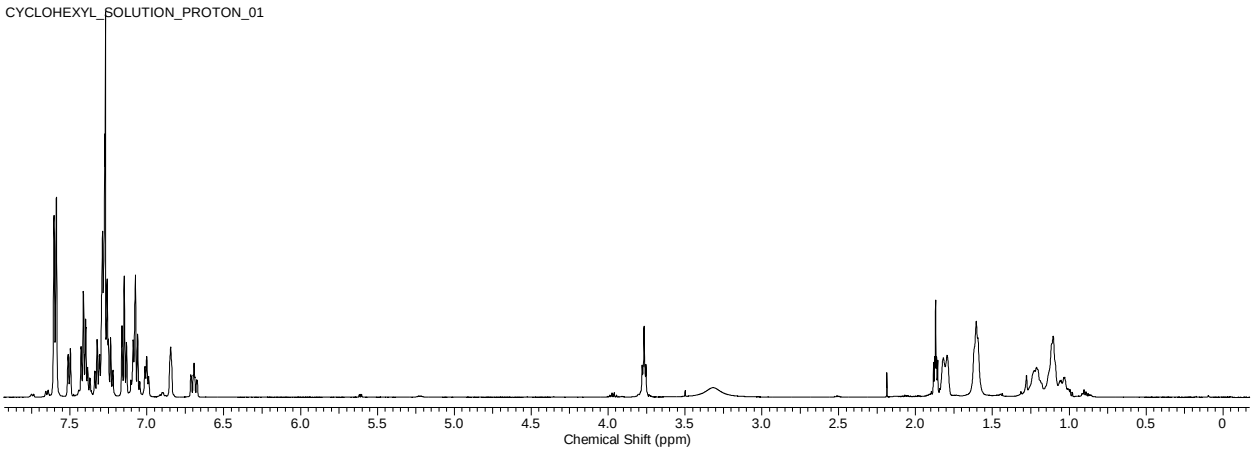

Figure I-10. ^{1}H-NMR ($CDCl_3$, 500 MHz) for DDQS-((cyclohexyl)(meta-aniline))

DDSQ-2((methyl)(hydroxyl))

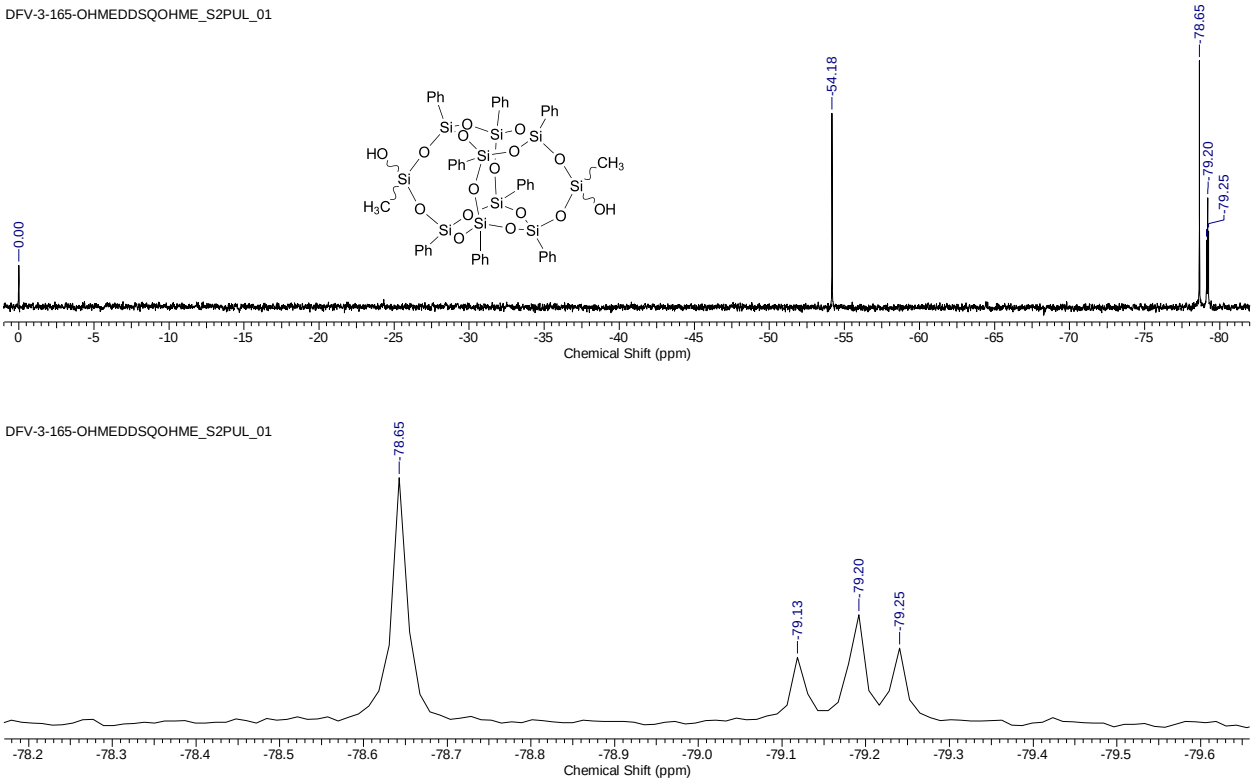

Figure I-11. ^{29}Si-NMR ($CDCl_3$, 99 MHz) for DDSQ-2((methyl)(hydroxyl))

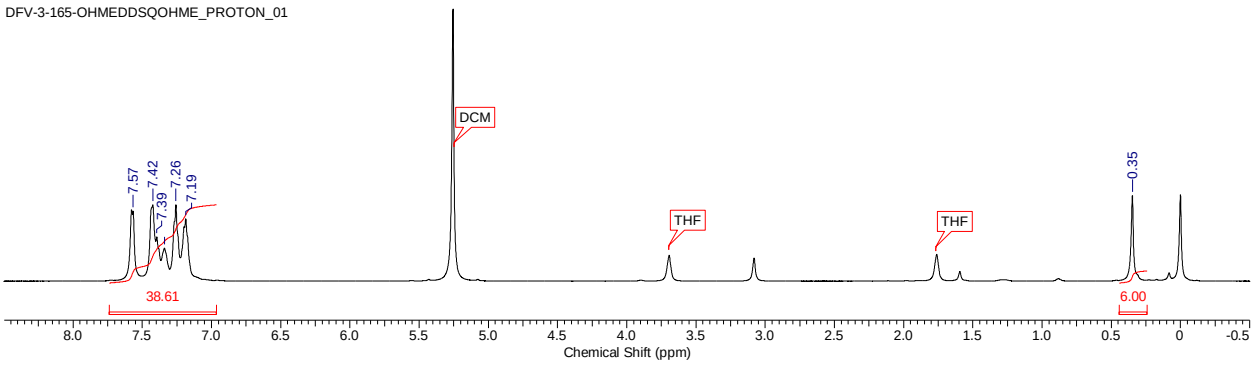

Figure I-12. ^{1}H-NMR ($CDCl_3$, 500 MHz) for DDSQ-2((methyl)(hydroxyl))

DDSQ-2((vinyl)(hydroxyl))

^{29}Si-NMR ($CDCl_3$, 99 MHz)

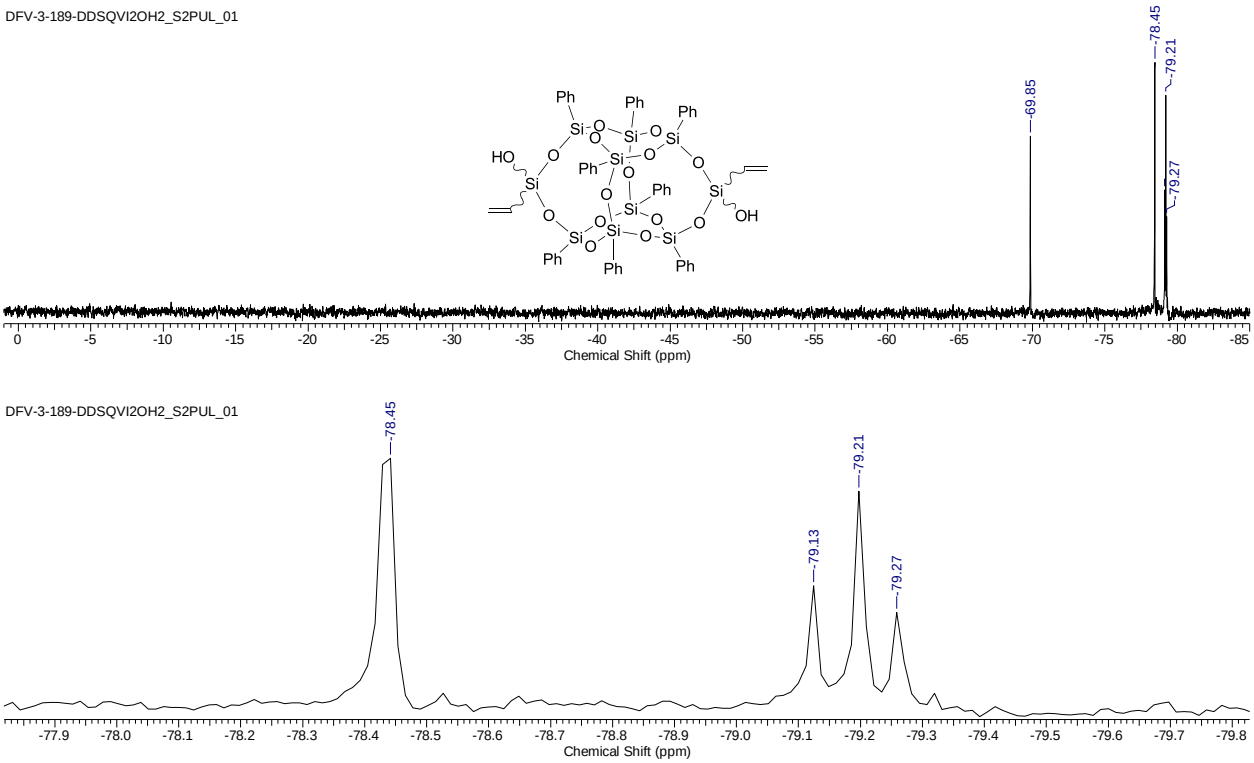

Figure I-13. ^{29}Si-NMR ($CDCl_3$, 99 MHz) for DDSQ-2((vinyl)(hydroxyl))

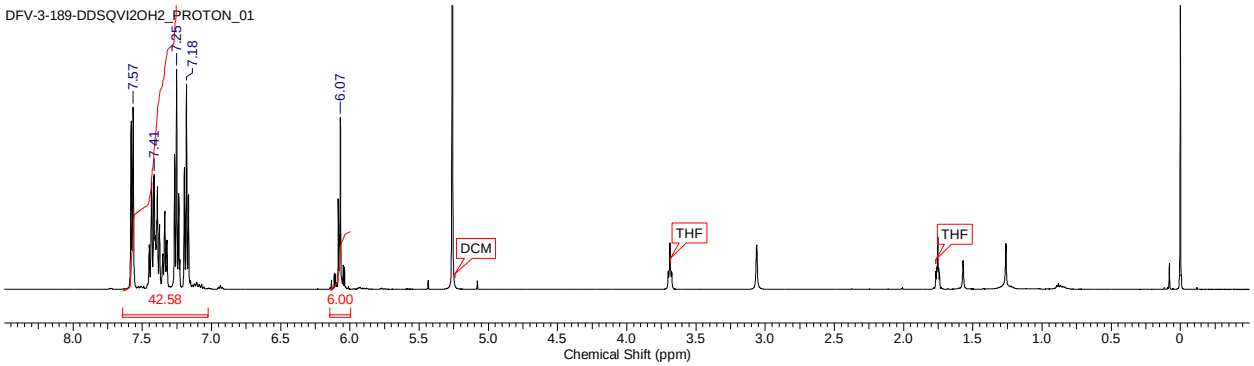

Figure I-14. ^{1}H-NMR ($CDCl_3$, 500 MHz) for DDSQ-2((vinyl)(hydroxyl))

DDSQ-2((isopropyl)(hydroxyl))

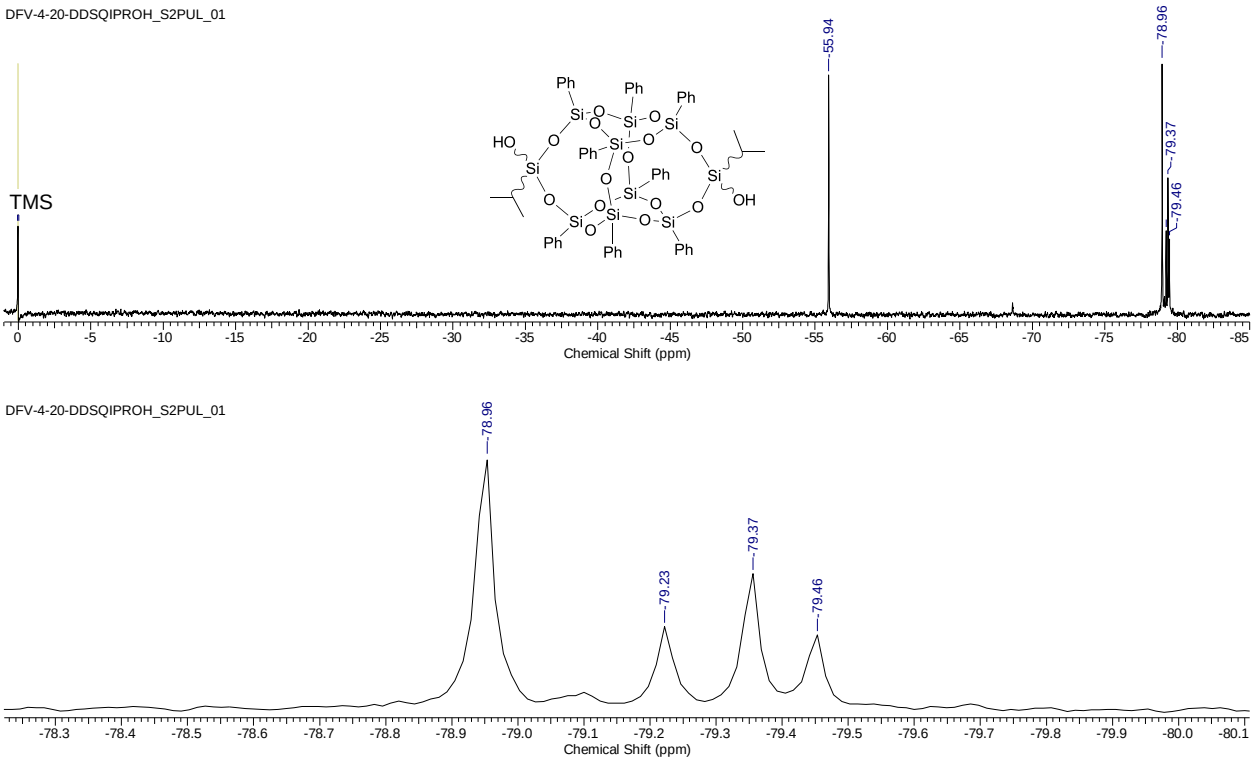

Figure I-15. ^{29}Si-NMR ($CDCl_3$, 99 MHz) for DDSQ-2((isopropyl)(hydroxyl))

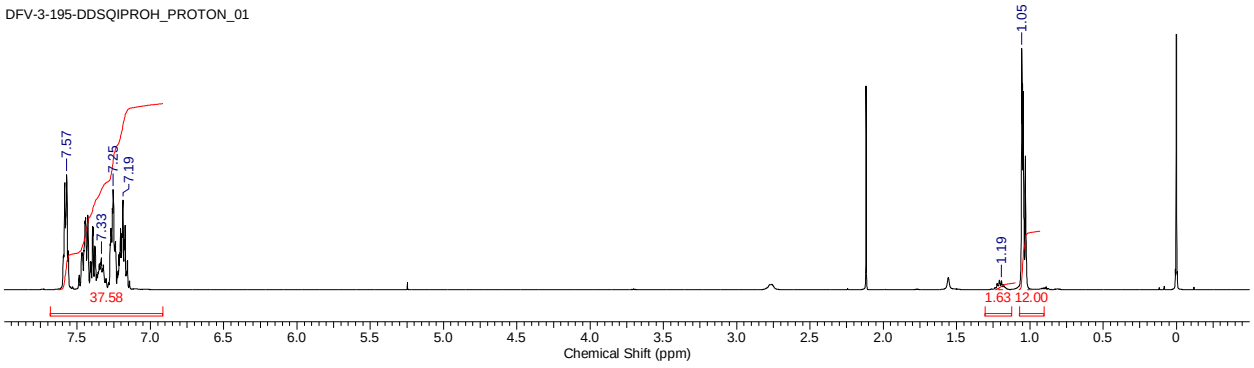

Figure I-16. ^{1}H-NMR ($CDCl_3$, 500 MHz) for DDSQ-2((isopropyl)(hydroxyl))

DDSQ-2((isobutyl)(hydroxyl))

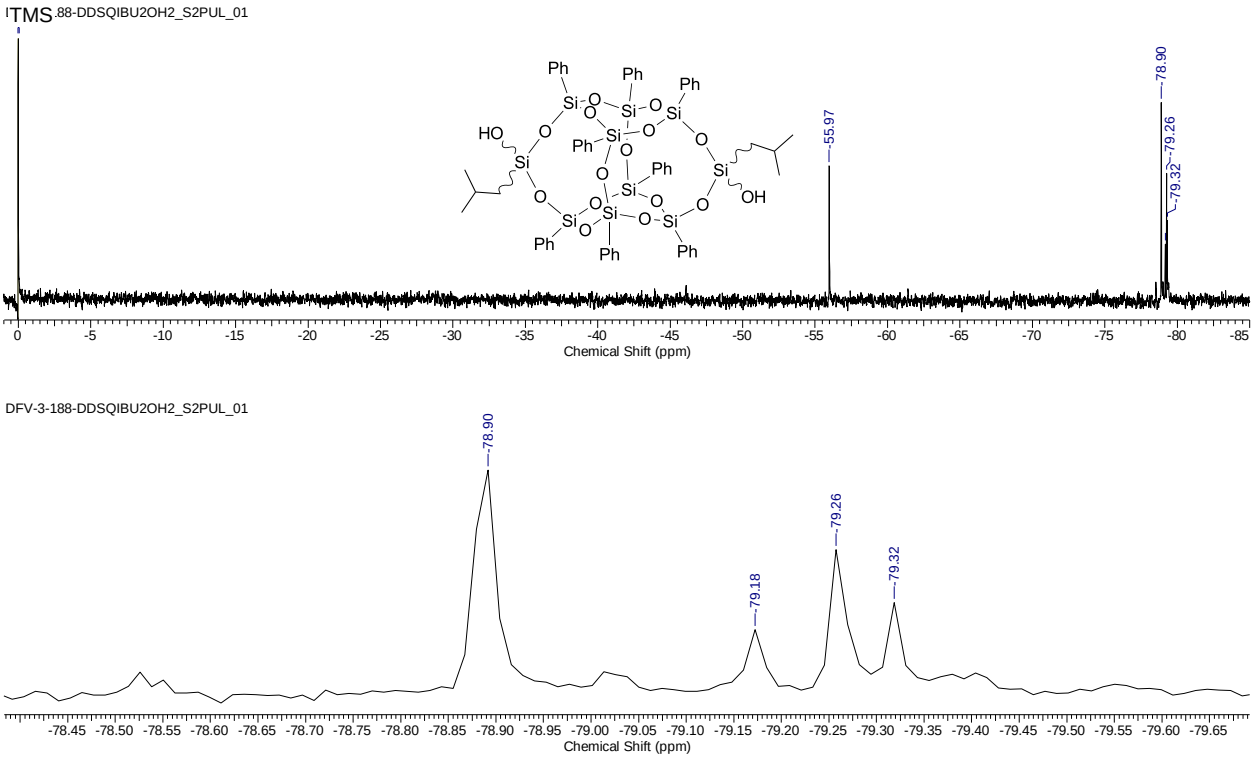

Figure I-17. ^{29}Si-NMR ($CDCl_3$, 99 MHz) for DDSQ-2((isobutyl)(hydroxyl))

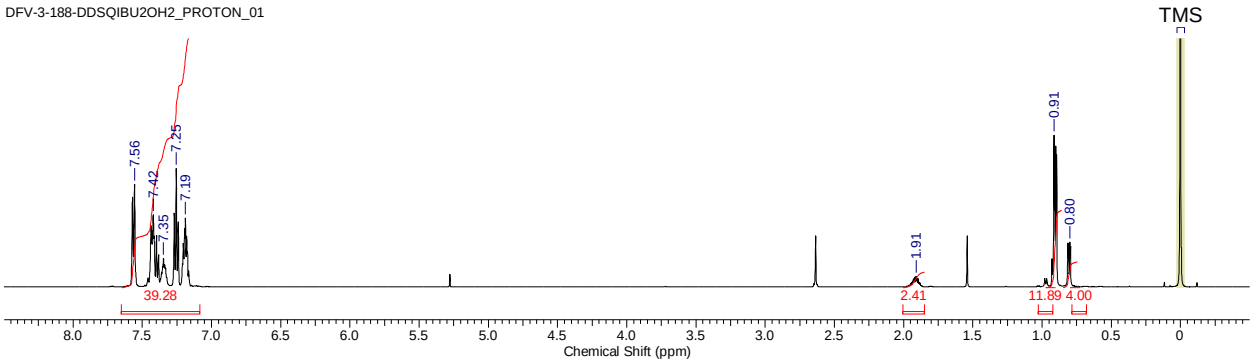

Figure I-18. ^{1}H-NMR ($CDCl_3$, 500 MHz) for DDSQ-2((isobutyl)(hydroxyl))

DDSQ-2((phenyl)(hydroxyl))

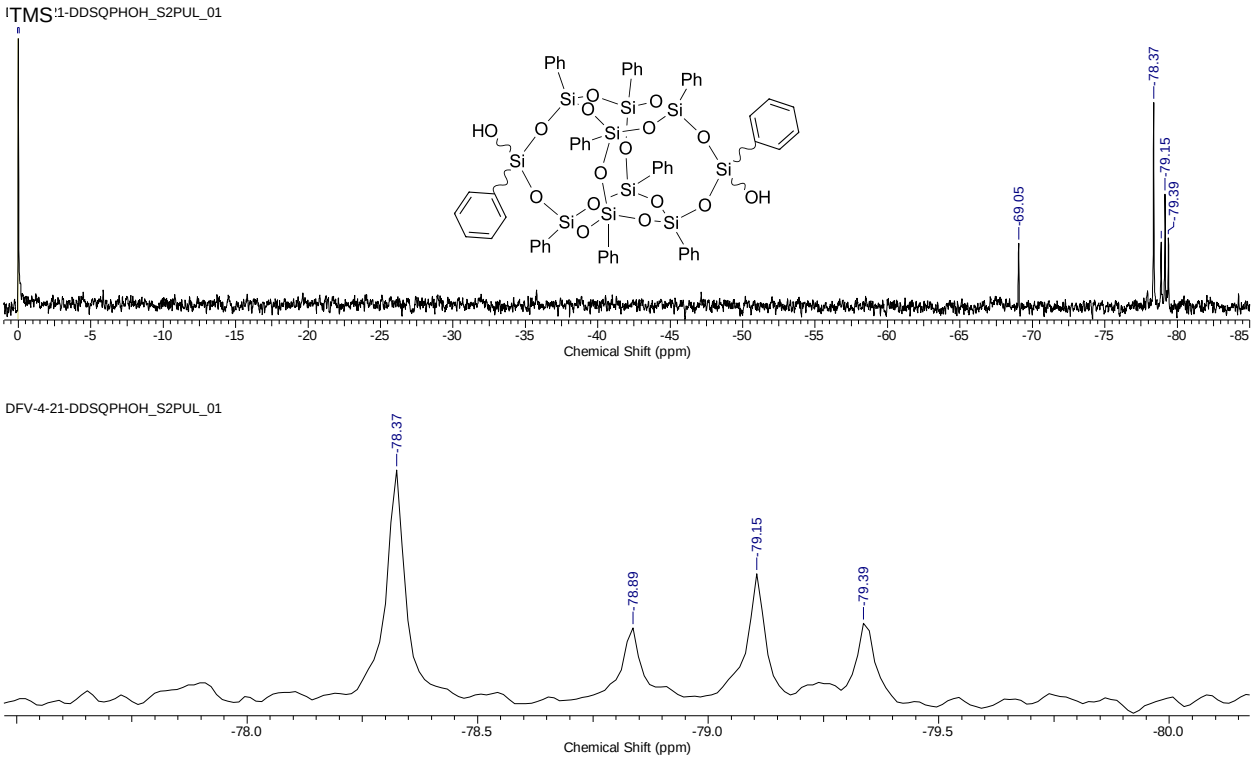

Figure I-19. ^{29}Si-NMR ($CDCl_3$, 99 MHz) for DDSQ-2((phenyl)(hydroxyl))

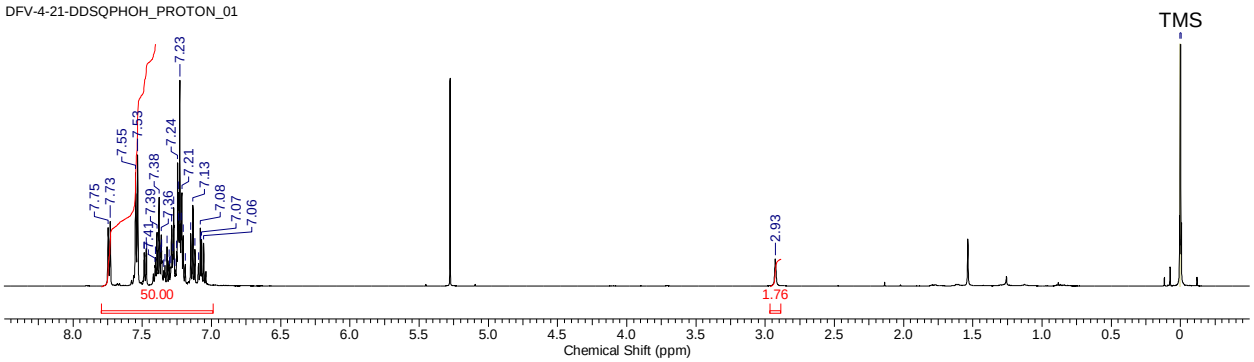

Figure I-20. ^{1}H-NMR ($CDCl_3$, 500 MHz) for DDSQ-2((phenyl)(hydroxyl))

DDSQ-2((methyl)(propyl-cyanide))

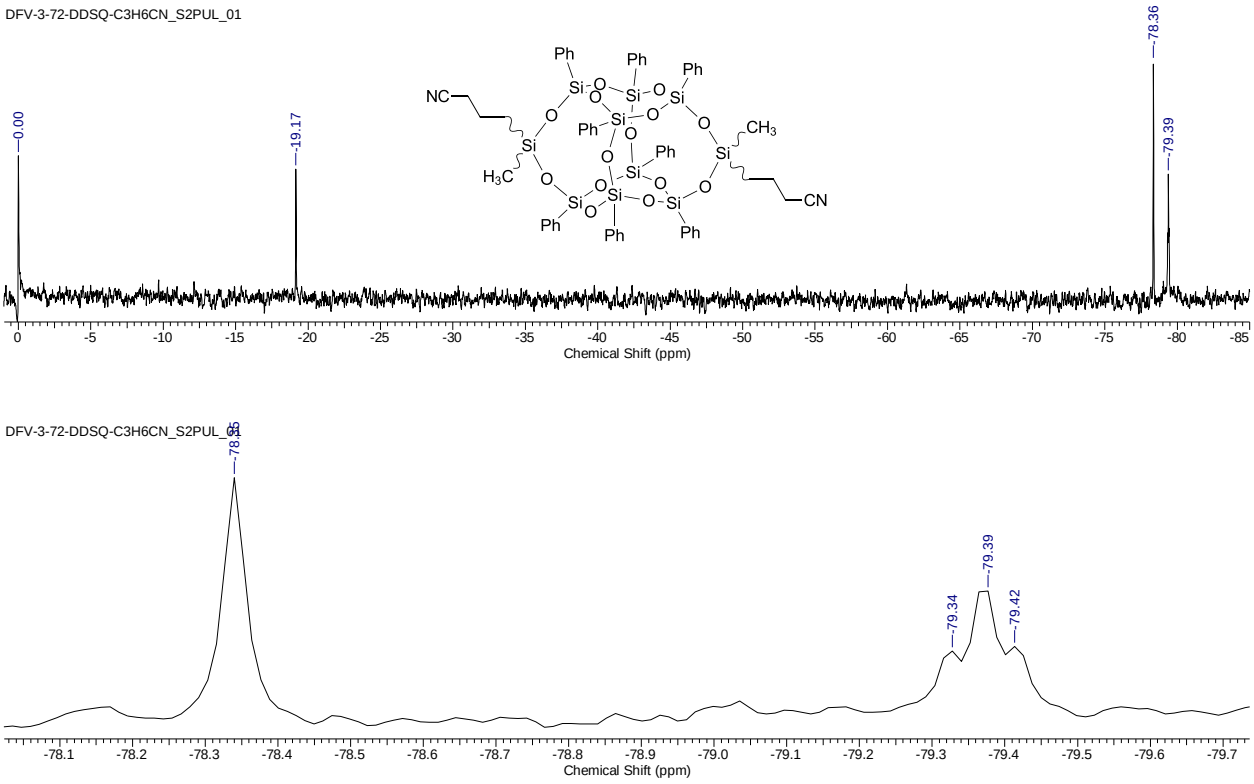

Figure I-21. ^{29}Si-NMR ($CDCl_3$, 99 MHz) for DDSQ-2((methyl)(propyl-cyanide))

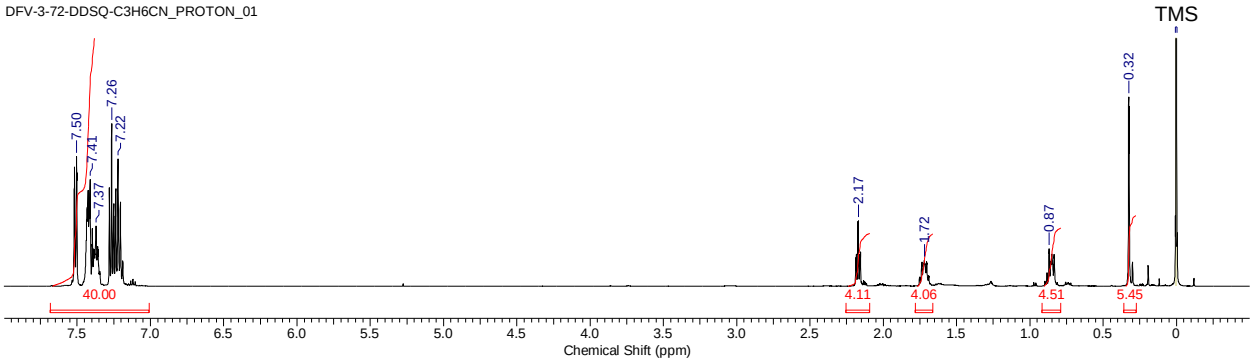

Figure I-22. ^{1}H-NMR ($CDCl_3$, 500 MHz) for DDSQ-2((methyl)(propyl-cyanide))

DDSQ-2((methyl)(hydro))

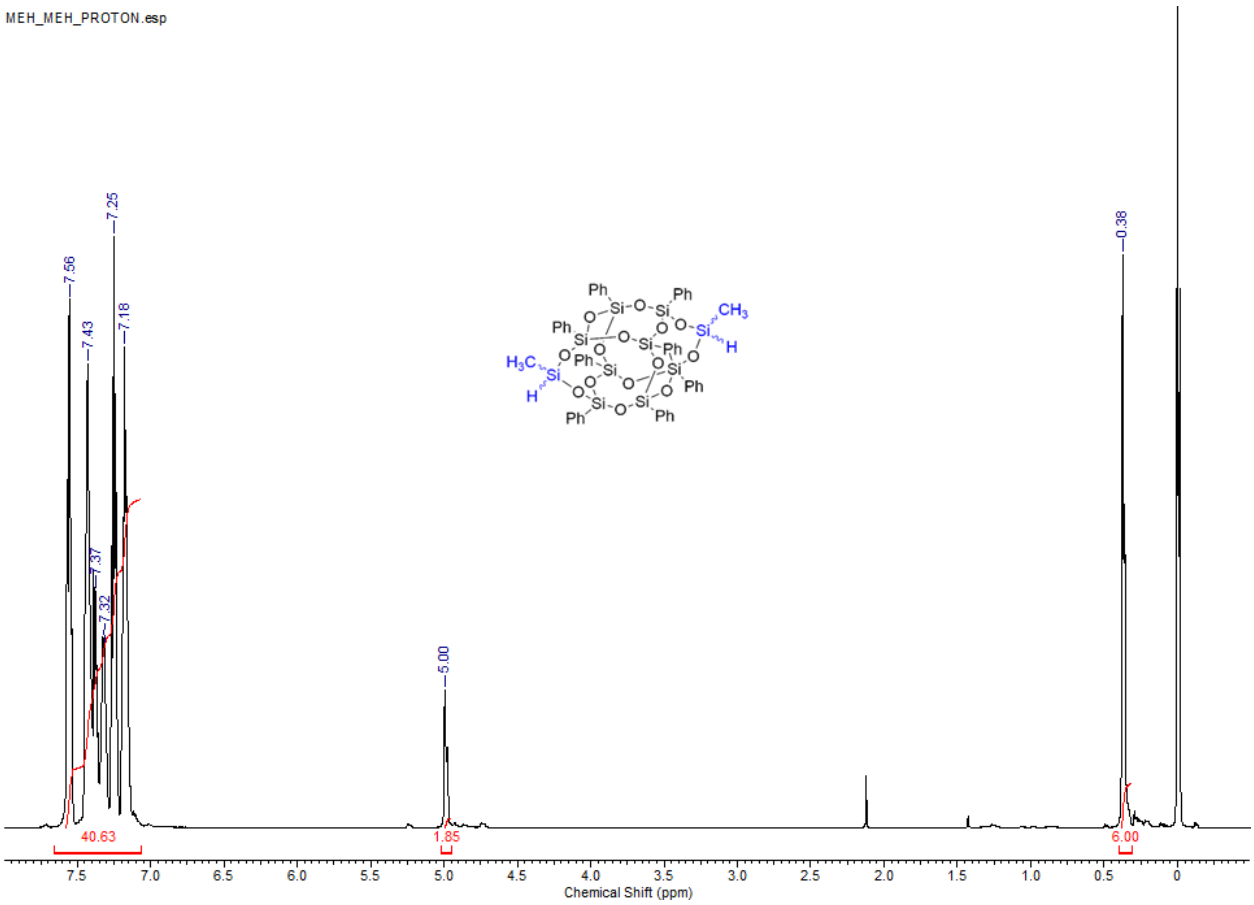

Figure I-23. ^{1}H-NMR (500 MHz, $CDCl_3$) for DDSQ-2((methyl)(hydro))

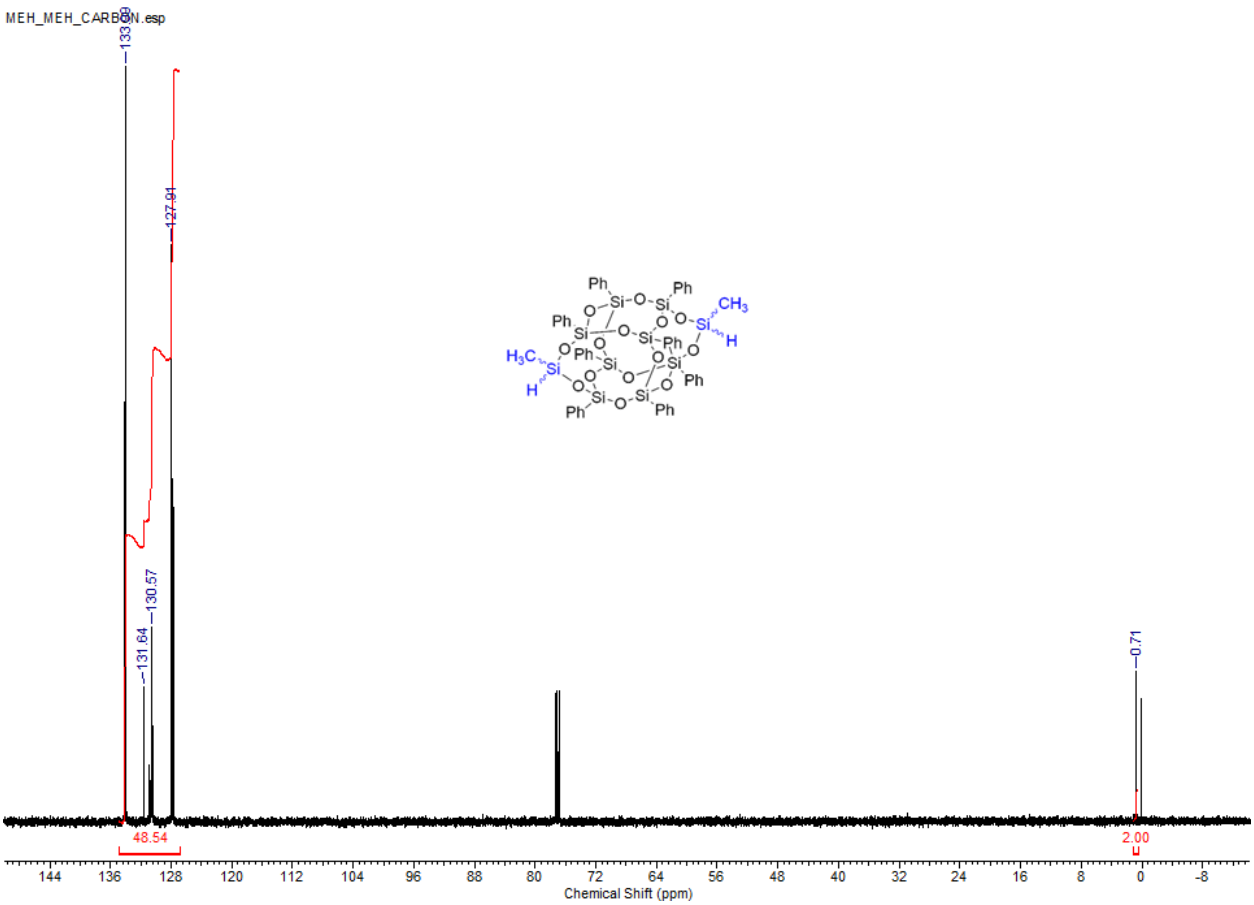

Figure I-24. ^{13}C-NMR (125 MHz, $CDCl_3$) for DDSQ-2((methyl)(hydro))

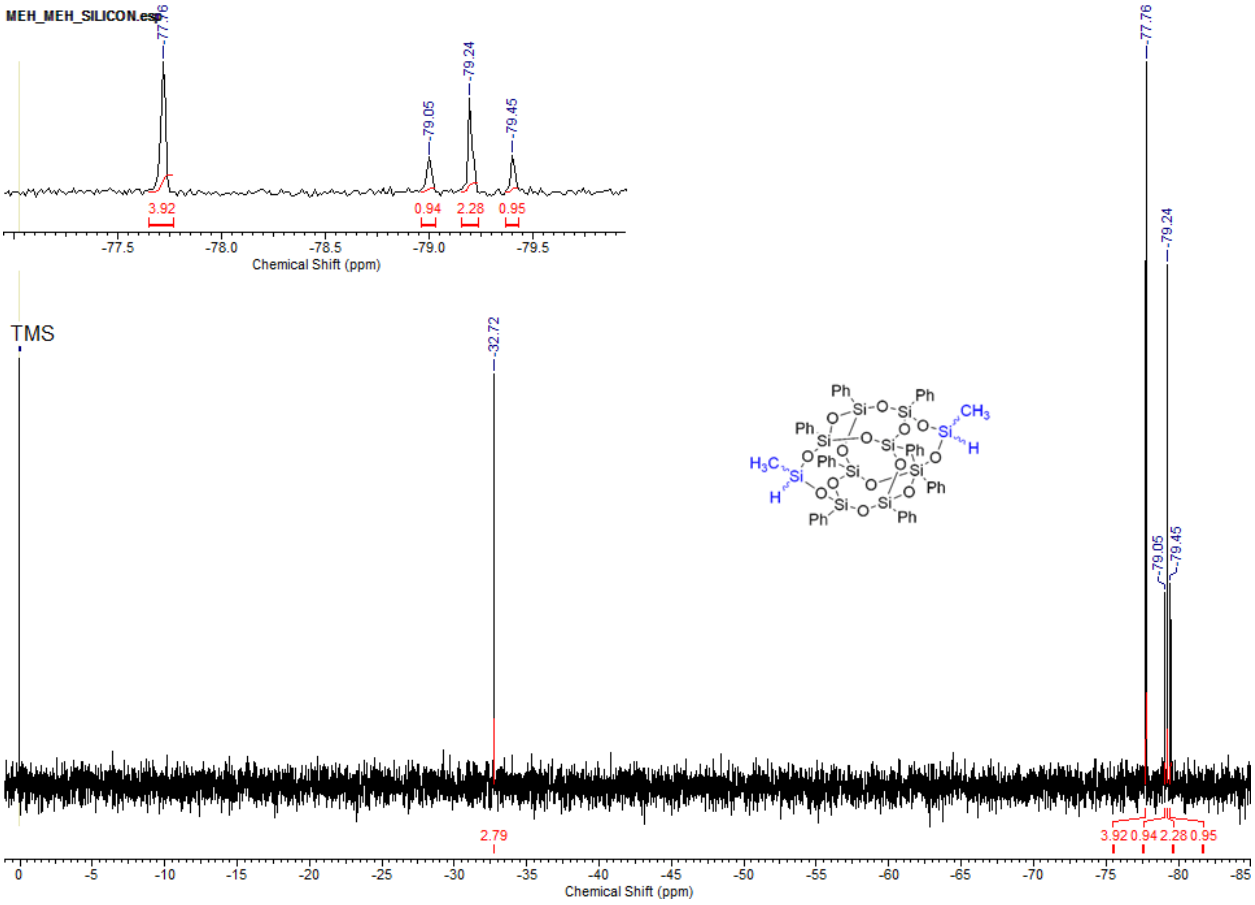

Figure I-25. ^{29}Si-NMR (99 MHz, $CDCl_3$) for DDSQ-2((methyl)(hydro))

DDSQ-2(methyl)$_2$

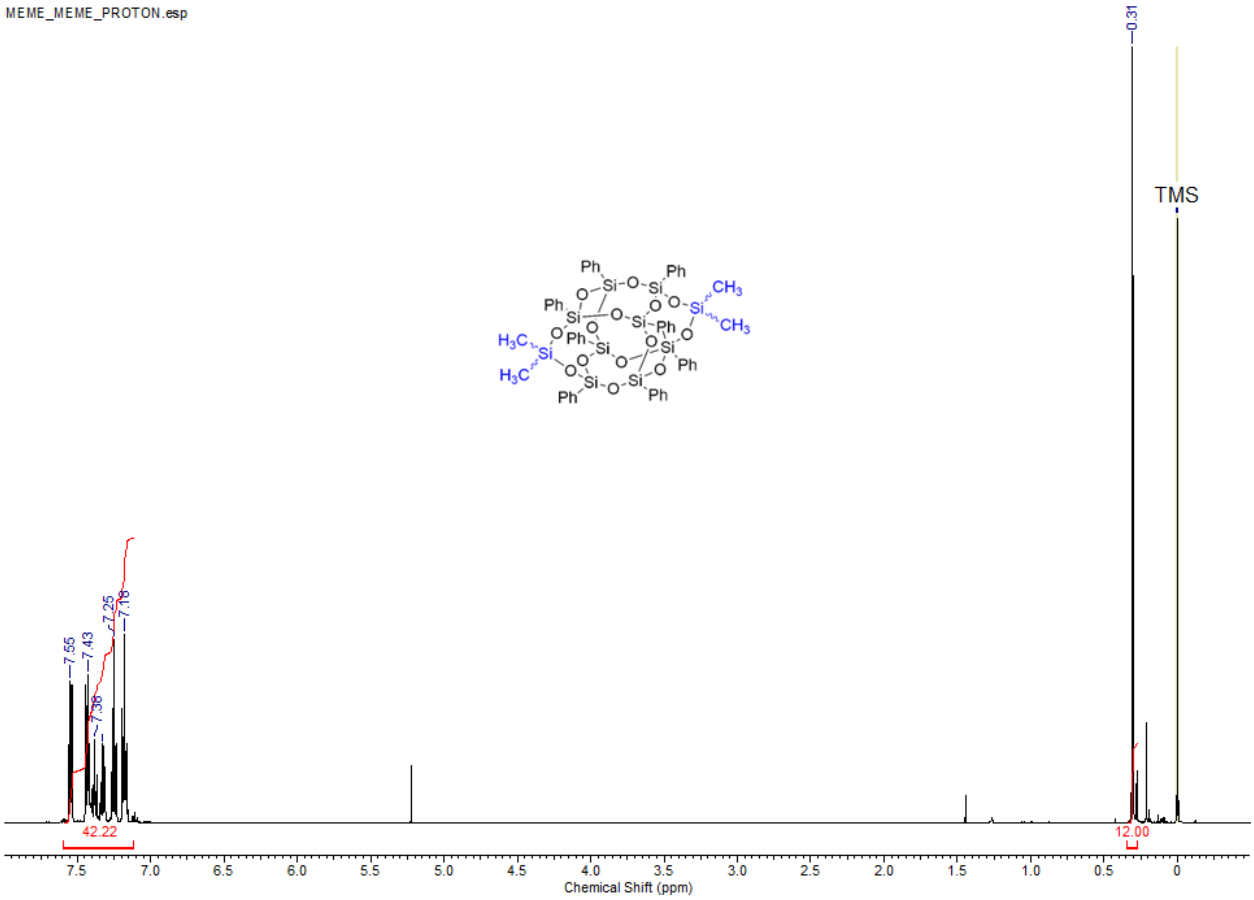

Figure I-26. ^{1}H-NMR (500 MHz, $CDCl_3$) for DDSQ-2(methyl)$_2$

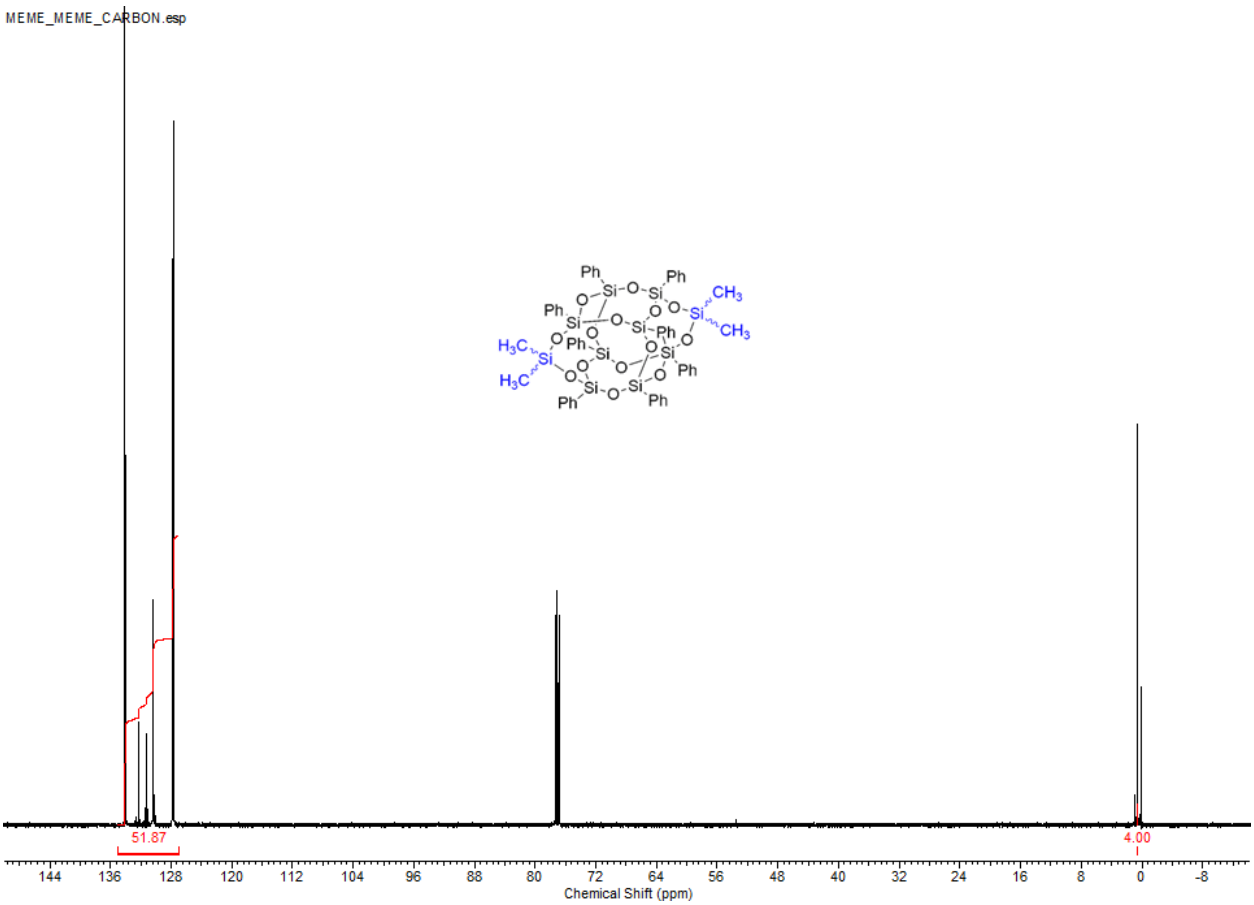

Figure I-27. ^{13}C-NMR (125 MHz, $CDCl_3$) for DDSQ-2(methyl)$_2$

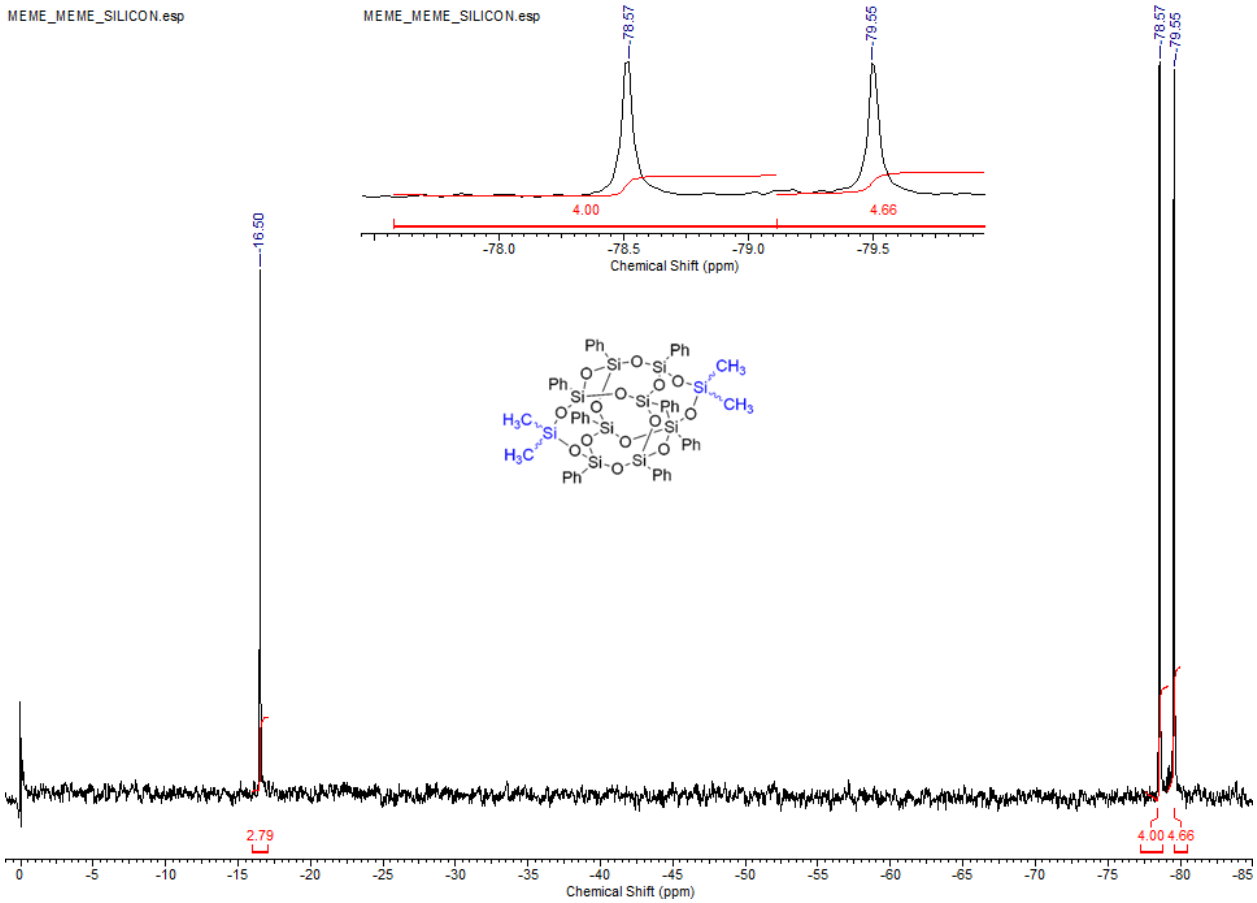

Figure I-28. ^{29}Si-NMR (99 MHz, $CDCl_3$) for DDSQ-2(methyl)$_2$

DDSQ-2((methyl)(vinyl))

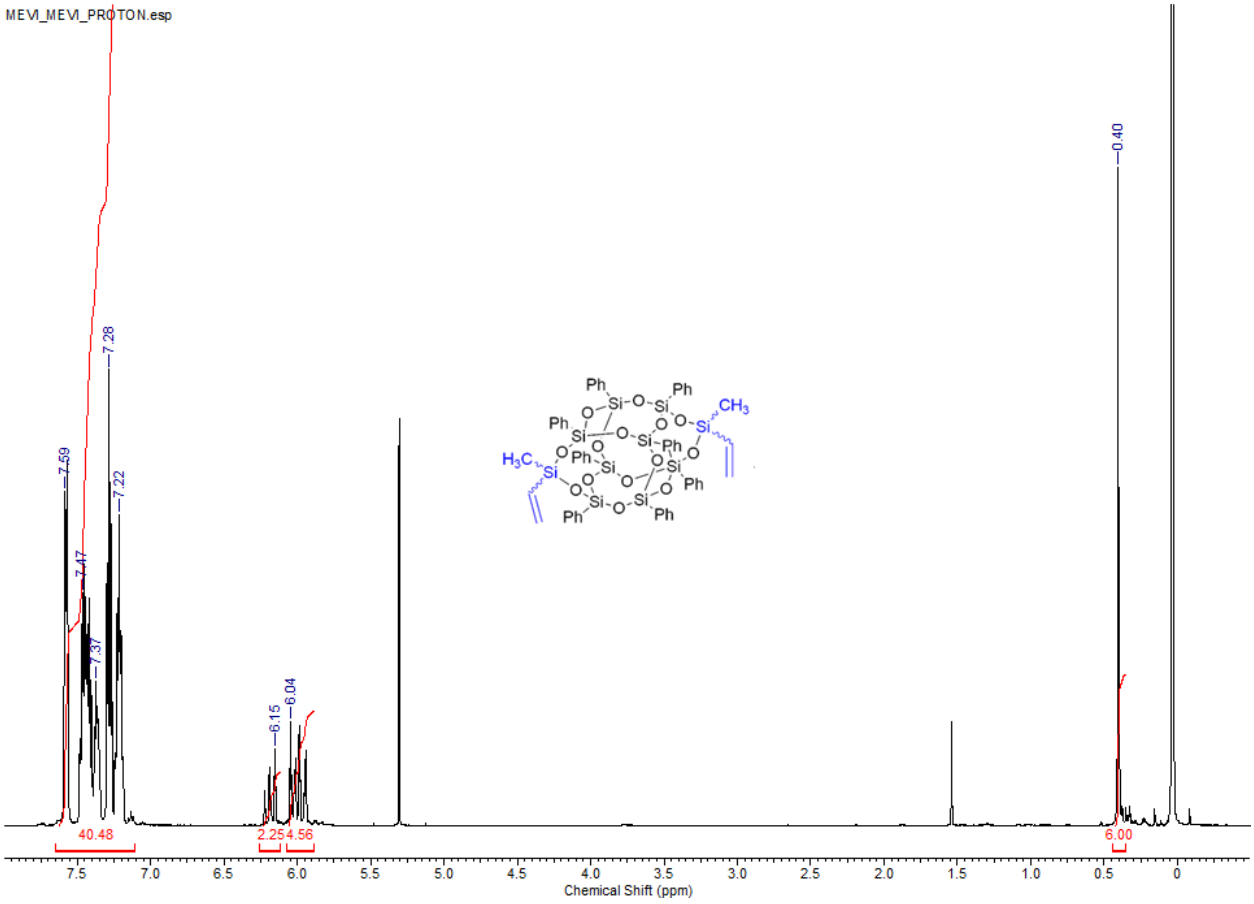

Figure I-29. ^{1}H-NMR (500 MHz, $CDCl_3$) for DDSQ-2((methyl)(vinyl))

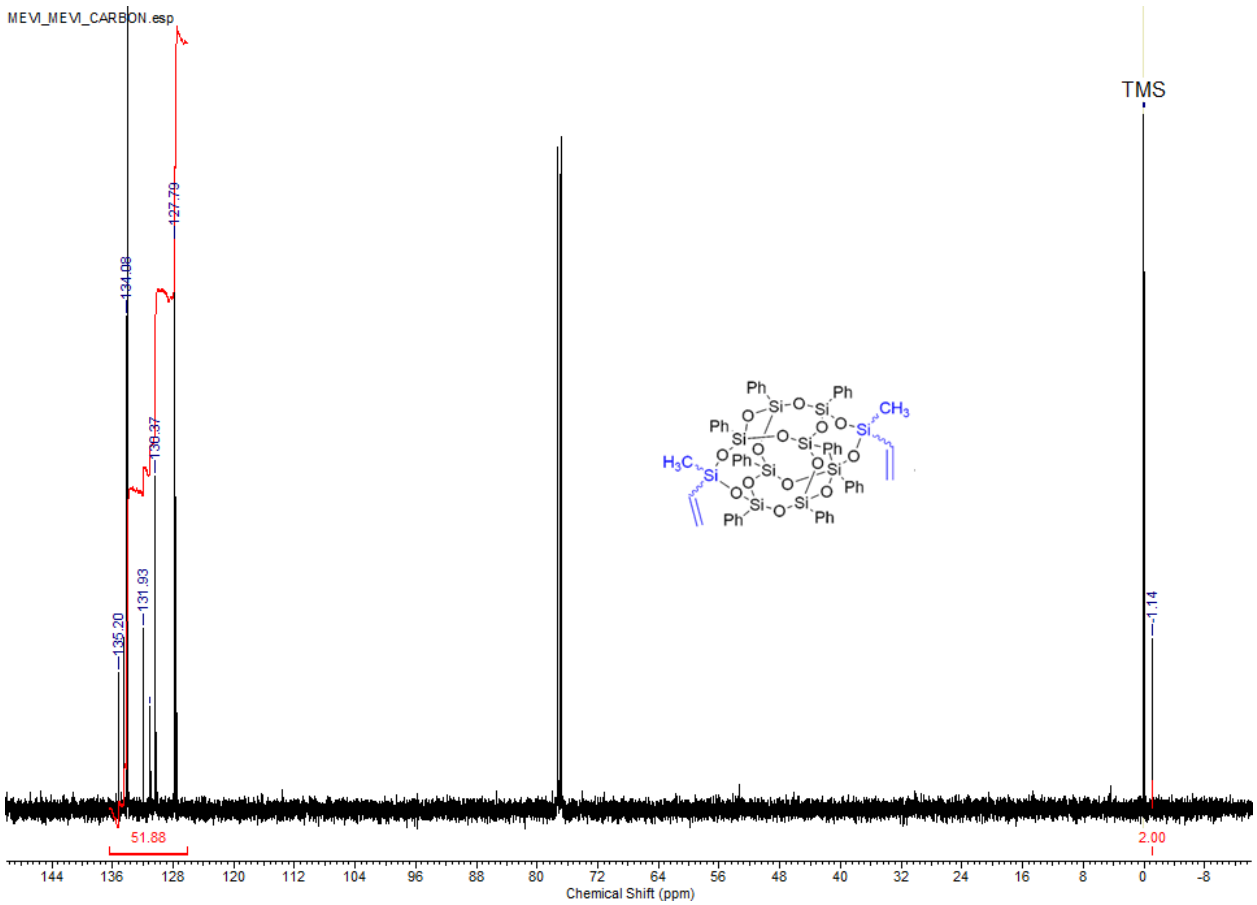

Figure I-30. ^{13}C-NMR (125 MHz, $CDCl_3$) for DDSQ-2((methyl)(vinyl))

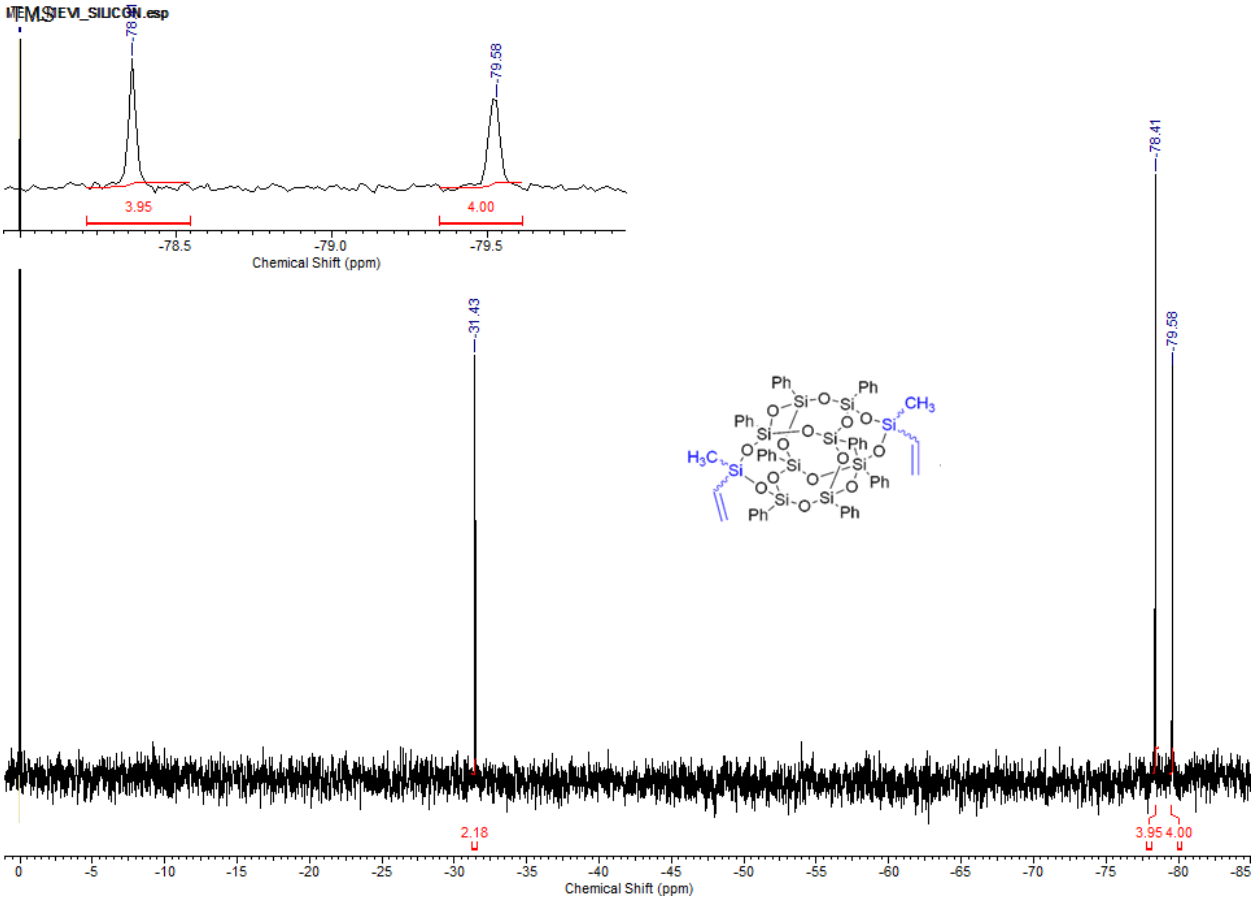

Figure I-31. ^{29}Si-NMR (99 MHz, $CDCl_3$) for DDSQ-2((methyl)(vinyl))

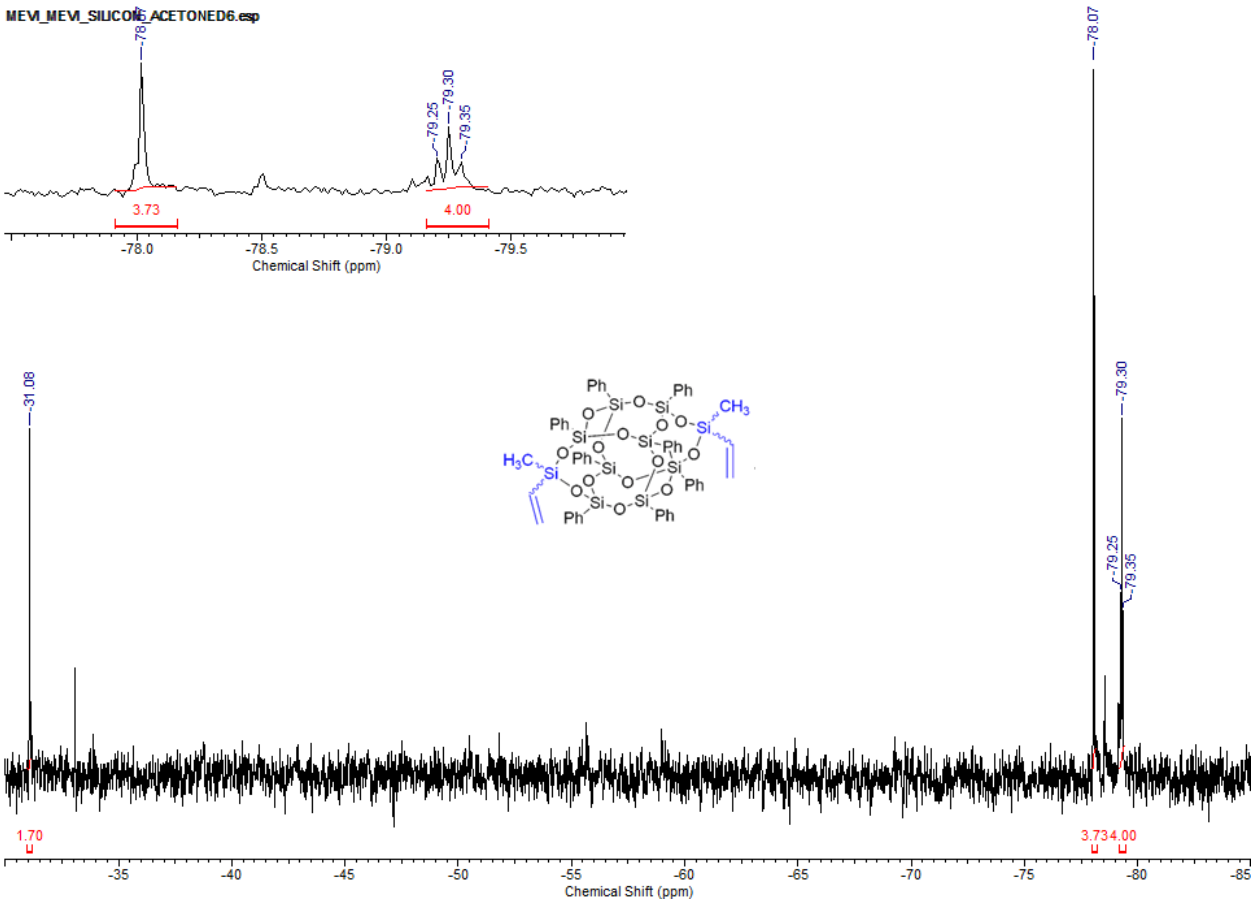

Figure I-32. ^{29}Si-NMR (99 MHz, Acetone-D6) for DDSQ-2((methyl)(vinyl))

DDSQ-2(methyl)(3-propyl-chloride)

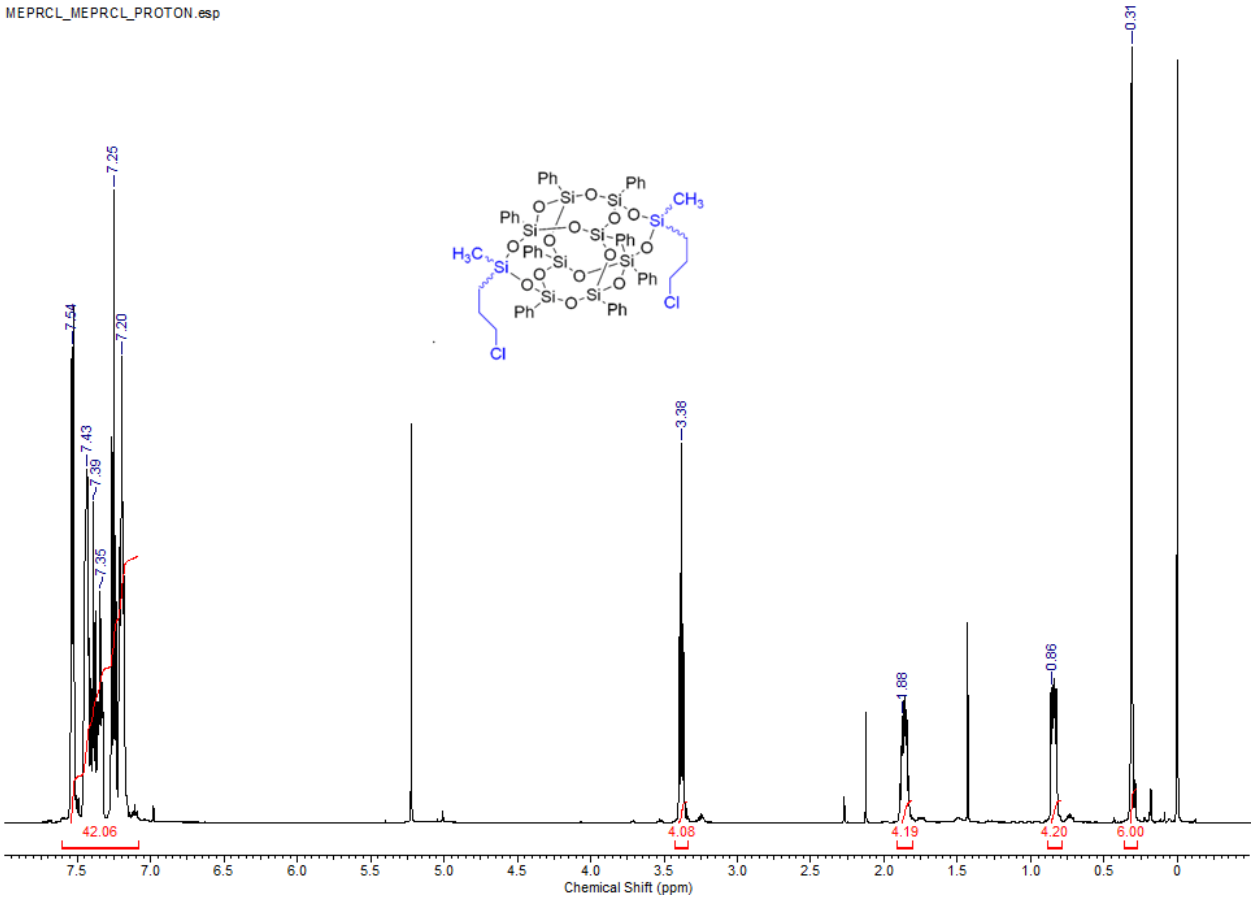

Figure I-33. ^{1}H-NMR (500 MHz, $CDCl_3$) for DDSQ-2(methyl)(3-propyl-chloride)

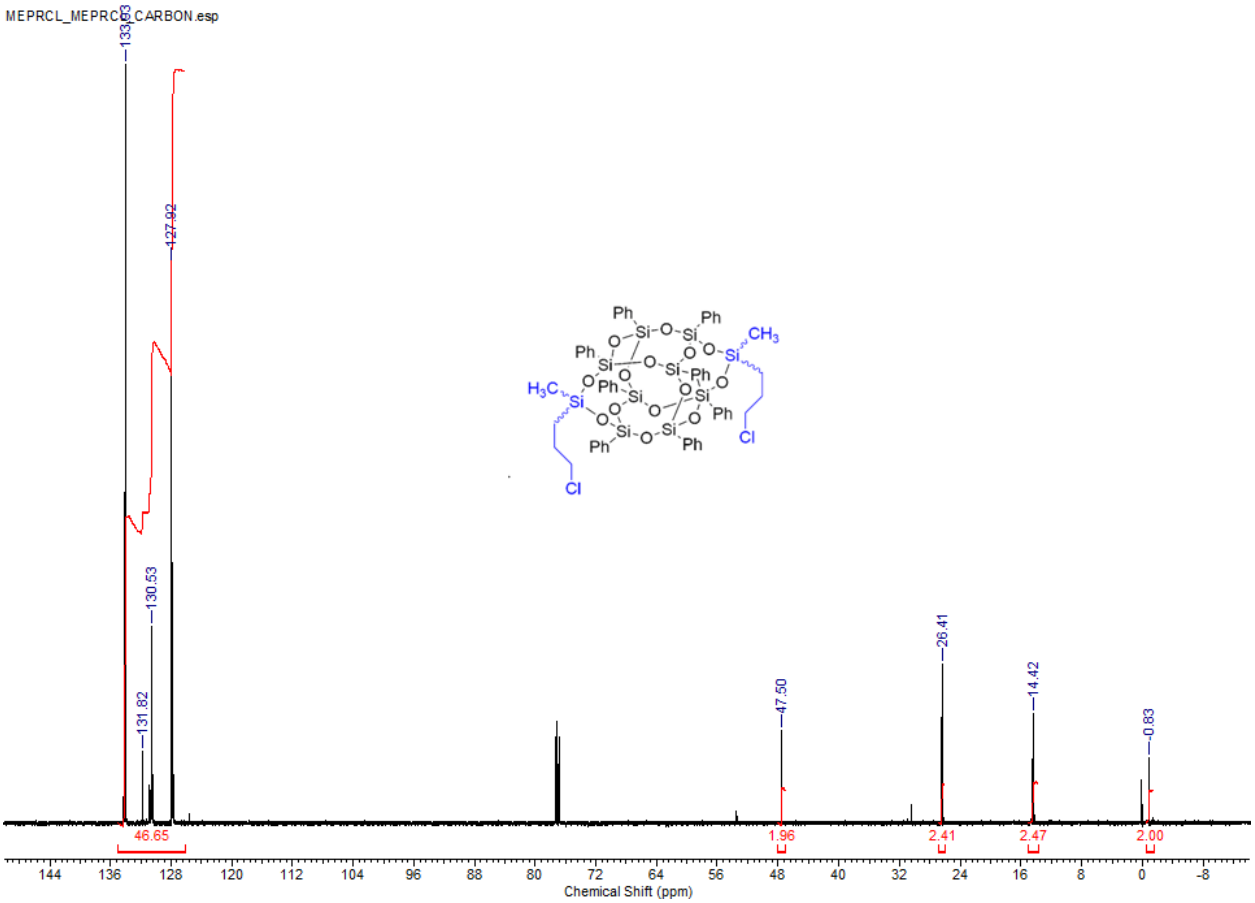

Figure I-34. ^{13}C-NMR (125 MHz, $CDCl_3$) for DDSQ-2(methyl)(3-propyl-chloride)

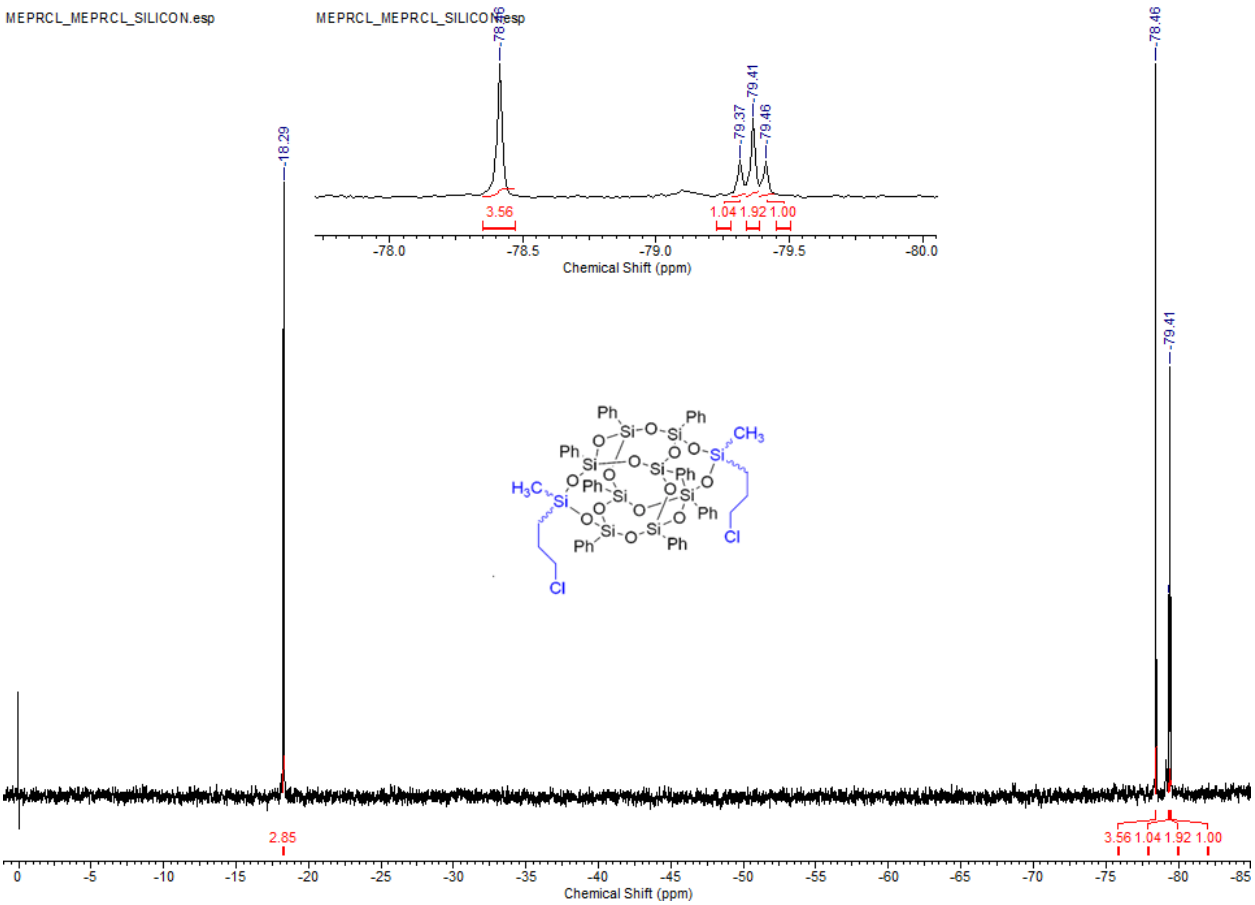

Figure I-35. ^{29}Si-NMR (99 MHz, $CDCl_3$) for DDSQ-2(methyl)(3-propyl-chloride)

DDSQ-2((methyl)(hydroxyl))

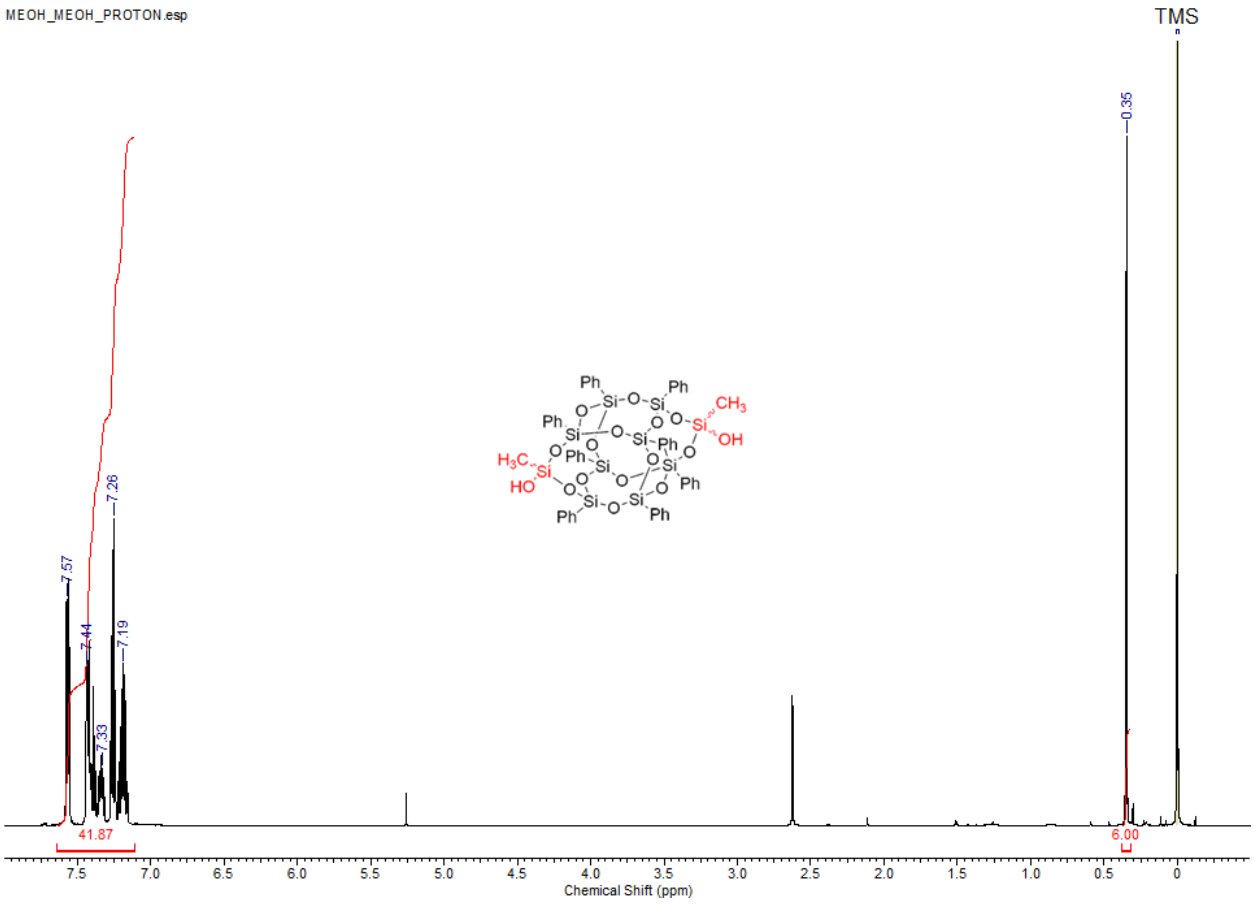

Figure I-36. ^{1}H-NMR (500 MHz, $CDCl_3$) for DDSQ-2((methyl)(hydroxyl))

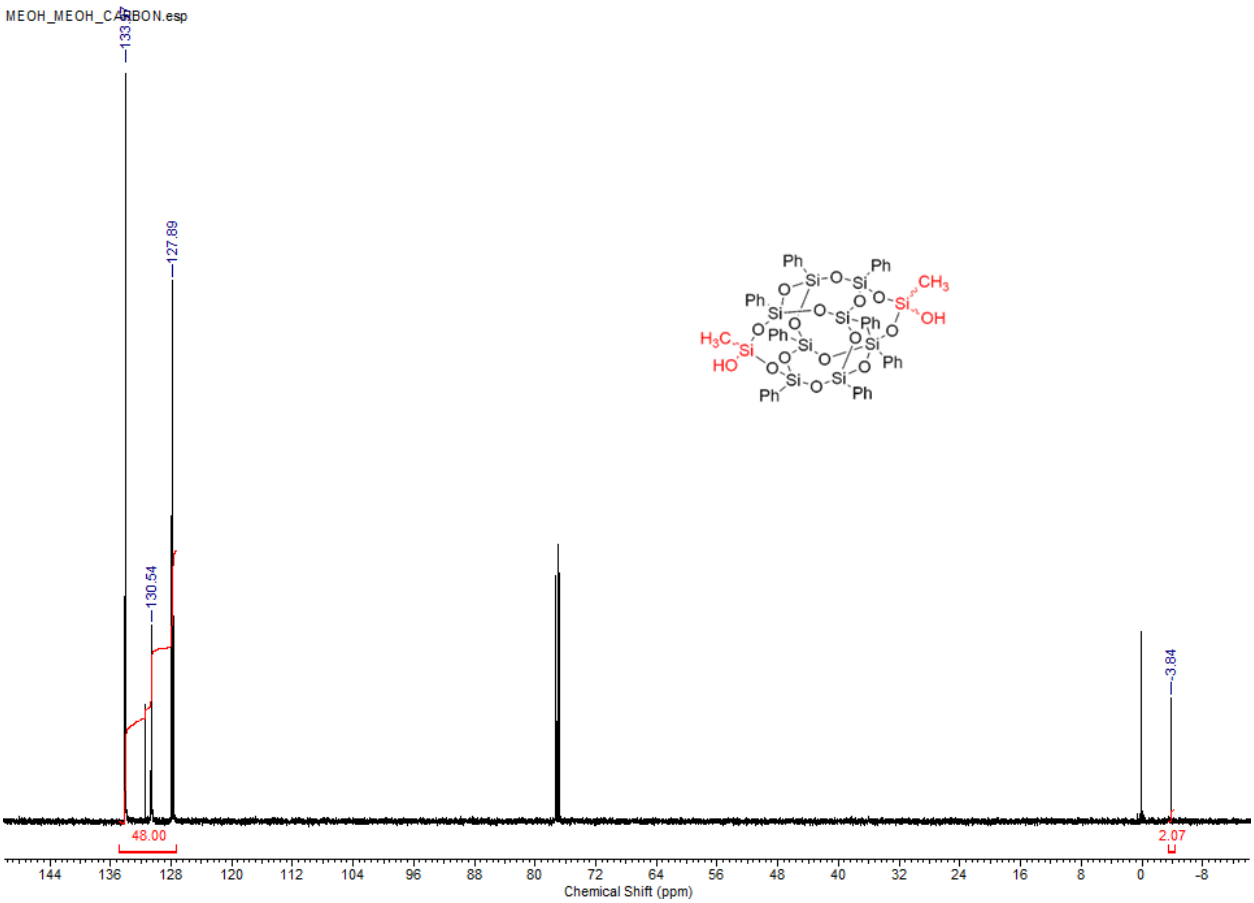

Figure I-37. ^{13}C-NMR (125 MHz, $CDCl_3$) for DDSQ-2((methyl)(hydroxyl))

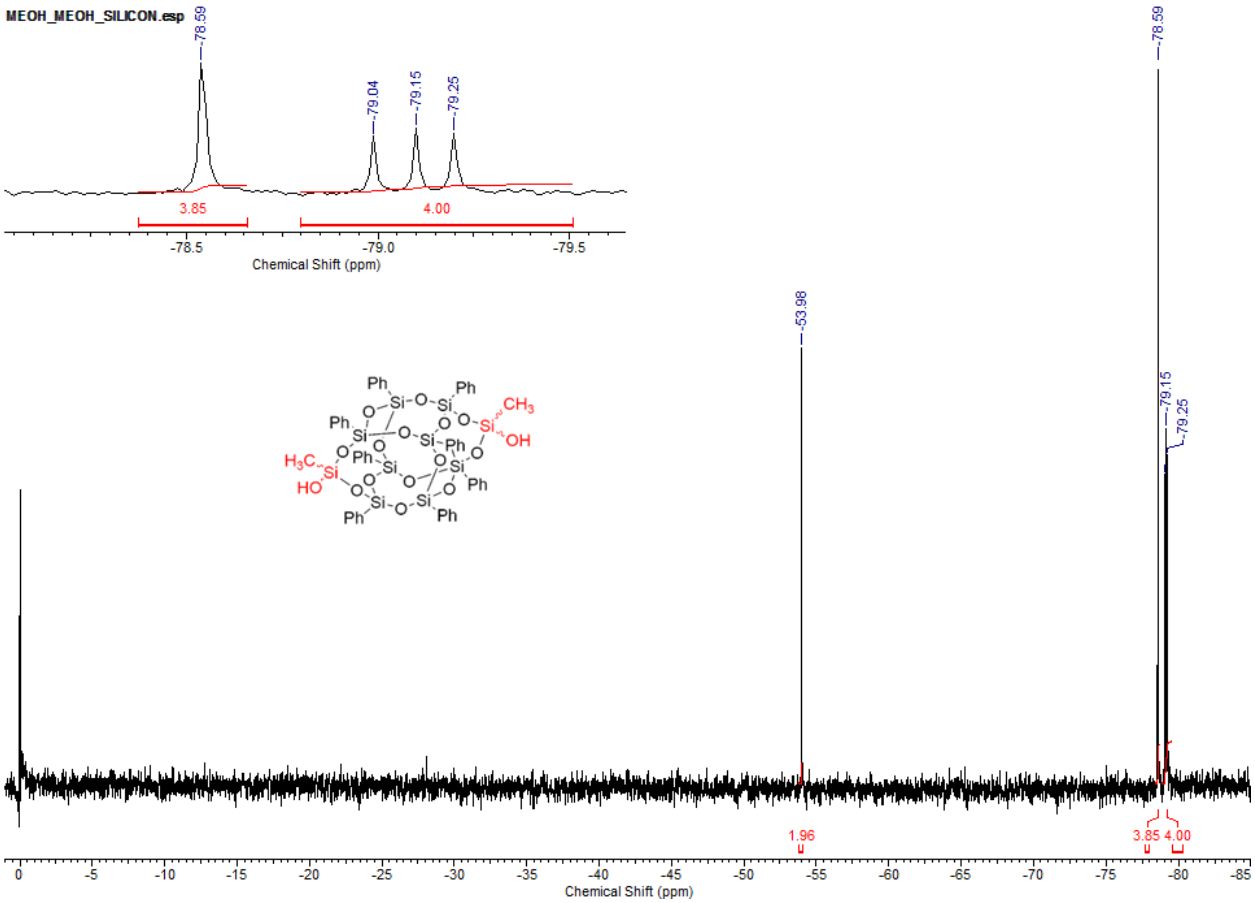

Figure I-38. ^{29}Si-NMR (99 MHz, $CDCl_3$) for DDSQ-2((methyl)(hydroxyl)) hydrolyzed by column chromatography

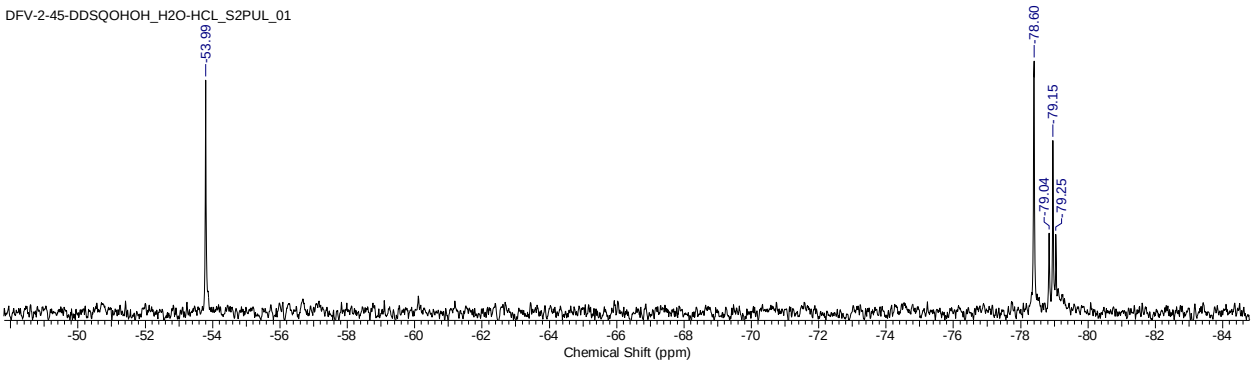

Figure I-39. ^{29}Si-NMR (99 MHz, $CDCl_3$) for DDSQ-2((methyl)(hydroxyl)) hydrolyzed with acidified H_2O

DDSQ-(methyl)(hydro)(methyl)(hydroxyl)

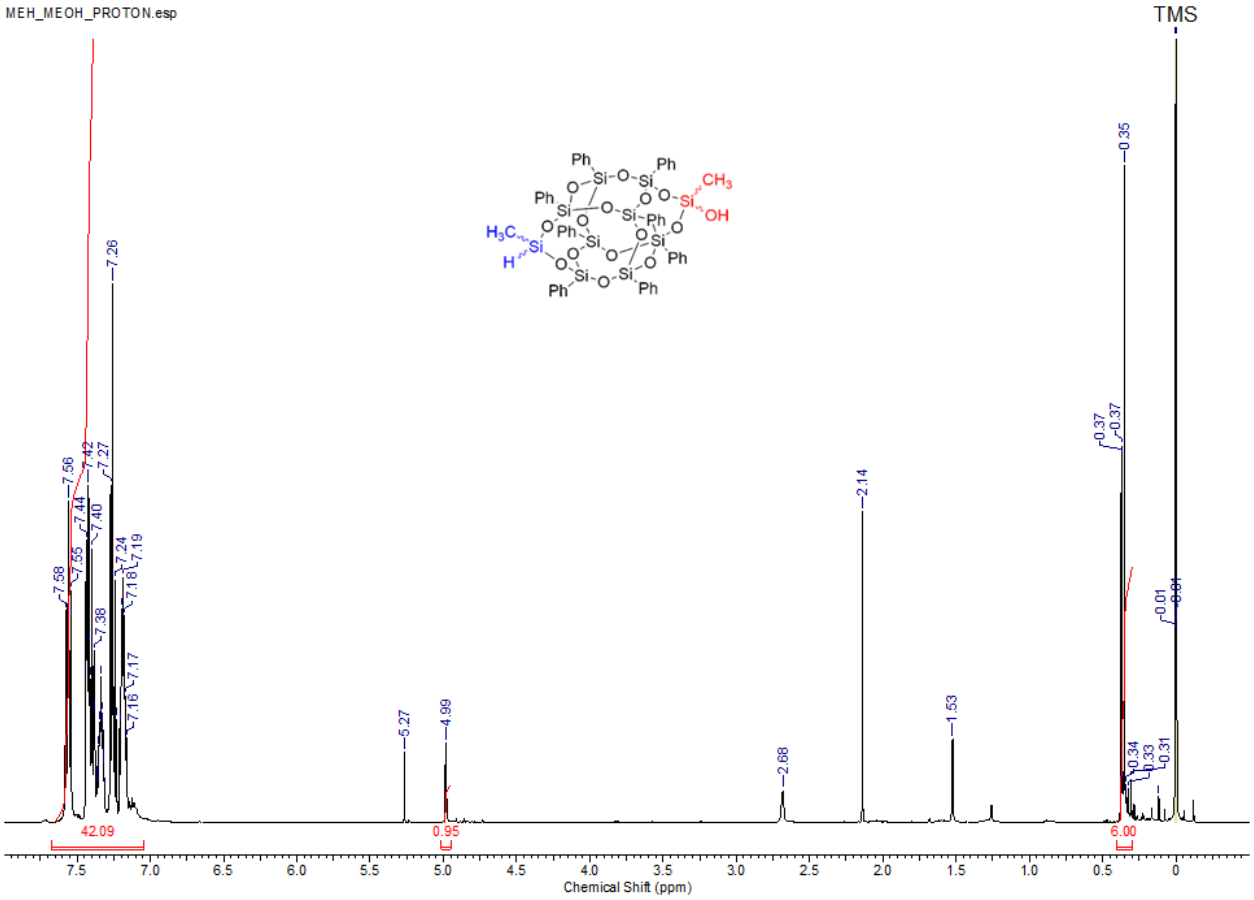

Figure I-40. ^{1}H-NMR (500 MHz, $CDCl_3$) for DDSQ-(methyl)(hydro)(methyl)(hydroxyl)

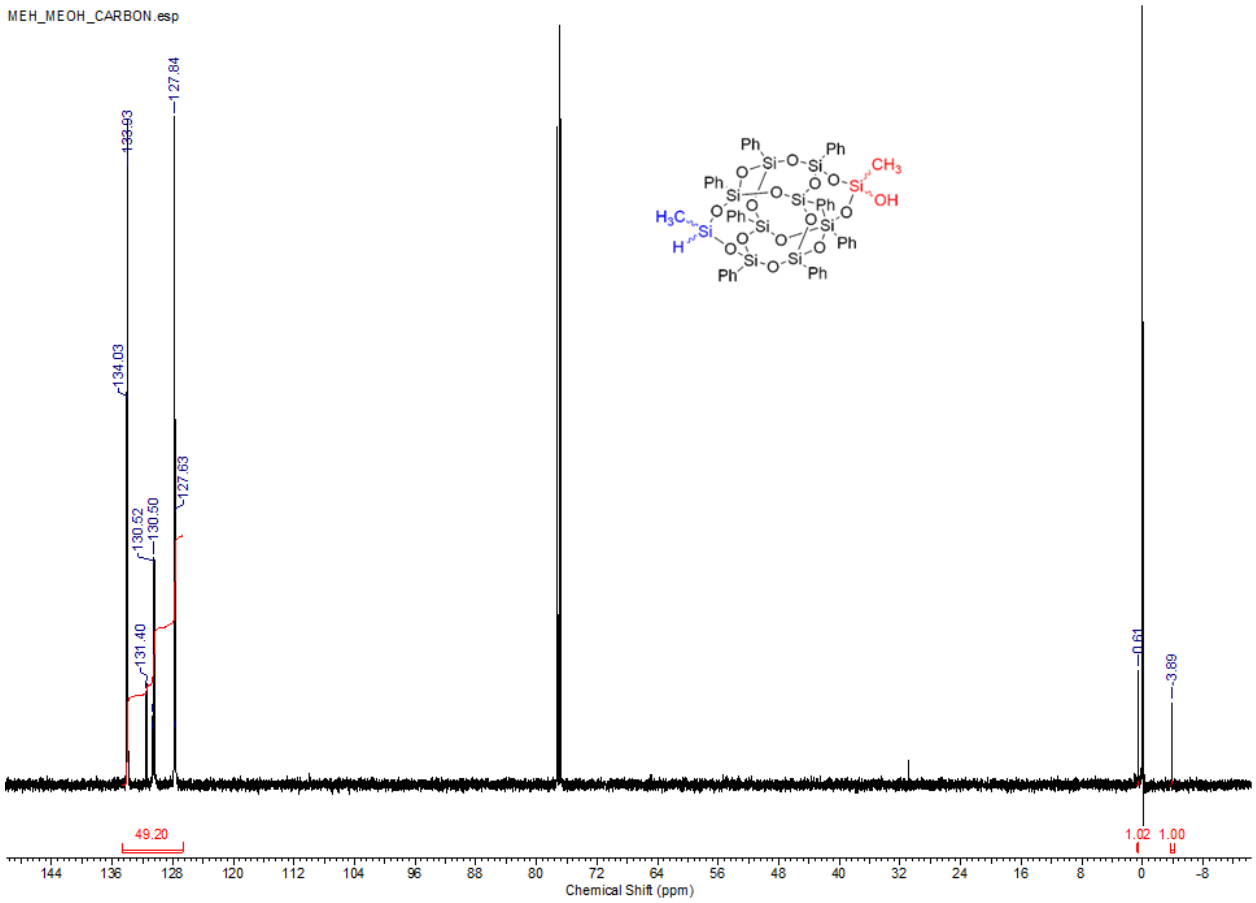

Figure I-41. ^{13}C-NMR (125 MHz, $CDCl_3$) for DDSQ-(methyl)(hydro)(methyl)(hydroxyl)

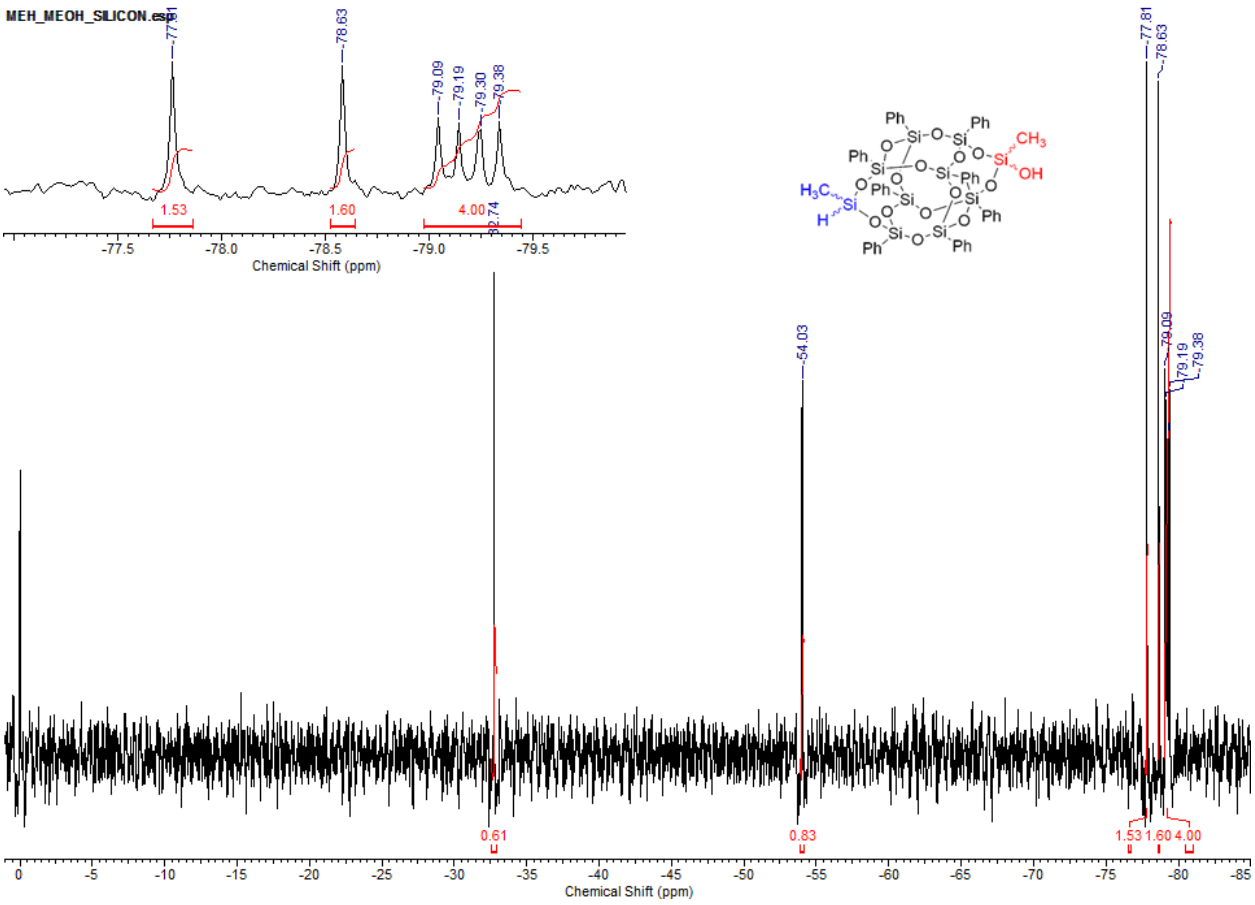

Figure I-42. ^{29}Si-NMR (99 MHz, $CDCl_3$) for DDSQ-(methyl)(hydro)(methyl)(hydroxyl)

DDSQ-(methyl)$_2$(methyl)(hydroxyl)

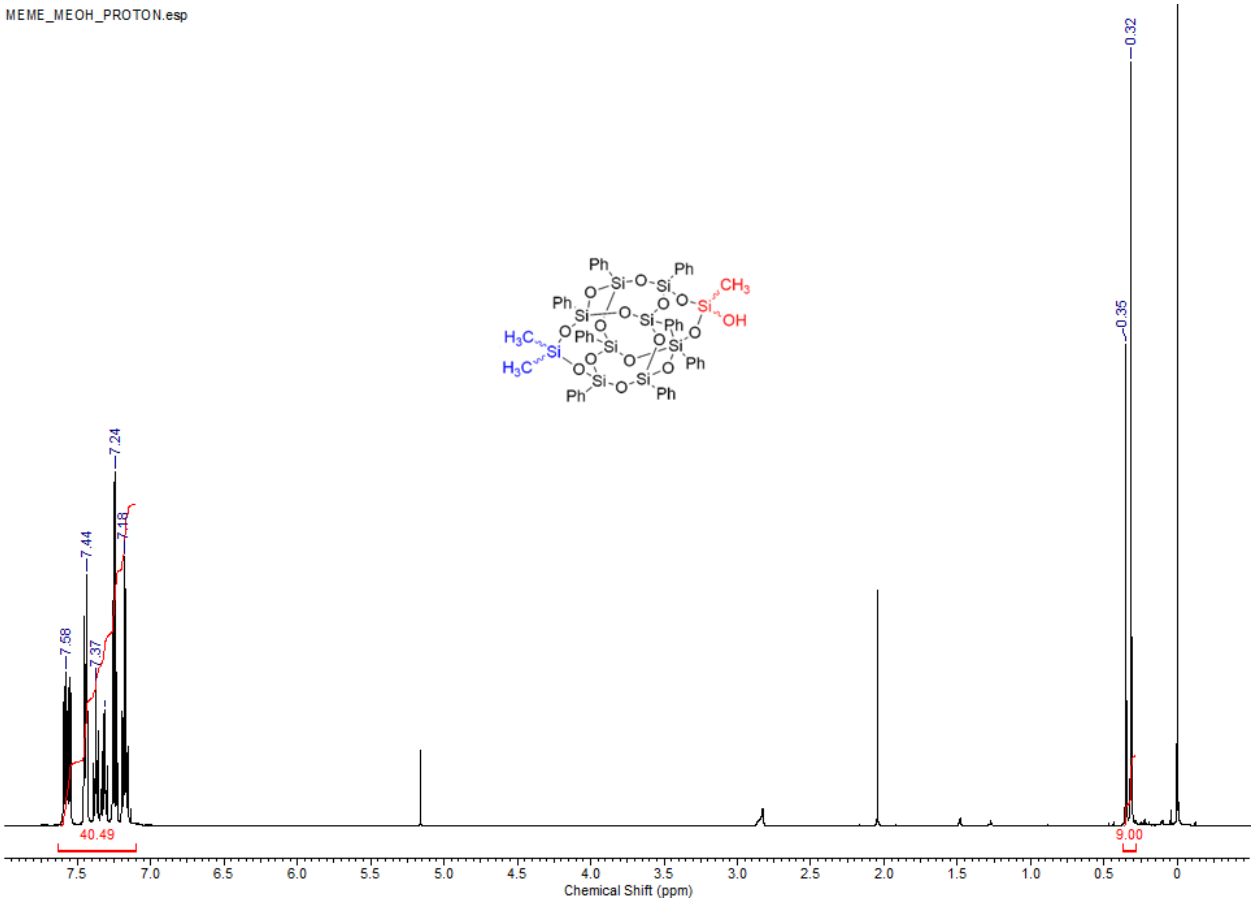

Figure I-43. ^{1}H-NMR (500 MHz, $CDCl_3$) for DDSQ-(methyl)$_2$(methyl)(hydroxyl)

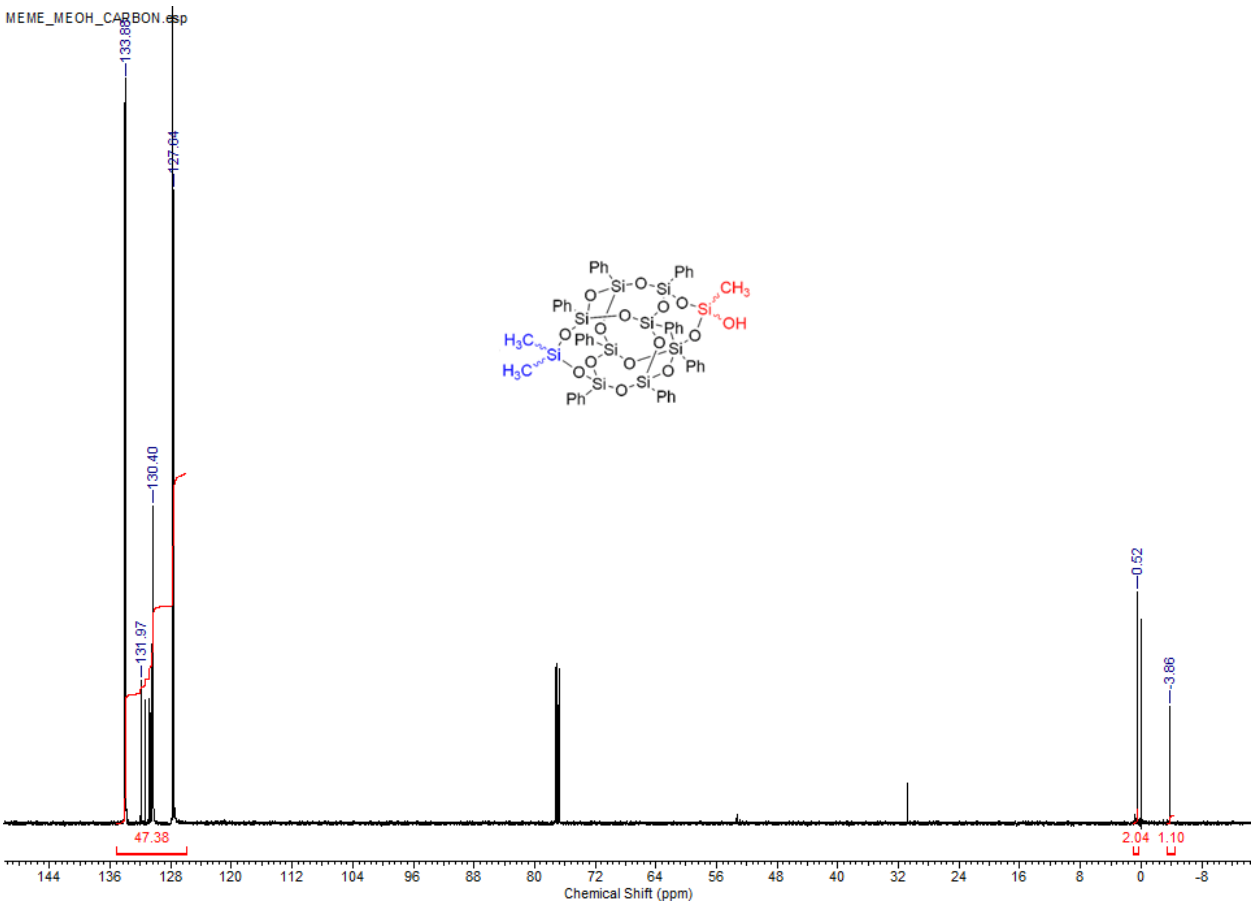

Figure I-44. ^{13}C-NMR (125 MHz, $CDCl_3$) for DDSQ-(methyl)$_2$(methyl)(hydroxyl)

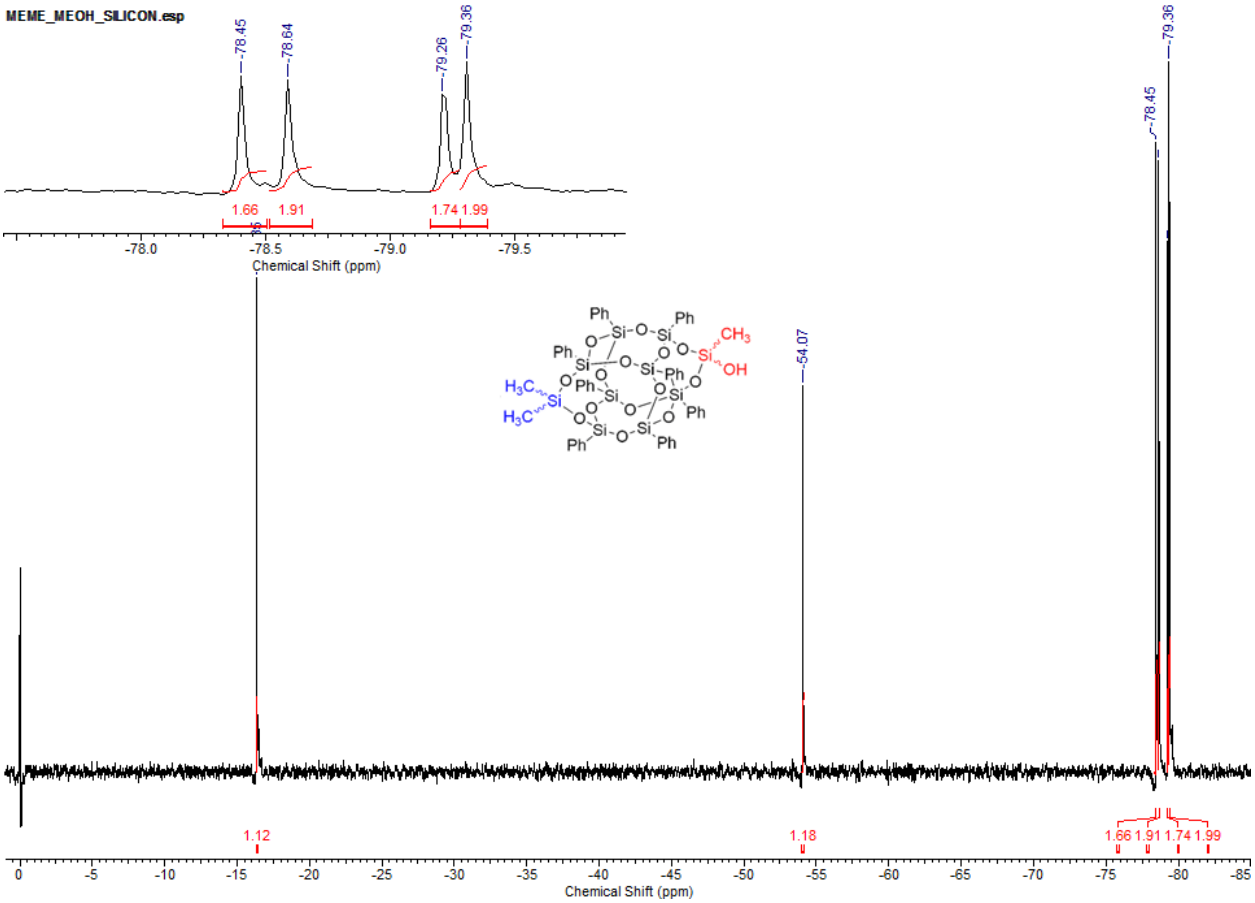

Figure I-45. ^{29}Si-NMR (99 MHz, $CDCl_3$) for DDSQ-(methyl)$_2$(methyl)(hydroxyl)

DDSQ-(methyl)(vinyl)(methyl)(hydroxyl)

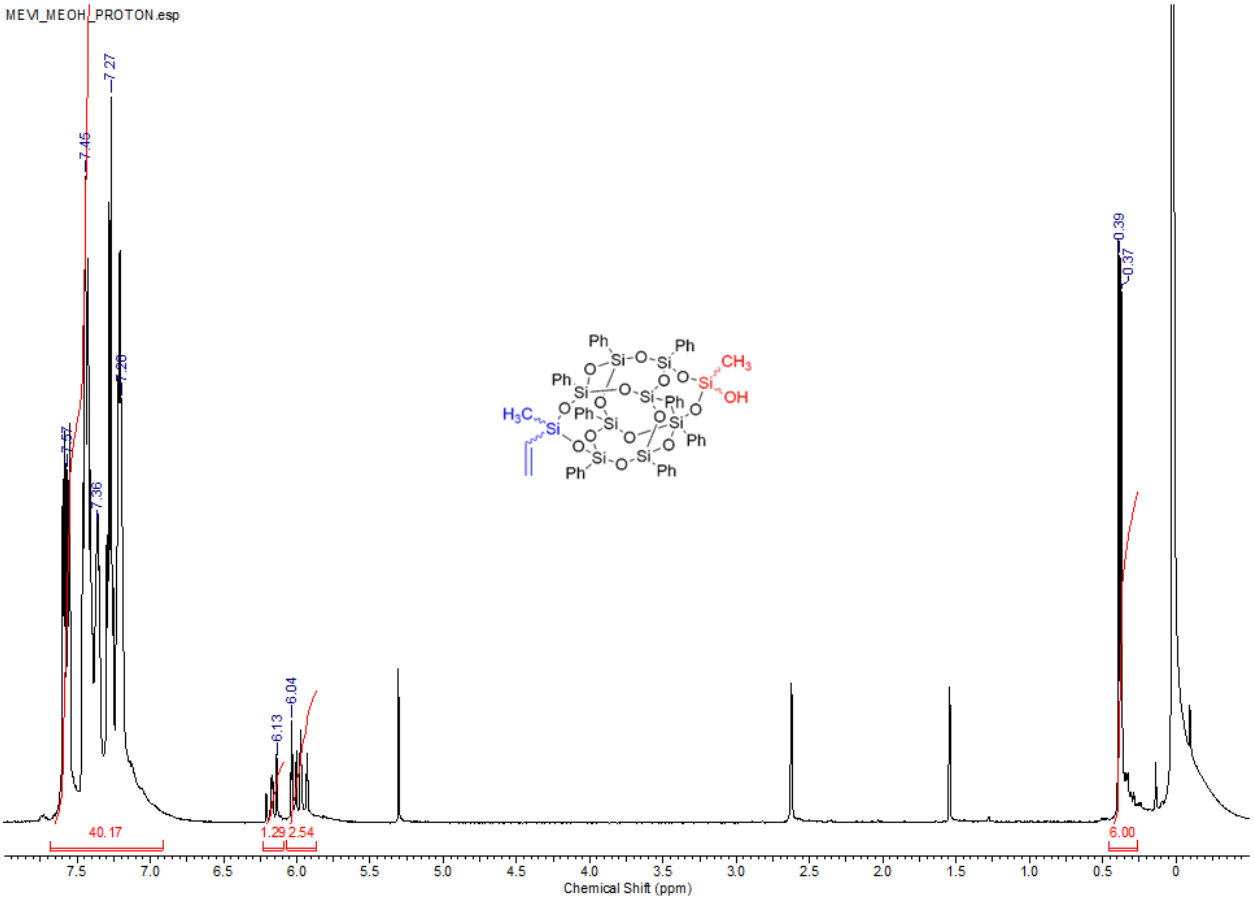

Figure I-46. ^{1}H-NMR (500 MHz, $CDCl_3$) for DDSQ-(methyl)(vinyl)(methyl)(hydroxyl)

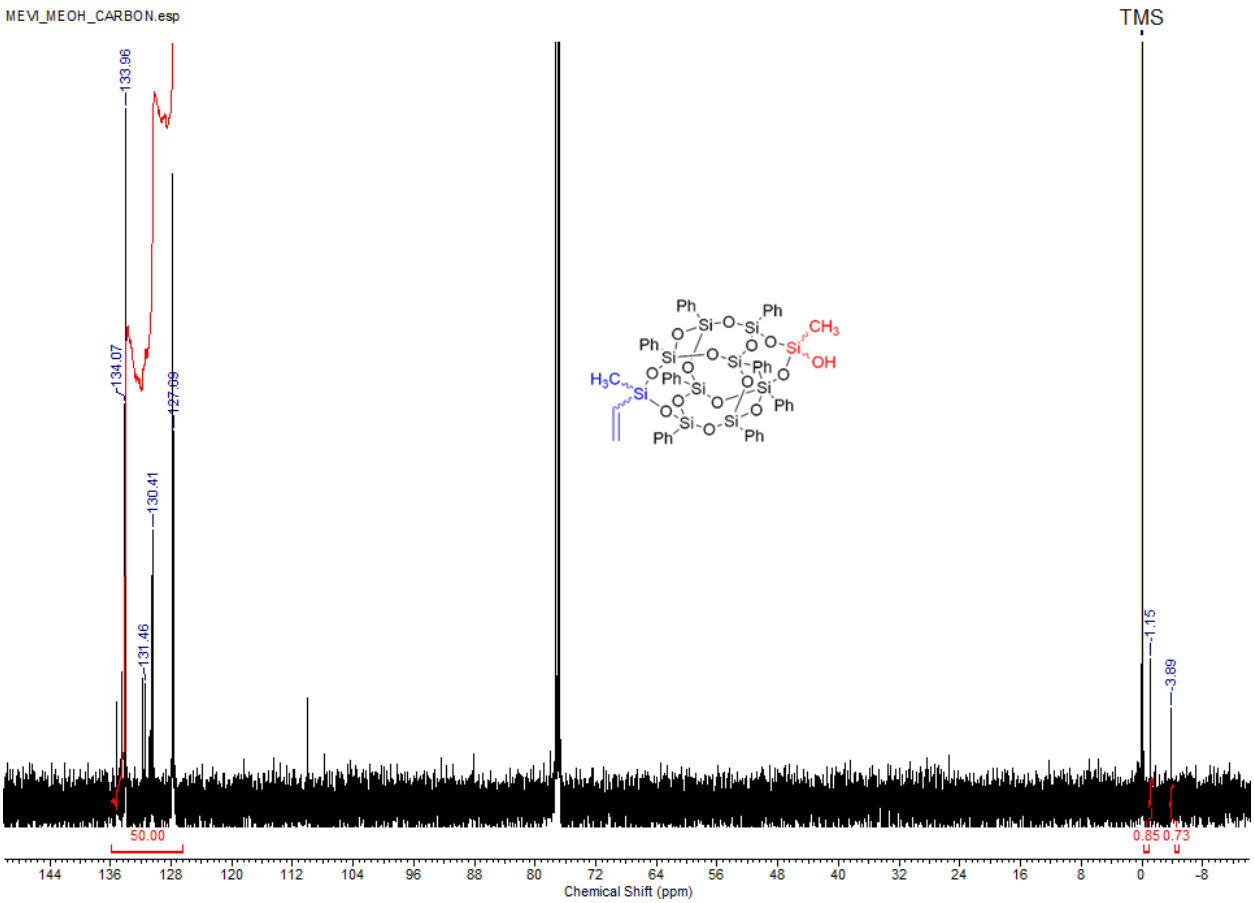

Figure I-47. ^{13}C-NMR (125 MHz, $CDCl_3$) for DDSQ-(methyl)(vinyl)(methyl)(hydroxyl)

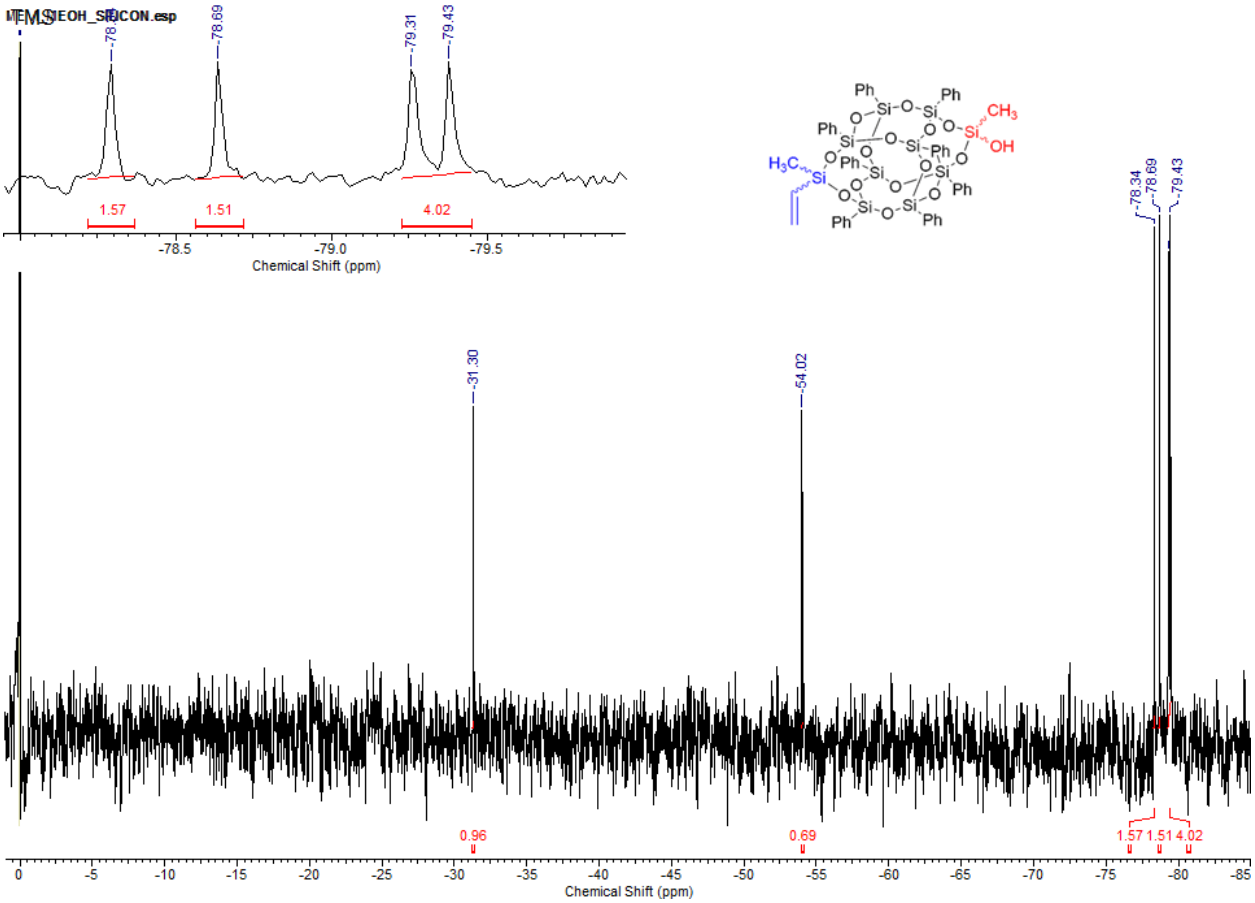

Figure I-48. ^{29}Si-NMR (99 MHz, $CDCl_3$) for DDSQ-(methyl)(vinyl)(methyl)(hydroxyl)

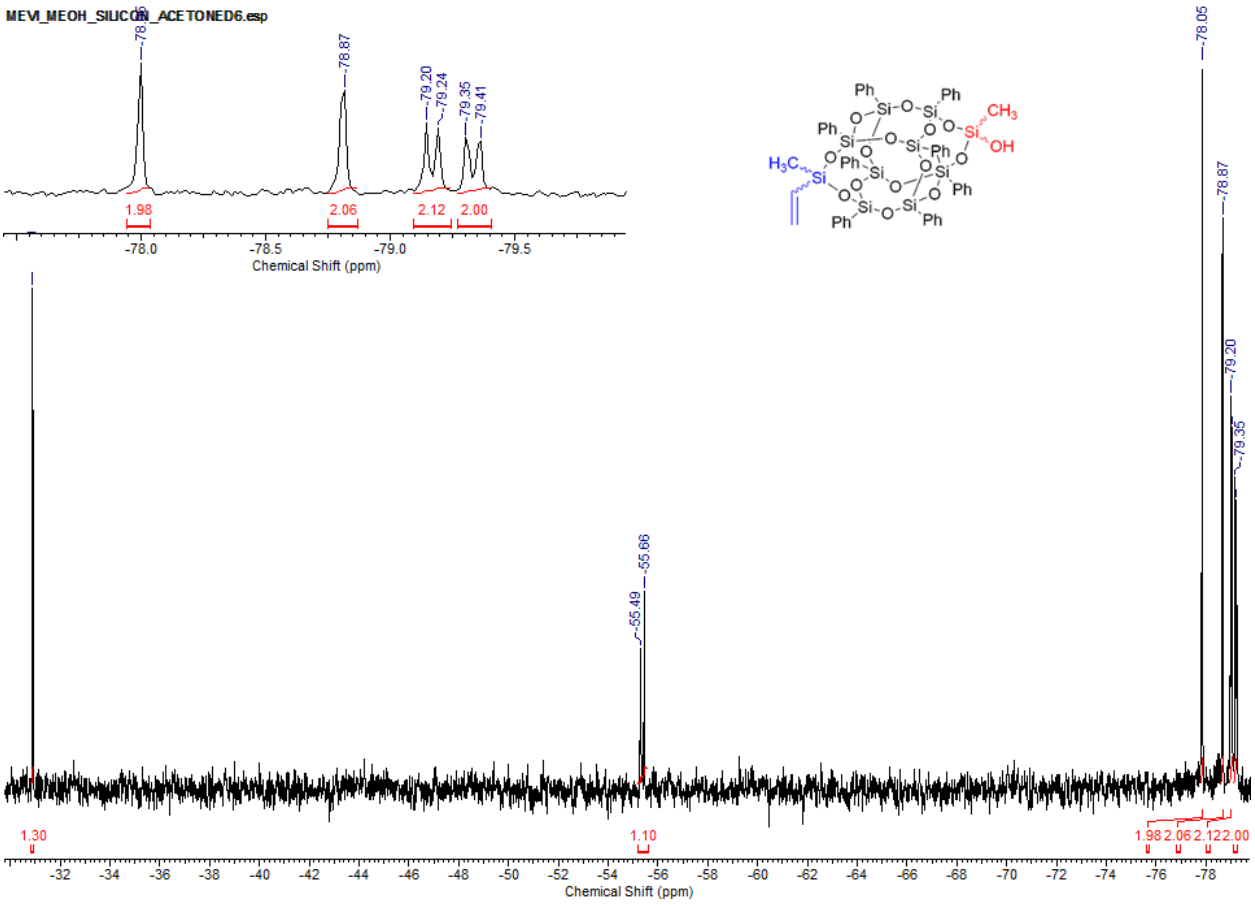

Figure I-49. ^{29}Si-NMR (99 MHz, Acetone-D6) for DDSQ-(methyl)(vinyl)(methyl)(hydroxyl)

DDSQ-(methyl)(3-propyl-chloride)(methyl)(hydroxyl)

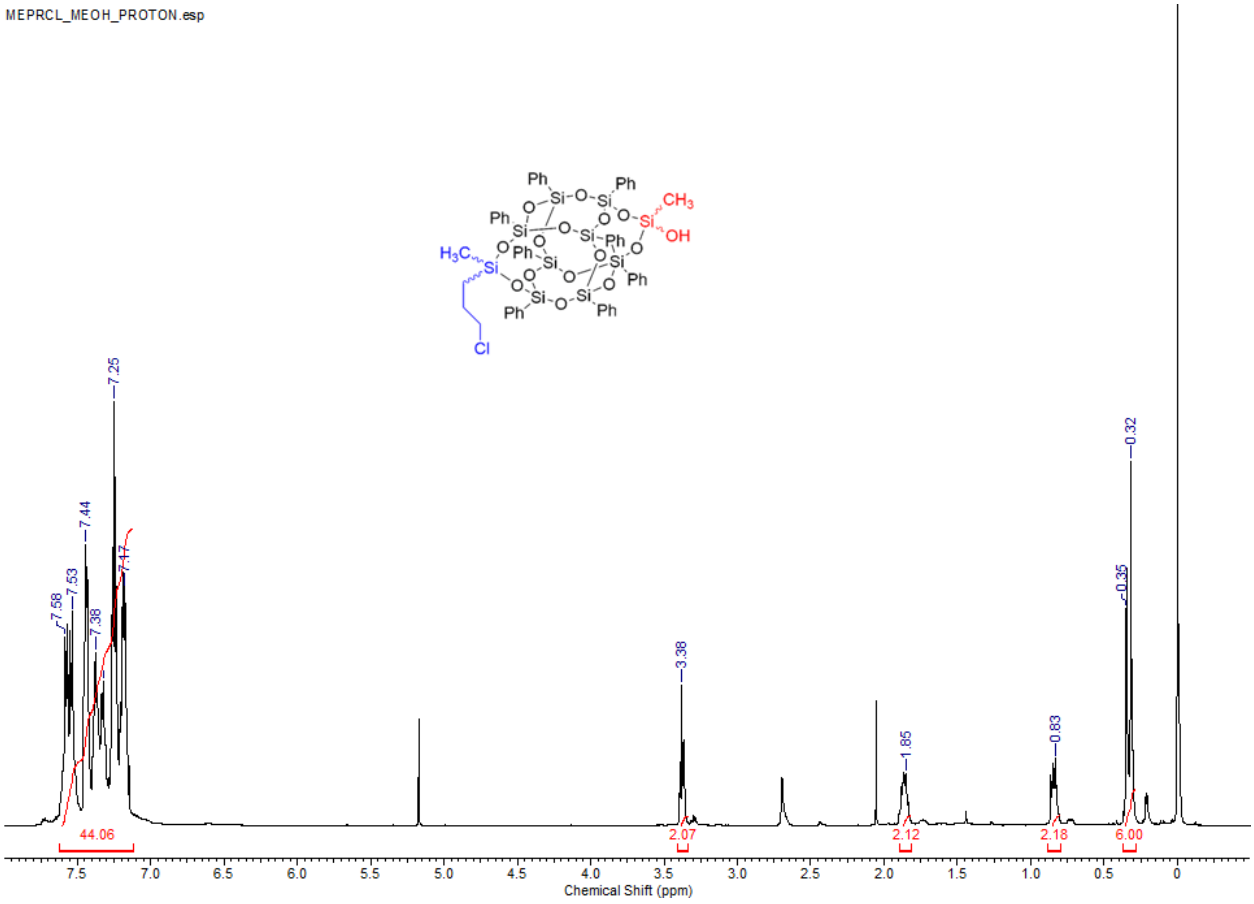

Figure I-50. ^{1}H-NMR (500 MHz, $CDCl_3$) for DDSQ-(methyl)(3-propyl-chloride)(methyl)(hydroxyl)

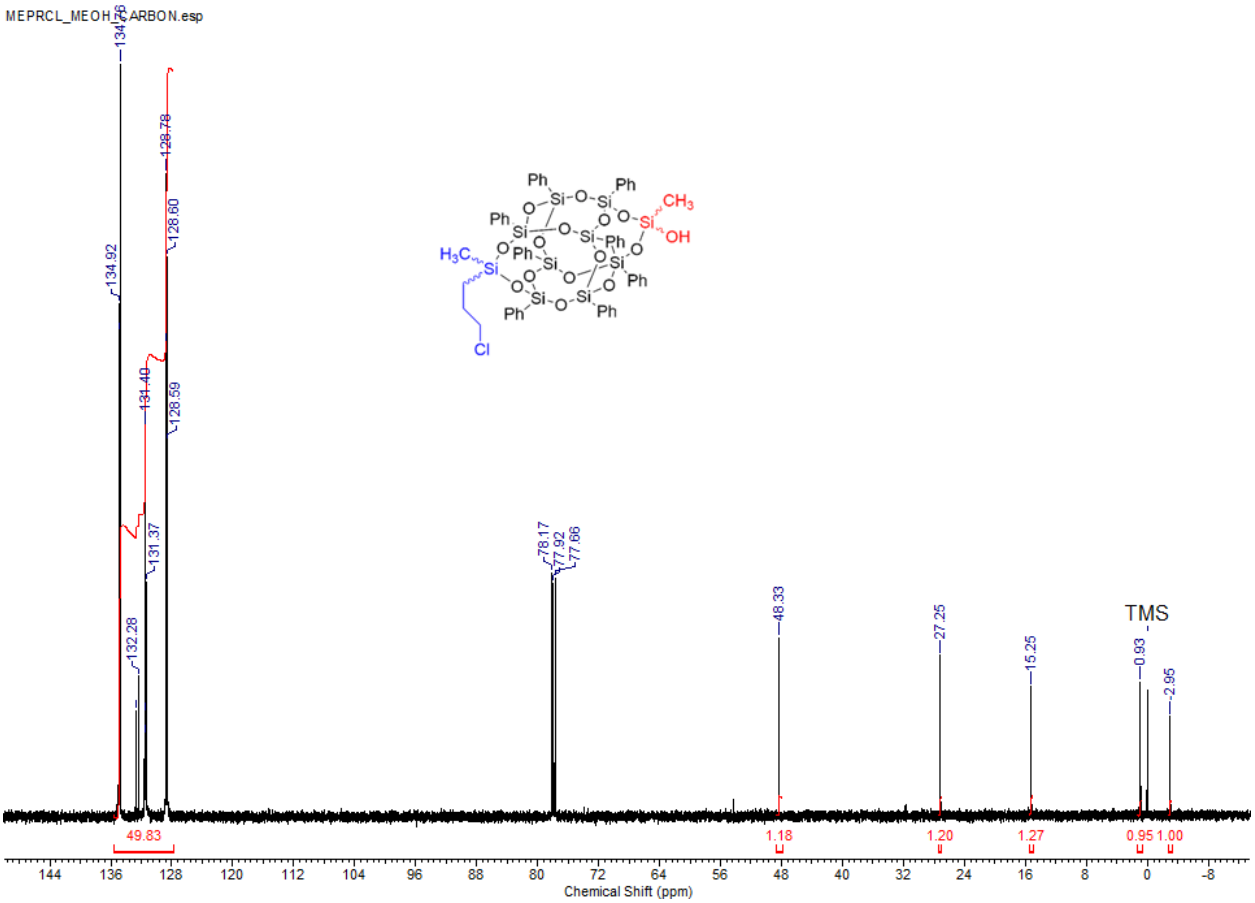

Figure I-51. ^{13}C-NMR (125 MHz, $CDCl_3$) for DDSQ-(methyl)(3-propyl-chloride)(methyl)(hydroxyl)

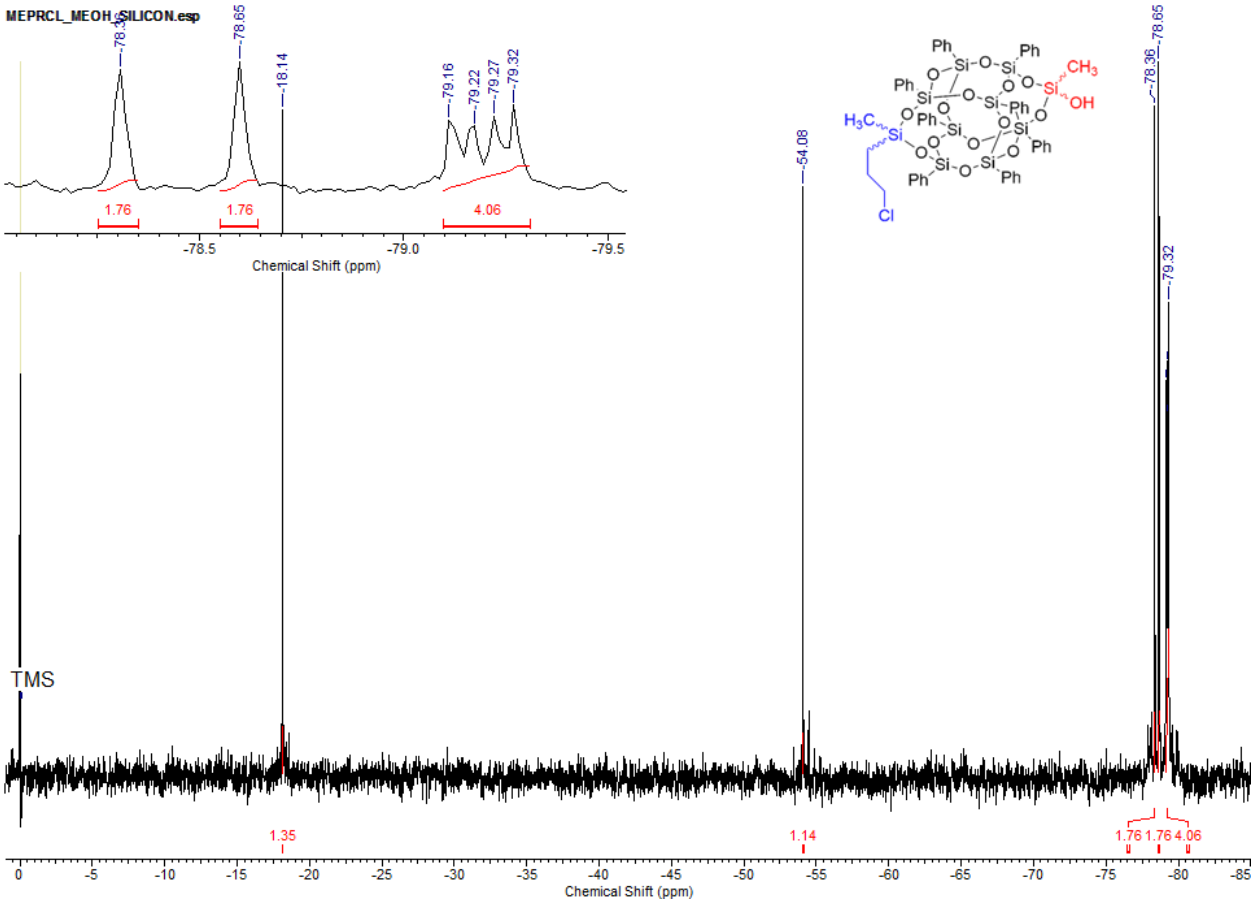

Figure I-52. ^{29}Si-NMR (99 MHz, $CDCl_3$) for DDSQ-(methyl)(3-propyl-chloride)(methyl)(hydroxyl)

DDSQ-(methyl)$_2$(vinyl)(hydroxyl)

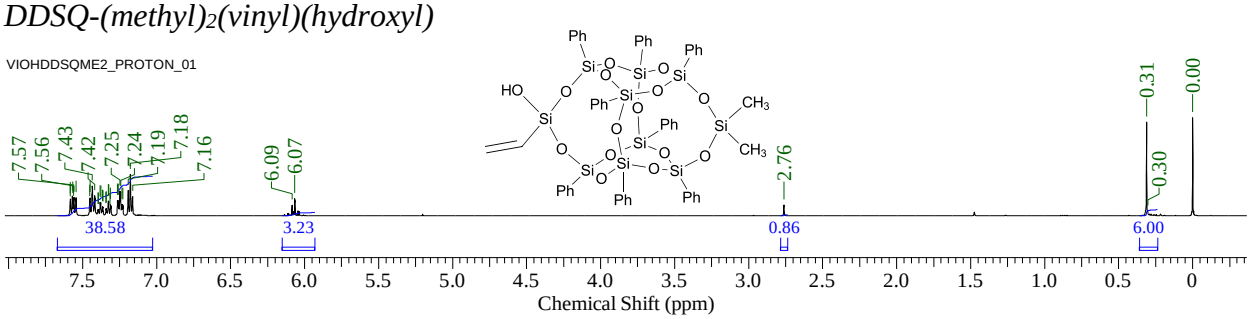

Figure I-53. ^{1}H-NMR (500 MHz, $CDCl_3$) for DDSQ-(methyl)$_2$(vinyl)(hydroxyl)

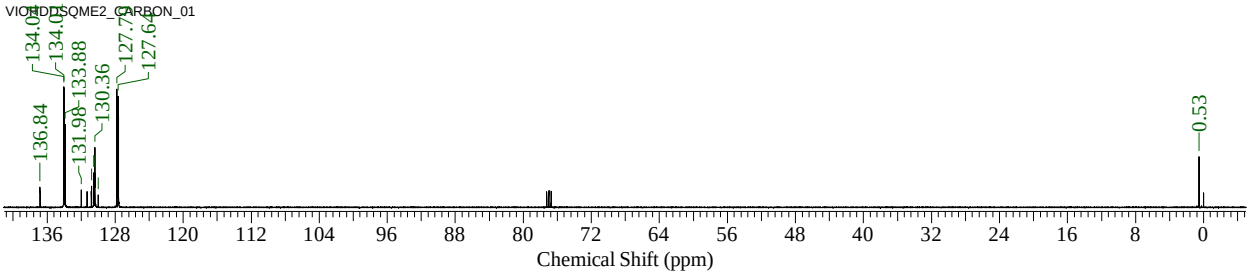

Figure I-54. ^{13}C-NMR (125 MHz, $CDCl_3$) for DDSQ-(methyl)$_2$(vinyl)(hydroxyl)

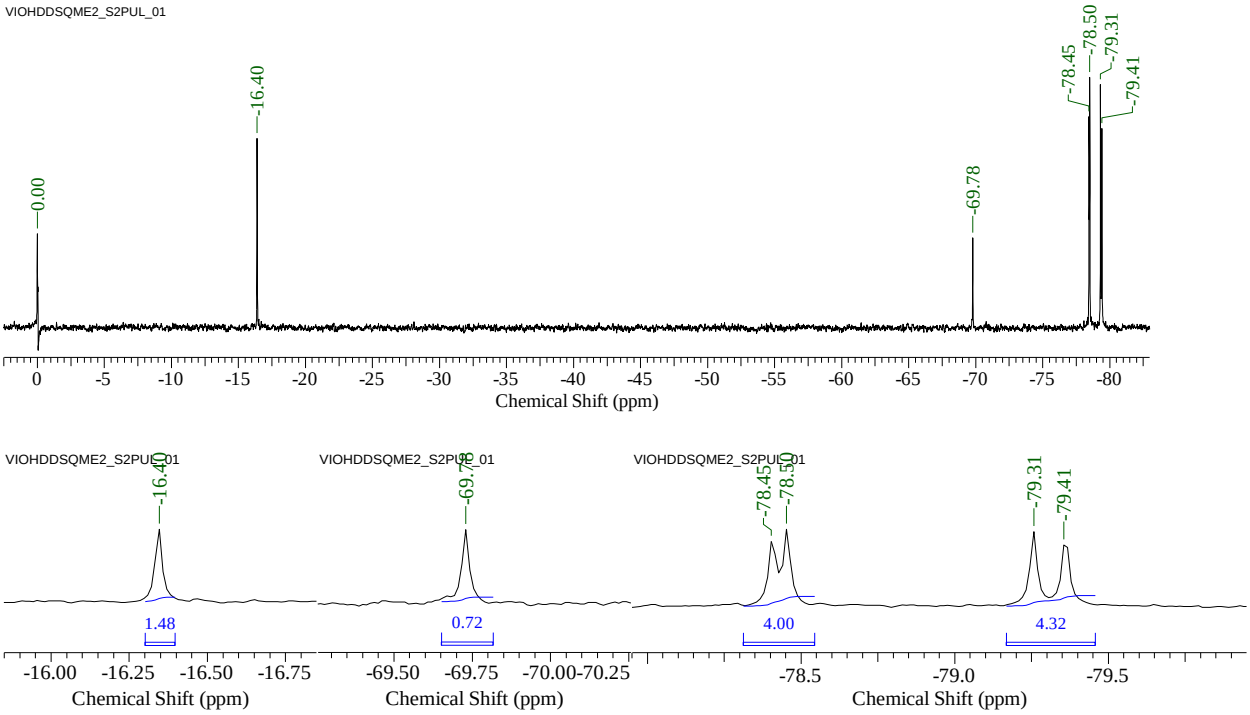

Figure I-55. ^{29}Si-NMR (99 MHz, $CDCl_3$) for DDSQ-(methyl)$_2$(vinyl)(hydroxyl)

DDSQ-(methyl)$_2$(isobutyl)(hydroxyl)

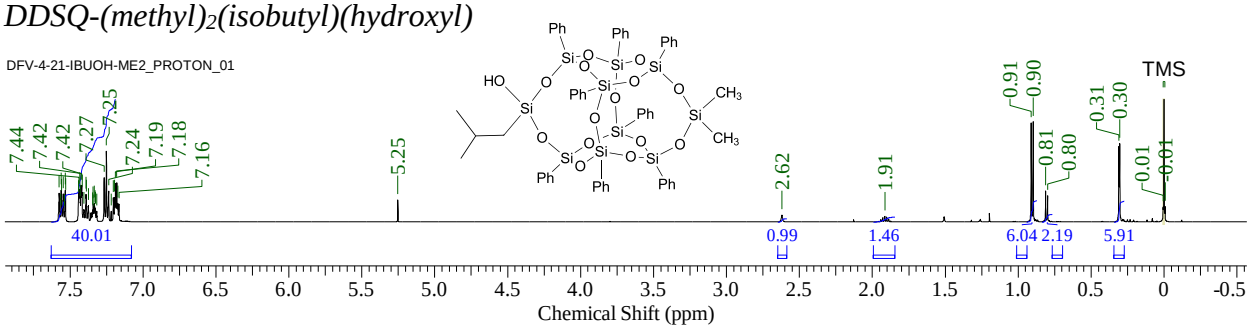

Figure I-56. ^{1}H-NMR (500 MHz, $CDCl_3$) for DDSQ-(methyl)$_2$(isobutyl)(hydroxyl)

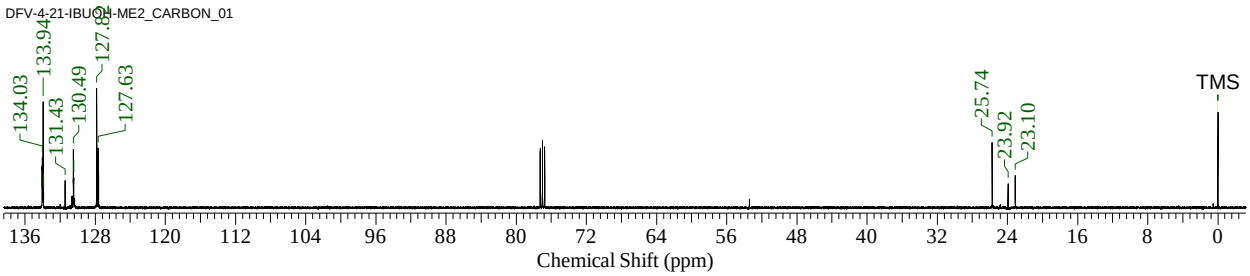

Figure I-57. ^{13}C-NMR (125 MHz, $CDCl_3$) for DDSQ-(methyl)$_2$(isobutyl)(hydroxyl)

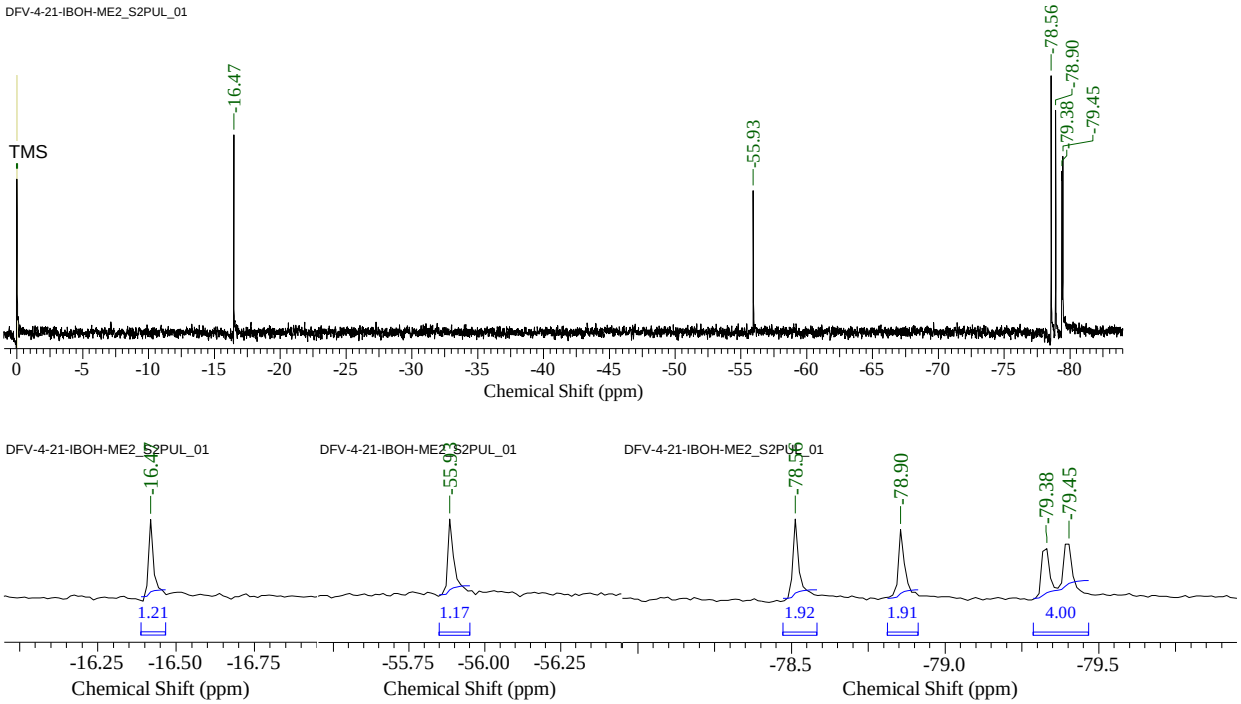

Figure I-58. ^{29}Si-NMR (99 MHz, $CDCl_3$) for DDSQ-(methyl)$_2$(isobutyl)(hydroxyl)

(Methyl)(para-aniline(trimethylsilyl))dichlorosilane

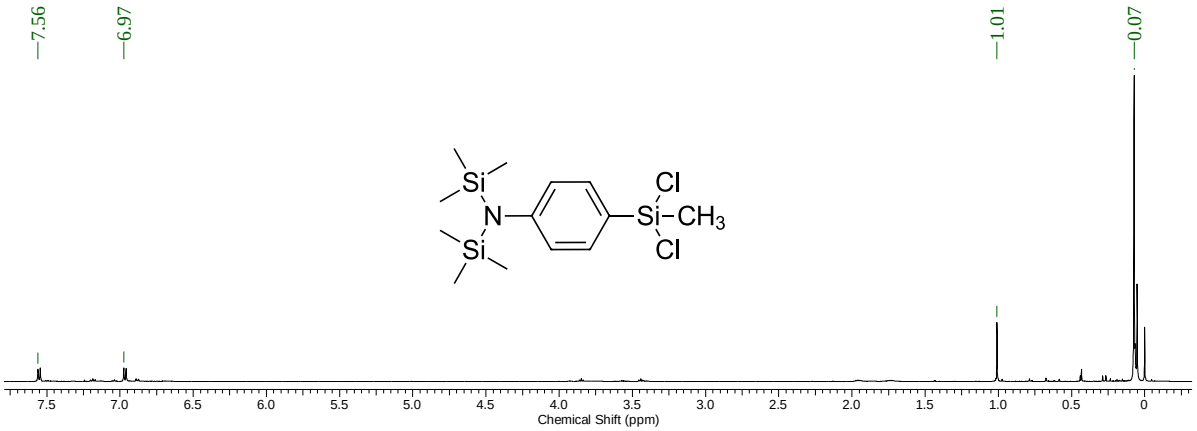

Figure I-59. ^{1}H NMR (500 MHz, $CDCl_3$) for (methyl)(para-aniline(trimethylsilyl))dichlorosilane

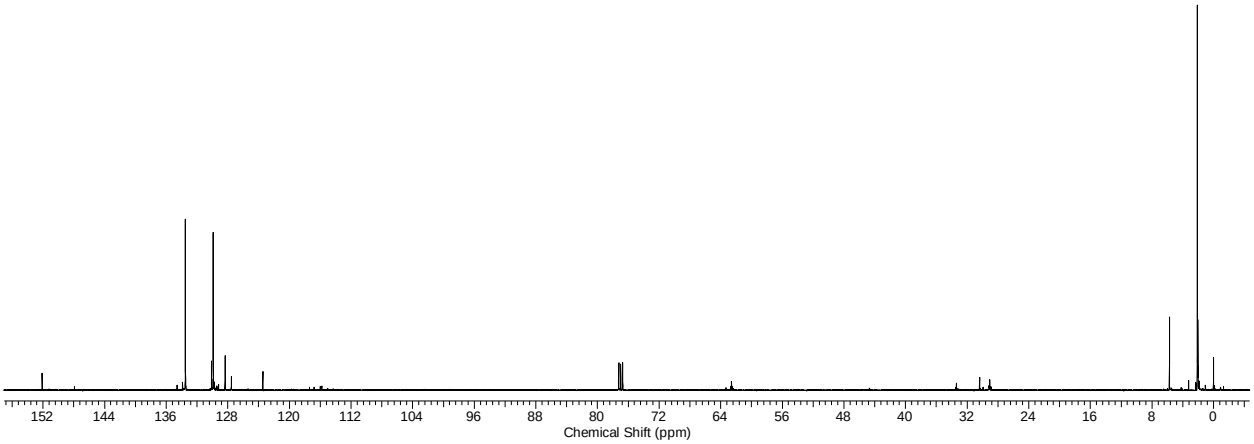

Figure I-60. ^{13}C NMR (125 MHz, $CDCl_3$) for (methyl)(para-aniline(trimethylsilyl))dichlorosilane

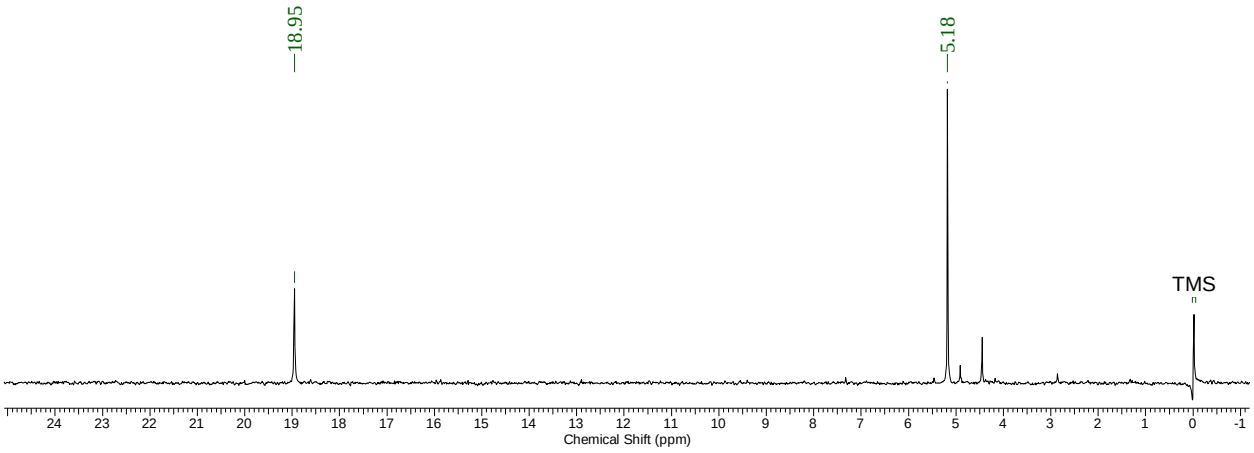

Figure I-61. ^{29}Si NMR (99 MHz, $CDCl_3$) for (methyl)(para-aniline(trimethylsilyl))dichlorosilane

1,4-Bromophenylethynylbenzene

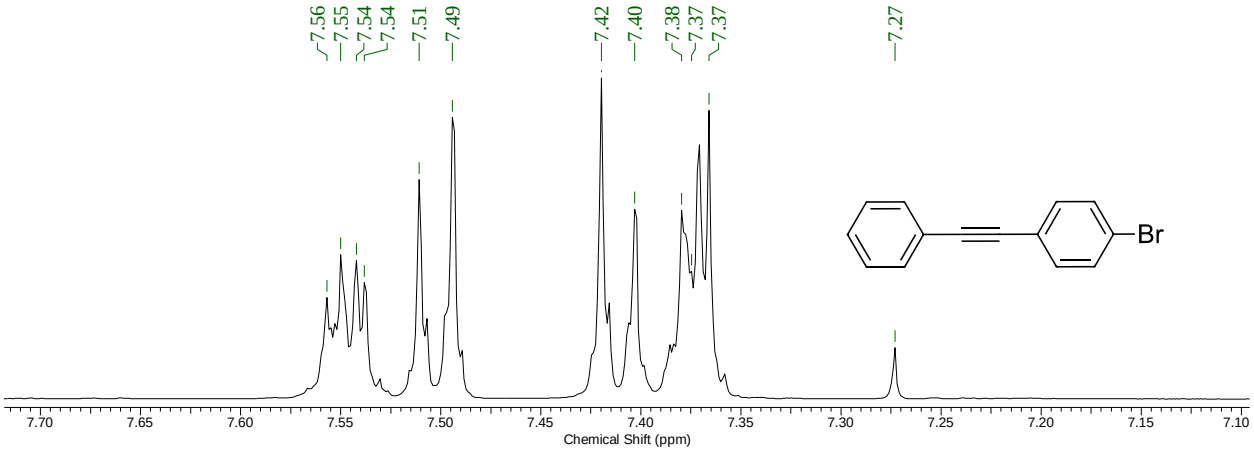

Figure I-62. ^{1}H NMR (500 MHz, $CDCl_3$) for 1,4-Bromophenylethynylbenzene

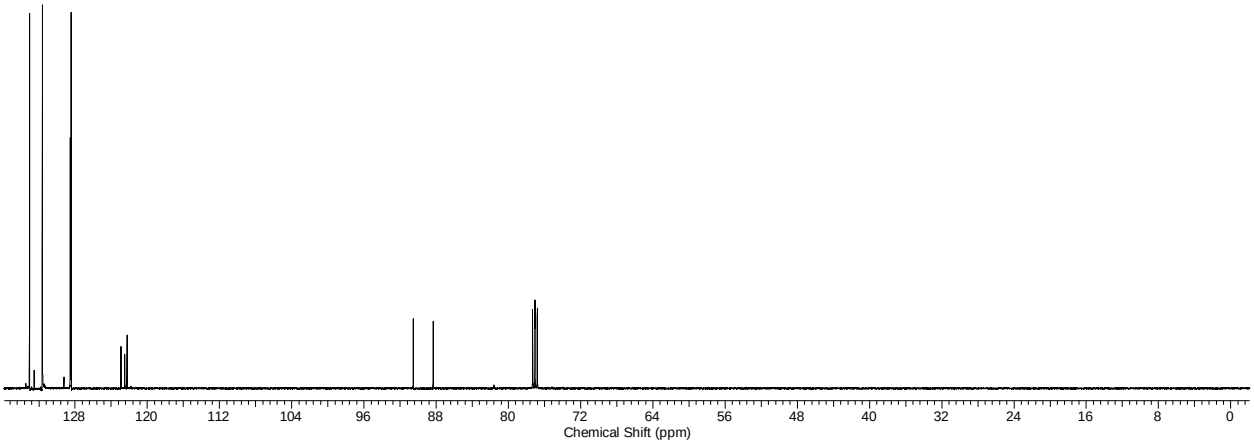

Figure I-63. ^{13}C NMR (125 MHz, $CDCl_3$) for 1,4-Bromophenylethynylbenzene

1,4-(Phenylethynyl)phenyl methyldichlorosilane

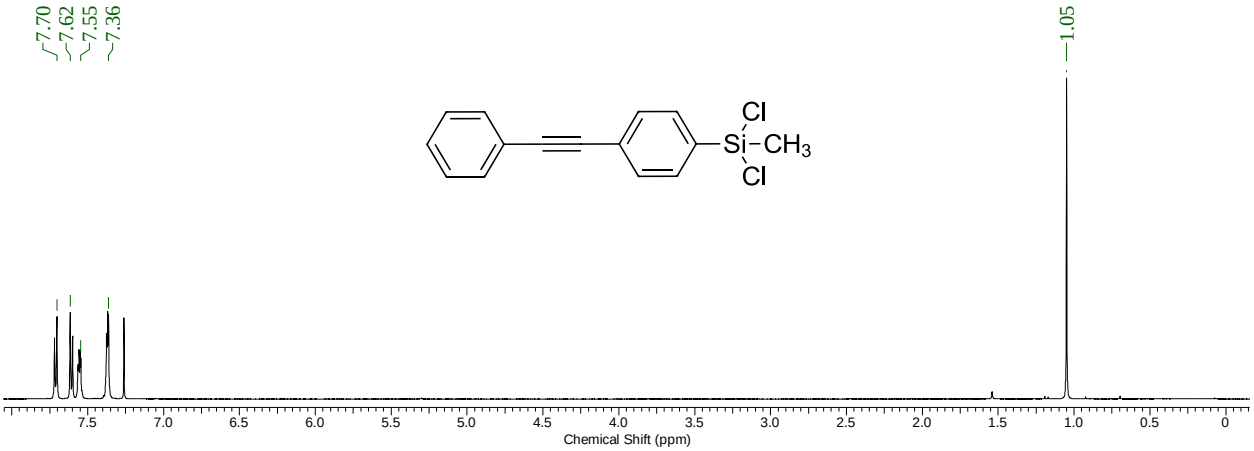

Figure I-64. ^{1}H NMR (500 MHz, $CDCl_3$) for 1,4-(Phenylethynyl)phenyl methyldichlorosilane

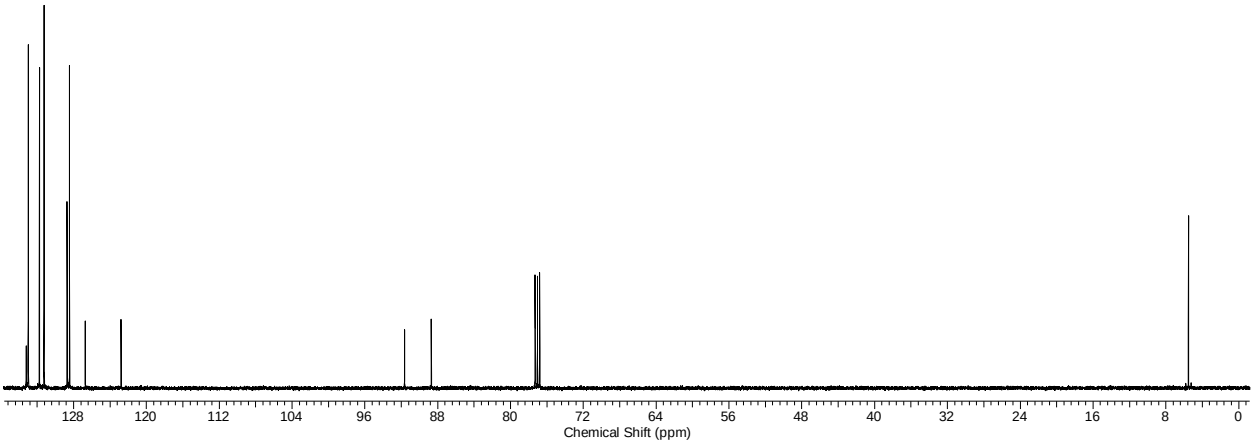

Figure I-65. ^{13}C NMR (125 MHz, $CDCl_3$) for 1,4-(Phenylethynyl)phenyl methyldichlorosilane

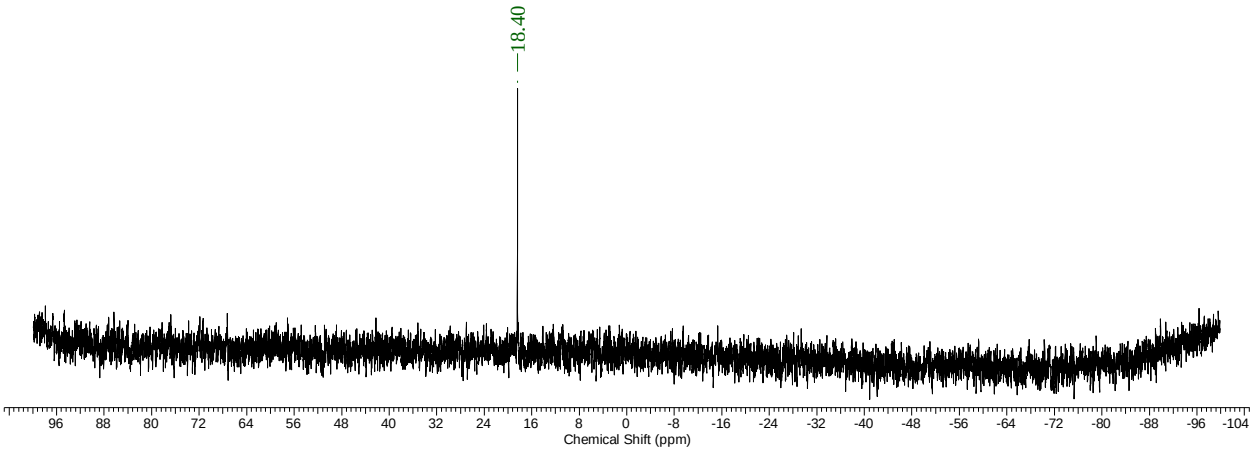

Figure I-66. ^{29}Si NMR (99 MHz, $CDCl_3$) for 1,4-(Phenylethynyl)phenyl methyldichlorosilane

DDSQ-2((methyl)(para-phenylethynyl phenyl))

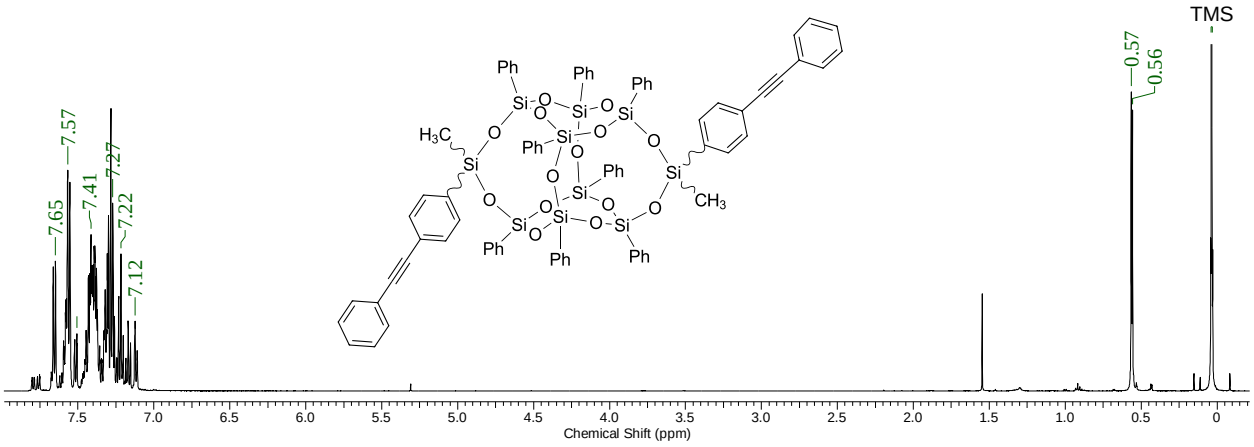

Figure I-67. ^{1}H NMR (500 MHz, $CDCl_3$) for DDSQ-2((methyl)(para-phenylethynyl phenyl))

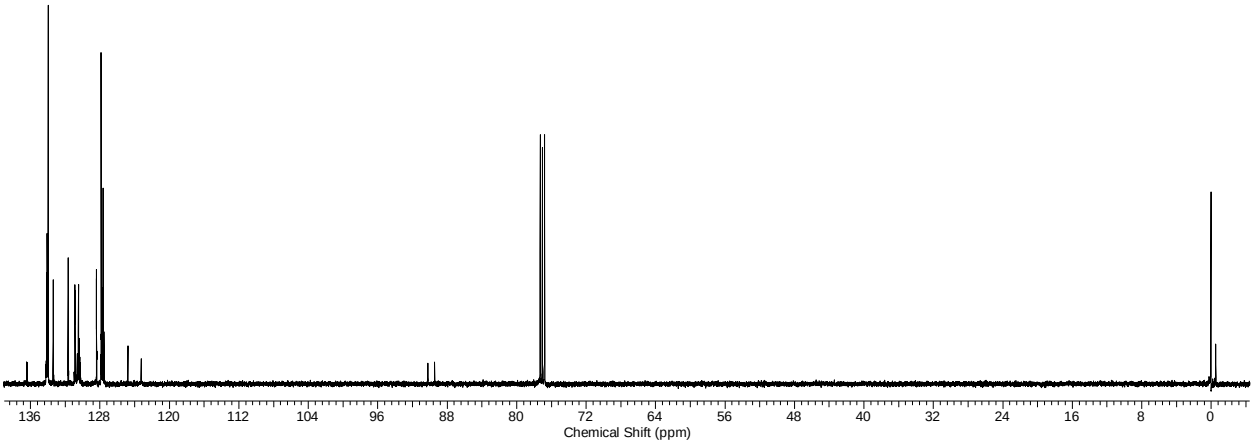

Figure I-68. ^{13}C NMR (125 MHz, $CDCl_3$) for DDSQ-2((methyl)(para-phenylethynyl phenyl))

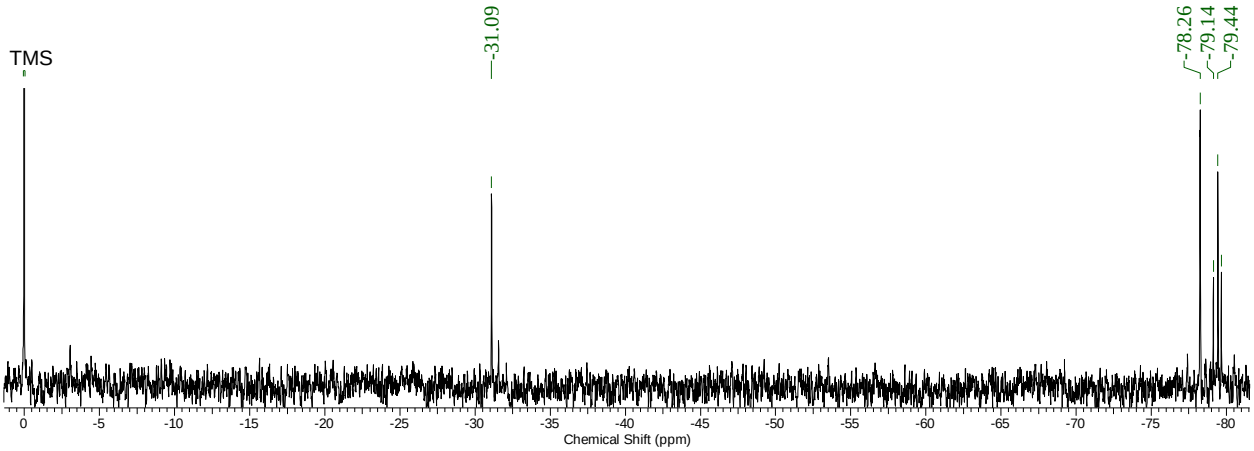

Figure I-69. ^{29}Si NMR (99 MHz, $CDCl_3$) for DDSQ-2((methyl)(para-phenylethynyl phenyl))

DDSQ-2((methyl)(phenyl))

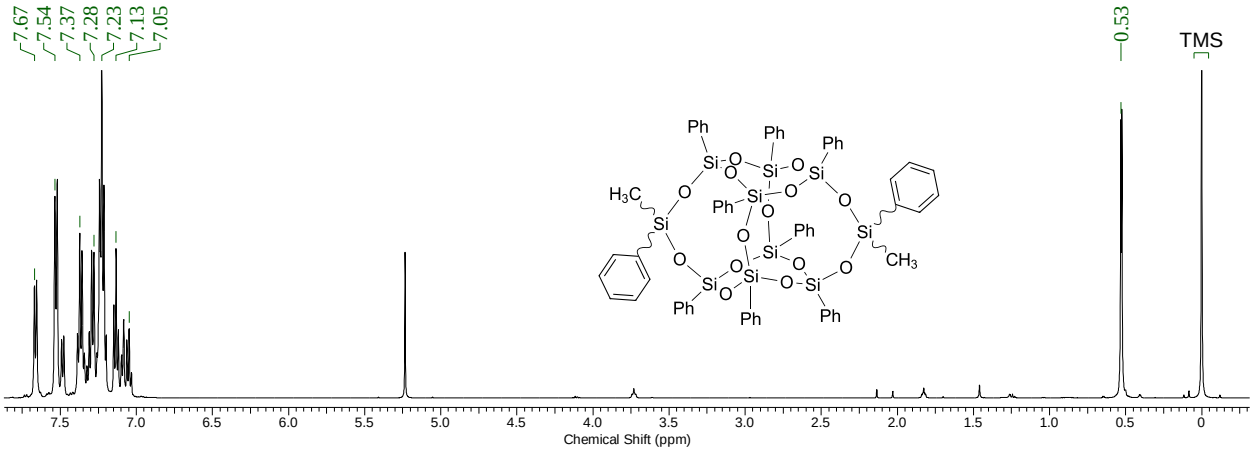

Figure I-70. ^{1}H NMR (500 MHz, $CDCl_3$) for DDSQ-2((methyl)(phenyl))

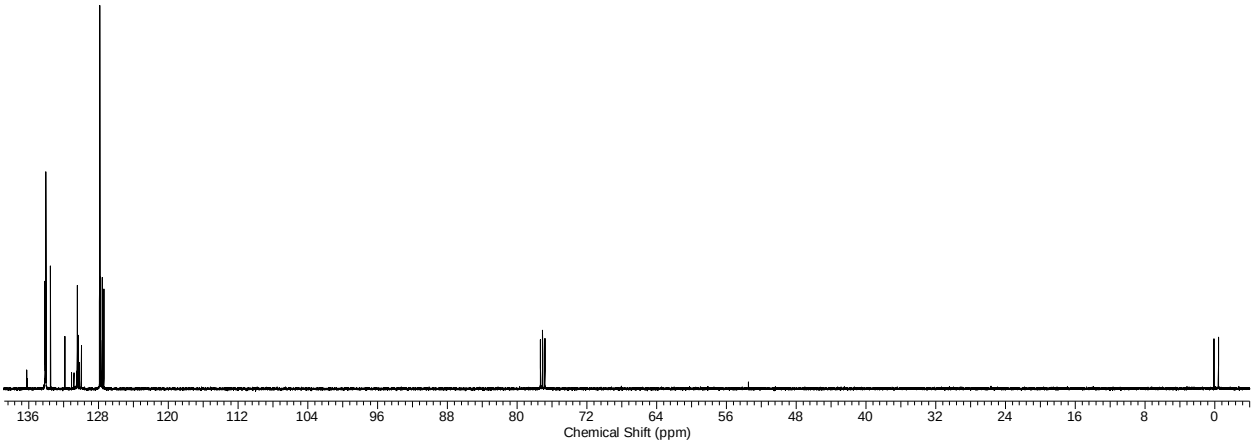

Figure I-71. ^{13}C NMR (125 MHz, $CDCl_3$) for DDSQ-2((methyl)(phenyl))

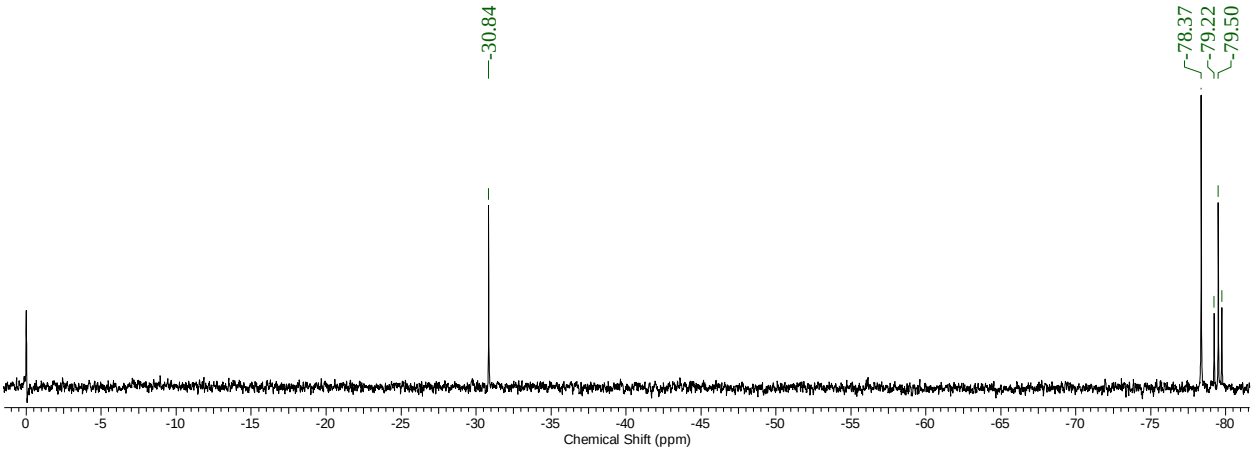

Figure I-72. ^{29}Si NMR (99 MHz, $CDCl_3$) for DDSQ-2((methyl)(phenyl))

APPENDIX J.

CRYSTALLOGRAPHIC INFORMATION

J. Crystallographic information

cis-DDSQ-2((methyl)(para-phenylamine))

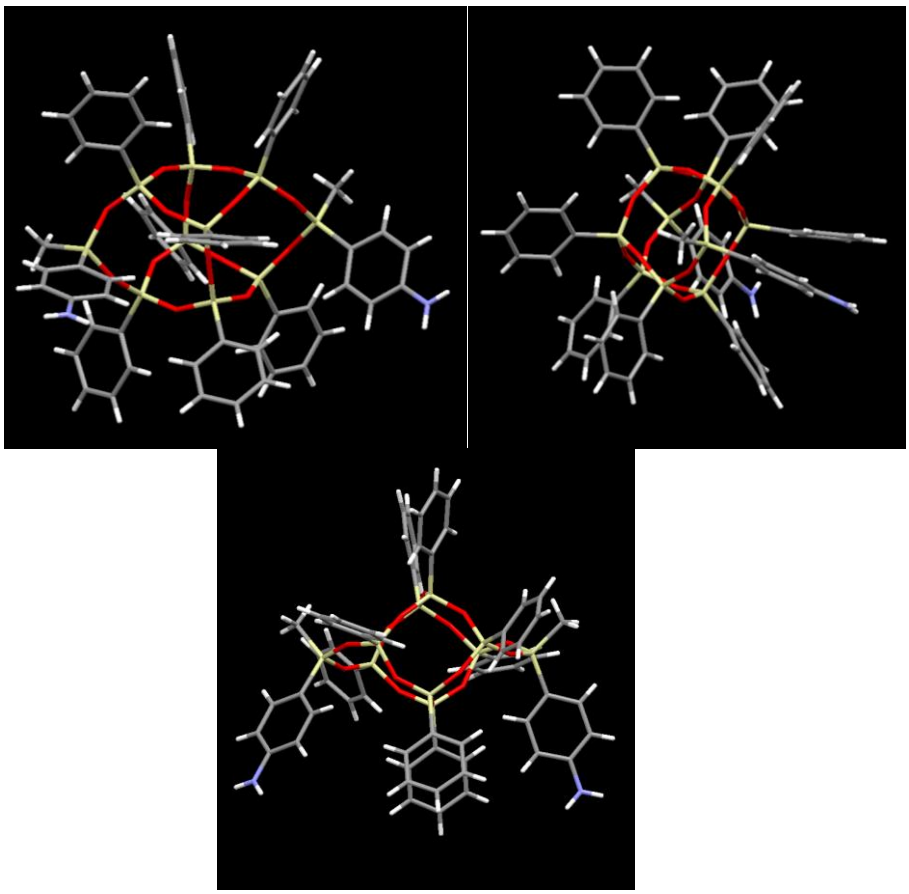

Figure J-1. Molecular structure of *cis*-DDSQ-2((methyl)(para-phenylamine)). White = H, Red = 0, Gray = C, Yellow = Si, Blue = N

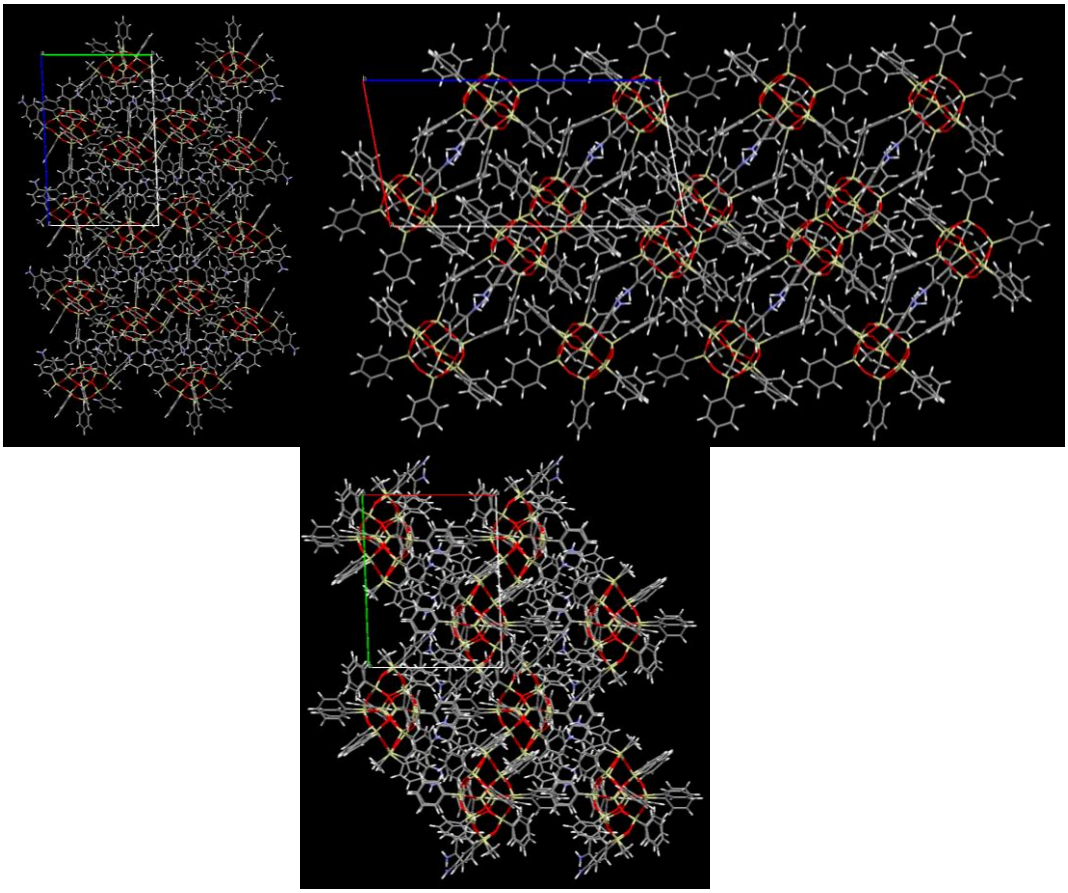

Figure J-2. Packing structure for *cis*-DDSQ-2((methyl)(para-phenylamine))

trans-DDSQ-2((methyl)(para-phenylamine))

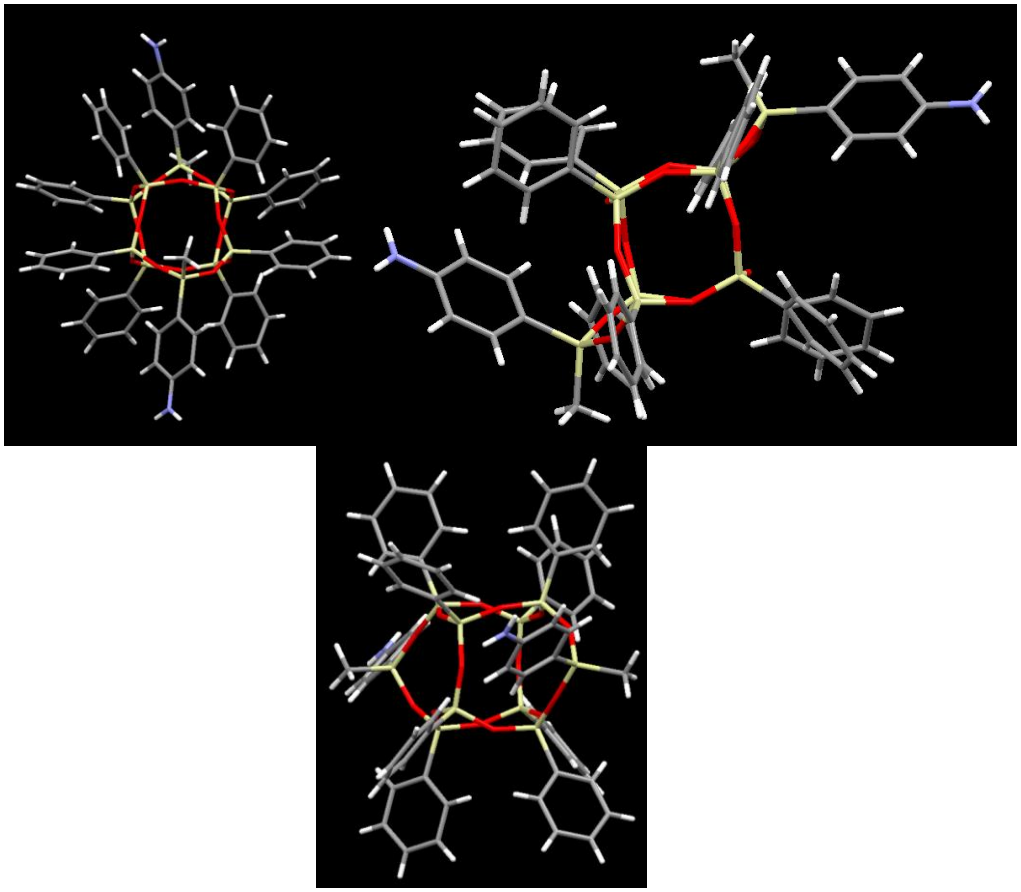

Figure J-3. Molecular structure of *trans*-DDSQ-2((methyl)(para-phenylamine)). White = H, Red = 0, Gray = C, Yellow = Si, Blue = N

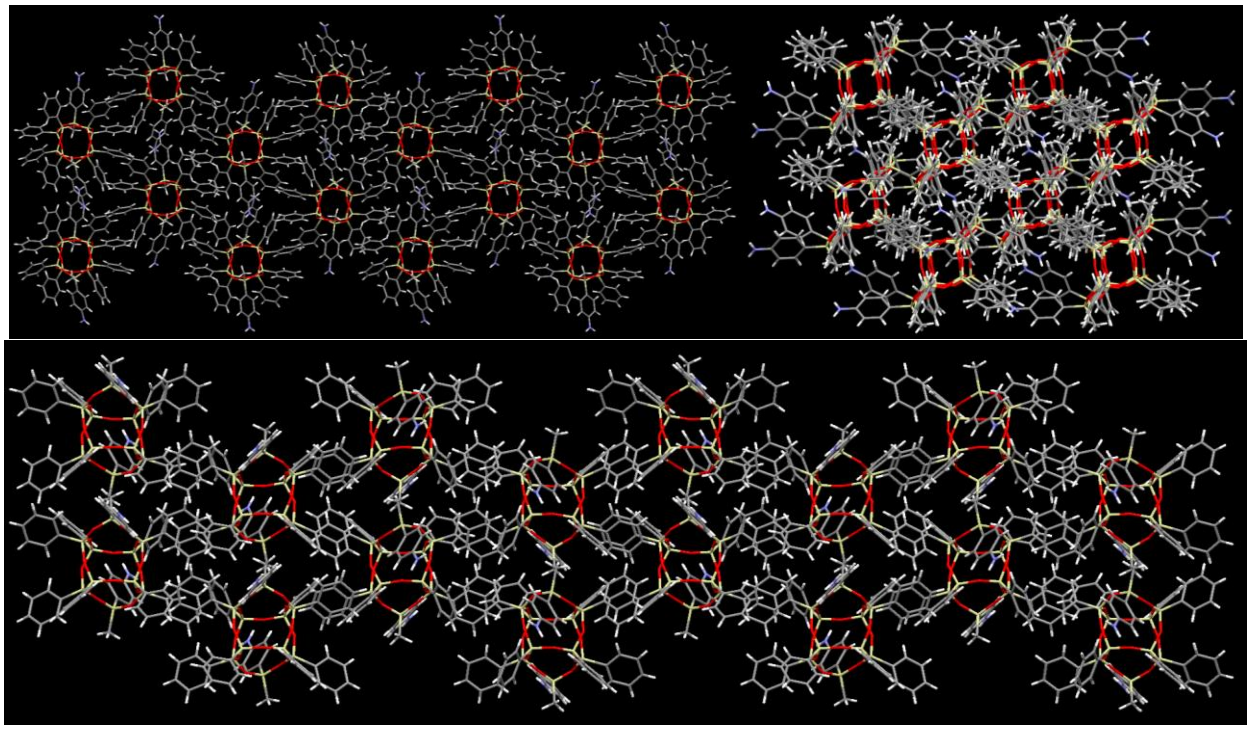

Figure J-4. Packing structure for *trans*-DDSQ-2((methyl)(para-phenylamine))

cis-DDSQ-2((methyl)(para-phenylethynyl phenyl))

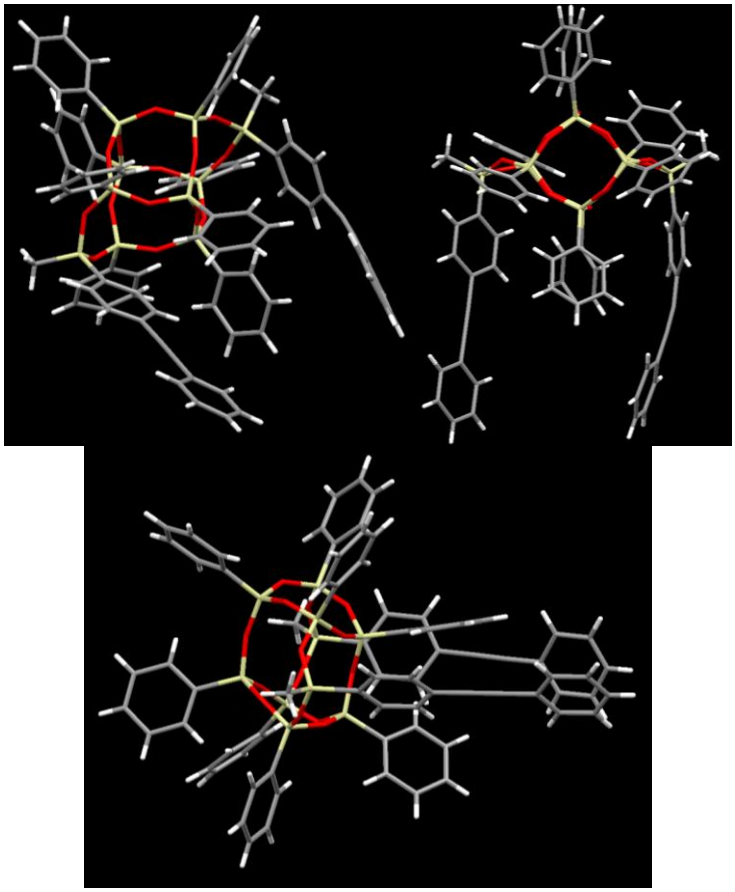

Figure J-5. Molecular structure of *cis*-DDSQ-2((methyl)(para-phenylethynyl phenyl)) White = H, Red = 0, Gray = C, Yellow = Si, Blue = N

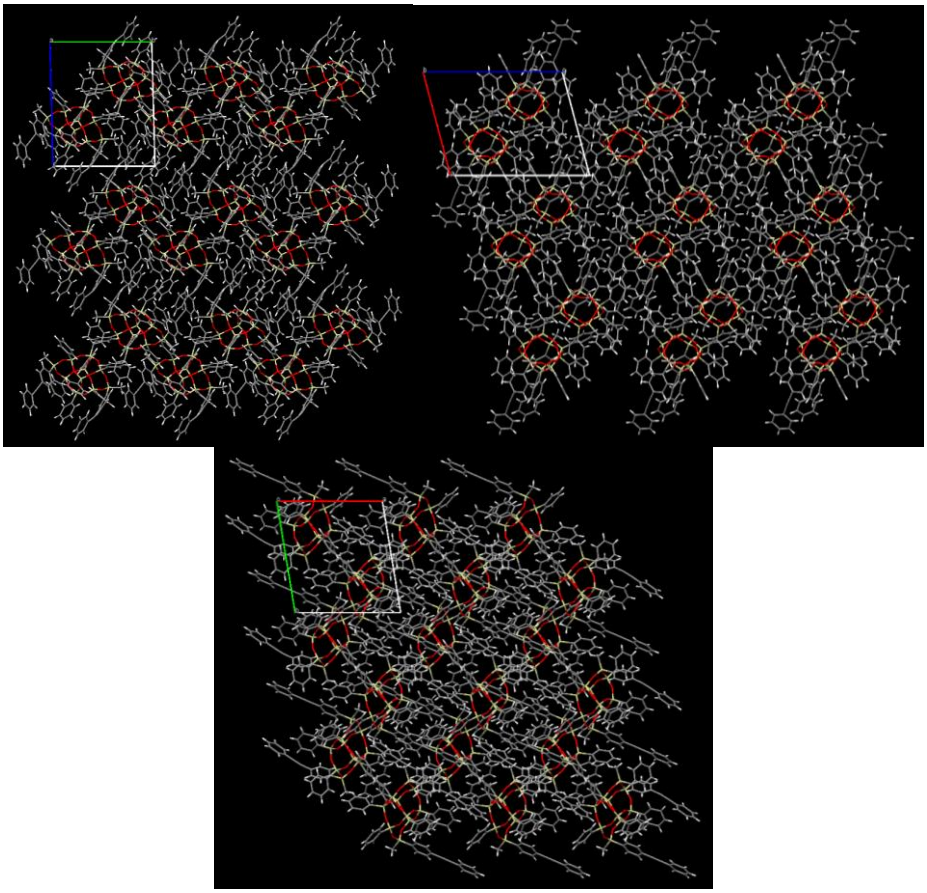

Figure J-6. Packing structure for *cis*-DDSQ-2((methyl)(para-phenylethynyl phenyl))

trans-DDSQ-2((methyl)(para-phenylethynyl phenyl))

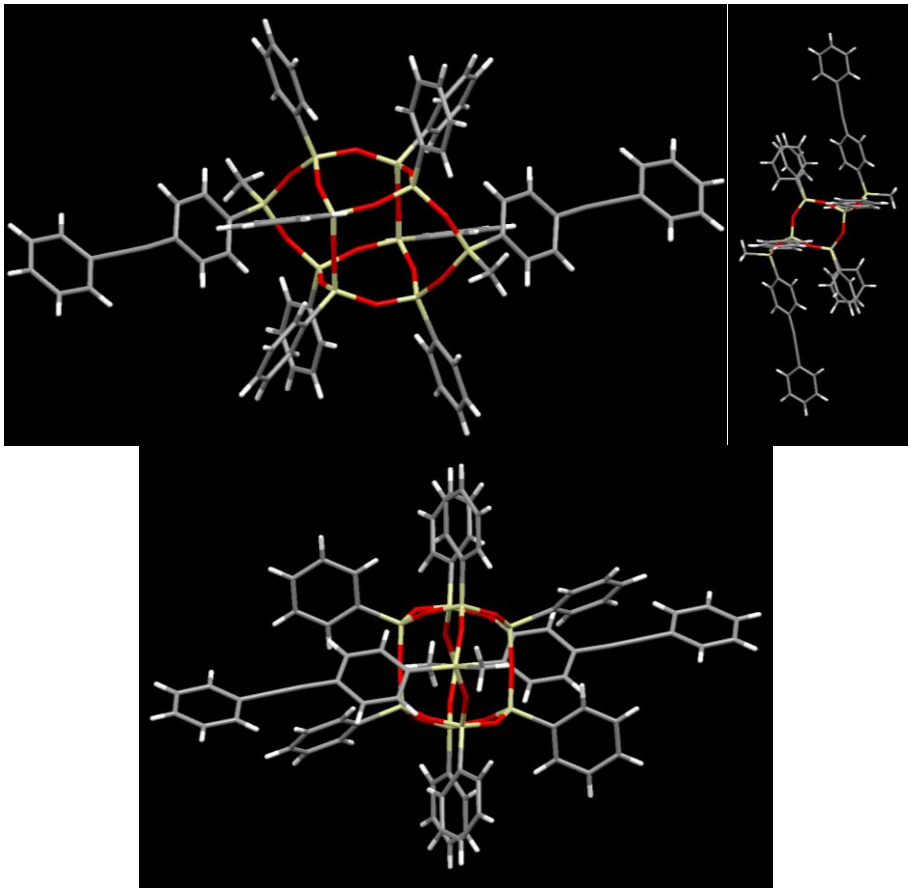

Figure J-7. Molecular structure of *trans*-DDSQ-2((methyl)(para-phenylethynyl phenyl)) White = H, Red = 0, Gray = C, Yellow = Si, Blue = N

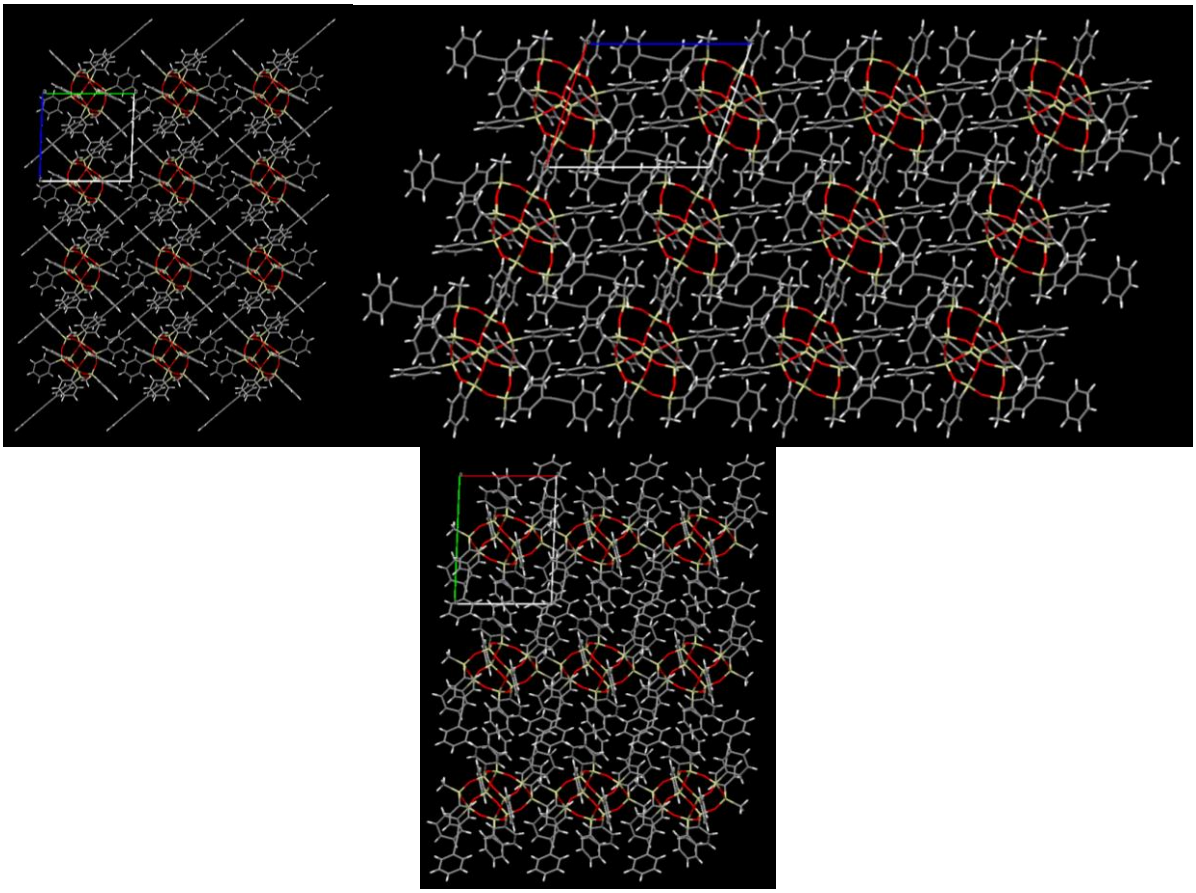

Figure J-8. Packing structure for *trans*-DDSQ-2((methyl)(para-phenylethynyl phenyl))

trans-DDSQ-2((methyl)(phenyl))

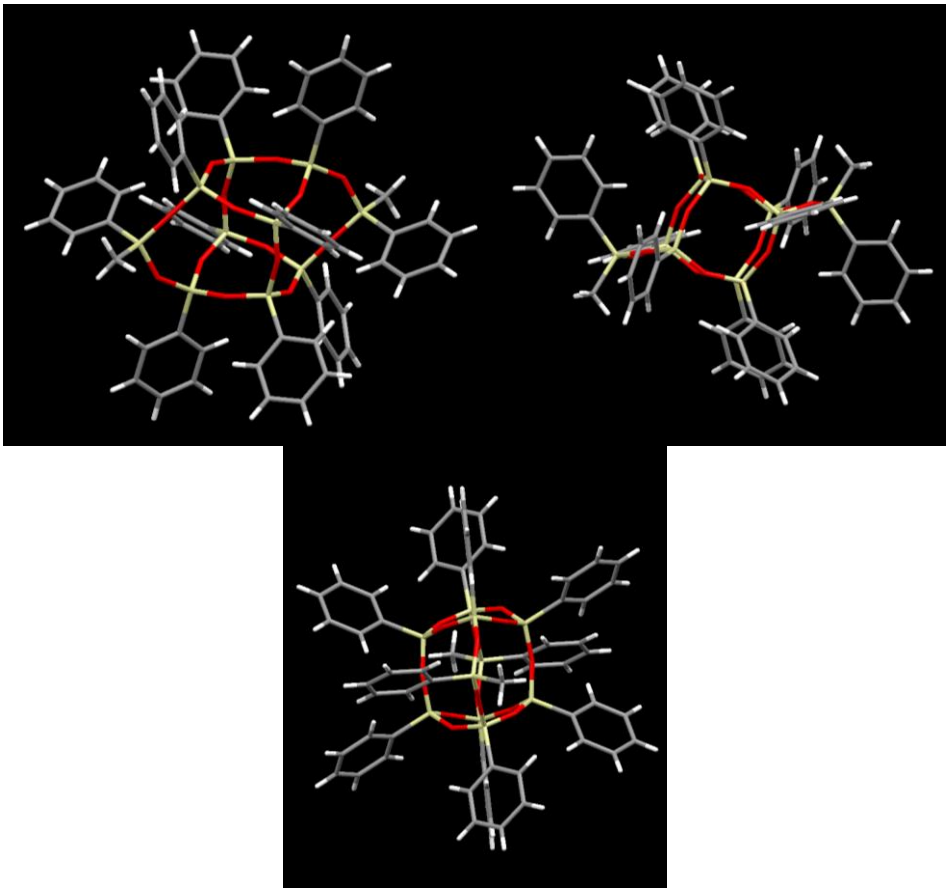

Figure J-9. Molecular structure of *trans*-DDSQ-2((methyl)(phenyl)) White = H, Red = 0, Gray = C, Yellow = Si, Blue = N

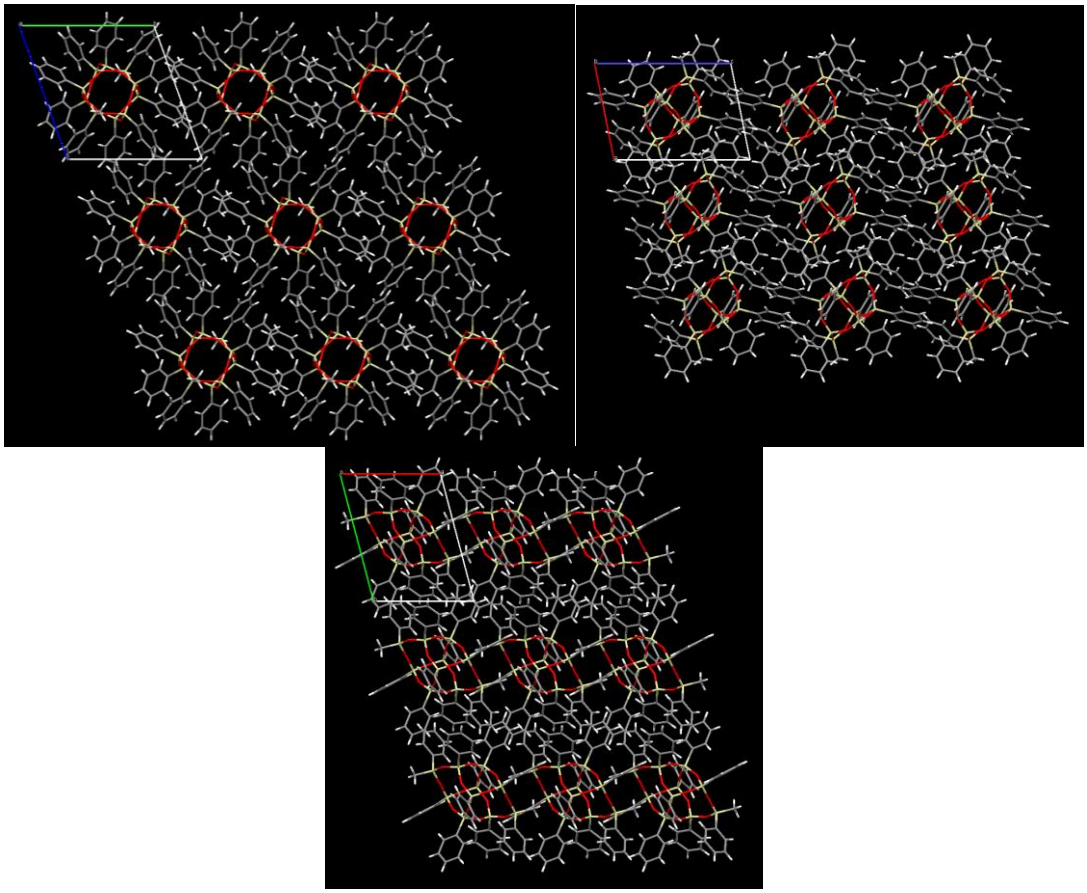

Figure J-10. Packing structure for *trans*-DDSQ-2((methyl)(phenyl))

REFERENCES

REFERENCES

(1) Hartmann-Thompson, C. *Applications of Polyhedral Oligomeric Silsesquioxanes*; Springer Science & Business Media, **2011**.

(2) Zhang, X.; Huang, Y.; Wang, T.; Liu, L. Influence of Fibre Surface Oxidation–reduction Followed by Silsesquioxane Coating Treatment on Interfacial Mechanical Properties of Carbon Fibre/polyarylacetylene Composites. *Compos. Part A Appl. Sci. Manuf.* **2007**, *38*, 936–944.

(3) Cordes, D. B.; Lickiss, P. D.; Rataboul, F. Recent Developments in the Chemistry of Cubic Polyhedral Oligosilsesquioxanes. *Chem. Rev.* **2010**, *110*, 2081–2173.

(4) Walczak, M.; Januszewski, R.; Majchrzak, M.; Kubicki, M.; Dudziec, B.; Marciniec, B. Unusual Cis and Trans Architecture of Dihydrofunctional Double-Decker Shaped Silsesquioxane and Synthesis of Its Ethyl Bridged π-Conjugated Arene Derivatives. *New J. Chem.* **2017**, *41*, 3290–3296.

(5) Ghanbari, H.; Cousins, B. G.; Seifalian, A. M. A Nanocage for Nanomedicine: Polyhedral Oligomeric Silsesquioxane (POSS). *Macromol. Rapid Commun.* **2011**, *32*, 1032–1046.

(6) Feher, F. J.; Newman, D. A.; Walzer, J. F. Silsesquioxanes as Models for Silica Surfaces. *J. Am. Chem. Soc.* **1989**, *111*, 1741–1748.

(7) Feher, F. J.; Phillips, S. H.; Ziller, J. W. Facile and Remarkably Selective Substitution Reactions Involving Framework Silicon Atoms in Silsesquioxane Frameworks. *J. Am. Chem. Soc.* **1997**, *119*, 3397–3398.

(8) Phillips, S. H.; Haddad, T. S.; Tomczak, S. J. Developments in Nanoscience: Polyhedral Oligomeric Silsesquioxane (POSS)-Polymers. *Curr. Opin. Solid State Mater. Sci.* **2004**, *8*, 21–29.

(9) Morimoto, Y.; Watanabe, K.; Ootake, N.; Inagaki, J.-I.; Yoshida, K.; Ohguma, K. Silsesquioxane Derivatives and Process for Production Thereof. 20040249103A1, December 9, **2004**.

(10) Ootake, N.; Yoshida, K. Organic Silicon Compound and Method for Producing Same, and Polysiloxane and Method for Producing Same. 20060155091:A1, July 13, **2006**.

(11) Lee, D. W.; Kawakami, Y. Incompletely Condensed Silsesquioxanes: Formation and Reactivity. *Polym. J.* **2007**, *39*, 230–238.

(12) Li, Z.; Kawakami, Y. Formation of Incompletely Condensed Oligosilsesquioxanes by Hydrolysis of Completely Condensed POSS via Reshuffling. *Chem. Lett.* **2008**, *37*, 804–805.

(13) Schoen, B. W.; Holmes, D.; Lee, A. Identification and Quantification of Cis and Trans Isomers in Aminophenyl Double-Decker Silsesquioxanes Using 1H--29Si gHMBC NMR. *Magn. Reson. Chem.* **2013**, *51*, 490–496.

(14) Schoen, B. W.; Lira, C. T.; Lee, A. Separation and Solubility of Cis and Trans Isomers in Nanostructured Double-Decker Silsequioxanes. *J. Chem. Eng. Data* **2014**, *59*, 1483–1493.

(15) Schoen, B. W. Aminophenyl Double Decker Silsesquioxanes: Spectroscopic Elucidation, Physical and Thermal Characterization, and Their Applications; **2013**.

(16) Ervithayasuporn, V.; Sodkhomkhum, R.; Teerawatananond, T.; Phurat, C.; Phinyocheep, P.; Somsook, E.; Osotchan, T. Unprecedented Formation of Cis-and Trans-Di [(3-Chloropropyl) Isopropoxysilyl]-Bridged Double-Decker Octaphenylsilsesquioxanes. *Eur. J. Inorg. Chem.* **2013**, *2013*, 3292–3296.

(17) Hoque, M. A.; Kakihana, Y.; Shinke, S.; Kawakami, Y. Polysiloxanes with Periodically Distributed Isomeric Double-Decker Silsesquioxane in the Main Chain. *Macromolecules* **2009**, *42*, 3309–3315.

(18) Cao, J.; Fan, H.; Li, B.-G.; Zhu, S. Synthesis and Evaluation of Double-Decker Silsesquioxanes as Modifying Agent for Epoxy Resin. *Polymer* **2017**, *124*, 157–167.

(19) Xu, S.; Zhao, B.; Wei, K.; Zheng, S. Organic-Inorganic Polyurethanes with Double Decker Silsesquioxanes in the Main Chains: Morphologies, Surface Hydrophobicity, and Shape Memory Properties. *J. Polym. Sci. B Polym. Phys.* **2018**, *56*, 893–906.

(20) Laberty-Robert, C.; Vallé, K.; Pereira, F.; Sanchez, C. Design and Properties of Functional Hybrid Organic–inorganic Membranes for Fuel Cells. *Chem. Soc. Rev.* **2011**, *40*, 961–1005.

(21) Liu, N.; Wei, K.; Wang, L.; Zheng, S. Organic–inorganic Polyimides with Double Decker Silsesquioxane in the Main Chains. *Polym. Chem.* **2016**, *7*, 1158–1167.

(22) Liu, N.; Li, L.; Wang, L.; Zheng, S. Organic-Inorganic Polybenzoxazine Copolymers with Double Decker Silsesquioxanes in the Main Chains: Synthesis and Thermally Activated Ring-Opening Polymerization Behavior. *Polymer* **2017**, *109*, 254–265.

(23) Wei, K.; Wang, L.; Zheng, S. Organic–inorganic Polyurethanes with 3,13-Dihydroxypropyloctaphenyl Double-Decker Silsesquioxane Chain Extender. *Polym. Chem.* **2013**, *4*, 1491–1501.

(24) Wu, S.; Hayakawa, T.; Kakimoto, M.-A.; Oikawa, H. Synthesis and Characterization of Organosoluble Aromatic Polyimides Containing POSS in Main Chain Derived from Double-Decker-Shaped Silsesquioxane. *Macromolecules* **2008**, *41*, 3481–3487.

(25) Wu, S.; Hayakawa, T.; Kikuchi, R.; Grunzinger, S. J.; Kakimoto, M.-A.; Oikawa, H. Synthesis and Characterization of Semiaromatic Polyimides Containing POSS in Main

Chain Derived from Double-Decker-Shaped Silsesquioxane. *Macromolecules* **2007**, *40*, 5698–5705.

(26) Jiang, Q.; Zhang, W.; Hao, J.; Wei, Y.; Mu, J.; Jiang, Z. A Unique "cage–cage" Shaped Hydrophobic Fluoropolymer Film Derived from a Novel Double-Decker Structural POSS with a Low Dielectric Constant. *J. Mater. Chem.* **2015**, *3*, 11729–11734.

(27) Moore, L. M. J.; Zavala, J. J.; Lamb, J. T.; Reams, J. T.; Yandek, G. R.; Guenthner, A. J.; Haddad, T. S.; Ghiassi, K. B. Bis-Phenylethynyl Polyhedral Oligomeric Silsesquioxanes: New High-Temperature, Processable Thermosetting Materials. *RSC Adv.* **2018**, *8*, 27400–27405.

(28) Seurer, B.; Vij, V.; Haddad, T.; Mabry, J. M.; Lee, A. Thermal Transitions and Reaction Kinetics of Polyhederal Silsesquioxane Containing Phenylethynylphthalimides. *Macromolecules* **2010**, *43*, 9337–9347.

(29) Crystallization: Basic Concepts and Industrial Applications; Beckmann, W., Ed.; 1st ed.; Wiley-VCH: Weinheim, **2011**.

(30) Cisternas, L. A.; Rudd, D. F. Process Designs for Fractional Crystallization from Solution. *Ind. Eng. Chem. Res.* **1993**, *32*, 1993–2005.

(31) Walas, S. M. 16 - CRYSTALLIZATION FROM SOLUTIONS AND MELTS. In *Chemical Process Equipment*; Walas, S. M., Ed.; Butterworth-Heinemann: Boston, **1990**; pp. 523–548.

(32) Smolik, M. Chemical, Physicochemical and Crystal-Chemical Aspects of Crystallization from Aqueous Solutions as a Method of Purification. In *Crystallization - Science and Technology*; Andreeta, M., Ed.; InTech, **2012**.

(33) Ahn, H. W.; Clarson, S. J. Synthesis and Characterization of Cis- and Trans-Trimethyltriphenylcyclotrisiloxane. *J. Inorg. Organomet. Polym.* **2001**, *11*, 203–216.

(34) Snyder, L. R. Linear Elution Adsorption Chromatography: XII. Functional Grou Adsorption Energies on the Metal Oxide Adsorbents. *J. Chromatogr. A* **1966**, *23*, 388–402.

(35) Snyder, L. R.; Dolan, J. W. Chapter 7 - Liquid–Solid Chromatography. In *Liquid Chromatography*; Fanali, S.; Haddad, P. R.; Poole, C. F.; Schoenmakers, P.; Lloyd, D., Eds.; Elsevier: Amsterdam, **2013**; pp. 143–156.

(36) Snyder, L. R.; Kirkland, J. J.; Dolan, J. W. *Introduction to Modern Liquid Chromatography*; 3rd ed.; Wiley: Hoboken, N.J., **2010**.

(37) Khopkar, S. M. *Basic Concepts of Analytical Chemistry*; New Academic Science: Kent, UNITED KINGDOM, **2011**.

(38) International Union of Pure; Chemistry, A. IUPAC Gold Book - partition chromatography http://dx.doi.org/10.1351/goldbook.P04436 (accessed Oct 13, **2018**).

(39) Ahuja, S. *Chromatography and Separation Science*; Elsevier, **2003**.

(40) Wingren, C.; Hansson, U.-B. CHROMATOGRAPHY: LIQUID | Partition Chromatography (Liquid–Liquid). In *Encyclopedia of Separation Science*; Wilson, I. D., Ed.; Academic Press: Oxford, **2000**; pp. 760–770.

(41) Scott, R. P. W. The Role of Molecular Interactions in Chromatography. *J. Chromatogr. A* **1976**, *122*, 35–53.

(42) Szucs, R.; Brunelli, C.; Lestremau, F.; Hanna-Brown, M. Chapter 17 - Liquid Chromatography in the Pharmaceutical Industry. In *Liquid Chromatography (Second Edition)*; Fanali, S.; Haddad, P. R.; Poole, C. F.; Riekkola, M.-L., Eds.; Elsevier, **2017**; pp. 515–537.

(43) Čelić, M.; Farré, M.; Lopez de Alda, M.; Perez, S.; Barceló, D.; Petrović, M. Chapter 15 - Environmental Analysis: Emerging Pollutants. In *Liquid Chromatography (Second Edition)*; Fanali, S.; Haddad, P. R.; Poole, C. F.; Riekkola, M.-L., Eds.; Elsevier, **2017**; pp. 451–477.

(44) Gika, H.; Theodoridis, G.; Rainville, P.; Plumb, R. S.; Wilson, I. D. Chapter 9 - Metabolic Phenotyping (metabonomics/metabolomics) by Liquid Chromatography-Mass Spectrometry. In *Liquid Chromatography (Second Edition)*; Fanali, S.; Haddad, P. R.; Poole, C. F.; Riekkola, M.-L., Eds.; Elsevier, **2017**; pp. 245–265.

(45) Gilbert-López, B.; Valdés, A.; Acunha, T.; García-Cañas, V.; Simó, C.; Cifuentes, A. Chapter 10 - Foodomics: LC and LC-MS-Based Omics Strategies in Food Science and Nutrition. In *Liquid Chromatography (Second Edition)*; Fanali, S.; Haddad, P. R.; Poole, C. F.; Riekkola, M.-L., Eds.; Elsevier, **2017**; pp. 267–299.

(46) Donato, P.; Dugo, P.; Mondello, L. Chapter 8 - Separation of Lipids. In *Liquid Chromatography (Second Edition)*; Fanali, S.; Haddad, P. R.; Poole, C. F.; Riekkola, M.-L., Eds.; Elsevier, **2017**; pp. 201–243.

(47) Royle, L. Chapter 7 - Separation of Glycans and Monosaccharides. In *Liquid Chromatography (Second Edition)*; Fanali, S.; Haddad, P. R.; Poole, C. F.; Riekkola, M.-L., Eds.; Elsevier, **2017**; pp. 183–200.

(48) Koga, R.; Miyoshi, Y.; Todoroki, K.; Hamase, K. Chapter 4 - Amino Acid and Bioamine Separations. In *Liquid Chromatography (Second Edition)*; Fanali, S.; Haddad, P. R.; Poole, C. F.; Riekkola, M.-L., Eds.; Elsevier, **2017**; pp. 87–106.

(49) Andjelković, U.; Giacometti, J.; Josić, D. Chapter 5 - Protein and Peptide Separations. In *Liquid Chromatography (Second Edition)*; Fanali, S.; Haddad, P. R.; Poole, C. F.; Riekkola, M.-L., Eds.; Elsevier, **2017**; pp. 107–157.

(50) Chankvetadze, B. Chapter 3 - Liquid Chromatographic Separation of Enantiomers. In *Liquid Chromatography (Second Edition)*; Fanali, S.; Haddad, P. R.; Poole, C. F.; Riekkola, M.-L., Eds.; Elsevier, **2017**; pp. 69–86.

(51) Panfili, G.; Fratianni, A.; Irano, M. Normal Phase High-Performance Liquid Chromatography Method for the Determination of Tocopherols and Tocotrienols in Cereals. *J. Agric. Food Chem.* **2003**, *51*, 3940–3944.

(52) Anumula, K. R.; Dhume, S. T. High Resolution and High Sensitivity Methods for Oligosaccharide Mapping and Characterization by Normal Phase High Performance Liquid Chromatography Following Derivatization with Highly Fluorescent Anthranilic Acid. *Glycobiology* **1998**, *8*, 685–694.

(53) Grossmann, C.; Langel, C.; Mazzotti, M.; Morbidelli, M.; Morari, M. Multi-Rate Optimizing Control of Simulated Moving Beds. *J. Process Control* **2010**, *20*, 490–505.

(54) Migliorini, C.; Mazzotti, M.; Morbidelli, M. Continuous Chromatographic Separation through Simulated Moving Beds under Linear and Nonlinear Conditions. *J. Chromatogr. A* **1998**, *827*, 161–173.

(55) Wankat, P. C. *Separation Process Engineering: Includes Mass Transfer Analysis, 3rd Edition*; Hall, P., Ed.; **2007**.

(56) Still, W. C.; Kahn, M.; Mitra, A. Rapid Chromatographic Technique for Preparative Separations with Moderate Resolution. *J. Org. Chem.* **1978**, *43*, 2923–2925.

(57) Fornstedt, T.; Forssén, P.; Samuelsson, J. Chapter 18 - Modeling of Preparative Liquid Chromatography. In *Liquid Chromatography*; Fanali, S.; Haddad, P. R.; Poole, C. F.; Schoenmakers, P.; Lloyd, D., Eds.; Elsevier: Amsterdam, **2013**; pp. 407–425.

(58) ASPEN. *Help File in ASPEN Chromatography V 10*; **2017**.

(59) Wang, Z.; Yonggang, L.; Huijuan, M.; Wenpeng, S.; Tao, L.; Cuifen, L.; Junqi, N.; Guichun, Y.; Zuxing, C. Novel Phosphorus-Nitrogen-Silicon Copolymers with Double-Decker Silsesquioxane in the Main Chain and Their Flame Retardancy Application in PC/ABS. *Fire Mater.* **2018**, *2*, 16230.

(60) Hoque, M. A.; Kawakami, Y. Synthesis of Polysilsesquioxanes with Double-Decker Silsesquioxane Repeating Units. *Journal of Scientific Research* **2016**, *8*, 217–227.

(61) Żak, P.; Dudziec, B.; Dutkiewicz, M.; Ludwiczak, M.; Marciniec, B.; Nowicki, M. A New Class of Stereoregular Vinylene-Arylene Copolymers with Double-Decker Silsesquioxane in the Main Chain. *J. Polym. Sci. Part A: Polym. Chem.* **2016**, *54*, 1044–1055.

(62) Seino, M.; Hayakawa, T.; Ishida, Y.; Kakimoto, M.-A.; Watanabe, K.; Oikawa, H. Hydrosilylation Polymerization of Double-Decker-Shaped Silsesquioxane Having Hydrosilane with Diynes. *Macromolecules* **2006**, *39*, 3473–3475.

(63) Kucuk, A. C.; Matsui, J.; Miyashita, T. Langmuir-Blodgett Films Composed of Amphiphilic Double-Decker Shaped Polyhedral Oligomeric Silsesquioxanes. *J. Colloid Interface Sci.* **2011**, *355*, 106–114.

(64) Díaz, U.; Brunel, D.; Corma, A. Catalysis Using Multifunctional Organosiliceous Hybrid Materials. *Chem. Soc. Rev.* **2013**, *42*, 4083–4097.

(65) Espinas, J.; Pelletier, J. D. A.; Abou-Hamad, E.; Emsley, L.; Basset, J.-M. A Silica-Supported Double-Decker Silsesquioxane Provides a Second Skin for the Selective Generation of Bipodal Surface Organometallic Complexes. *Organometallics* **2012**, *31*, 7610–7617.

(66) Laine, R. M.; Choi, J.; Lee, I. Organic--Inorganic Nanocomposites with Completely Defined Interfacial Interactions. *Adv. Mater.* **2001**, *13*, 800–803.

(67) Wu, S.; Hayakawa, T.; Kikuchi, R.; Grunzinger, S. J.; Kakimoto, M.-A.; Oikawa, H. Synthesis and Characterization of Semiaromatic Polyimides Containing POSS in Main Chain Derived from Double-Decker-Shaped Silsesquioxane. *Macromolecules* **2007**, *40* (16), 5698–5705.

(68) Żak, P.; Majchrzak, M.; Wilkowski, G.; Dudziec, B.; Dutkiewicz, M.; Marciniec, B. Synthesis and Characterization of Functionalized Molecular and Macromolecular Double-Decker Silsesquioxane Systems. *RSC Adv.* **2016**, *6* (12), 10054–10063.

(69) Liu, N.; Wei, K.; Wang, L.; Zheng, S. Organic–inorganic Polyimides with Double Decker Silsesquioxane in the Main Chains. *Polym. Chem.* **2016**, *7* (5), 1158–1167.

(70) Liu, N.; Li, L.; Wang, L.; Zheng, S. Organic-Inorganic Polybenzoxazine Copolymers with Double Decker Silsesquioxanes in the Main Chains: Synthesis and Thermally Activated Ring-Opening Polymerization Behavior. *Polymer* **2017**, *109* (Supplement C), 254–265.

(71) Schoen, B. W. *Aminophenyl Double Decker Silsesquioxanes: Spectroscopic Elucidation, Physical and Thermal Characterization, and Their Applications*; 2013.

(72) Wei, K.; Wang, L.; Zheng, S. Organic–inorganic Polyurethanes with 3,13-Dihydroxypropyloctaphenyl Double-Decker Silsesquioxane Chain Extender. *Polym. Chem.* **2013**, *4* (5), 1491–1501.

(73) Hoque, M. A.; Kawakami, Y. Synthesis of Polysilsesquioxanes with Double-Decker Silsesquioxane Repeating Units. *Journal of Scientific Research* **2016**, *8* (2), 217–227.

(74) Hoque, M. A.; Kakihana, Y.; Shinke, S.; Kawakami, Y. Polysiloxanes with Periodically Distributed Isomeric Double-Decker Silsesquioxane in the Main Chain. *Macromolecules* **2009**, *42* (9), 3309–3315.

(75) Schoen, B. W.; Lira, C. T.; Lee, A. Separation and Solubility of Cis and Trans Isomers in Nanostructured Double-Decker Silsequioxanes. *J. Chem. Eng. Data* **2014**, *59* (5), 1483–1493.

(76) Schoen, B. W.; Holmes, D.; Lee, A. Identification and Quantification of Cis and Trans Isomers in Aminophenyl Double-Decker Silsesquioxanes Using 1H--29Si gHMBC NMR. *Magn. Reson. Chem.* **2013**, *51* (8), 490–496.

(77) Walczak, M.; Januszewski, R.; Majchrzak, M.; Kubicki, M.; Dudziec, B.; Marciniec, B. Unusual Cis and Trans Architecture of Dihydrofunctional Double-Decker Shaped Silsesquioxane and Synthesis of Its Ethyl Bridged π-Conjugated Arene Derivatives. *New J. Chem.* **2017**, *41* (9), 3290–3296.

(78) Ervithayasuporn, V.; Sodkhomkhum, R.; Teerawatananond, T.; Phurat, C.; Phinyocheep, P.; Somsook, E.; Osotchan, T. Unprecedented Formation of Cis-and Trans-Di [(3-Chloropropyl) Isopropoxysilyl]-Bridged Double-Decker Octaphenylsilsesquioxanes. *Eur. J. Inorg. Chem.* **2013**, *2013* (19), 3292–3296.

(79) Seurer, B.; Vij, V.; Haddad, T.;, Mabry J.M.; Lee, A. Thermal transitions and reaction kinetics of Polyhedral Silsesquioxanes containing Phenylethynylphtalimides. *Macromolecules* **2010**, 43, 9337-9347.

(80) Lee, A. Separation and Phase Behavior of Double-Decker Silsesquioxane Isomers. In *Proceedings of the 3rd World Congress on Recent Advances in Nanotechnology*; World Congress on Recent Advances in Nanotechnology; Avestia Publishing, 2018.

(81) Vogelsang, D. F.; Dannatt, J. E.; Maleczka, R. E.; Lee, A. Separation of Asymmetrically Capped Double-Decker Silsesquioxanes Mixtures. *Polyhedron* **2018**, *155*, 189–193.

(82) Snyder, L. R.; Kirkland, J. J.; Dolan, J. W. *Introduction to Modern Liquid Chromatography*, 3rd ed.; Wiley: Hoboken, N.J., 2010.

(83) Ghasemi, J.; Niazi, A. Spectrophotometric Simultaneous Determination of Nitroaniline Isomers by Orthogonal Signal Correction-Partial Least Squares. *Talanta* **2005**, *65* (5), 1168–1173.

(84) Howell, J. A.; Sutton, R. E. Ultraviolet and Absorption Light Spectrometry. *Anal. Chem.* **1998**, *70* (12), 107–118.

(85) Scott, R. P. W. The Role of Molecular Interactions in Chromatography. *J. Chromatogr. A* **1976**, *122*, 35–53.

(86) Liu, N.; Wei, K.; Wang, L.; Zheng, S. Organic–inorganic Polyimides with Double Decker Silsesquioxane in the Main Chains. *Polym. Chem.* **2016**, *7* (5), 1158–1167.

(87) Liu, N.; Li, L.; Wang, L.; Zheng, S. Organic-Inorganic Polybenzoxazine Copolymers with Double Decker Silsesquioxanes in the Main Chains: Synthesis and Thermally Activated Ring-Opening Polymerization Behavior. *Polymer* **2017**, *109* (Supplement C), 254–265.

(88) Jiang, Q.; Zhang, W.; Hao, J.; Wei, Y.; Mu, J.; Jiang, Z. A Unique "cage–cage" Shaped Hydrophobic Fluoropolymer Film Derived from a Novel Double-Decker Structural POSS with a Low Dielectric Constant. *J. Mater. Chem.* **2015**, *3* (44), 11729–11734.

(89) Wei, K.; Wang, L.; Zheng, S. Organic–inorganic Polyurethanes with 3,13-Dihydroxypropyloctaphenyl Double-Decker Silsesquioxane Chain Extender. *Polym. Chem.* **2013**, *4* (5), 1491–1501.

(90) Hoque, M. A.; Kakihana, Y.; Shinke, S.; Kawakami, Y. Polysiloxanes with Periodically Distributed Isomeric Double-Decker Silsesquioxane in the Main Chain. *Macromolecules* **2009**, *42* (9), 3309–3315.

(91) Vij, V.; Haddad, T. S.; Yandek, G. R.; Ramirez, S. M.; Mabry, J. M. Synthesis of Aromatic Polyhedral Oligomeric SilSesquioxane (POSS) Dianilines for Use in High-Temperature Polyimides. *Silicon Chem.* **2012**, *4* (4), 267–280.

(92) Hoque, M. A.; Kawakami, Y. Synthesis of Polysilsesquioxanes with Double-Decker Silsesquioxane Repeating Units. *Journal of Scientific Research* **2016**, *8* (2), 217–227.

(93) Schoen, B. W.; Lira, C. T.; Lee, A. Separation and Solubility of Cis and Trans Isomers in Nanostructured Double-Decker Silsequioxanes. *J. Chem. Eng. Data* **2014**, *59* (5), 1483–1493.

(94) Walczak, M.; Januszewski, R.; Majchrzak, M.; Kubicki, M.; Dudziec, B.; Marciniec, B. Unusual Cis and Trans Architecture of Dihydrofunctional Double-Decker Shaped Silsesquioxane and Synthesis of Its Ethyl Bridged π-Conjugated Arene Derivatives. *New J. Chem.* **2017**, *41* (9), 3290–3296.

(95) *Crystallization : Basic Concepts and Industrial Applications*, 1st ed.; Beckmann, W., Ed.; Wiley-VCH: Weinheim, 2011.

(96) Snyder, L. R.; Kirkland, J. J.; Dolan, J. W. *Introduction to Modern Liquid Chromatography*, 3rd ed.; Wiley: Hoboken, N.J., 2010.

(97) Migliorini, C.; Mazzotti, M.; Morbidelli, M. Continuous Chromatographic Separation through Simulated Moving Beds under Linear and Nonlinear Conditions. *J. Chromatogr. A* **1998**, *827* (2), 161–173.

(98) Grossmann, C.; Langel, C.; Mazzotti, M.; Morbidelli, M.; Morari, M. Multi-Rate Optimizing Control of Simulated Moving Beds. *J. Process Control* **2010**, *20* (4), 490–505.

(99) Ahuja, S. *Chromatography and Separation Science*; Elsevier, 2003.

(100) Kamarei, F.; Gritti, F.; Guiochon, G.; Burchell, J. Accurate Measurements of Frontal Analysis for the Determination of Adsorption Isotherms in Supercritical Fluid Chromatography. *J. Chromatogr. A* **2014**, *1329*, 71–77.

(101) Panfili, G.; Fratianni, A.; Irano, M. Normal Phase High-Performance Liquid Chromatography Method for the Determination of Tocopherols and Tocotrienols in Cereals. *J. Agric. Food Chem.* **2003**, *51* (14), 3940–3944.

(102) Anumula, K. R.; Dhume, S. T. High Resolution and High Sensitivity Methods for Oligosaccharide Mapping and Characterization by Normal Phase High Performance Liquid Chromatography Following Derivatization with Highly Fluorescent Anthranilic Acid. *Glycobiology* **1998**, *8* (7), 685–694.

(103) Glinski, J. A.; Davey, M. H.; Kane, R. E.; Glinski, V. B. Quantification of Activin® Grape Seed Extracts for Procyanidin Composition with Reverse Phase and Normal Phase HPLC. *Planta Med.* **2008**, *74* (09), SL39.

(104) Rao, D. B. S. METHOD DEVELOPMENT AND VALIDATION OF REVERSE PHASE HPLC FOR PREGABALIN IN PHARMACEUTICAL DOSAGE BY REVERSE PHASE HPLC. *WJPPS* **2017**, 2001–2012.

(105) Narine, S. S.; Yue, J.; Kong, X. Production of Polyols from Canola Oil and Their Chemical Identification and Physical Properties. *J. Am. Oil Chem. Soc.* **2007**, *84* (2), 173–179.

(106) Andrews, G. D.; Vatvars, A. HPLC Analysis of Polymers. Separation of Hydroxy-Functional Poly(methyl Methacrylate) by Number of Hydroxyls and Separation of Poly(methyl Methacrylate) Oligomers. *Macromolecules* **1981**, *14* (5), 1603–1605.

(107) Ootake, N.; Yoshida, K. Organic Silicon Compound and Method for Producing Same, and Polysiloxane and Method for Producing Same. 20060155091:A1, July 13, 2006.

(108) Morimoto, Y.; Watanabe, K.; Ootake, N.; Inagaki, J.-I.; Yoshida, K.; Ohguma, K. Silsesquioxane Derivatives and Process for Production Thereof. 20040249103A1, December 9, 2004.

(109) Lee, D. W.; Kawakami, Y. Incompletely Condensed Silsesquioxanes: Formation and Reactivity. *Polym. J.* **2007**, *39*, 230–238.

(110) Mituła, K.; Duszczak, J.; Brząkalski, D.; Dudziec, B.; Kubicki, M.; Marciniec, B. Tetra-Functional Double-Decker Silsesquioxanes as Anchors for Reactive Functional Groups and Potential Synthons for Hybrid Materials. *Chem. Commun.* **2017**, *53*, 10370–10373.

(111) Schoen, B. W. *Aminophenyl Double Decker Silsesquioxanes: Spectroscopic Elucidation, Physical and Thermal Characterization, and Their Applications*; 2013.

(112) Schoen, B. W.; Holmes, D.; Lee, A. Identification and Quantification of Cis and Trans Isomers in Aminophenyl Double-Decker Silsesquioxanes Using 1H--29Si gHMBC NMR. *Magn. Reson. Chem.* **2013**, *51*, 490–496.

(113) Schoen, B. W.; Lira, C. T.; Lee, A. Separation and Solubility of Cis and Trans Isomers in Nanostructured Double-Decker Silsesquioxanes. J. Chem. Eng. Data 2014, 59, 1483–1493.

(114) Seurer, B.; Vij, V.; Haddad, T.; Mabry, J. M.; Lee, A. Thermal Transitions and Reaction Kinetics of Polyhedral Silsesquioxane Containing Phenylethynylphthalimides. Macromolecules 2010, 43, 9337–9347.

(115) Kohri, M.; Matsui, J.; Watanabe, A.; Miyashita, T. Synthesis and Optoelectronic Properties of Completely Carbazole-Substituted Double-Decker-Shaped Silsesquioxane. *Chem. Lett.* **2010**, *39*, 1162–1163.

(116) Xu, S.; Zhao, B.; Wei, K.; Zheng, S. Organic-Inorganic Polyurethanes with Double Decker Silsesquioxanes in the Main Chains: Morphologies, Surface Hydrophobicity, and Shape Memory Properties. *J. Polym. Sci. B Polym. Phys.* **2018**, *56*, 893–906.

(117) Wang, Z.; Yonggang, L.; Huijuan, M.; Wenpeng, S.; Tao, L.; Cuifen, L.; Junqi, N.; Guichun, Y.; Zuxing, C. Novel Phosphorus-Nitrogen-Silicon Copolymers with Double-Decker Silsesquioxane in the Main Chain and Their Flame Retardancy Application in PC/ABS. *Fire Mater.* **2018**, *2*, 16230.

(118) Liu, N.; Wei, K.; Wang, L.; Zheng, S. Organic-inorganic Polyimides with Double Decker Silsesquioxane in the Main Chains. Polym. Chem. 2016, 7, 1158–1167.

(119) Wei, K.; Wang, L.; Zheng, S. Organic-inorganic Polyurethanes with 3,13-Dihydroxypropyloctaphenyl Double-Decker Silsesquioxane Chain Extender. Polym. Chem. 2013, 4, 1491–1501.

(120) Hoque, M. A.; Kakihana, Y.; Shinke, S.; Kawakami, Y. Polysiloxanes with Periodically Distributed Isomeric Double-Decker Silsesquioxane in the Main Chain. *Macromolecules* **2009**, *42*, 3309–3315.

(121) Ervithayasuporn, V.; Sodkhomkhum, R.; Teerawatananond, T.; Phurat, C.; Phinyocheep, P.; Somsook, E.; Osotchan, T. Unprecedented Formation of Cis-and Trans-Di [(3-Chloropropyl) Isopropoxysilyl]-Bridged Double-Decker Octaphenylsilsesquioxanes. *Eur. J. Inorg. Chem.* **2013**, *2013*, 3292–3296.

(122) Walczak, M.; Januszewski, R.; Majchrzak, M.; Kubicki, M.; Dudziec, B.; Marciniec, B. Unusual Cis and Trans Architecture of Dihydrofunctional Double-Decker Shaped Silsesquioxane and Synthesis of Its Ethyl Bridged π-Conjugated Arene Derivatives. *New J. Chem.* **2017**, *41*, 3290–3296.

(123) Kucuk, A. C.; Matsui, J.; Miyashita, T. Langmuir-Blodgett Films Composed of Amphiphilic Double-Decker Shaped Polyhedral Oligomeric Silsesquioxanes. *J. Colloid Interface Sci.* **2011**, *355*, 106–114.

(124) Kucuk, A. C.; Matsui, J.; Miyashita, T. Synthesis and Photochemical Response of Ru(Ii)-Coordinated Double-Decker Silsesquioxane. *RSC Adv.* **2018**, *8*, 2148–2156.

(125) Espinas, J.; Pelletier, J. D. A.; Abou-Hamad, E.; Emsley, L.; Basset, J.-M. A Silica-Supported Double-Decker Silsesquioxane Provides a Second Skin for the Selective Generation of Bipodal Surface Organometallic Complexes. *Organometallics* **2012**, *31*, 7610–7617.

(126) Żak, P.; Dudziec, B.; Dutkiewicz, M.; Ludwiczak, M.; Marciniec, B.; Nowicki, M. A New Class of Stereoregular Vinylene-Arylene Copolymers with Double-Decker Silsesquioxane in the Main Chain. *J. Polym. Sci. Part A: Polym. Chem.* **2016**, *54*, 1044–1055.

(127) Liu, N.; Li, L.; Wang, L.; Zheng, S. Organic-Inorganic Polybenzoxazine Copolymers with Double Decker Silsesquioxanes in the Main Chains: Synthesis and Thermally Activated Ring-Opening Polymerization Behavior. *Polymer* **2017**, *109*, 254–265.

(128) Wu, S.; Hayakawa, T.; Kikuchi, R.; Grunzinger, S. J.; Kakimoto, M.-A.; Oikawa, H. Synthesis and Characterization of Semiaromatic Polyimides Containing POSS in Main Chain Derived from Double-Decker-Shaped Silsesquioxane. *Macromolecules* **2007**, *40*, 5698–5705.

(129) Hoque, M. A.; Kawakami, Y. Synthesis of Polysilsesquioxanes with Double-Decker Silsesquioxane Repeating Units. *Journal of Scientific Research* **2016**, *8*, 217–227.

(130) Wu, S.; Hayakawa, T.; Kakimoto, M.-A.; Oikawa, H. Synthesis and Characterization of Organosoluble Aromatic Polyimides Containing POSS in Main Chain Derived from Double-Decker-Shaped Silsesquioxane. *Macromolecules* **2008**, *41*, 3481–3487.

(131) Vogelsang, D. F.; Dannatt, J. E.; Maleczka, R. E.; Lee, A. Separation of Asymmetrically Capped Double-Decker Silsesquioxanes Mixtures. *Polyhedron* **2018**, *155*, 189–193.

(132) Fornstedt, T.; Forssén, P.; Samuelsson, J. Chapter 18 - Modeling of Preparative Liquid Chromatography. In *Liquid Chromatography*; Fanali, S.; Haddad, P. R.; Poole, C. F.; Schoenmakers, P.; Lloyd, D., Eds.; Elsevier: Amsterdam, 2013; pp. 407–425.

(133) Snyder, L. R.; Kirkland, J. J.; Dolan, J. W. *Introduction to Modern Liquid Chromatography*; 3rd ed.; Wiley: Hoboken, N.J., 2010.

(134) Gritti, F.; Guiochon, G. Systematic Errors in the Measurement of Adsorption Isotherms by Frontal Analysis Impact of the Choice of Column Hold-up Volume, Range and Density of the Data Points. *J. Chromatogr. A* **2005**, *1097*, 98–115.

(135) Manual, I. Agilent ChemStation for LC and CE Systems.

(136) ASPEN. *Help File in ASPEN Chromatography V 10*; **2017**.

(137) Vogelsang, D.; Maleczka, R.; Lee, A. HPLC Characterization of cis and trans mixtures of Double-Decker Shaped Silsesquioxanes. *Silicon J.* Submitted **2018**.

(138) Phillips, S. H.; Haddad, T. S.; Tomczak, S. J. Developments in Nanoscience: Polyhedral Oligomeric Silsesquioxane (POSS)-Polymers. *Curr. Opin. Solid State Mater. Sci.* **2004**, *8* (1), 21–29. https://doi.org/10.1016/j.cossms.2004.03.002.

(139) Li, G.; Wang, L.; Ni, H.; Pittman, C. U. Polyhedral Oligomeric Silsesquioxane (POSS) Polymers and Copolymers: A Review. *J. Inorg. Organomet. Polym.* **2001**, *11* (3), 123–154. https://doi.org/10.1023/A:1015287910502.

(140) Feher, F. J.; Phillips, S. H.; Ziller, J. W. Facile and Remarkably Selective Substitution Reactions Involving Framework Silicon Atoms in Silsesquioxane Frameworks. *J. Am. Chem. Soc.* **1997**, *119* (14), 3397–3398. https://doi.org/10.1021/ja963904m.

(141) Feher, F. J.; Newman, D. A.; Walzer, J. F. Silsesquioxanes as Models for Silica Surfaces. *J. Am. Chem. Soc.* **1989**, *111* (5), 1741–1748. https://doi.org/10.1021/ja00187a028.

(142) Feher, F. J.; Walzer, J. F. Synthesis and Characterization of Vanadium-Containing Silsesquioxanes. *Inorg. Chem.* **1991**, *30* (8), 1689–1694. https://doi.org/10.1021/ic00008a005.

(143) Morimoto, Y.; Watanabe, K.; Ootake, N.; Inagaki, J.-I.; Yoshida, K.; Ohguma, K. Silsesquioxane Derivatives and Process for Production Thereof. 20040249103A1, December 9, 2004.

(144) Lee, D. W.; Kawakami, Y. Incompletely Condensed Silsesquioxanes: Formation and Reactivity. *Polym. J.* **2007**, *39* (3), 230–238. https://doi.org/10.1295/polymj.PJ2006169.

(145) Hoque, M. A.; Kakihana, Y.; Shinke, S.; Kawakami, Y. Polysiloxanes with Periodically Distributed Isomeric Double-Decker Silsesquioxane in the Main Chain. *Macromolecules* **2009**, *42* (9), 3309–3315. https://doi.org/10.1021/ma900124x.

(146) Kawabata, K.; Tajima, A.; Matsuo, T.; Watanabe, Y.; Ayama, K. Compound Including Organopolysiloxane or Silsesquioxane Skeleton Having Isocyanuric Skeleton, Epoxy Group and SiH Group, Thermosetting Resin Composition Containing the Compound as Adhesion-Imparting Agent, Hardened Material and Sealing Agent for Optical Semiconductor. U.S. Patent 20140148536:A1, May 29, 2014.

(147) Au-Yeung, H.-L.; Leung, S. Y.-L.; Yam, V. W.-W. Supramolecular Assemblies of Dinuclear Alkynylplatinum(II) Terpyridine Complexes with Double-Decker Silsesquioxane Nano-Cores: The Role of Isomerism in Constructing Nano-Structures. *Chem. Commun.* **2018**, *54* (33), 4128–4131. https://doi.org/10.1039/c8cc00557e.

(148) Wu, S.; Hayakawa, T.; Kakimoto, M.-A.; Oikawa, H. Synthesis and Characterization of Organosoluble Aromatic Polyimides Containing POSS in Main Chain Derived from Double-Decker-Shaped Silsesquioxane. *Macromolecules* **2008**, *41* (10), 3481–3487. https://doi.org/10.1021/ma7027227.

(149) Kucuk, A. C.; Matsui, J.; Miyashita, T. Langmuir-Blodgett Films Composed of Amphiphilic Double-Decker Shaped Polyhedral Oligomeric Silsesquioxanes. *J. Colloid Interface Sci.* **2011**, *355* (1), 106–114. https://doi.org/10.1016/j.jcis.2010.12.033.

(150) Wu, S.; Hayakawa, T.; Kikuchi, R.; Grunzinger, S. J.; Kakimoto, M.-A.; Oikawa, H. Synthesis and Characterization of Semiaromatic Polyimides Containing POSS in Main Chain Derived from Double-Decker-Shaped Silsesquioxane. *Macromolecules* **2007**, *40* (16), 5698–5705. https://doi.org/10.1021/ma070547z.

(151) Jiang, Q.; Zhang, W.; Hao, J.; Wei, Y.; Mu, J.; Jiang, Z. A Unique "cage–cage" Shaped Hydrophobic Fluoropolymer Film Derived from a Novel Double-Decker Structural POSS with a Low Dielectric Constant. *J. Mater. Chem.* **2015**, *3* (44), 11729–11734. https://doi.org/10.1039/C5TC02432C.

(152) Liu, N.; Li, L.; Wang, L.; Zheng, S. Organic-Inorganic Polybenzoxazine Copolymers with Double Decker Silsesquioxanes in the Main Chains: Synthesis and Thermally Activated Ring-Opening Polymerization Behavior. *Polymer* **2017**, *109* (Supplement C), 254–265. https://doi.org/10.1016/j.polymer.2016.12.049.

(153) Hoque, M. A.; Kawakami, Y. Synthesis of Polysilsesquioxanes with Double-Decker Silsesquioxane Repeating Units. *Journal of Scientific Research* **2016**, *8* (2), 217–227. https://doi.org/10.3329/jsr.v8i2.26791.

(154) Żak, P.; Majchrzak, M.; Wilkowski, G.; Dudziec, B.; Dutkiewicz, M.; Marciniec, B. Synthesis and Characterization of Functionalized Molecular and Macromolecular Double-Decker Silsesquioxane Systems. *RSC Adv.* **2016**, *6* (12), 10054–10063. https://doi.org/10.1039/C5RA20848C.

(155) Haddad, T. S.; Viers, B. D.; Phillips, S. H. Polyhedral Oligomeric Silsesquioxane (POSS)-Styrene Macromers. *J. Inorg. Organomet. Polym.* **2001**, *11* (3), 155–164. https://doi.org/10.1023/A:1015237627340.

(156) Leu, C.-M.; Chang, Y.-T.; Wei, K.-H. Polyimide-Side-Chain Tethered Polyhedral Oligomeric Silsesquioxane Nanocomposites for Low-Dielectric Film Applications. *Chem. Mater.* **2003**, *15* (19), 3721–3727. https://doi.org/10.1021/cm030393b.

(157) Lichtenhan, J. D.; Schwab, J. J.; An, Y.; Liu, Q.; Haddad, T. S. Process for the Functionalization of Polyhedral Oligomeric Silsesquioxanes. U.S. Patent 6927270, August 9, 2005.

(158) Li, Y.; Dong, X.-H.; Zou, Y.; Wang, Z.; Yue, K.; Huang, M.; Liu, H.; Feng, X.; Lin, Z.; Zhang, W.; et al. Polyhedral Oligomeric Silsesquioxane Meets "click" Chemistry: Rational Design and Facile Preparation of Functional Hybrid Materials. *Polymer* **2017**, *125*, 303–329. https://doi.org/10.1016/j.polymer.2017.08.008.

(159) Cao, J.; Fan, H.; Li, B.-G.; Zhu, S. Synthesis and Evaluation of Double-Decker Silsesquioxanes as Modifying Agent for Epoxy Resin. *Polymer* **2017**, *124*, 157–167. https://doi.org/10.1016/j.polymer.2017.07.056.

(160) Xu, S.; Zhao, B.; Wei, K.; Zheng, S. Organic-Inorganic Polyurethanes with Double Decker Silsesquioxanes in the Main Chains: Morphologies, Surface Hydrophobicity, and Shape Memory Properties. *J. Polym. Sci. B Polym. Phys.* **2018**, *56* (12), 893–906. https://doi.org/10.1002/polb.24603.

(161) Haddad, T. S.; Mabry, J. M.; Ramirez, S. Synthesis of Functional Fluorinated Polyhedral Oligomeric Silsesquioxane (F-POSS). U.S. Patent 9249313, February 2, 2016.

(162) Lee, A.; Lu, Y.; Roche, A.; Pan, T.-Y. Influence of Nano-Structured Silanols on the Microstructure and Mechanical Properties of A4047 and A359 Aluminum Casting Alloys. *Int. J. Metalcast* **2016**, *10* (3), 338–341. https://doi.org/10.1007/s40962-016-0044-4.

(163) Blanco, I.; Abate, L.; Bottino, F. A.; Bottino, P. Thermal Degradation of Hepta Cyclopentyl, Mono Phenyl-Polyhedral Oligomeric Silsesquioxane (hcp-POSS)/polystyrene (PS) Nanocomposites. *Polym. Degrad. Stab.* **2012**, *97* (6), 849–855. https://doi.org/10.1016/j.polymdegradstab.2012.03.041.

(164) Jin, L.; Ishida, H. New Thermo-Oxidative Protective Coating for Carbon/carbon Composites in Mid-Temperature Range Using a Combination of Nano-Filler and Macro-Filler with Polybenzoxazine as a Carbon-Forming Matrix. *Polym. Compos.* **2011**, *32* (8), 1164–1173. https://doi.org/10.1002/pc.21135.

(165) Vahabi, H.; Eterradossi, O.; Ferry, L.; Longuet, C.; Sonnier, R.; Lopez-Cuesta, J.-M. Polycarbonate Nanocomposite with Improved Fire Behavior, Physical and Psychophysical Transparency. *Eur. Polym. J.* **2013**, *49* (2), 319–327. https://doi.org/10.1016/j.eurpolymj.2012.10.031.

(166) Ke, F.; Zhang, C.; Guang, S.; Xu, H. POSS Core Star-Shape Molecular Hybrid Materials: Effect of the Chain Length and POSS Content on Dielectric Properties. *J. Appl. Polym. Sci.* **2013**, *127* (4), 2628–2634.

(167) Ramirez, N. V.; Sanchez-Soto, M. Effects of POSS Nanoparticles on ABS-G-Ma Thermo Oxidation Resistance. *Polym. Compos.* **2012**, *33* (10), 1707–1718.

(168) Wang, Z.; Yonggang, L.; Huijuan, M.; Wenpeng, S.; Tao, L.; Cuifen, L.; Junqi, N.; Guichun, Y.; Zuxing, C. Novel Phosphorus-Nitrogen-Silicon Copolymers with Double-Decker Silsesquioxane in the Main Chain and Their Flame Retardancy Application in PC/ABS. *Fire Mater.* **2018**, *2*, 16230. https://doi.org/10.1002/fam.2649.

(169) Seurer, B.; Vij, V.; Haddad, T.; Mabry, J. M.; Lee, A. Thermal Transitions and Reaction Kinetics of Polyhederal Silsesquioxane Containing Phenylethynylphthalimides. *Macromolecules* **2010**, *43* (22), 9337–9347. https://doi.org/10.1021/ma101640q.

(170) Liu, N.; Wei, K.; Wang, L.; Zheng, S. Organic–inorganic Polyimides with Double Decker Silsesquioxane in the Main Chains. *Polym. Chem.* **2016**, *7* (5), 1158–1167. https://doi.org/10.1039/C5PY01827G.

(171) Cardiano, P.; Lazzara, G.; Manickam, S.; Mineo, P.; Milioto, S.; Lo Schiavo, S. POSS–Tetraalkylammonium Salts: A New Class of Ionic Liquids. *Eur. J. Inorg. Chem.* **2012**, *2012* (34), 5668–5676. https://doi.org/10.1002/ejic.201200874.

(172) Li, H.; Zhao, X.; Chu, G.; Zhang, S.; Yuan, X. One-Step Fabrication of a Superhydrophobic Polymer Surface from an Acrylic Copolymer Containing POSS by Spraying. *RSC Adv.* **2014**, *4* (107), 62694–62697. https://doi.org/10.1039/C4RA07113A.

(173) Xue, Y.; Wang, H.; Yu, D.; Feng, L.; Dai, L.; Wang, X.; Lin, T. Superhydrophobic Electrospun POSS-PMMA Copolymer Fibres with Highly Ordered Nanofibrillar and Surface Structures. *Chem. Commun.* **2009**, (42), 6418–6420. https://doi.org/10.1039/b911509a.

(174) Kucuk, A. C.; Matsui, J.; Miyashita, T. Synthesis and Photochemical Response of Ru(II)-Coordinated Double-Decker Silsesquioxane. *RSC Adv.* **2018**, *8* (4), 2148–2156. https://doi.org/10.1039/C7RA12290J.

(175) Espinas, J.; Pelletier, J. D. A.; Abou-Hamad, E.; Emsley, L.; Basset, J.-M. A Silica-Supported Double-Decker Silsesquioxane Provides a Second Skin for the Selective Generation of Bipodal Surface Organometallic Complexes. *Organometallics* **2012**, *31* (21), 7610–7617. https://doi.org/10.1021/om300918v.

(176) Hartmann-Thompson, C. *Applications of Polyhedral Oligomeric Silsesquioxanes*; Springer Science & Business Media, 2011.

(177) He, F.-A.; Zhang, L.-M. Using Inorganic POSS-Modified Laponite Clay to Support a Nickel α-Diimine Catalyst for in Situ Formation of High Performance Polyethylene Nanocomposites. *Nanotechnology* **2006**, *17* (24), 5941. https://doi.org/10.1088/0957-4484/17/24/007.

(178) Tanaka, K.; Ishiguro, F.; Chujo, Y. POSS Ionic Liquid. *J. Am. Chem. Soc.* **2010**, *132* (50), 17649–17651. https://doi.org/10.1021/ja105631j.

(179) Tanaka, K.; Ishiguro, F.; Jeon, J.-H.; Hiraoka, T.; Chujo, Y. POSS Ionic Liquid Crystals. *Npg Asia Materials* **2015**, *7*, e174. https://doi.org/10.1038/am.2015.28.

(180) Tanaka, K.; Ishiguro, F.; Chujo, Y. Thermodynamic Study of POSS-Based Ionic Liquids with Various Numbers of Ion Pairs. *Polym. J.* **2011**, *43*, 708. https://doi.org/10.1038/pj.2011.54.

(181) Zhao, R.; Chen, Y.; Liu, G.; Jiang, Y.; Chen, K. Fabrication of Self-Healing Waterbased Superhydrophobic Coatings from POSS Modified Silica Nanoparticles. *Mater. Lett.* **2018**, *229*, 281–285. https://doi.org/10.1016/j.matlet.2018.07.040.

(182) Rizvi, S. B.; Yildirimer, L.; Ghaderi, S.; Ramesh, B.; Seifalian, A. M.; Keshtgar, M. A Novel POSS-Coated Quantum Dot for Biological Application. *Int. J. Nanomedicine* **2012**, *7*, 3915–3927. https://doi.org/10.2147/IJN.S28577.

(183) Ganesh, V. A.; Nair, A. S.; Raut, H. K.; Tan, T. T. Y.; He, C.; Ramakrishna, S.; Xu, J. Superhydrophobic Fluorinated POSS-PVDF-HFP Nanocomposite Coating on Glass by Electrospinning. *J. Mater. Chem.* **2012**, *22* (35), 18479–18485.

(184) Wang, D. K.; Varanasi, S.; Strounina, E.; Hill, D. J. T.; Symons, A. L.; Whittaker, A. K.; Rasoul, F. Synthesis and Characterization of a POSS-PEG Macromonomer and POSS-PEG-PLA Hydrogels for Periodontal Applications. *Biomacromolecules* **2014**, *15* (2), 666–679. https://doi.org/10.1021/bm401728p.

(185) Tanaka, K.; Ohashi, W.; Kitamura, N.; Chujo, Y. Reductive Glutathione-Responsive Molecular Release Using Water-Soluble POSS Network Polymers. *BCSJ* **2011**, *84* (6), 612–616. https://doi.org/10.1246/bcsj.20110032.

(186) Kolel-Veetil, M. K.; Fears, K. P.; Qadri, S. B.; Klug, C. A.; Keller, T. M. Formation of a Crosslinked POSS Network by an Unusual Hydrosilylation: Thermo-Oxidative Stabilization of the α-Cristobalite Phase in Its Amorphous Regions. *J. Polym. Sci. A Polym. Chem.* **2012**, *50* (15), 3158–3170.

(187) Bagheri, H.; Soofi, G.; Javanmardi, H.; Karimi, M. A 3D Nanoscale Polyhedral Oligomeric Silsesquioxanes Network for Microextraction of Polycyclic Aromatic Hydrocarbons. *Mikrochim. Acta* **2018**, *185* (9), 418. https://doi.org/10.1007/s00604-018-2950-z.

(188) Ghanbari, H.; Cousins, B. G.; Seifalian, A. M. A Nanocage for Nanomedicine: Polyhedral Oligomeric Silsesquioxane (POSS). *Macromol. Rapid Commun.* **2011**, *32* (14), 1032–1046. https://doi.org/10.1002/marc.201100126.

(189) Tan, A.; Farhatnia, Y.; Seifalian, A. M. Polyhedral Oligomeric Silsesquioxane Poly (carbonate-Urea) Urethane (POSS-PCU): Applications in Nanotechnology and Regenerative Medicine. *Crit. Rev. Biomed. Eng.* **2013**, *41* (6), 495–513.

(190) Olivero, F.; Renò, F.; Carniato, F.; Rizzi, M.; Cannas, M.; Marchese, L. A Novel Luminescent Bifunctional POSS as a Molecular Platform for Biomedical Applications. *Dalton Trans.* **2012**, *41* (25), 7467–7473. https://doi.org/10.1039/C2DT30218G.

(191) Pu, Y.; Zhang, L.; Zheng, H.; He, B.; Gu, Z. Drug Release of pH-Sensitive poly(L-Aspartate)-B-Poly(ethylene Glycol) Micelles with POSS Cores. *Polym. Chem.* **2013**, *5* (2), 463–470. https://doi.org/10.1039/C3PY00965C.

(192) Schoen, B. W. *Aminophenyl Double Decker Silsesquioxanes: Spectroscopic Elucidation, Physical and Thermal Characterization, and Their Applications*; Ph.D. Thesis, Michigan State University, East Lansing, MI, 2013.

(193) Guo, T.; Wang, B. Isothermal Cold Crystallization and Melting Behaviors of Poly(lactic acid)/Epoxy Vinyl Polyhedral Oligomeric Silsesquioxanes Nanocomposites. *Polym. Plast. Technol. Eng.* **2014**, *53* (9), 917–926. https://doi.org/10.1080/03602559.2014.886061.

(194) Li, Y.; Morgan, R. J. Thermal Cure of Phenylethynyl-Terminated AFR-PEPA-4 Imide Oligomer and a Model Compound. *J. Appl. Polym. Sci.* **2006**, *101* (6), 4446–4453. https://doi.org/10.1002/app.24047.

(195) Schoen, B. W.; Holmes, D.; Lee, A. Identification and Quantification of Cis and Trans Isomers in Aminophenyl Double-Decker Silsesquioxanes Using 1H--29Si gHMBC NMR. *Magn. Reson. Chem.* **2013**, *51* (8), 490–496.

(196) Walczak, M.; Januszewski, R.; Majchrzak, M.; Kubicki, M.; Dudziec, B.; Marciniec, B. Unusual Cis and Trans Architecture of Dihydrofunctional Double-Decker Shaped Silsesquioxane and Synthesis of Its Ethyl Bridged π-Conjugated Arene Derivatives. *New J. Chem.* **2017**, *41* (9), 3290–3296. https://doi.org/10.1039/C7NJ00255F.

(197) Vogelsang, D. F.; Maleczka, R. E.; Lee, A. HPLC Characterization of Cis and Trans Mixtures of Double-Decker Shaped Silsesquioxanes. *Silicon* **2018**. https://doi.org/10.1007/s12633-018-0045-4.

(198) Attanayake, G. K. *Study of Different Routes to Develop Asymmetric Double Decker Silsesquioxane (DDSQ)*; Master's Thesis, Michigan State University, East Lansing, MI, 2015.

(199) Schoen, B. W.; Lira, C. T.; Lee, A. Separation and Solubility of Cis and Trans Isomers in Nanostructured Double-Decker Silsequioxanes. *J. Chem. Eng. Data* **2014**, *59* (5), 1483–1493. https://doi.org/10.1021/je4010245.

(200) Ervithayasuporn, V.; Sodkhomkhum, R.; Teerawatananond, T.; Phurat, C.; Phinyocheep, P.; Somsook, E.; Osotchan, T. Unprecedented Formation of Cis-and Trans-Di [(3-Chloropropyl) Isopropoxysilyl]-Bridged Double-Decker Octaphenylsilsesquioxanes. *Eur. J. Inorg. Chem.* **2013**, *2013* (19), 3292–3296.

(201) Moore, L. M. J.; Zavala, J. J.; Lamb, J. T.; Reams, J. T.; Yandek, G. R.; Guenthner, A. J.; Haddad, T. S.; Ghiassi, K. B. Bis-Phenylethynyl Polyhedral Oligomeric Silsesquioxanes: New High-Temperature, Processable Thermosetting Materials. *RSC Adv.* **2018**, *8* (48), 27400–27405. https://doi.org/10.1039/C8RA05954C.

(202) Thogiti, S.; Parvathaneni, S. P.; Keesara, S. Polymer Anchored 3-Benzoyl-1-(1-Benzylpiperidin-4-Yl)-2-Thiopseudourea-Pd(II) Complex: An Efficient Catalyst for the Copper and Solvent Free Sonogashira Cross-Coupling Reaction. *J. Organomet. Chem.* **2016**, *822*, 165–172. https://doi.org/10.1016/j.jorganchem.2016.08.029.

(203) Vogelsang, D. F.; Dannatt, J. E.; Maleczka, R. E., Jr.; Lee, A. Separation of Asymmetrically Capped Double-Decker Silsesquioxanes Mixtures. *Polyhedron* **2018**, *155*, 189–193. https://doi.org/10.1016/j.poly.2018.08.016.

(204) Vij, V.; Haddad, T. S.; Yandek, G. R.; Ramirez, S. M.; Mabry, J. M. Synthesis of Aromatic Polyhedral Oligomeric SilSesquioxane (POSS) Dianilines for Use in High-Temperature Polyimides *Silicon* **2012**, *4*, 267–280. https://doi.org/10.1007/s12633-012-9130-2.

(205) van Laar, J. J. Die Schmelz- Oder Erstarrungskurven Bei Binären Systemen, Wenn Die Feste Phase Ein Gemisch (amorphe Feste Lösung Oder Mischkristalle) Der Beiden Komponenten Ist. *Zeitschrift für Physikalische Chemie* **1908**, *63U* (1). https://doi.org/10.1515/zpch-1908-6314.

(206) Boettinger, W. J.; Kattner, U. R.; Moon, K.-W.; Perepezko, J. NIST Recommended Practice Guide: DTA and Heat-Flux DSC Measurements of Alloy Melting and Freezing. **2006**.